UNIVERSITÉ DU QUÉBEC À TROIS-RIVIÈRES

DÉVELOPPEMENT D'UNE CULTURE *IN VITRO*, ÉTUDE TRANSCRIPTOMIQUE COMPARATIVE ET CARACTÉRISATION FONCTIONNELLE DES GÈNES DE BIOSYNTHÈSE POUR UNE MEILLEURE COMPRÉHENSION DE LA VOIE DE BIOSYNTHÈSE DES ALCALOÏDES DES AMARYLLIDACEAE

DEVELOPMENT OF *IN VITRO* CULTURE, COMPARATIVE TRANSCRIPTOMIC STUDY, AND FUNCTIONAL CHARACTERIZATION OF BIOSYNTHETIC GENES FOR BETTER UNDERSTANDING OF AMARYLLIDACEAE ALKALOIDS BIOSYNTHESIS PATHWAY

THÈSE PRÉSENTÉE

COMME EXIGENCE PARTIELLE DE LA

DU DOCTORAT EN BIOLOGIE CELLULAIR ET MOLÉCULAIRE

PAR

MANOJ KOIRALA

JANVIER 2024

Avertissement

UNIVERSITÉ DU QUÉBEC À TROIS-RIVIÈRES

BIOLOGIE CELLULAIRE ET MOLÉCULAIRE (DOCTORAT)

Direction de recherche :

Isabel Desgagné-Penix, Ph.D	Université du Québec à Trois-Rivières
Prénom et nom	Directeur de recherche

Jury d'évaluation

Isabel Desgagné-Penix, Ph.D	Directeur de recherche
Prénom et nom	Fonction du membre de jury
Hugo Germain, Ph.D	Président du jury
Prénom et nom	Fonction du membre de jury
Thu-Thuy Dang, Ph.D	Évaluateur externe
Prénom et nom	Fonction du membre de jury
Degbedji Tagnon Missihoun, Ph.D	Évaluateur interne
Prénom et nom	Fonction du membre de jury

ACKNOWLEDGEMENT

Life is full of ups and downs, effusive gains, and maudlin pains, but some moments are forever. Getting through an accomplishment, looking back, and admiring oneself are the most cherishing fascinations of life. But that, too, the moment to pay my extreme gratitude and sincere thanks to my mentor and supervisor, Professor Isabel Desgagne-Penix, for her fruitful guidance, constructive ideas, support, and encouragement throughout my research. Her knowledge, expertise, and mentorship have shaped my research interests and career aspirations. I am also indebted to Dr. Natacha Merindol, who generously shared her time, expertise, and insights to help me navigate the research challenges. Their patience, kindness, and willingness to answer my questions were essential to my growth as a researcher. I am very thankful to Fatma Meddeb for her technical and administrative support during my study in Isabel's lab.

I want to acknowledge Professor Hugo Germain (Université du Québec à Trois-Rivières) for his support and for providing instrumental and reagent support during my study. I am grateful to Mélodie B. Plourde for teaching basic laboratory techniques. I am very thankful to Dr. Seydou Ka for his guidance on metabolite extraction. Special thanks go to Sarah-Eve Gélinas for her help in analyzing my sample with special attention throughout this study.

I want to extend my gratitude to Ariane Garand, who introduced me to the fascinating world of bioinformatics and the tools and skills necessary to analyze and interpret complex transcriptomic data. I am also grateful to Professor Marek Mutwill and his research team at Nanyang Technological University, Singapore, where I completed my internship in plant system biology. Their generosity in sharing their resources and knowledge with me was invaluable. I am truly honored to have had the opportunity to work alongside such talented and inspiring researchers who told me bioinformatics is not rocket science.

I am grateful to all my colleagues and seniors who contributed to my research project and finally helped me summarize my research work in a scientific article. I am thankful to my family, seniors, colleagues, and my interns for their unwavering support, patience, and encouragement throughout my Ph.D. journey. Their love and belief in me kept me motivated and inspired, and I am forever grateful for their presence in my life.

RÉSUMÉ EN FRANÇAIS

Les plantes produisent une large gamme de métabolites spécialisés (MS). Bien que le rôle physiologique des MS ne soit pas clair, les plantes les synthétisent pour s'adapter aux conditions environnementales changeantes et difficiles. Outre leur rôle défensif, ces composés ont également une valeur thérapeutique pour l'être humain. Les MS végétaux, bien connus pour leur valeur pharmacologique, constituent l'une des plus grandes classes de MS. Les alcaloïdes exclusivement extraits des Amaryllidaceae sont connus sous le nom d'alcaloïdes d'Amaryllidaceae (AAs). Les AAs, comme de nombreux MS, s'accumulent dans la plante en petites quantités variables et certains types d'AA sont restreints à certaines espèces d'Amaryllidaceae, ce qui limite encore davantage leur application pharmacologique. Par conséquent, une meilleure compréhension de la biosynthèse de ces alcaloïdes est intéressante pour de nombreux biochimistes, biologistes synthétiques, ingénieurs métaboliques et biologistes végétaux. Au cours de notre étude, nous avons développé la culture *in vitro* de *Crinum* x *powellii* ″Album″ qui est bien connu pour produire des AAs antiviraux tels que la cherylline et la lycorine. Pour comprendre l'effet des facteurs de croissance sur les cultures *in vitro* de *C.* x *powellii* ″Album″, nous avons cultivé des cals dans des conditions de lumière ou d'obscurité avec un apport exogène de phytohormones à différentes concentrations. Nos résultats démontrent que la combinaison d'auxine et de lumière influence de manière significative la croissance, la survie et la morphogenèse des tissus *in vitro* par rapport aux traitements individuels. De plus, la combinaison d'auxine et de lumière régule également positivement l'expression des gènes codant pour des enzymes biosynthétiques des alcaloïdes et conduit à une augmentation de la teneur en certains alcaloïdes, suggérant un impact positif sur le potentiel de défense des cals. Nos résultats fournissent un aperçu de la régulation des gènes codant pour les protéines impliquées dans la biosynthèse des alcaloïdes dans les cals de *C.* x *powellii* ″Album″ et soulignent le potentiel de l'auxine et de la lumière en tant qu'outils pour améliorer leur production dans les plantes médicinales. Cette étude constitue une base pour une exploration plus approfondie des cals de *C.* x *powellii* ″Album″ en tant que source durable de composés bioactifs pour des applications pharmaceutiques et agricoles. De plus, cette étude ouvre la voie à la découverte de la voie de biosynthèse de MS de *C.* x *powellii* ″Album″, comme la cherylline et la lycorine. Pour avancer la caractérisation de la voie de biosynthèse des AAs au niveau enzymatique, nous avons caractérisé la norbelladine *O*-méthyltransférase de l'Amaryllidaceae *Narcisssus papyraceus (Np*OMT*)*. Contrairement à la norbelladine *O*-méthyltransférase précédemment

caractérisée par d'autres équipes, la *Np*OMT catalyse la méthylation régiosélective de la norbelladine ainsi que la méthylation non régiosélective du 3,4-dihydroxybenzylaldéhyde et de l'acide caféique. De plus, *Np*OMT peut produire de la 3ˈ,4ˈ-diméthylnorbelladine à partir de la norbelladine, ce qui n'a jamais été rapporté auparavant. Des analyses d'arrimage et de dynamique moléculaire approfondies suggèrent que la formation de 4ˈ- par rapport à la 3ˈ-*O*-méthylnorbelladine est favorisée dans le site actif de la *Np*OMT dans les conditions physiologiques, ce qui est confirmé par un test enzymatique *in vivo* chez *Nicotiana benthamiana*. Notre étude révèle un nouveau potentiel catalytique de la *O*-méthyltransférase, qui peut être utilisé pour développer de nouvelles connaissances concernant la régio-spécificité et la promiscuité de substrat de ces *O*-méthyltransférases. En conclusion, nos recherches fournissent des connaissances et des outils permettant de supporter la production durable d'AA en utilisant des approches biotechnologiques.

Mots-clés : Métabolites spécialisés, culture *in vitro*, stress, étude transcriptomique, norbelladine-*O*-méthyltransférase, promiscuité, régiosélectif

Abstract

Plants produce a wide range of specialized metabolites (SM). Although the physiological role of these SM in plants is not clear, plants synthesize these SM to adapt themselves to changing harsh environmental conditions. In addition, to plant SM's defensive role, these compounds may also have therapeutic value for human beings. Among several classes of plant SM, alkaloids are one the largest types of plant SM, which are well known for their pharmacological significance. Alkaloid exclusively extracted from the Amaryllidaceae plant family are known as Amaryllidaceae alkaloids (AAs). AAs, with many plants SM, are also accumulated *in planta* in only traceable quantities, and certain types of AAs are only limited to specific genera of the Amaryllidaceae plant family which further limits pharmacological applications. Therefore, a better understanding of the biosynthesis of these structurally diverse and pharmacologically potential alkaloids is attractive for biochemists, synthetic biologists, metabolic engineers, and plant biologists. During our study, we developed the *in vitro* culture of *Crinum*. x *powellii "Album"* which is well known for producing antiviral AAs such as cherylline and lycorine. To understand the effect of growth factors on the *in-vitro* of *C.* x *powellii* "Album", we culture *C.* x *powellii* "Album" on the light and dark conditions with the exogenous supply of NAA and 2,4-D at three different concentrations (2 mg/L, 4 mg/L, and 8 mg/L). Our results demonstrate that the combination of auxin and light significantly influences *in vitro* tissue growth, survival, and morphogenesis compared to individual treatments. Furthermore, the combination of auxin and light also upregulates the expression of genes encoding enzymes involved in alkaloid biosynthesis. It leads to an increase in the content of certain alkaloids, suggesting a positive impact on the defense potential of the callus. Our findings provide insights into the regulation of genes encoding proteins involved in alkaloid biosynthesis in *C.* x *powellii* "Album" callus and underline the potential of auxin and light as tools for enhancing their production in medicinal plants. This study provides a foundation for further exploration of *C.* x *powellii* "Album" callus as a sustainable source of bioactive compounds for pharmaceutical and agricultural applications. Furthermore, this study paves the way for the discovery of the biosynthetic pathway of SM from *C.* x *powellii* "Album", such as cherylline and lycorine. To develop deep knowledge regarding the biosynthesis of AAs at the enzyme level we characterized norbelladine *O*-methyltransferase from *N. papyraceus.* Unlike previously reported enzymes, *N. papyraceus* norbelladine *O*-methyltransferase catalyzed the regioselective methylation of norbelladine together with non-regioselective methylation of 3,4-dihydroxybenzylaldehyde and

caffeic acid. Moreover, *O*-methyltransferase can produce 3ˈ,4ˈ-dimethylnorbelladine from norbelladine *in vitro* assay. In depth molecular docking and molecular dynamic study suggest that *Np*OMT more favoured the formation of 4ˈ-*O*-methylnorbelladine in physiological conditions which is supported by *in vivo* enzymatic assay in *Nicotiana benthamiana*. Our study reveals the novel catalytic potential of *O*-methyltransferase, which can be utilized to develop knowledge regarding the regiospecificity and substrate promiscuity of such *O*-methyltransferase. In a nutshell, our research provides a comprehensive understanding and tools to support the development for the sustainable production of AAs by using biotechnological approaches.

Keywords: Specialized metabolites, *In vitro* culture, stress, transcriptomic study, norbelladine-*O*-methyltransferase, promiscuous, regioselective

Contents

List of figures

List of Tables

List of abbreviations

2,4-D	2,4-Dicholophenoxyacetic acid
4CL	4-hydroxyphenylacetyldehyde
4HPAA	4-hydroxyphenylpuruvate decarboxylase
AAs	Amaryllidaceae alkaloids
AAOMT	Amaryllidaceae alkaloids *O*-methyltransferase
BLAST	Basic local alignment search tool
BSA	Bovine serum albumin
BUSCO	Benchmarking Universal Single-Copy Orthologs
CatOMT	Catechol *O*-methyltransferase
CCoAOMT	Caffeoyl CoA *O*-methyltransferase
COMT	Caffeic acid *O*-methyltransferase
CYP	Cytochrome P450
C3H	*p*-coumarate hydroxylase
C4H	*Trans*-cinnamate hydroxylase
DAPI	4′,6-diamidino-2-phenylindole
DMSO	Dimethyl sulfoxide
GAM-HRP	Goat anti-mouse-horse radish peroxidase
*Ge*OMT	*Galanthus elwesii* O-methyltransferase
HBS	Hydroxybenzaldehyde synthase
HCT	Hydroxycinnamoyl transferase
IPTG	Isopropyl β-D-thiogalactopyranoside
*La*OMT	*Lycoris radiata O*-methyltransferase
LB	Luria Bertani
LC-MS/MS	Liquid chromatography with tandem mass spectrometry
*Lr*OMT	*Lycoris radiata O*-methyltransferase
MRM	Multiple reaction monitoring
N4OMT	Norbelladine 4' *O*-methyltransferase
NAA	1-Naphthaleneacetic acid

NBS	Norbelladine synthase
NGS	Next-generation sequencing
NMR	Nuclear magnetic resonance
*Np*OMT	*Narcissus papyraceus O*-methyltransferase
*Np*N4OMT	*Narcissus* sp. aff *pseudonarcissus O*-methyltransferase
NorRed	Noroxomaritidine reductase
OMT	*O*-methyltransferase
ORF	Open reading frame
PAL	Phenylalanine ammonium lyase
PCR	Polymerase chain reaction
PVDF	Polyvinylidene difluoride
RIN	RNA Integrity number
RT-qPCR	Quantitative reverse transcription polymerase chain reaction
SAM	*S*-adenosyl methionine
SDS-PAGE	Sodium dodecyl sulfate-polyacrylamide gel electrophoresis
SM	Specialized metabolites
TBST	Tris-buffered saline (TBS) containing Tween 20
TYDC	Tyrosine decarboxylase
V11H	Vittatine 11-hydroxylase
*Vp*OMT	*Vanilla panifolia O*-methyltransferase

Chapter I[1]

1. General Introduction

1.1 Specialized metabolites

Plants evolutive adaptation to harsh environmental conditions is considered one of the most significant developments in Earth's history (Kenrick and Crane 1997). During this process, plants have developed a plethora of chemical depositories by using complex metabolic networks to protect themselves from coevolving living organisms (Jacobowitz and Weng 2020). Chemical compounds that plants synthesized explicitly for interactions with their surrounding environment and to protect themselves from predators are known as plant specialized metabolites (SM) (Hagel and Facchini 2013). Although the physiological role of many SM is not clear, they have a tremendous biological role in plants ability to colonize almost all types of habitats on the earth. Generally, SM are not involved in development and reproduction (Krug and Proksch 1993, Kenrick and Crane 1997), but may provide defense or support adaptation to stresses. Moreover, they have a wide range of beneficial applications for humans, such as dyes and food flavorings, nutraceuticals, pharmaceuticals, natural preservatives, and chemical adjuvants (Facchini, Bohlmann et al. 2012, Koirala, Karimzadegan et al. 2022). As such, there is a considerable interest in producing them in large quantities and in sufficiently pure form (Kallscheuer, Classen et al. 2019).

From the beginning of human civilization, people used plant-based materials to combat diseases in the form traditional medicine, and later, they became a vital part of modern medicine (De Smet 1997, Tu 2016). For instance, parts of snowdrops (*Galanthus woronowii,* Amaryllidaceae) are used in Russia and Europe as a traditional medicine to ease migraines and headaches. Later, galanthamine was extracted from snowdrops, shown to possess anti-cholinesterase activity, and approved for the treatment of early symptoms of Alzheimer's disease (Howes and Perry 2011).

---

1 Introduction of this thesis was adapted from our published review article "Biotechnological approaches to optimize the production of Amaryllidaceae alkaloids. *Biomolecules*, Koirala *et. al* 2022

The development of modern science and technology has revealed that the plant's medicinal properties are indeed related to their phytochemical content. SM are derived from the primary metabolites and are broadly classified into different groups, such as phenylpropanoids, terpenoids, peptides, and alkaloids. A brief classification of specialized metabolites is shown in Figure 1.1 (Jacobowitz and Weng 2020).

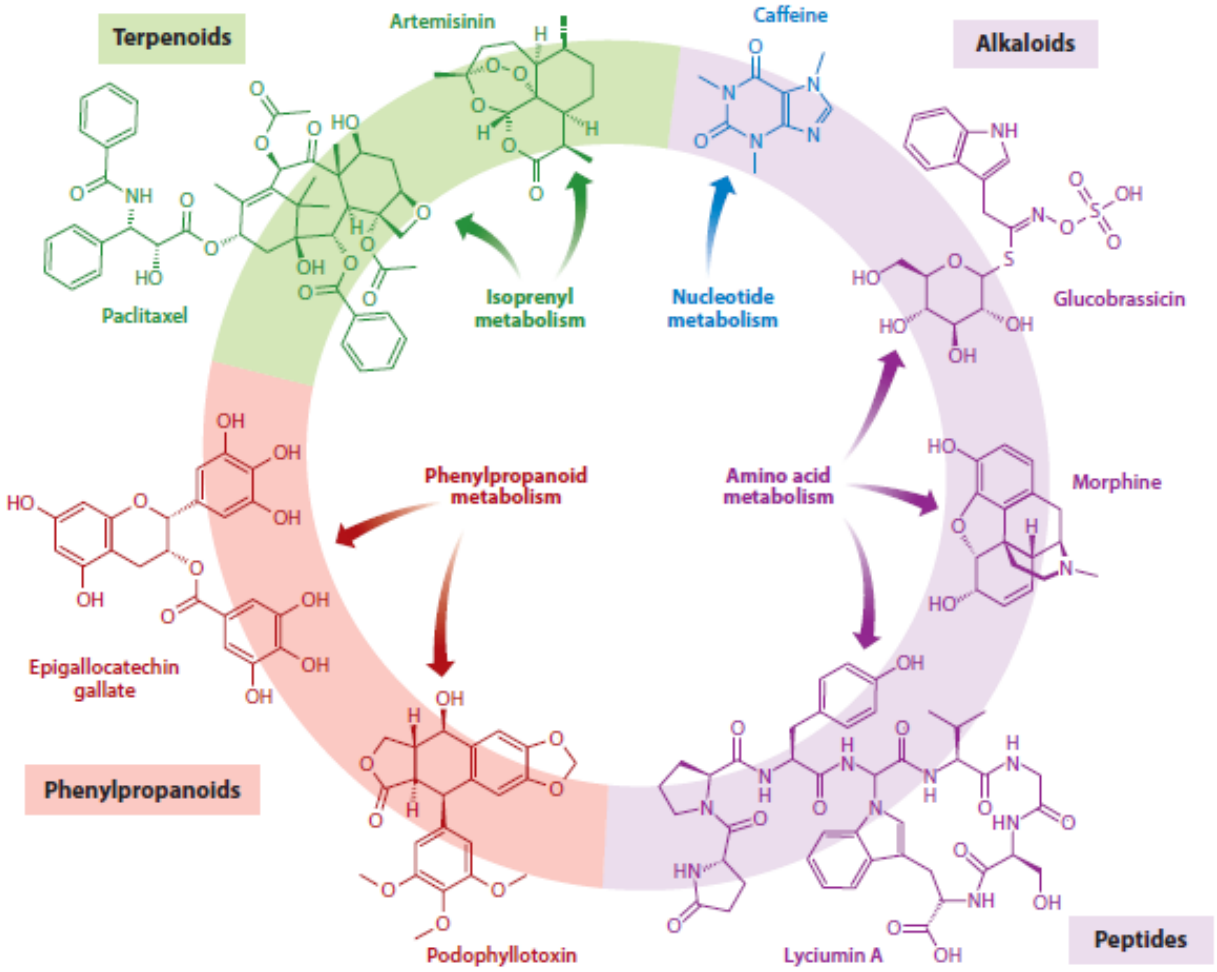

Figure 1.1 Classification of plant specialized metabolites. Plant specialized metabolites are classified into phenylpropanoids, alkaloids, terpenoids, and peptides. Specialized metabolites are derived from primary metabolites: phenylpropanoids metabolism, amino acid metabolism, nucleotide metabolism, and isoprenyl metabolism. (Jacobowitz and Weng 2020).

Plants accumulate a bewildering array of SM, estimated to be anywhere from 200 000 to 1 million structurally diverse chemical compounds in all plant species (Facchini, Bohlmann et al. 2012, Wang, Alseekh et al. 2019). Alkaloids are important class of SM and are known for their therapeutic potential (Cordell, Quinn-Beattie et al. 2001, Kurek 2019). Alkaloids are nitrogen-containing SM, reported from bacteria and fungi, but are more specially produced by higher plants (Evans 2009). Nitrogen atom in alkaloids molecules make them often alkaline (basic) in nature, allowing them to exit as water-soluble salt of organic acid in plant tissue (Dostál 2000). Although alkaloid structure is diverse, the presence of a nitrogen atom in the form of a primary amine (RNH_2), a secondary amine (R_2NH), or a tertiary amine (R_3N) (Cushnie, Cushnie et al. 2014) is considered as unifying feature. Based on their biosynthetic route (derived from amino acid or not), alkaloids are classified as true-, proto-, or pseudoalkaloid. Pseudoalkaloids feature a basic carbon skeleton not derived from an amino acid. True- and proto-alkaloids have an amino acid as a precursor, but they differ in the presence or absence of the N-atom in the heterocycle ring, respectively (Casciaro, Mangiardi et al. 2020). As heterocyclic alkaloids possess diverse and complex ring structures, they are further classified into 14 different classes such as pyrrole, pyrrolidines, imidazoles, piperidines, pyridine, indole, purine, indolizidine, pyrrolizidine, isoquinoline, quinolone, quinolizidines, tropanes, and aporphine (Othman, Sleiman et al. 2019). The cores of ring structures of heterocyclic alkaloids are shown in Figure 1.2.

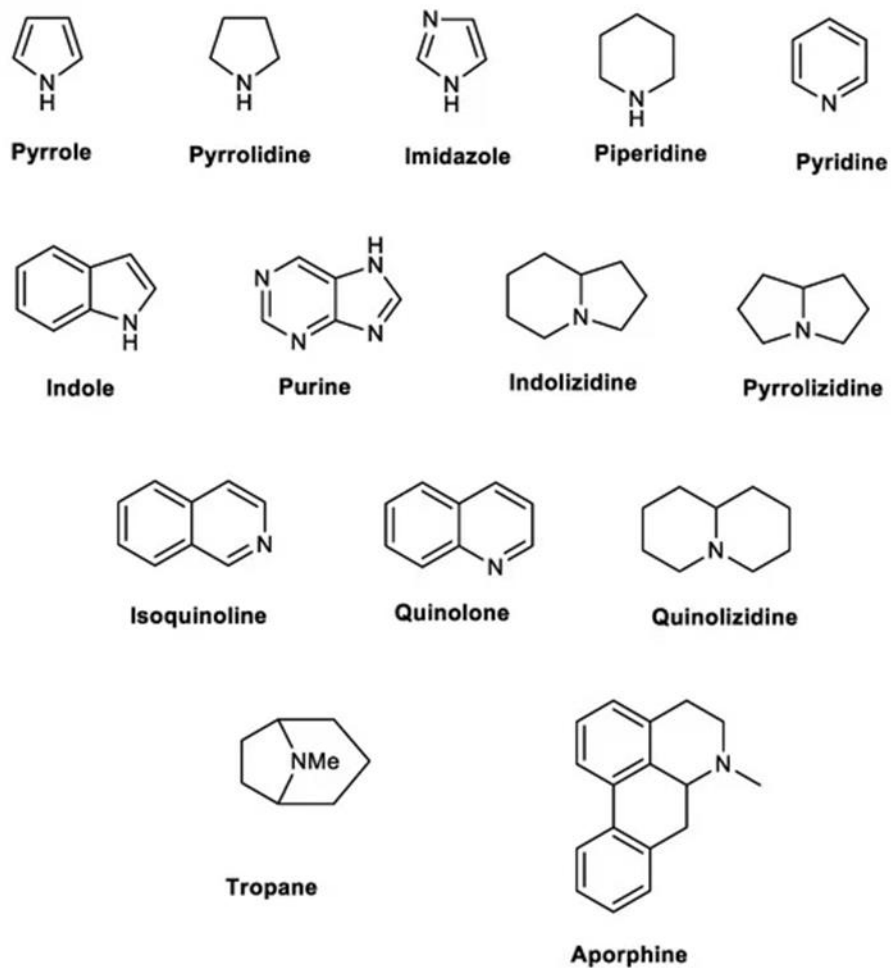

Figure 1.2 Sub-groups of heterocyclic alkaloids. (Casciaro, Mangiardi et al. 2020)

1.2 Amaryllidaceae alkaloids and their biological activities

Alkaloids were reported in almost 20 % of plants (Facchini and De Luca 2008). Plant families such as Amaryllidaceae, Annonaceae, Apocynaceae, Papaveraceae, Asteraceae, Solanaceae, Rutaceae, Fabaceae, Rubiaceae, Berberidaceae, Boraginaceae, Goetaceae, and Ranunculaceae are well known for alkaloid synthesis (Cordell, Quinn-Beattie et al. 2001).

Amaryllidaceae plants are herbaceous perennial plant that belongs to the order Asparagales, and this family was further divided into three sub-families *i.e.,* Amaryllidoideae, Agapanthoideae, and Allioideae (Chase, Reveal et al. 2009, Group, Chase et al. 2016). This plant family consists of 75 genera and 1600 species, which are mostly distributed from subtropical to tropical habitats

(Desgagné-Penix 2021). Many species of Amaryllidaceae plants were domesticated for their big, beautiful flowers and are mostly geophytes (Berkov, Osorio et al. 2020). They have been used in traditional medicine for a long time (Fennell and Van Staden 2001). For example, in southern Nigeria, medicine produced from bulbs of *Crinum jagus* is traditionally recommended for memory loss and mental illnesses (Houghton, Agbedahunsi et al. 2004, Idu, Obaruyi et al. 2008). The medicinal properties of these Amaryllidaceae plants are due to their phytochemical content, especially alkaloids (Ding, Qu et al. 2017). Alkaloids which are exclusively synthesize by Amaryllidaceae plant family are known as Amaryllidaceae alkaloids (AAs). These alkaloids are belonging to isoquinoline types of alkaloids (Desgagné-Penix 2021). Within the Amaryllidaceae family, AAs are the chemotaxonomic features of Amaryllidoideae sub-families (Berkov, Osorio et al. 2020). Since the isolation of lycorine from *Narcissus pseudonarcissus*, more than 650 AAs have been reported from Amaryllidaceae (Ka, Koirala et al. 2020). Despite having a wide range of structural variations, these AAs can be grouped into different types based on their chemical properties, such as their molecular skeleton and ring structure (Kornienko and Evidente 2008, He, Qu et al. 2015, Jin and Yao 2019). Ka *et al*., 2020 classified AAs into 9 types based on their biosynthetic origin. A 10^{th} type includes AAs whose biosynthetic route is unclear (Table 1.1 and Figure 1.3)(Ka, Koirala et al. 2020).

Table 1.1: Different types of Amaryllidaceae alkaloids. Categorised was done based on their biogenetic route and core ring structure (Ka et al., 2020).

Number	Type Name	Ring-Type
I	Norbelladine	N-(3,4-Dioxybenzyl)-4-oxyphenethylamine
II	Cherylline	Tetrahydroisoquinolineoxy phenethylamine
III	Galanthamine	6H-Benzof-2-benzazepine
IV	Lycorine	Pyrrolo[d,e]phenanthridine
V	Homolycorine	2-Benzopyrano-[3,4-g]indole
VI	Crinine	5,10b-Ethanophenanthridine
VII	Narciclasine	Lycoridine
VIII	Pretazettine	2-Benzopyrano[3,4-c]indole
IX	Montanine	5,11-Methanomorphanthridine
X	Other	Different ring types and biogenetic origin

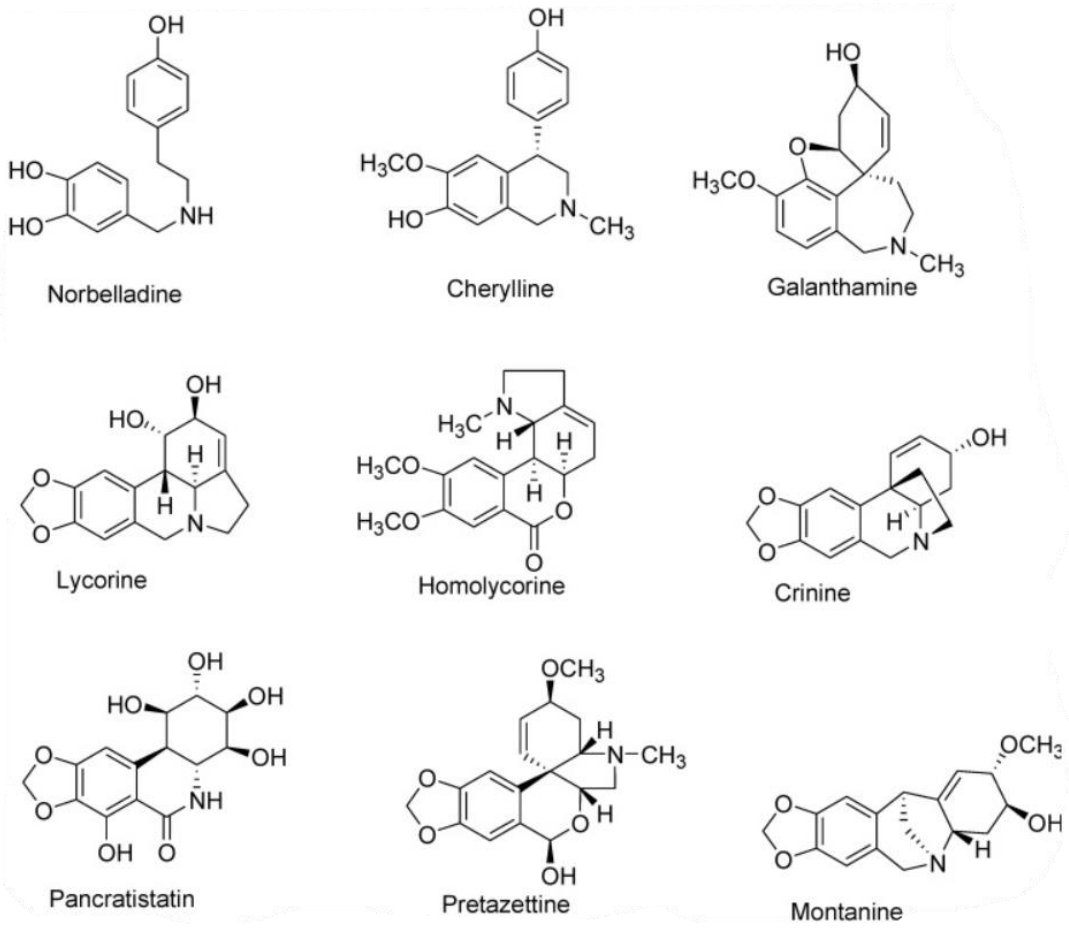

Figure 1.3: Representative structure of different Amaryllidaceae alkaloids types (Ka, Koirala et al. 2020)

Although the ecophysiologcial role of many AAs is unknown, plants produce AAs to protect themselves from pathogens and herbivores, for example, galanthamine possesses cholinergic effect to insects and can act like insecticides (Houghton, Ren et al. 2006). AAs are also well known for their bioactivities, such as antifungal antitumor, antiviral, antibacterial, antimalarial, and analgesic. As mentioned above, galanthamine, an AAs with acetylcholinesterase (AChE) inhibitory activity, is used to treat early symptoms of Alzheimer's disease (He, Qu et al. 2015, Desgagné-Penix 2021). Lycorine and its derivatives are a major type of AAs that exhibits antiproliferative activity against multidrug resistant and apoptosis-resistant cancers cells at micromolar concentration when investigated with preclinical model of human cancer cell *in vitro* and *in vivo*. The strong relationship between lycorine's lipophilicity and anticancer activities makes it an a ideal candidate

for designing new anticancer therapeutics (Dasari, Banuls et al. 2014). Cytotoxic properties of AAs that belong to crinine types such as haemanthamine and haemanthidine have been well studied. AAs derived from haemanthidine, *i.e. N*-methylhaemanthidine possesses increased cytotoxicity against pancreatic cancer cells by inhibiting AKT signaling pathway (Cahlíková, Kawano et al. 2021). Montanine type AAs were found to have anti-microbial activity against *Staphyloccocus aureus* and *Pseudomonas aeruginosa* (Maafi 2023). A study on the crude extract of *C. jagus* showed its antiviral properties. Further study on specific AAs from *C. jagus, i.e.* cherylline, showed it can efficiently inhibit dengue virus (DENV) and Zika virus (ZIKV) replication with EC_{50} of 8.8 μM and 20.3 μM, respectively (Ka, Merindol et al. 2021).

1.3 Factors affecting the biosynthesis Amaryllidaceae alkaloids in *planta*

Although the biosynthesis of AAs from endophytic soil microorganisms associated with Amaryllidaceae plants was reported, the plant is considered to be the major source of AAs (Berkov, Osorio et al. 2020, Ptak, Morańska et al. 2022). Still, the accumulation of AAs is very low *in planta*. For example, 1 kg of galanthamine is extracted from about one ton of bulbs of *Leucojum aestivum*, with galanthamine levels of 0.1 – 0.2% dry weight (Diop, Hehn et al. 2007). Also, some AAs are rare and often associated with specific genera within the Amaryllidaceae plant family. One example is the cherylline-type, which is mostly extracted from *Crinum* genus, and represents 0.004% of alkali-solution extracted from *Crinum* plant (Brossi, Grethe et al. 1970). A study done with *N. papyraceus* and *N. tazetta* shows the ontogenic variation of AAs profile. AAs profiling of different organs showed remarkable differences in their alkaloid pattern, the main alkaloid detected, and their number. Lycorine-type dominated in *N. papyraceus*, while narciclasine-, galanthamine- and homolycorine-types were found in *N. tazetta* (Shawky, Abou-Donia et al. 2015). Besides the plant genotypes, AAs content fluctuates during plant life cycle. In *N. papyraceus*, AAs alkaloid content and expression of AAs biosynthetic gene vary during the six development stages (*i.e.*, unplanted bulbs, emergence with presence of young leaves, presence of stems with unopened flower buds, blossoming with emergence of immature flowers, flowering with mature flowers and senescence with wilting flowers) (Hotchandani, de Villers et al. 2019).

AAs accumulation is not only affected by endogenous factors but also by external biotic and abiotic environment factors. Often plants respond to adverse environmental conditions by triggering SM biosynthesis. A study on *L. aestivum*, *Narcissus* sp., and *Crinum* sp. shows that their alkaloid

profiles vary with seasonal changes (Elgorashi, Drewes et al. 2003, Lubbe, Gude et al. 2013, Demir, Yildirim et al. 2022). Higher seasonal temperature favors the accumulation of AAs in bulbs, whereas lower seasonal temperature supports their accumulation in leaves. Furthermore, soil neutral to alkaline pH and organic matter content enhances AAs accumulation in *L. aestivum* (Demir, Yildirim et al. 2022).

The extended chemical library of AAs increases the pharmacological interests of Amaryllidaceae as a potential source for novel drug discovery. However, variations in AAs profile between Amaryllidaceae species, differences in site of accumulation, fluctuation with seasonal changes, and various environmental factors make sustainable production of AAs from plants a challenging task.

1.4 Alternative approaches for Amaryllidaceae alkaloids production

According to Bright focus foundation (https://www.brightfocus.org/alzheimers/article/alzheimers-disease-facts-figures) in 2022, over 55 million people are living with Alzheimer's disease or other kind of dementia worldwide, among them over 60% people live in low- or middle-income countries. Yet, galanthamine accumulated at traceable quantity in native plant, which restricts the supply chain of this drug, and eventually increases the market price. Extensive demand requires a huge amount of plant as raw materials, and over-harvesting makes them as endangered species, such as *L. aestivum* categorized as such and listed in the Red Data Book of Bulgaria (Kathe, Honnef et al. 2003). Moreover, extraction and purification of targeted SM from native plant requires extensive effort and can be time consuming because plants accumulate similar class of SM which demand for precise extraction and separation of target compound (Brusotti, Cesari et al. 2014). Therefore, native plant is not sufficient to fulfil the growing demand of AAs.

There have been several attempts to produce AAs by chemical synthesis. Reports show on the successful chemical synthesis of AAs such as norbelladine, galanthamine, lycorine, cherylline, montanine, crinine, plicamine tazettine, phenanthridone, phenanthridine, tazettine, mesembrine and gracilamine (Banwell, Edwards et al. 2001, Lebrun, Couture et al. 2003, Marco-Contelles, Rodríguez et al. 2005, Girard, Karimzadegan et al. 2022, Miller, McLean et al. 2022). Synthesis of AAs involves multiple reaction steps leading to a low overall yield, and often a mixture of enantiomers (Lebrun, Couture et al. 2003, Marco-Contelles, Rodríguez et al. 2005, Shin, Jung et al. 2014, Manolov, Atanasova et al. 2015, Miller, McLean et al. 2022). This is problematic as pharmacological potential of molecules depends on their complex chemical structure, including

their regiospecific functionalization and chirality (Nonn, Binder et al. 2020). Consequently, it is often challenging to chemically synthesize AAs having highly oxygenated cyclic system with multiple chiral centers, and not cost-effective, nor ecological.

As an alternative, biotechnological strategies offer many advantages to produce plant SM (Diop, Hehn et al. 2007, Pavlov, Berkov et al. 2007, Laurain-Mattar and Ptak 2018). This includes *in vitro* culture of plant, *i.e*., cultivation of plant or plant parts in sterile controlled condition, or metabolic engineering of heterologous hosts such as *E. coli*, yeast, or *N. benthamiana* with AAs pathway genes**.** However, the biosynthesis route of most AAs is still not clear, this knowledge is essential to engineer host organism. Together with the production of AAs, *in vitro* culture can be utilized to generate samples for transcriptomic-level studies on alkaloid-producing and non-producing tissue and elucidate biosynthetic pathways (Gallego, Rojas et al. 2018). *In vitro* culture can serve as a platform to generated deeper genetic level understanding of SM biosynthesis, a step toward more advanced genetic engineering approach.

1.4.1 Amaryllidaceae alkaloid from *in vitro* culture

Production of plant SM through *in vitro* tissue culture is a well-established strategy. Harvesting of anti-inflammatory and anti-bacterial naphtoquinone shikonin from *Lithospermum erythrorhizon*, bioactive berberine from *Coptis japonica* cultures, chemotherapy drug paclitaxel from *Taxus baccata*, sanguinarine from *Papaver somniferum* cells and antioxidant saponins from *Panax ginseng* cells, are few examples of commercially available therapeutics that have been produced using *in vitro* cultures (Sato and Yamada 1984, Shimomura, Sudo et al. 1991, Bourgaud, Gravot et al. 2001, Parc, Canaguier et al. 2002). The common strategy to synthesize plant SM from *in vitro* culture is summarized in figure 1.4. Organ- and genotype-specific accumulation of SM were reported from Amaryllidaceae plant species (Hotchandani, de Villers et al. 2019, Demir, Yildirim et al. 2022). During *in vitro* culture system, it is possible to manipulate growth parameters, which is a challenging task in nature, and gives researchers the chance to study how various parameters affect the synthesis of targeted SM (Carbone, Preuss et al. 2009). Precise selection of plant genotypes, culture conditions and optimal composition of growth media can enhance our ability to develop specialized plant tissue, and higher production of targeted SM.

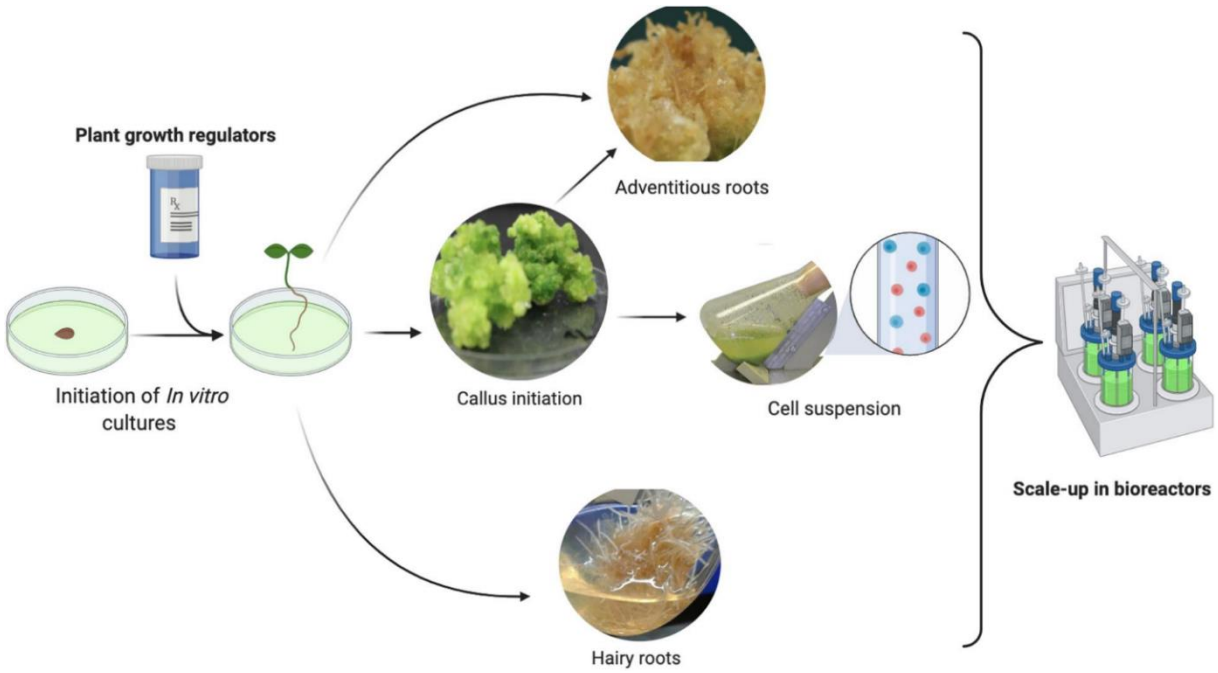

Figure 1.4 Pictorial representation of the *in vitro* culture strategy. Figure shows various *in vitro* cultures generated through plant biotechnology methods and their potential for the commercial scale production of phytomedicines (Khan et al., 2021).

The specific interest on Amaryllidaceae *in vitro* cultures as a mean to produce alkaloids was first reported in 1963 by Fales *et al.* (Mann and Mudd 1963) and has been since intensively and continuously studied. Micropropagation, a technique that enables rapid vegetative clonal multiplication of plants from limited or small size explants, has been applied in Amaryllidaceae species such as *Rhodophiala pratensis*, *Lapiedra martinezii*, *Eucrosia stricklandii*, and *Lycoris sprengeri* leading to plant development with similar morphometric traits (Colque, Viladomat et al. 2002, Santos, Fidalgo et al. 2002, Juan-Vicedo, Pavlov et al. 2019, Trujillo-Chacon, Pastene-Navarrete et al. 2020, Ren, Lin et al. 2021). Other cultivation methods of plant material *in vitro* (bulblets, seedlings, plantlets, shoots, roots, shoot-clump, callus) also provide an interesting opportunity to produce AAs, being effective for both conservation, long term growth and industrial purposes (Table 1.2).

Table 1.2: Yields of AAs of therapeutical interest from *in vitro* cultures. (Koirala, Karimzadegan et al. 2022)

Target metabolites	Species	Tissue type	Maximum yield	Ref
Cherylline	*Crinum moorei*	Bulblets	6.9 mg/100 g DW	(Fennell, Elgorashi et al. 2003)
Haemanthamine	*Rhodophiala pratensis*	Callus	6.9 µg/mg Ext	(Trujillo-Chacón, Pastene-Navarrete et al. 2020)
	Narcissus cv. Hawera	Plants	25.5 µg/100 mg Ext	(Berkov, Georgieva et al. 2021)
Powelline	*Crinum moorei*	Bulblets	46.84 mg/100 g DW	(Fennell, Elgorashi et al. 2003)
Tazettine	*Rhodophiala pratensis*	Callus	2.68 µg/mg Ext	(Trujillo-Chacón, Pastene-Navarrete et al. 2020)
	Narcissus confusus	Shoot-clump culture	0.043 % DW	(Sellés, Bergoñón et al. 1997)
Mesembrenone	*Narcissus pallidulus*	Plants	337.6 µg/100 mg Ext	(Berkov, Georgieva et al. 2021)
	N. cv. Hawera	Plants	214.8 µg/100 mg Ext	(Berkov, Georgieva et al. 2021)

DW = Dry weight, Ext: Extract.

Callus induction is defined as the growth of undifferentiated tissues from any plant parts. Because different plant parts accumulate different types and amounts of alkaloids, the obtained type of callus may be related to the type of tissue used as a starting material (Hotchandani, de Villers et al. 2019). Undifferentiated tissues do not always yield to high amounts of alkaloids, especially without elicitation (Tarakemeh, Azizi et al. 2019, Ferdausi, Chang et al. 2020) (Table 1.3). Still callus culture can be beneficial because such tissue can be maintained for a long duration, and used as a gateway for micropropagation, plant cell suspension cultures, or other *in vitro* systems to produce alkaloids (Ferdausi, Chang et al. 2020).

Table 1.3 Enhancement of Amaryllidaceae alkaloids in *in vitro* cultures with elicitor treatment (Koirala, Karimzadegan et al. 2022).

Species	Culture condition (tissue type)	Amaryllidaceae alkaloid	Yield and type of condition	Elicitor and yield	Ref
Narcissus confusus	Liquid-shaked culture (shoot clumps)	Galanthamine	ut. 2-2.5 mg / culture	MeJa (3.8 X)	(Colque, Viladomat et al. 2004)
N. pseudonarcissus cv. Carlton	Callus	Galanthamine	ut. 7.88 µg/g FW	MeJa (5.6 X) Chitosan (3 X)	(Ferdausi, Chang et al. 2021)
Lycoris longituba	Liquid medium	Galanthamine	ut. n.a.	MeJa (2.71 X)	(Li, Xu et al. 2021)
	(seedling)	Lycorine	ut. n.a.	MeJa (2.01 X)	
		Lycoramine	ut.n.a.	MeJa (2.85 X)	
	Seedling (culture in tray)	Galanthamine	white light n.a.	Blue light (2.45X)	(Li, Xu et al. 2021)
		Lycorine	white light n.a.	Blue light (1.74 X)	
		Lycoramine	white light n.a.	Blue light (1.92 X)	
Lycoris chinensis	seedling	Galanthamine	ut. n.a.	MeJa (1.49 X) YE (1.62 X) SNP (1.72 X)	(Mu, Wang et al. 2009)
		Lycorine	ut. n.a.	MeJA (1.37 X) YE (1.38 X)	
L. aestivum	*In vitro* plants	Galanthamine	ut. n.a.	Melatonin (58.6X)	(Ptak, Simlat et al. 2019)
		Lycorine	ut. n.a.	Melatonin (1.5 X)	
	Liquid shoot culture	Galanthamine	ut. n.a.	JA (1.36 X)	(Ivanov, Georgiev et al. 2013)
		Lycorine	ut. n.a.	JA (1.40-1.67 X) MeJa (1.3 X)	

		Norgalanthamine	ut. n.a.	JA (2X) MeJa (2X)	
	temporary immersion system (bulblets, leaves)	Galanthamine	ut. 372.2-1719.6 µg/g DW	MeJa (468.6-2202.5 µg/g DW)	(Schumann, Torras-Claveria et al. 2013)
L. aestivum L.	RITA Bioreactor	Galanthamine	ut. n.a.	MeJa (0.1 mg /g DW) ACC (0.10 mg/ g DW)	(Ptak, Morańska et al. 2017)
		Lycorine	ut. 0.2-0.25 mg /g DW	MeJa (0.6 mg /g DW) SA (1 mg /g DW) Ethephon (0.46 mg /g DW)	
L. aestivum Gravety Giant	RITA Bioreactor	Galanthamine	ut. 0.08-0.1 mg/g DW	MeJa (0.4 mg/g 5X DW) SA (8x) ACC (0.60 mg/g)	(Ptak, Morańska et al. 2017)
		Lycorine	ut. 0.15 -0.62 mg/g DW	MeJa (1.15 mg/g DW 1.85X) SA (5X) ACC (0.54mg/g DW, 3.6X)	

Abbreviation; n.a.: not available; ut: untreated, basal condition, MeJa: methy jasmonate, JA : ,jasmonic acid SA: salicylic acid, ACC: 1-aminocyclopropane-1-carboxylic acid, FW: Fresh weight, DW : Dry weight, X: fold change, YE, SNP. Ref: reference

In addition to proper selection of tissue and of *in vitro* propagation technique, many other factors affect the growth and the efficiency of alkaloid production understanding and managing both growth conditions and stress is required to increase biomass production with higher yields of SM (Gupta, Sengupta et al. 2016, Espinosa-Leal, Mora-Vásquez et al. 2022). Remarkably, many growth parameters can be monitored and optimized using *in vitro* methods. Amaryllidaceae plants

grow differently under distinctive artificial conditions. The focus of most of the current research is the production of galanthamine, while there is also abundant data on lycorine. Table 1.2 and Table 1.3 illustrate production of AAs and the impact of different conditions of elicitation on AAs production in *in vitro* systems. Bergoñón *et al* achieved a total production of 2.50 mg of galanthamine per culture by cultivating shoot-clumps in shaking-liquid media. This is the highest amount of galanthamine produced *in vitro* ever reported (Bergoñón, Codina et al. 1996). *In vitro* biosynthesis of less common AAs such as cherylline, tazettine, haemanthamine, mesembrenone were reported in various studies of *in vitro* propagation of Amaryllidaceae species and are summarized in Table 1.2. Both physical and chemical parameters can be manipulated during *in vitro* culture and influence the growth and development of plants, and alkaloid accumulation.

1.4.1.1 Physical parameters

Different cultivation methods such as solid media culture, shaken-flask submerged condition, and temporary immersion or fully-submersive techniques in RITA® bioreactor have been applied in Amaryllidaceae plants (Table 1.2 and 1.3) (Bergoñón, Codina et al. 1996, Colque, Viladomat et al. 2002, Ivanov, Georgiev et al. 2011). Berkov *et al.* 2009 grew *L. aestivum* shoot culture in shaken-flasks following induction from callus and monitored their growth-index. The maximum biomass was obtained at day 35 and AAs biosynthesis intensified at late exponential to early stationary growth phase (Berkov, Pavlov et al. 2009). In the following study, to optimize production of target metabolites (mostly galanthamine), *L. aestivum* shoots were cultivated in temporary immersion RITA system with a higher growth index (*i.e.* 2.98) compared to shaken-flasks culture. The main advantage of the temporary immersion system is that cultivated shoots increased significantly, then shoot generated from meristematic cell (Ivanov, Georgiev et al. 2011). The system was further improved for *L. aestivum* shoot culture using advanced modified gas column bioreactor with a 1.7 mg/L maximum production of galanthamine (Georgiev, Ivanov et al. 2012). *L. aestivum* shoot cultures show balanced growth at all tested regimens in modified gas column bioreactor. Similar techniques using twin scale explant from bulbs as starting materials have shown that *N. confusus* shoot-clump culture in liquid media lead to an efficient micropropagation of plant tissue to produce galanthamine (2.50 mg per culture in day long photoperiod) (Bergoñón, Codina et al. 1996).

In addition to culture system, temperature is one of the key factors that modulates growth and alkaloid production in Amaryllidaceae. Some studies have shown that the maximum yield of

galanthamine was achieved at 26°C (range 18°C-30°C), whereas the best combination of highest amount of dry mass (20.8 g/L) and galanthamine content (1.7 g/L) was achieved at 22°C when shoot culture were grown under 18 L/(L·h) flow rate of inlet air (Ivanov, Georgiev et al. 2011, Georgiev, Ivanov et al. 2012, Ivanov, Georgiev et al. 2012). Ivanov, I. *et al* 2012 obtained 18 different AAs from shoot culture of *L. aestivum* and reported that lower temperature (18℃) favoured the production of galanthamine, while inhibiting the production of other lycorine- and haemanthamine-type of alkaloids. Temperature possibly alters the activity of the enzymes catalyzing phenol-oxidative coupling reaction of 4'-*O*-methylnorbelladine (Ivanov, Georgiev et al. 2012).

Light can boost the production of AAs in *in vitro* culture (Bergoñón, Codina et al. 1996, Pavlov, Berkov et al. 2007, Berkov, Pavlov et al. 2009, Rahimi Khonakdari, Rezadoost et al. 2020). In shoot cultures of *N. confusus*, light affected both morphology and alkaloid content (Bergoñón, Codina et al. 1996). In *N. tazetta L*., bulblets and leaves proliferation per explant was higher in light condition (16:8h, light:dark photoperiod), as compared to a 24h dark condition. Also, regenerated bulblets contained 40 µg/g dry weight of galanthamine under exposed photoperiod compared to 20 µg/g dry weight for 24 h dark condition (Rahimi Khonakdari, Rezadoost et al. 2020). Light quality also impacts on the production of AAs. For example, it was observed that production of galanthamine (2.45 times), lycorine (1.74 times) and lycoramine (1.92 times) were increased in blue compared to white light in *in vitro* plantlets of *Lycoris longituba* (Li, Xu et al. 2021). These studies demonstrate that a complex combination of physical parameters impacts alkaloid production, and that cultivation parameters, light and temperature should be optimized in each system, and for each species.

1.4.1.2 Chemical factors

Plants require diverse types of micro- and macro-elements for their growth and development. The quantity of carbon and nitrogen in the media affects the growth and the profile of SM accumulation. The type and the concentration of carbon source play an important role in plant tissue culture. Sucrose is widely used, the effect of its concentration on *N. confuses* culture was measured following growth in liquid-shaken medium by Sellés *et al* 1997 (Sellés, Bergoñón et al. 1997). Assessing the effects of concentrations ranging between 3% - 18% of sucrose, optimal combination of growth and galanthamine production was achieved with 9% (Sellés, Bergoñón et al. 1997). Ptak

et al. 2020 demonstrated that both type of carbohydrate and concentration have important role in synthesis of AAs. Like Sellés study, they reveal that the highest amount of *L. aestivum* biomass was obtained with 9% sucrose when cultivated in RITA® bioreactor. However, they also show that alternative source of carbon can enhance the AAs, as the highest amount of galanthamine was recorded with 3% fructose (Ptak, Morańska et al. 2020).

The type and concentration of phytohormones play a key role in tissue survival and differentiation, including organogenesis and synthesis of AAs. Auxins, abscisic acid, cytokinins, ethylene, and gibberellins are commonly recognized as the five main classes of naturally occurring plant hormones. The isolated or combined effect of auxin or cytokinin on *in vitro* cultures' nutrient uptake and metabolism was demonstrated (Gaspar, Kevers et al. 1996). In 2011, Tahchy *et al* observed that an increment of auxin (2,4-dicholophenoxyacetic acid (2,4-D)) in growth media reduced the survival of *in vitro* cultured tissues of *N. pseudonarcissus, G. elwesii* and *L. aestivum*, whereas an increment of cytokinin (6-benzylaminopurine, BAP) increased survival rate (El Tahchy, Bordage et al. 2011). Phytohormone concentration and type also influence the type of tissue that will develop, which eventually affects the alkaloid profile. Development of undifferentiated calli from different varieties of *Narcissus* was induced following treatment with auxin concentrations of 25 µM of 1-napthaleneacetic acid (NAA), 50 µM of 2,4-D and picloram, whereas organogenesis only happened when treated with NAA, or using higher concentrations of picloram. AAs such as demethylmaritidine and tazettine were only detected on the differentiated tissues (Tarakemeh, Azizi et al. 2019). AAs profile of *L. aestivum* and *N. pseudonarcissus cv. Carlton* obtained from *in vitro* system revealed that differentiated cells are more suitable for production of AAs, as compared to undifferentiated cells (callus) in which alkaloid content was lower. Lower concentration of NAA favoured the tissue differentiation, while higher concentration was suitable for callus induction (Ferdausi, Chang et al. 2020). Most studies have confirmed that the amount and the type of auxin correlated with the alkaloid profile and with tissue differentiation during *in vitro* culture (Tarakemeh, Azizi et al. 2019, Ferdausi, Chang et al. 2020), although no consensus combination can be clearly defined at this point.

Although, the ecophysiological role of many plants specialized metabolites is not clear, biotic and abiotic factors or signaling agents (elicitors) can boost the production of AAs (Mu, Wang et al. 2009, Ptak, Simlat et al. 2019, Liu, Zhou et al. 2020, Zhou, Liu et al. 2020). Different types of

elicitors such as fungal elicitors, methyl jasmonate, jasmonic acid, salicylic acid, and melatonin enhance the synthesis of AAs in *in vitro* culture (Table 1.3). The induction of AAs using methyl jasmonate treatment on seedling of *Lycoris aurea* was well studied by Wang *et al.* in 2017 (Wang, Xu et al. 2017). Methyl jasmonate and jasmonic acid increase the production of AAs in *L. aestivum.* shoot cultures cultivated in submerged condition by stimulating the AAs precursor enzymes of the pathway (Ivanov, Georgiev et al. 2013). Melatonin addition (10 μM) during *in vitro* culture of *L. aestivum L.* reduced the negative effect of NaCl (*i.e.* salt stress) and enhanced the biomass production together with an increased accumulation of galanthamine and lycorine by 58.6 and 1.5 folds, respectively (Table 1.3) (Ptak, Simlat et al. 2019). In conclusion, the optimization of media components and of elicitor type in *in vitro* culture of Amaryllidaceae plant provides an alternative and sustainable platform for AAs production.

1.4.2 Gene engineering approaches

As mentioned above, production of AAs from the plant source is not always sustainable. Furthermore, in native plant similar type of SM accumulates, as these compounds are of similar nature, this makes downstream purification of target metabolite a challenging task (Xu, Bhan et al. 2013, Pyne, Narcross et al. 2019). Accumulation of AAs in *in vitro* culture is still very low and cannot fulfill the increasing demand. *In vitro* culture can however, serves as system to generate sample for genetic level study. *In vitro* cultures grown under different condition have been used to perform transcriptomic study and update the knowledge regarding biosynthetic route of plant SM (Gallego, Rojas et al. 2018). Then, bioengineered microbial with SM biosynthesis route can produce target plant specialized metabolites faster as compared to whole plant system. Production of targeted plant metabolites in heterologous hosts can reduce downstream extraction process, which eventually becomes more economically sustainable (Xu, Bhan et al. 2013). This demands a better understanding of biosynthetic pathways, biochemistry of target metabolites biosynthesis, and of heterologous host system biology (Koirala, Karimzadegan et al. 2022). Knowledge based approach for production of AAs is in its pace, our understanding of biosynthetic route and role of synthetic biological approach to produce AAs is described in the following sections.

1.4.2.1 Molecular understanding of Amaryllidaceae alkaloids biosynthesis

Even though therapeutic properties of AAs have been extensively studied, the full understanding of the biosynthetic pathway and characterization of enzymes responsible for catalyzing different biosynthetic reactions need more efforts. Combined application of early labeling studies followed by omics strategies have accelerated the discovery of AAs biosynthetic enzymes (El Tahchy, Ptak et al. 2011, Li, Xu et al. 2021). After the discovery of the biosynthetic route of different intermediates, many biosynthetic enzymes were predicted based on the nature of the biochemical reaction and by homology with enzymes involved in the alkaloid biosynthesis from other plant families. Databases generated from transcriptomic and metabolic analysis of several Amaryllidaceae species support the presence of enzyme families that catalyze the different biochemical reaction in AAs pathway (Singh and Desgagné-Penix 2017, Hotchandani, de Villers et al. 2019, Park, Yeo et al. 2019, Ferdausi, Chang et al. 2021, Li, Xu et al. 2021, Tousignant, Diaz-Garza et al. 2022).

Biosynthesis of AAs involves a series of biochemicals reaction such as bond formations, rearrangements, breakages, functional group additions and modifications to connect primary metabolism to AAs metabolism (Figure 1.5). The amino acids involved in protein synthesis also serve as precursor molecules for many SM such as flavonoids, phenylpropanoids, coumarins, lignin and alkaloids (Wink 2011). In AAs pathway, aromatic amino acid derived from seven steps shikimate acid pathway contribute for amine and aldehyde building block, *i.e.* tyramine (amine precursor) and 3,4-dihydroxybenzylaldehyde (3,4-DHBA) (aldehyde precursor) derived from $_{L}$-tyrosine and $_{L}$-phenylalanine, respectively. Biosynthesis of both precursor amino acids begins from chorismate, the final product from shikimate pathway, occurring inside the plastid (Desgagné-Penix 2021). Chorismate is transformed into prephenate by a chorismate mutase, and then to arogenate by an aminotransferase. From arogenate, under the action of arogenate dehydratase, phenylalanine is synthesized whereas the arogenate dehydrogenase catalyses tyrosine synthesis from arogenate (Desgagné-Penix 2021). Tyrosine is decarboxylated by the enzyme tyrosine decarboxylase (TYDC) to give tyramine while production of the second building block, 3,4-DHBA), is achieved from phenylpropanoid pathway by the action of enzymes such as phenylalanine ammonia-lyase (PAL), cinnamate 4-hydoxylase (C4H), *p*-coumarate 3-hydroxylase (C3H), to name but a few. TYDC was characterized from *Lycoris radiata,* a galanthamine

producing Amaryllidaceae plant (Hu, Li et al. 2021). The functional characterization of PAL and C4H from *Lycoris sp.* was reported using heterologous expression in *E.coli* (Jiang, Xia et al. 2011, Li, Li et al. 2018). All genes candidates which encode enzymes that catalyze biochemical reactions involved in the synthesis of precursor molecules of AAs as a AAs-precursor genes have been identified in (Hotchandani, de Villers et al. 2019).

Biosynthesis of AAs specifically begins with the condensation of the two precursor molecules tyramine and 3,4-DHBA to yield norbelladine. Despite having a remarkable diversity in structure and biological activity, norbelladine is considered as first common intermediate of all AAs. *Singh et al* characterized a single enzyme as catalyzing norbelladine synthesis, *i.e* norbelladine synthase (NBS). However, later other research showed that condensation of tyramine and 3,4-DHBA into norbelladine was catalysed by NBS and noroxomaritidine/norcraugsodine reductase (NR)(Kilgore, Holland et al. 2016, Majhi, Gélinas et al. 2023). Further NBS and NR are shown to be localized in the cytosol and their observed physically interaction in yeast and plant, indicates that both NR and NBS are involved in biosynthesis of norbelladine (Tousignant, Diaz-Garza et al. 2022, Majhi, Gélinas et al. 2023).

Conversion of norbelladine to it *O*-methylated form is consider as a major step in AAs pathway. *S*-adnosyl-$_L$-methionine (SAM) dependent *O*-methyltransferases (OMT) which catalyse the transfer of methyl group from methyl-donor (SAM) to free hydroxyl group of acceptor substrate are common in plants (Ibrahim, Bruneau et al. 1998). Based on the amino acid sequence alignment, substrate and size, plant OMT can be broadly classified into two groups, *i.e* class I OMT (23-27 kDa) and class II OMTs (38-43 kDa). Class I OMTs require divalent cation for methylation reaction, whereas class II OMTs are metal independent. In AAs pathway, class I OMTs involved in *O*-methylation of norbelladine were characterized. The specific synthesis of both 3ˈ-*O*- and 4ˈ-*O*-methylated AAs suggests that regio-selective methylation is important to determine the types of the end product of AAs biosynthesis route (Desgagné-Penix 2021). Early labeling studies reveal that 4ˈ-*O*-methylnorbelladine is involved in the biosynthesis of AAs such as lycorine, haemanthamine and galanthamine (El Tahchy, Ptak et al. 2011). One step deeper in the pathway, the structural feature of cherylline-type of AAs suggests the occurrence of 3ˈ-*O*-methylation during the biosynthesis of these type of AAs, although it remains to be proven. Therefore, *O*-methylated norbelladine was considered as key intermediate of AAs pathway. The characterization of

norbelladine *O*-methyltransferase (OMT) from *Narcissus sp.* aff. *pseudonarsissus* (*Np*N4OMT) by Kilgore *et al* revealed that the enzyme catalyzed the transfer of a methyl-group from SAM to alkaloid substrate at 4' -*O* position of norbelladine and of its N-methylated form (Kilgore, Augustin et al. 2014). However, later studies on homologous norbelladine OMT from *Lycoris radiata* (*Lr*OMT), *L. aurea* (*La*OMT) and *Galanthus elwesii* (*Ge*OMT) revealed that methylation can occur either in the 3'-*O* or 4'-*O* position of norbelladine, and in 3-*O* and 4-*O* position of 3,4-DHBA, or caffeic acid (precursor molecules). The kinetic study of *Lr*OMT and *La*OMT indicates that it has a higher affinity for AAs precursor molecules as substrate, compared to norbelladine. This generated alternative hypothesis for formation of methylated norbelladine *i.e* (3′- or 4′-*O*-methylnorbelladine) by condensation of methylated 3,4-DHBA (*i.e.* vanillin and isovanillin) with tyramine (Sun, Wang et al. 2018, Li, Qiao et al. 2019). However, up to now, none of the possible methylated forms of 3, 4-DHBA or caffeic acid were tested as a substrate for norbelladine synthesizing enzymes.

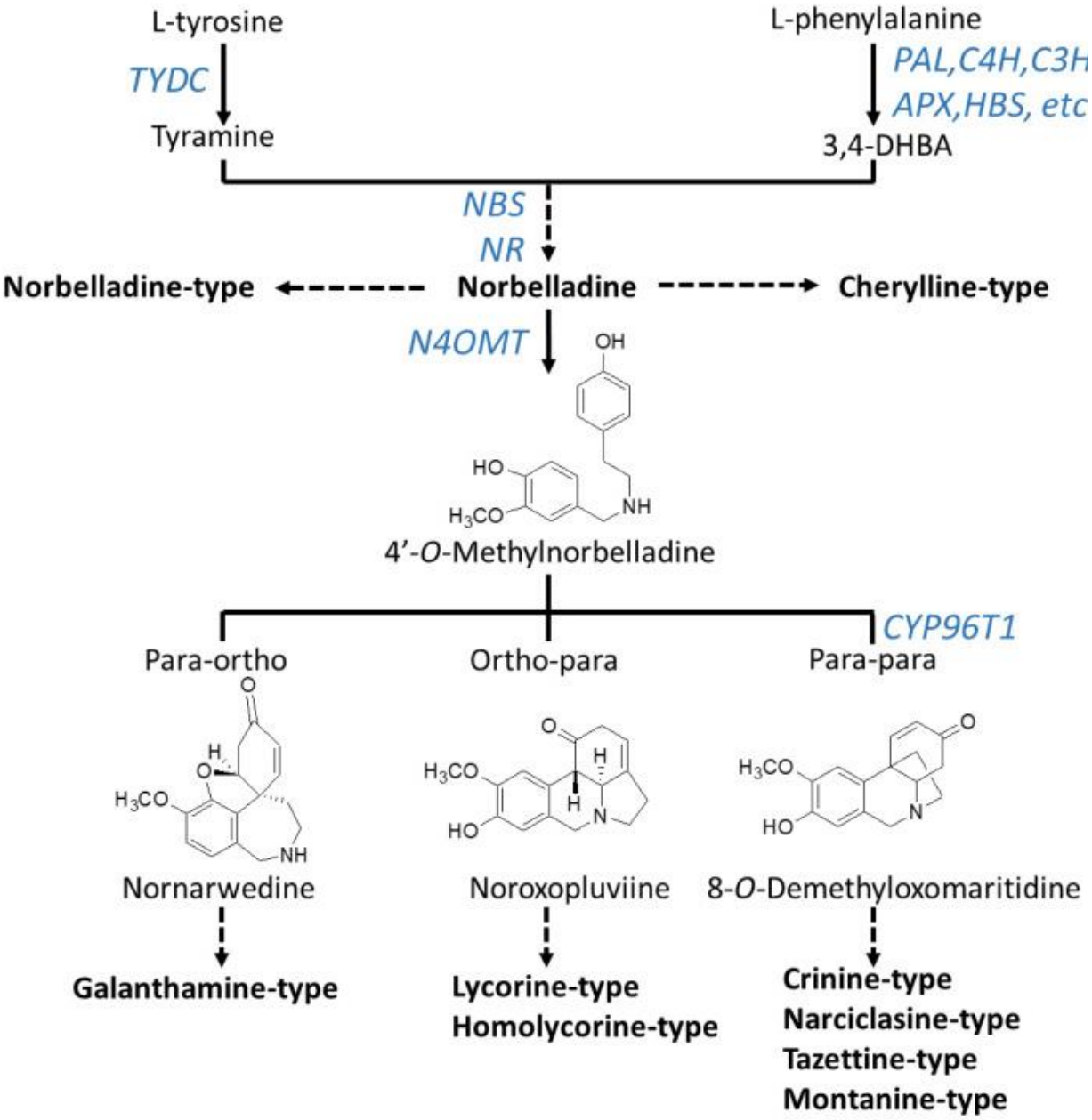

Figure 1.5 Biosynthetic routes to main types of Amaryllidaceae alkaloids. Black arrow represents one reaction whereas dotted arrow represents several reactions. Genes written in blue were functional characterized from AAs pathway (Ka, Koirala et al. 2020).

Following the formation of 4'-*O*-methylnorbelladine, its cyclization by three alternative way leads formation of different types of AAs. 4'-*O*-methylnorbelladine can be directed to 1) galanthamine-type AAs by *para-ortho'*, 2) lycorine-type AAs by *ortho-para'* and 3) crinine-type of AAs by *para-para'* phenol coupling reactions (Figure 1.5). These various phenol oxidative couplings involve the same biochemical reaction and are catalysed by the cytochrome P450 enzyme family. As an

example for this class of enzymes, a CYP96T1 that catalyse *para-para'* oxidative reaction of 4′*O*-methylnorbelladine has been characterized (Kilgore, Augustin et al. 2016). Further modifications of alkaloids intermediates generate the diverse range of AAs. Thus, plants synthesize specialized metabolites by using complex biosynthetic routes that derive from primary metabolic pathways.

AAs biosynthesis is a multifaceted process that involves different regulatory elements and gene functions. The expression of certain genes involved in plant metabolism also changes with climatic and environmental factors (Ncube, Nair et al. 2015). It also varies with developmental stage of plant (Hotchandani, de Villers et al. 2019). It remains challenging to correlate gene expression and metabolite accumulation *in planta*, as the site of metabolite synthesis may differ from the site of accumulation. For example nicotine biosynthesis occurs in root of tobacco but the alkaloid accumulates in the aerial part of the plant (Katoh, Ohki et al. 2005). For all these reasons*, in vitro* cultures have been an essential tool to decipher the alkaloid biosynthesis pathway. In 2011, Tahchy *et al* used deuterium-labeled precursors fed to *in vitro* cultures of *L. aestivum*. In this study, the authors followed the transfer of labeled precursor 4'-*O*-methyl-d_3-norbelladine from media into shoot and then its metabolization into lycorine and galanthamine. This study demonstrated that 4'-*O*-methylnorbelladine was a key intermediate AAs (El Tahchy, Ptak et al. 2011). Until now, AAs specific genes such as NBS, N4OMT, CYP96T1, and NR have been characterized and confirmed from *Leucojum sp., Narcissus sp*., *Lycoris sp.* cultures (Kilgore, Augustin et al. 2016, Kilgore, Holland et al. 2016, Majhi, Gélinas et al. 2022). However, our molecular understanding regarding the complex biosynthesis route of AAs and its regulation is still unclear. Sequence specificity implicated in enzymes regioselectivity, and with enrichment of specific AAs are not known yet. Furthermore, the pattern of relative expression of putative AAs biosynthesis genes in fields versus *in vitro* and in differentiated *versus* undifferentiated tissues of *Narcissus* development added some clear knowledge regarding their role in alkaloid biosynthesis (Aleya, Xianmin et al. 2021). A study performed on callus culture of *L. radiata* showed how different factors, such as temperature (cold treatment), osmotic pressure (PEG treatment) or elicitor treatment (methyl jasmonate) can influence *Lr*OMT (an AAs biosynthesis gene) gene expression pattern (Sun, Wang et al. 2018). *In vitro* system cultures are a powerful tool to uncover AAs biosynthesis and gene regulation that should be more thoroughly exploited.

1.4.2.2 Genetic engineering strategy for SM biosynthesis

Recent achievement in synthetic biological approaches includes the production of complex biomolecules such as noscapine (a benzylisoquinoline alkaloid from opium poppy) and its halogenated derivatives (anticancer) in *Saccharomyces cerevisiae*, assembling 30 biosynthetic enzymes from plant, bacteria and mammal and yeast itself, including seven plant endoplasmic reticulum localized genes (Li, Li et al. 2018). This success raises the hope to produce complex biomolecules such as AAs by using synthetic biological approach.

Proper selection of host organism is the starting point of synthetic biological approach. The chosen organism should be producing (or easily modified to produce) enough core metabolites such as aromatic amino acids L-phenylalanine and tyrosine, precursors needed for biosynthesis target specialized metabolite like AAs. Selection of host species will also rely on prior knowledge of their ease of engineering, established cloning tools, culture techniques, and possibility to scale up to industrial requirements. Due to rapid growth and easy handling, microbial hosts such as yeast (*Saccharomyces cerevisiae*) and to a lesser extent *E. coli,* were used to produce plant derived high value compounds, like morphinan alkaloids (Facchini, Bohlmann et al. 2012, Fossati, Narcross et al. 2015, Diamond and Desgagné-Penix 2016). Furthermore, the production of aromatic amino acid (precursor for AAs) and associated upstream gene/enzyme were well studies in yeast and *E. coli* (Cao, Gao et al. 2020). Precursors such as tyrosine and *p*-coumaric acid have been already produced in *E. coli* (Patnaik, Zolandz et al. 2008, Li, Li et al. 2018). Recently unicellular photosynthetic organism, such as microalgae and cyanobacteria became new research platforms because of their unicellular physiology together with their photosynthetic, heterotrophic, and mixotrophic lifestyles (Slattery, Diamond et al. 2018). Moreover, plant based genetic engineering technique is also emerging in model plant such as *Nicotiana tabacum* and *N. benthamiana* (Farhi, Marhevka et al. 2011).

Gene deletion, expression of endogenous metabolic genes or swapping of endogenous enzymes with more active homologues are common techniques to enhance production of intrinsic metabolites in selected heterologous host. Then, a path to the targeted SM can be designed and implemented. A candidate pathway is first outlined through selection of stepwise chemical intermediates leading from host metabolism to the target compound, followed by selection of enzymes to carry out each specified reaction (Kitney and Freemont 2012, Ausländer, Ausländer et

al. 2017). Although, different biochemical routes for AAs have been proposed, still we need a lot of knowledge regarding biosynthesis gene and underline of biochemical reaction. Muti-omics (genomic transcriptomics, metabolomic) of different Amaryllidaceae plants which produce unique types of AAs can be helpful to identify candidate biosynthetic genes (Ferdausi, Chang et al. 2021, Li, Xu et al. 2021, Tousignant, Diaz-Garza et al. 2022). Plant species from *Crinum* genus such as *C.* x *powellii* are known to be produce cherylline type of AAs and still none of genes involved in AA metabolism from this plant is known (Velten, Erdelen et al. 1998, Niño, Hincapié et al. 2007). Enzyme level of understanding of biosynthetic pathway can enhance our ability to synthesize targeted molecule by using genetic engineering approaches (Koirala, Karimzadegan et al. 2022).

1.5 Importance, hypothesis, and objectives

Although, there are several AAs with potential therapeutic properties, only galanthamine is used as therapeutic agent. Currently, the main source of AAs is the native plant with limited accumulation of AAs, restraining their further pharmaceutical application and research (Desgagné-Penix 2021). Their accumulation is affected by environmental factors (Lubbe, Gude et al. 2013, Ncube, Nair et al. 2015). Alternative to native plant source, *in vitro* tissue culture can provide powerful platform to produce SM (Koirala, Karimzadegan et al. 2022).

Currently, most of the research on *in vitro* tissue culture on Amaryllidaceae plant concentrates on galanthamine producing species (Bergoñón, Codina et al. 1996, Diop, Hehn et al. 2007, Ferdausi, Chang et al. 2020, Ferdausi, Chang et al. 2021). However, there are several Amaryllidaceae plant from which distinct types of AAs are reported. Therefore, our study focuses on *in vitro* culture development of *C.* x *powellii* "Album" which is well known to produce AAs such as cherylline, an antiviral AA. Although research is limited to understand the effect of a single factor on AAs biosynthesis during *in vitro* culture, we hypothesized that understanding the combined effect of light and auxin on *in vitro* tissue development, morphogenesis and AAs biosynthesis at transcriptomic level would accelerate the sustainable and eco-friendly production of AAs.

Biosynthetic enzymes such TYDC, NBS, NR, OMT and CYP96 were biochemically characterized from different Amaryllidaceae plants. Although the biosynthetic pathway to AAs is still not fully elucidated, labeling studies established that 4'*O*-methylnorbelladine was the key intermediate alkaloid precursor of diverse types of AAs. Previously, class I type of *O*-methyltransferases from

different Amaryllidaceae plants were characterized, most accepting norbelladine as the substrate and methylated norbelladine at a single position (3ˈor 4ˈ-OH)(Sun, Wang et al. 2018, Li, Qiao et al. 2019). Intriguingly, other *O*-methylated forms of norbelladine were detected *in planta*. For a better understanding of catalytic potential of OMT, it is necessary to characterize homologous enzymes from various Amaryllidaceae plants. Homologous norbelladine *O*-methyltransferase from *N. papyraceus* (*Np*OMT) has not been functionally characterized before. We propose that characterization *O*-methyltransferase from *N. papyraceus* can be valuable tool to rewire AAs pathway in heterologous host for production of targeted types of AAs.

Therefore, based on previous study and with the aim to generate tools for sustainable production of AAs, our research hypothesis is that transcriptomic level understanding of the effect of growth factor in *in vitro* culture, and molecular characterization of biosynthetic gene can be valuable tools for sustainable production of AAs.

We divided our research goal with the following two objectives:

Objective 1: Uncover cherylline-pathway biosynthesis using comparative transcriptomic study between alkaloid producing and alkaloid non-producing *C.* x *powellii* "Album" tissue generated from *in vitro* culture.

As our first study, we conducted our experiments on *C.* x *powellii "*Album*"*, a non-model medicinal plant belonging to *Crinum* genus of Amaryllidaceae family. Studies on different Amaryllidaceae show that light and hormones can affect growth, morphogenesis, and AAs accumulation on *in vitro* tissue. To understand, the combined effect of light and auxin, we performed the comparative transcriptomic study on alkaloid producing and alkaloid non-producing tissue developed in dark and light conditions with exogenous supply of different concentration of auxin. For this study, we first develop *in vitro* culture of *C.* x *powellii* "Album" from twin scale explant extracted from bulbs. Then we performed target metabolites analysis of the different types of tissue developed during *in vitro* culture. Although callus produced less AAs, we selected callus as sample for transcriptomic study as they were responsive to light and auxin. This study was included as Chapter II in form of scientific article published in Phytochemistry (2023).

Objective 2. Functional characterization of homologous norbelladine *O*-methyltransferase from *N. papyraceus*.

As *O*-methylated norbelladine was considered as key intermediate compound of the AAs pathway by several studies (Chan 1973, El Tahchy, Ptak et al. 2011), we aimed to generate more comprehensive knowledge on the role of norbelladine *O*-methyltransferase. We functionally characterized *O*-methyltransferase from *N. papyraceus* (*Np*OMT). For this study, we cloned targeted *NpOMT* into pMAL-c2X and induced heterologous protein in *E. coli*. Enzymatic assay of heterologous *Np*OMT was performed with different substrates from AAs pathway having free OH-group including norbelladine. To elaborate our knowledge on *O*-methylation reaction regio-selectivity mechanism, we performed the *in silico* docking and molecular dynamic study. Sub-cellular localization study of *Np*OMT, and *in vivo* enzymatic assay show the potential of *Np*OMT to methylate norbelladine in 4'-O position in a heterologous cellular environment. Therefore, this study can extend our knowledge regarding catalytic potential of *O*-methyltransferase, their role in Amaryllidaceae biosynthetic pathway and can serve as important tool for synthetic biology to produce targeted AAs from heterologous host. These results are included as Chapter III as a manuscript to be submitted to journal of biological chemistry.

Chapter II contains a study that presents *in vitro* tissue development, effect of auxin and light on *in vitro* tissue development and comparative transcriptomic study between Amaryllidaceae alkaloid producing and alkaloid non-producing tissue of *C.* x *powellii* “Album”.

Chapter II

2. Auxin and light-mediated regulation of growth, morphogenesis, and alkaloid biosynthesis in *Crinum* x *powellii* "Album" callus

Manoj Koirala, Karen Cristine Goncalves dos Santos, Sarah-Eve Gélinas, Simon Ricard, Vahid Karimzadegan, Basanta Lamichhane, Nuwan Sameera Liyanage, Natacha Merindol, Isabel Desgagné-Penix

The manuscript was published in a phytochemistry 2023.

Contribution: Manoj Koirala established and sub-culture *in vitro* culture of *C* x *powellii* "Album" with the help of Vahid Karimzadegan, Basanta Lamichhane, and Nuwan Sameera Liyanage. Simon Ricard performed the GC-MS analysis and Sarah-Eve Gélinas performed the. Manoj Koirala did RNA-seq analysis with the help of Karen Cristine Goncalves dos Santos. Simon Ricard, Sarah-Eve Gélinas and Karen Cristine Goncalves dos Santos revised the manuscript. Manoj Koirala performed experiments with the supervision of Natacha Merindol and Isabel Desgagné-Penix.

2.1 Abstract

Crinum x *powellii* 'Album' belongs to the Amaryllidaceae medicinal plant family that produces a range of structurally diverse alkaloids with potential therapeutic properties. The optimal conditions for *in vitro* tissue growth, morphogenesis, and alkaloid biosynthesis remain unclear. Auxin and light play critical roles in regulating plant growth, development, and alkaloid biosynthesis in several Amaryllidaceae plants. Here, we have succeeded in showing, for the first time, that the combination of auxin and light significantly influence *C.* x *powellii* "Album" *in vitro* tissue growth, survival, and morphogenesis compared to individual treatments. Furthermore, this combination also upregulates the expression of alkaloid biosynthetic genes and led to an increase in the content of certain alkaloids, suggesting a positive impact on the defense and therapeutic potential of the calli. Our findings provide insights into the regulation of genes involved in alkaloid biosynthesis in *C.* x *powellii* "Album" callus and underline the potential of auxin and light as tools for enhancing their production in plants. This study provides a foundation for further exploration of *C*. x *powellii* "Album" calli as a sustainable source of bioactive alkaloids for pharmaceutical and agricultural applications. Furthermore, this study paves the way to the discovery of the biosynthetic pathway of specialized metabolites from *C.* x *powellii* "Album", such as cherylline and lycorine.

2.2 Introduction

Plant natural products have been an abundant source of chemical compounds for drug discovery (Rates 2001). Such molecules, whose biosynthesis is essential for plants to adapt and to interact with harsh ecological environments, are defined as plant specialized metabolites (SMs) (Jacobowitz and Weng 2020). Plant-derived alkaloids comprise one of the largest classes of SMs, reported in almost 20% of plants. Among them, alkaloids that are exclusively reported in the Amaryllidaceae plant family are known as Amaryllidaceae alkaloids (AAs) (Martin 1988, Lewis 1996, Dewick 2009, Singh and Desgagne-Penix 2015, Jin and Yao 2019, Desgagné-Penix 2020). AAs have chemotherapeutical effects on humans. For instance, galanthamine is marketed for the treatment of Alzheimer's disease, lycorine has cytotoxic and antiviral properties (Ieven, Vlietinck et al. 1982, Tallini, Osorio et al. 2017, Nair and van Staden 2023), and cherylline is a non-cytotoxic antiviral compound (Ka, Masi et al. 2020, Ka, Merindol et al. 2021). The *Crinum* genus from the Amaryllidaceae family, contains more than 130 species widely distributed among subtropical and tropical regions. Plants from this genus are used in traditional medicine as they display antitumor, immunostimulant, analgesic, antiviral, and antibacterial properties (Fennell and van Staden 2001). Accordingly, several *Crinum* species produce both cherylline and lycorine, together with copious AAs structures displaying a wide range of pharmacological activities (Abd el Hafiz, Ramadan et al. 1991, Fennell, Elgorashi et al. 2003, Refaat, Kamel et al. 2012, Tallini, Torras-Claveria et al. 2018, Ka, Merindol et al. 2021). *C.* x *powellii* "Album" (swamp lily) is an interspecies hybrid plant of *C. moorei* and *C. bulbispermum,* from which a number of AAs have been reported, including cherylline, lycorine, 1-*O*-acetyl-lycorine, cripowellin, and ismine, emphasizing its potential pharmacological interest (Velten, Erdelen et al. 1998, Brossi, Grethe et al. 2002, Nino, Hincapie et al. 2007).

In Amaryllidaceae, most of the metabolic enzymatic reactions yielding different AAs are not known. The biosynthesis involves the shikimate pathway that produces precursor aromatic amino acids, including L-phenylalanine and L-tyrosine (Figure 2.1). On one hand, L-phenylalanine follows the phenylpropanoid pathway to generate 3,4-dihydoxybenzylaldehyde (Desgagné-Penix 2020, Koirala, Karimzadegan et al. 2022). On the other hand, tyrosine is decarboxylated into tyramine under the action of tyrosine decarboxylase (TYDC) enzymes (Hu, Li et al. 2021). Reuniting both precursors, norbelladine synthase (NBS) (Singh, Massicotte et al. 2018, Tousignant,

Diaz-Garza et al. 2022) and norcraugsodine reductase (Kilgore, Holland et al. 2016) catalyze the condensation and reduction of tyramine and 3,4-dihydroxybenzyladehyde into norcraugsodine and then norbelladine (Majhi, Gélinas et al. 2022), the latter being the key intermediate compound of the pathway. Biochemical modifications of norbelladine or of its precursors by *O*-methyltransferase (*O*MT), and further modification by phenol-coupling reactions by cytochrome P450 (CYP), generate a diverse type of AAs. Up to date, more than 650 AAs of different ring types and biogenic origin such as norbelladine-, cherylline-, galanthamine-, crinine-, lycorine-types have been reported (Tallini, Osorio et al. 2017).

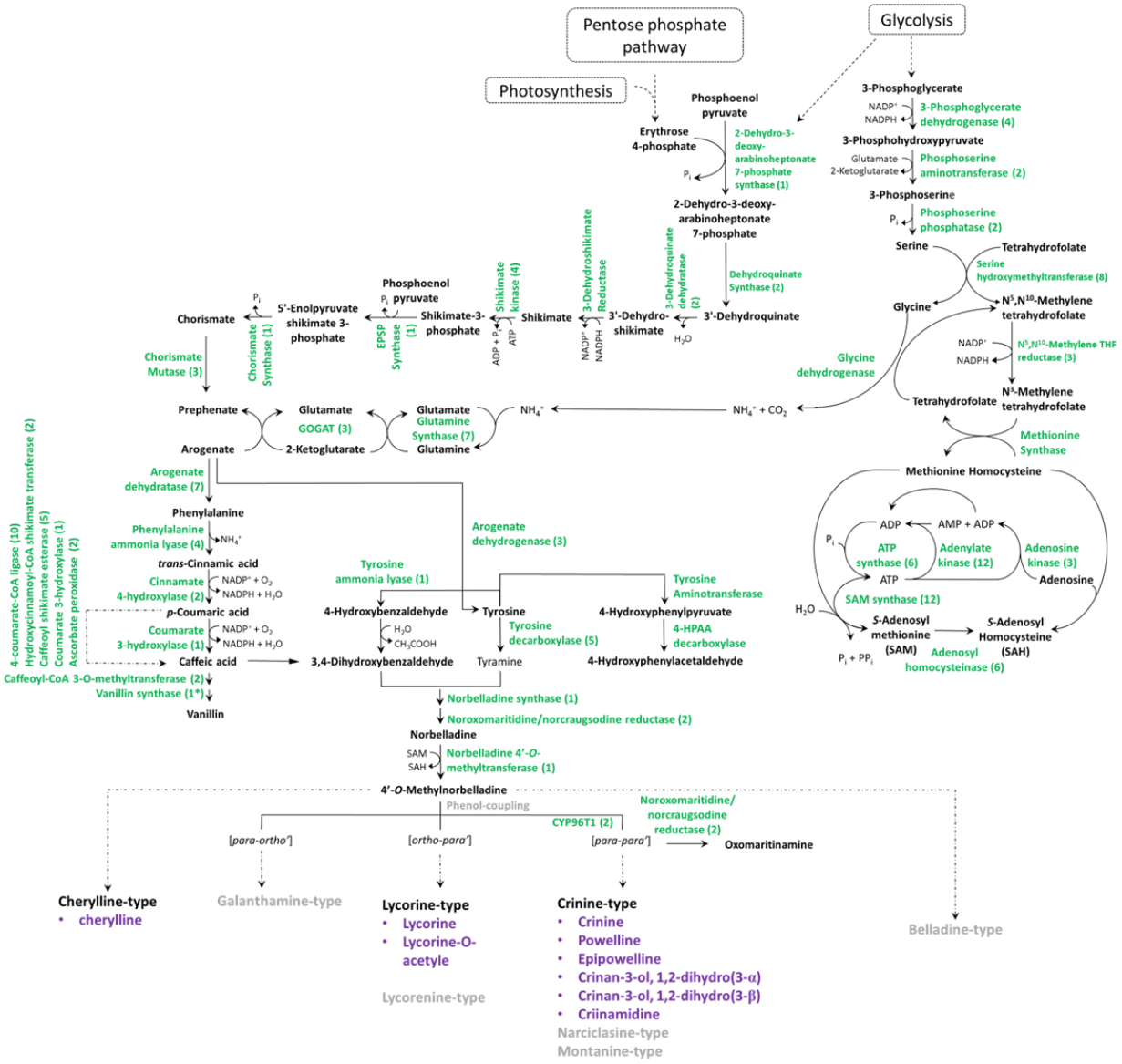

Figure 2.1 Proposed metabolic pathway leading to Amaryllidaceae alkaloids. Black arrow represents one reaction whereas dotted arrow represents several reactions. Enzyme catalyzing key reactions identified in *C* x *powelli* "Album" transcriptome in this study are written in green. Alkaloids written in purple were detected in this study in *C* x *powelii* "Album" extracted tissues whereas Amaryllidaceae alkaloids types written in gray were not detected. Numbers in small bracket represent the number of complete transcripts identified from *C*. x *powellii* "Album" transcriptome during this study.

Unfortunately, AAs biosynthesis and accumulation occur at low levels in planta, varying with developmental stages, tissues and seasonal changes (Lubbe, Gude et al. 2013, Hotchandani, de Villers et al. 2019). This issue impairs the commercial application of AAs, because their production requires large volumes of plant material (Brossi, Grethe et al. 2002, Lubbe, Gude et al. 2013,

Koirala, Karimzadegan et al. 2022). A successful alternative strategy includes the use of in vitro culture of specific plant tissues to produce SMs have been described before. The initiation and establishment of such methodology are influenced by several factors, such as exogenous supply of phytohormones and culture conditions (Gaba 2005, Trujillo Chacón, Leiva et al. 2023). Auxins are phytohormones known to induce cell elongation and to regulate diverse processes in plants, such as trophic responses to light and gravity, general shoot and root architecture, organogenesis, and growth in tissue culture. Exogenous supplies of auxins can greatly impact tissue differentiation and AAs accumulation (Ptak, Tahchy et al. 2013). The exposure to light is also an important parameter for plant *in vitro* culture. Recently, the effects of photoperiod on *in vitro* cultures of *Narcissus tazetta* showed that both tissue differentiation and alkaloid accumulation varied in relation to light conditions(Rahimi Khonakdari, Rezadoost et al. 2020). Lastly, in addition to its use as a mean of production of SMs, *in vitro* plant tissue culture technology can provide a powerful platform to uncover biosynthetic pathways and to generate a homogeneous sample that can be used in further studies (Gallego, Rojas et al. 2018).

In this study, we developed the in vitro culture of *C.* x *powellii* "Album" varying both light and auxins concentrations. Then, to explore the effect of different factors on the biosynthesis of AAs, we performed a comparative transcriptomic study between alkaloid-producing and non-producing callus generated with four culture conditions, varying both auxin treatment and light exposure. This study presents the first transcriptome analysis of a species that produce cherylline (Figure 2.1).

2.3 Results

2.3.1 *C.* x *powellii* "Album" clusters with *Crinum* species endemic to South Africa

To genotype *C.* x *powellii* "Album" (Figure 2.2a), a partial *ITS2* region was amplified from genomic DNA (Wang and Chen 2007, Ka, Merindol et al. 2021). The phylogenetic analysis was performed with 10 different species of the *Crinum* genus, using *Amaryllis belladonna* as outgroup (Figure 2.2b). Close analysis of the *ITS2* region reveals two subclades, (i) from *C. stuhlmannii* to *C. forbesii* highlighted in yellow color and (ii) from *C. yemenense* to *C. oliganthum* highlighted in blue color, which is consistent with Meerow, Lehmiller et al. (2003). Subclade (i) includes mostly African species together with *C. flaccidum,* endemic of Australia. *C.* x *powellii* clusters inside this group, more specifically with the South African endemics *C. stuhlmannii,* and *C. bulbispermum,* and *C. moorei* from which it derives. Subclade (ii) is formed by the American clade, together with tropical and North African species.

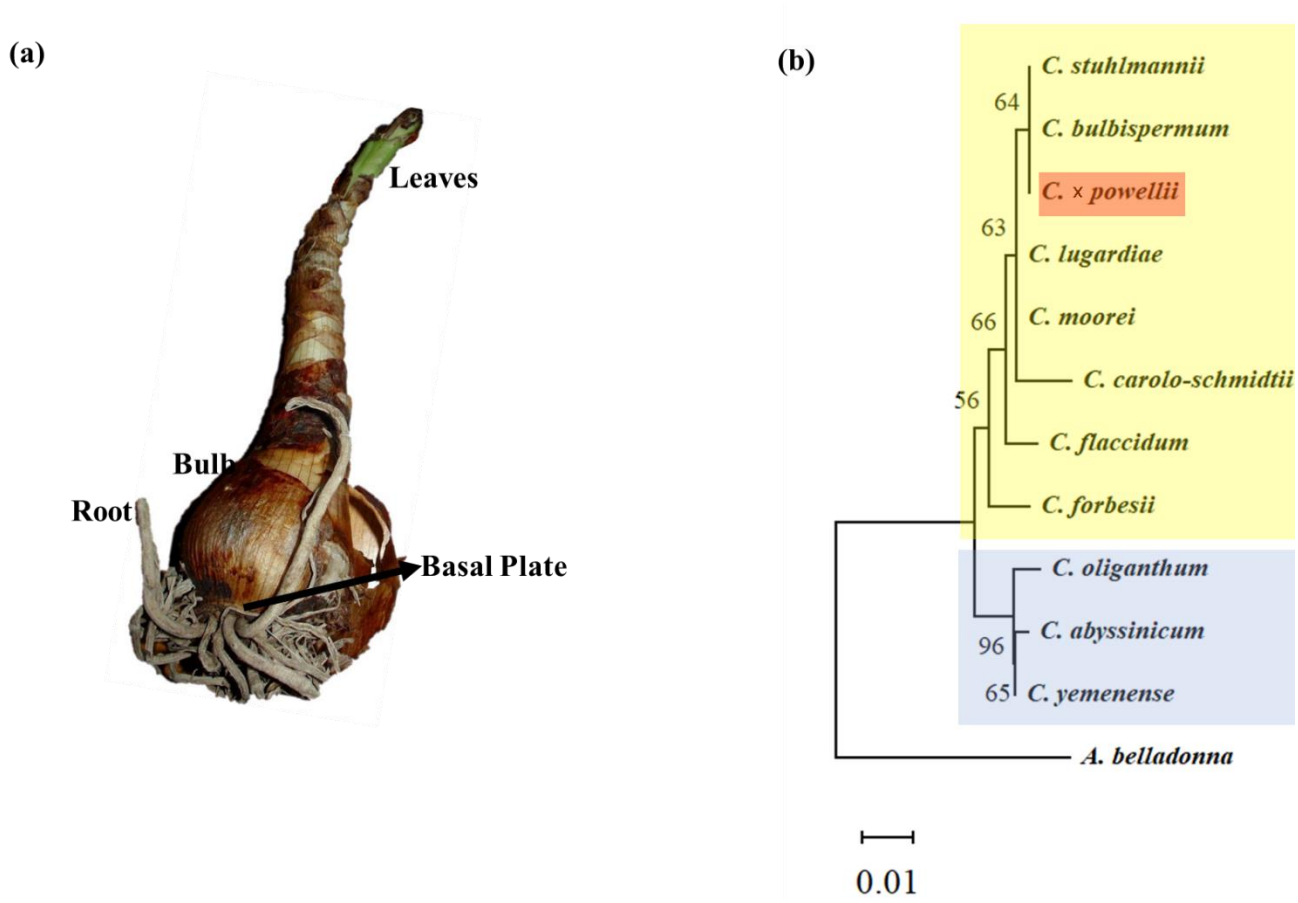

Figure 2.2 Verification of explant genus. (a) *C.* x *powellii* "album" tissues used during this study. (b) Genotyping of *C.* x *powellii* "Album". The phylogenetic analysis was performed using Molecular Evolutionary genetic analysis (MEGA 11.0.3) software. The evolutionary history was inferred using the Neighbor-Joining method and the optimal tree is shown. The percentage of replicate trees in which the associated taxa clustered together in the bootstrap test (1000 replicates) are shown next to the branches. The tree is drawn to scale, with branch lengths in the same units as those of the evolutionary distances used to infer the phylogenetic tree. The evolutionary distances were computed using the p-distance method and are in the units of the number of base differences per site. This analysis involved *ITS2* region from *C*. x *powellii* "Album", 10 ITS2 region nucleotide sequences from different *Crinum* species, *i.e*. (*C. abyssinicum* (AY139117.1), *C. oliganthum* (AY139142.1), *C. lugardiae* (JX464264.1), *C. yemenense* (AY139151.1), *C. moorei* (AY139141.1), C..stuhlmannii (JX464267.1), *C. carolo-schmidtii* (AY139125.1), *C.forbesii* (AY139133.1), *C. flaccidum* (AY139132.1), *C. bulbispermum* (AY139123.1)) and *A. belladonna* (JX464257.1) as a out-group. *C*. x *powellii* "Album" is highlighted in red.

2.3.2 *C.* x *powellii* "Album" *in vivo* tissues are enriched in crinine-, lycorine- and cherylline-type alkaloids.

Next, we explored the metabolite profile of crude methanolic extracts of *C.* x *powellii* "Album" tissues, including roots, basal plates, bulbs, and young leaves (Figure 2.2a). The GC-MS analysis showed the presence of 52 peaks, and the identity of some AAs was confirmed by comparing fragmentation pattern of detected compound with the NIST library 0.5 (ANNEX B Table S1). Overall, three different types of AAs were detected in *C.* x *powellii* "Album", namely crinine-type (powelline, epipowelline, crinine acetate and crinine), lycorine-type (lycorine and lycorine-*O*-acetyl) and cherylline-type (cherylline) (Table 2.1; Figure 2.3, and ANNEX B Figure S2). Lycorine was detected in all analyzed organs of *C.* x *powellii* "Album", however, its *O*-acetylated derivative was detected only in bulbs. Crinine-type alkaloids were detected in different parts of the plant. Cherylline was detected in all studied organs, except in the leaves. Basal plates and leaves contained the most diversified profile of alkaloids (Table 2.1).

Table 2.1 Amaryllidaceae alkaloid detection in different types of *C.* x *powellii* "Album" samples by GC-MS analysis. The number of m/z observed corresponds to the number of peaks observed in the samples ran in triplicates. n.a: not applicable. Shown are only tissues and conditions in which alkaloids were specifically detected. Experiments were done in triplicates. *, ** and *** indicate the number of replicates (*i.e.*, one, two or three out of three) where the corresponding metabolites were detected and identified. Our detection threshold consisted of a NIST05 hit >90% at a given retention time (see ANNEX B Table S1). Numbers in small brackets refer to ANNEX B Table S1 alkaloids and ANNEX B Figure S2 peaks.

Type	Light	Type of auxin (concentration)	Type of tissue	Number of m/z observed	Lycorine		Crinine						Cherylline
					Lycorine (8)	Lycorine -O-acetyl (7)	Epipowelline (6)	Crinan-3-ol,1,2-didehydro(3-alpha) (1)	Crinamidine (9)	Crinine acetate (4)	Crinan-3-ol,1,2-didehydro(3-beta) (2)	Powelline (5)	Cherylline (3)
In vivo	n.a.	n.a.	Leave	32	**	*	*	*		***	**		
			Bulb	23	***			***				***	***
			Root	22	***			***				***	***
			Basal plate		***			***		***		***	***
In vitro	-	NAA(2 mg/L)	Indirect bulblet	13								**	
	+	NAA (2 mg/L)	Callus	15				*				***	
			Indirect shoot	19	**			*	***			***	***
		NAA (4 mg/L)	Callus	15								**	
			Indirect shoot	15	**	*			**			**	**
		NAA (8 mg/L)	Callus	13								*	
			Indirect shoot	19	**		*	**	***			***	***

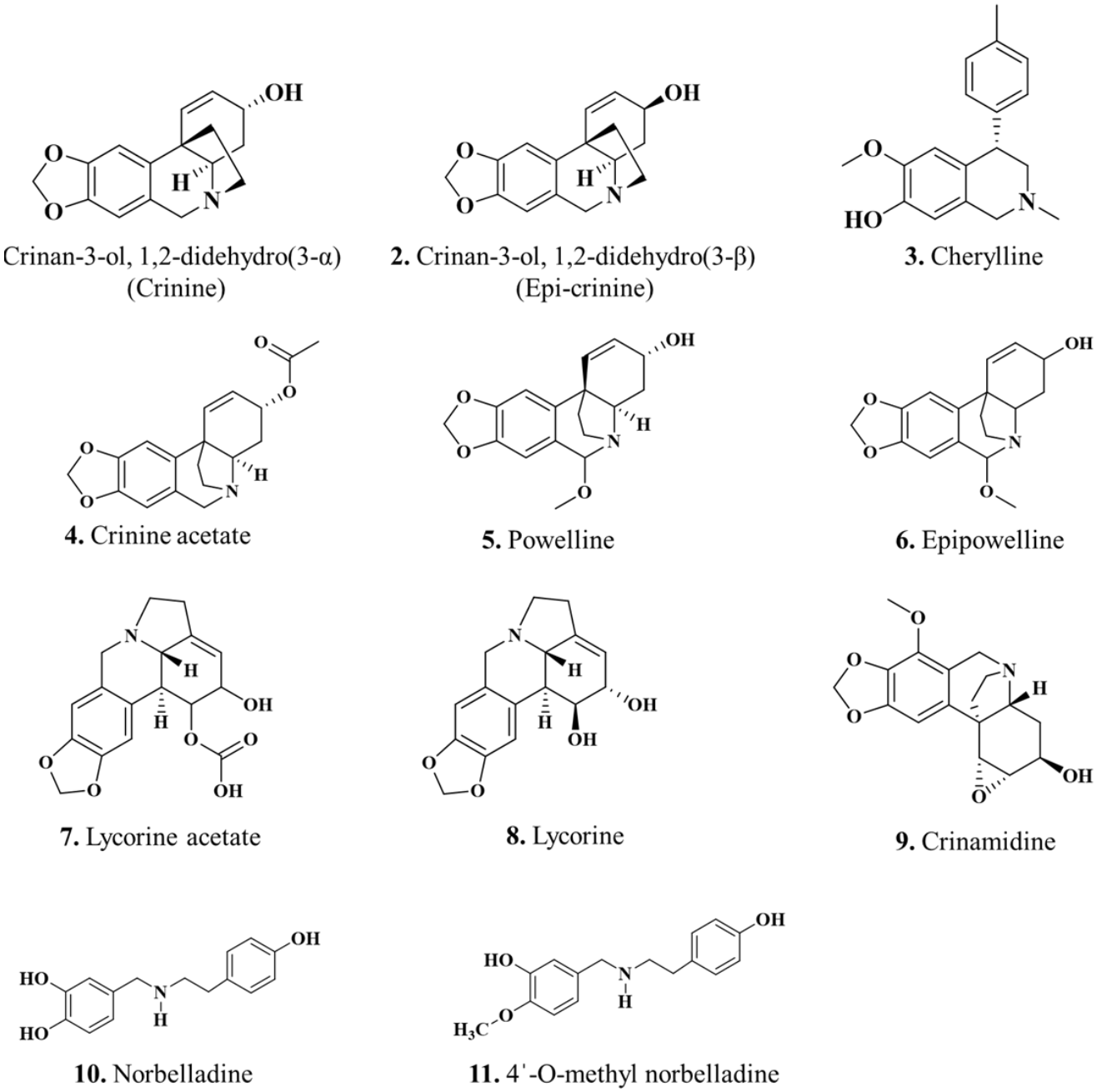

Figure 2.3 Structure of Amaryllidaceae alkaloids from *C.* x *powellii* "Album". Compound 1-9 were detected during GC-MS analysis, compounds 1, 3 and 8 was detected in both GC-MS and LC-MS/MS analysis and compound 10 and 11 were only detected during LC-MS/MS analysis of *C.* x *powellii "*Album" sample. Relative quantity of compounds 1,8, 10 and 12 were determined by using LC-MS/MS

2.3.3 Light and auxin greatly affect *in vitro* tissue survival and morphogenesis.

To develop *in vitro* culture of *C.* x *powellii* "Album", twin scale explants were extricated from bulbs after surface sterilization. Explants grown in light and dark conditions displayed distinct

morphologies. When grown in dark, explants were mostly white. By contrast, upon exposure to light, they were mainly green and brownish, depending on the type of auxin used. We observed a 5.60-fold increase in browning of explant during *in vitro* culture in light compared to dark condition (ANNEX B Figure. S3). Browning of most of explant was followed by death of explant or callus**.**

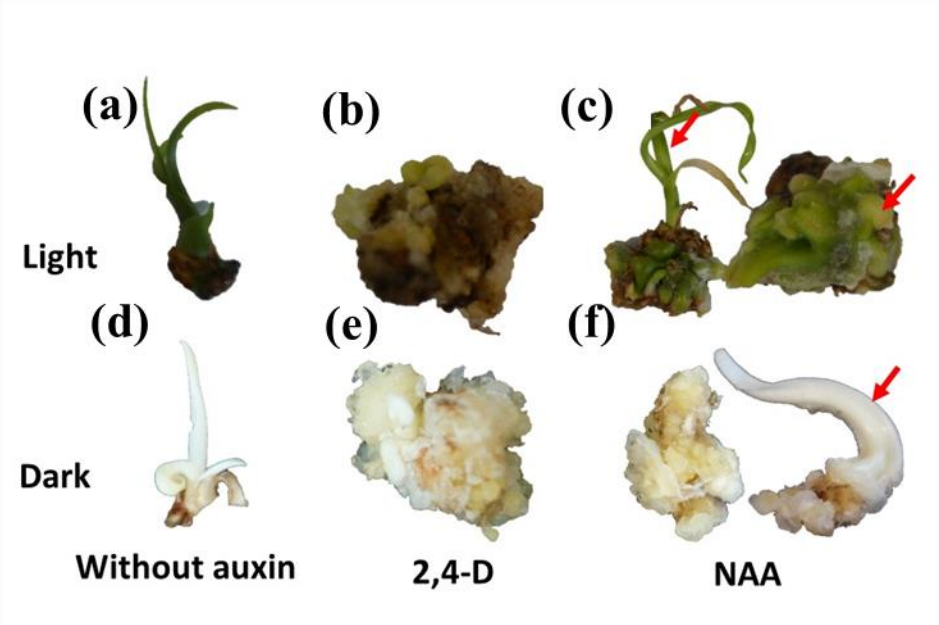

Figure 2.4 Different types of tissue generated from the *in vitro* culture of *C.* x *powellii* "Album". (a), (b) & (c) represent tissues developed in light conditions; (d), (e) & (f) represent tissues generated in the dark condition. (a) & (d), tissues generated without auxin (direct organogenesis); (b) & (e), tissues generated with 2,4-D (callus formation); (c) & (f), tissues generated with NAA (red arrow indicates indirect organogenesis). Shown are representative pictures of 6 months old tissues for each mentioned condition. Pictures were taken under the laminar hood from callus and explants grown in Petri dishes, they displayed approximately the same size.

Following this initial phase of culture, different types of tissues continued to develop depending on the conditions and types of hormones, over the 6 months study period of *C.* x *powellii* culture (Figure 2.4; ANNEX B Table S3). In absence of auxin, no callus induction was observed, but direct organogenesis (direct shoot formation) occurred for 100% of explants. Although overall survival rate of explants grown in light was lower (ANNEX Figure S3), tissues generated in darkness without auxin only survived for short periods, starting to die after 20-22 weeks of culture. Induction of callus was observed after 3-4 weeks, occurring more rapidly with media supplemented with 2,4-D (at every concentration), regardless of light exposure. When media were supplemented with NAA, callus induction occurred in 4-6 weeks, depending on its concentration. The type of auxin also affected the type of tissues generated. Initial callus morphogenesis in presence of 2,4-D was

globular, while NAA led to a swelling-type of callus. In the case of 2,4-D, explants grew as undifferentiated tissues (callus, 100% of explants) regardless of its concentration and light exposure, whereas light played a role in the explant development when NAA was supplied as auxin. In the light-exposed condition, with 2 and 4 mg/L of NAA, shoot generation occurred within 8 weeks, whereas with 8 mg/L, it took 14 weeks for tissue to become differentiated. In dark condition, tissue differentiation was observed on the 10^{th} week of culture when supplied with 2 and 4 mg/L of NAA; however, no shoot formation was seen with higher concentration of this hormone.

2.3.4 Light increases the production of metabolites in *in vitro* tissue.

To understand the alkaloid producing capability of *in vitro* tissues, GC-MS analysis of methanolic extracts was performed. Noteworthy, fewer AAs were identified from undifferentiated tissues compared to *in vivo* or *in vitro* differentiated samples (Table 2.1). Another remarkable difference was the near absence of AAs detection in tissues grown in the dark (with or without 2,4-D), compared to *in vivo* and light-exposed tissues, and NAA-treated, respectively. Four to fourteen metabolite peaks were detected in samples grown in dark condition, depending on auxin concentration. However, powelline was the only alkaloid identified in differentiated tissue (induced bulblet) generated in the culture supplemented with 2 mg/L of NAA in the dark (Table 2.1). By contrast, 8 to 19 metabolite peaks were observed in *in vitro* tissue samples exposed to light. Tissue differentiation following NAA treatment was associated with an increase in AAs detection in cultures exposed to light. In contrast to tissue growth in dark conditions, powelline was detected in all calli grown exposed to light with any of the tested NAA concentrations (Table 2.1). Interestingly, the types of AAs detected in *in vitro* tissues generated from the light with NAA were similar to the AAs detected from *in vivo* tissue. All three types of AAs, *i.e.,* lycorine-, crinine- and cherylline-type, were identified from differentiated tissues treated with NAA and exposed to light.

2.3.5 Lycorine and cherylline are triggered by light and 2,4-D in undifferentiated tissues.

AAs were undetectable (below lower limits of quantitation) in several *in vitro* tissues following GC-MS analysis, especially those treated with 2,4-D. To get a broader and more sensitive view of *in vitro* tissues AAs profile, we performed targeted metabolite analysis using LC-MS/MS. In general, a similar profile of metabolite enrichment according to tissue differentiation (compounds are more abundant in shoots), light exposure and auxin (NAA) treatment was observed using both

methods (ANNEX Figure S4). However, LC-MS/MS allowed for the sensitive detection of alkaloids in callus grown in darkness. Metabolites such, five AAs (*i.e*. norbelladine, 4'-*O*-methylnorbelladine, cherylline, lycorine and crinine) and six AAs precursors (*i.e.*, caffeic acid, ferulic acid, L-tyrosine, *p*-coumaric acid, phenylalanine, and tyramine) were identified based on their retention time and fragmentation pattern compared to available authentic standards (Figure 2.3, Figure 2.5; ANNEX Figure S4). In callus, the accumulation of these metabolites of interest was mostly affected by light, and then by 2,4-D (Figure 5). Hence, we focused our analysis on the combination of these two conditions. 4'-*O*-methylnorbelladine was detected in tissues exposed to light regardless of concentration of 2,4-D, however its accumulation was 3-fold higher in tissues grown with 4 compared to 2 mg/L of 2,4-D. The accumulation of lycorine was almost 2-fold higher in tissue cultured with 2 compared to 4 mg/L of 2,4-D. Cherylline was not detected in callus obtained from tissues cultured with 2 mg/L of 2,4-D, but was detected at 4 mg/L of 2,4-D, with an accumulation 2.5-fold higher in light compared to dark condition (Figure 2.5; ANNEX B Figure S4).

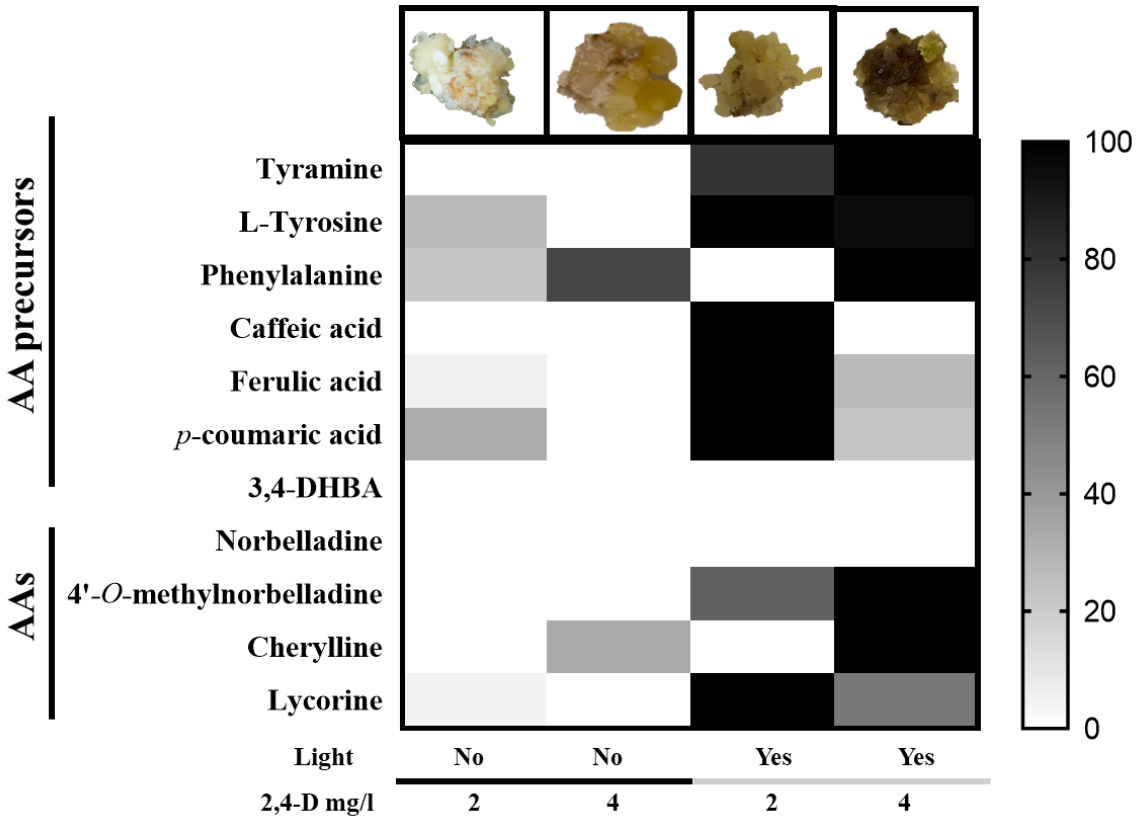

Figure 2.5 LC-MS/MS analysis of targeted metabolites in tissue generated from in vitro culture of *C.* x *powellii* "Album". On top, callus developed during *in-vitro* culture conditions, from left to right: dark:2 mg/L of 2,4-D, dark:4 mg/L of 2,4-D, light:2 mg/L of 2,4-D and light:4 mg/L of 2,4-D. Heatmap shows the relative abundance of target metabolites in tissue culture of *C.* x *powellii* "Album". Relative abundance corresponds to the mean value of three independent replicated values normalized to the sample with the highest level for each compound. The condition included in the analysis in which the highest quantity of a specific compound is detected is shown as the most intense box. Pictures were taken under the laminar hood from callus grown in Petri dishes, they displayed approximately the same size.

2.3.6 *De novo* transcriptomic assembly of *C* x *powellii* "Album"

To get insight into the biosynthesis route and uncover the genes involved in lycorine and cherylline production in *C.* x *powellii* "Album", we performed RNA sequencing (RNA-seq) from selected callus of *C.* x *powellii* "Album" cultured in light and dark conditions, with 2 mg/L or 4 mg/L of 2,4-D. The 8 mg/L of 2,4-D treatment was not included as it did not yield enough tissue for further analysis. Also, the NAA treatment was excluded since the organogenesis occurred in light condition only, which would result in an additional variable dimension. Furthermore, to generate a complete view of the species transcriptome, we also included the RNA-seq data obtained from *in vivo* tissues.

Altogether, a total of 1 240 830 608 raw reads were generated (ANNEX B Table S4). These were cleaned up using optimized fastp software, according to initial quality assessment performed with FastQC, resulting in 1 162 489 247 clean reads. These were assembled using Trinity software, yielding 1 261 988 of trinity transcripts and 785 475 trinity genes. BUSCO analysis revealed that 90.7% of the orthologs in the embryophyte database were found complete in *C.* x *powellii* "Album"s transcriptome. The assembly had N50 of 1 033, with mean and median contig lengths of 364 and 658.04 respectively (ANNEX B Table S4). In total, 133 843 transcripts were annotated using Pfam and Uniprot databases.

Next, the gene-size distribution, GO and COG analysis of assembled *C.* x *powellii* "Album" transcriptome were generated, and the GO term annotation of the transcripts based on UniProt, SwissProt and Pfam annotations was obtained (ANNEX B Figure S5). Most genes were associated with "binding" (GO:0005488, molecular function). The second largest number of transcripts were annotated with GO terms belonging to "cellular process" (GO:0009987, biological process) (ANNEX B Figure S5). There were fewer transcripts annotated with cellular component GO terms. Based on the sequence homology, 1008 assemble genes had COG (Clusters of Orthologous Genes) functional classification, resulting into 24 categories (ANNEX B Figure S5). "Energy production and conversion" was the most common category followed by "general function", whereas "cytoskeleton", "extracellular structure", "RNA processing and modification" and "chromatin structure and dynamic" were the ones with fewer transcripts.

2.3.7 A combination of light and 2,4-D modulates the expression of photosynthesis- and stress response-related gene categories.

To elucidate the effect of different factors in the underlying regulatory processes, we performed a comparative transcriptomic study between AAs producing and non-producing callus cultures in light and dark conditions, with 2 and 4 mg/L of 2,4-D. Principal component analysis of transcriptomic data revealed three main clusters well separated from one another (ANNEX B Figure S6). The exposure to light played a dominant role in the gene expression profile of the samples than the concentration of 2,4-D, and calli grown in the dark were more homogenous than when exposed to light. Two sub-clusters were observed in the dark-grown group according to the concentration of auxin used. Strikingly, in light-exposed callus, the concentration of the phytohormone played a greater role in the gene expression profiles, generating two distant clusters.

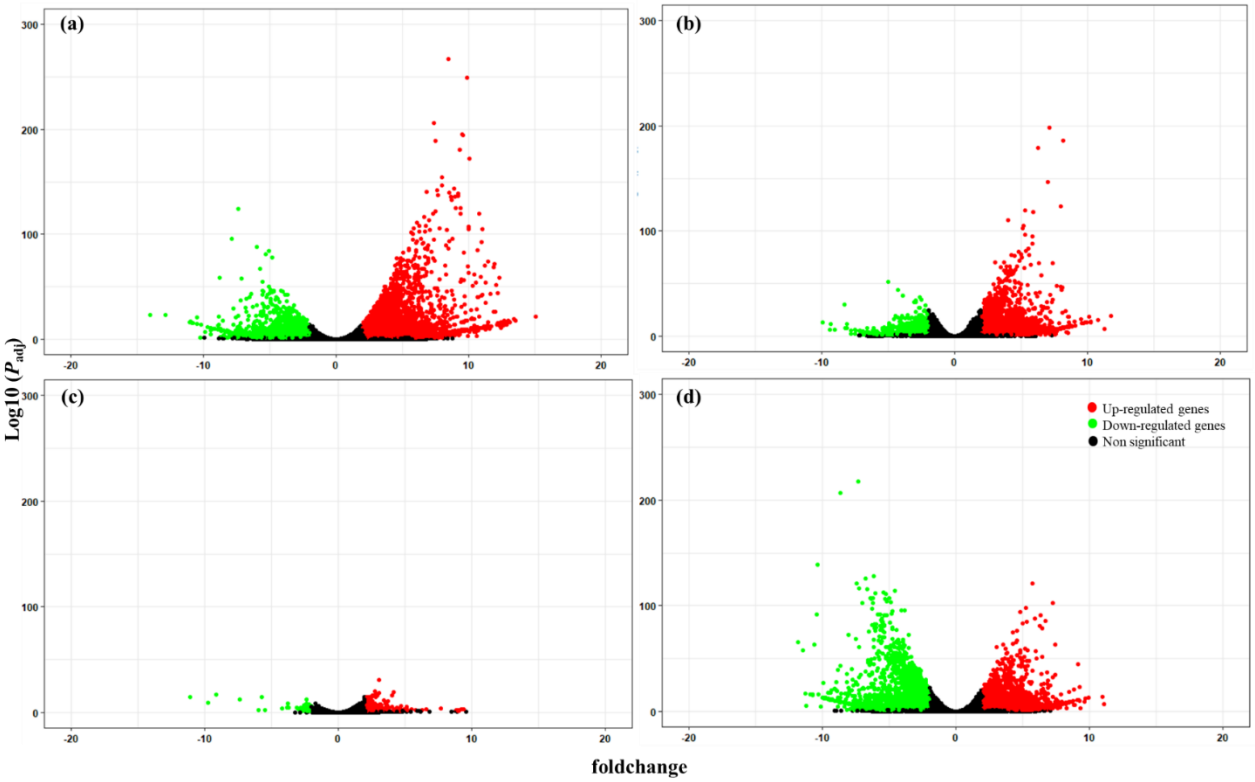

Figure 2.6 Volcano plots of differentially expressed genes identified in callus of *C.* x *powellii* "Album". (a) 2 mg/L of 2,4-D: Light Vs Dark , (b) 4 mg/L of 2,4-D: Light Vs Dark, (c) Dark: 4 mg/L Vs 2 mg/L of 2,4-D and (d) Light: 4 mg/l Vs 2 mg/L of 2,4-D. Differential expression analysis was performed using the R package DESeq2. p-values were adjusted for controlling the false discovery rate (FDR). Only genes with $|\log_2(\text{FoldChange})| > 2$ and an adjusted p-value < 0.05 were considered as significant differentially expressed. Red indicates up-regulated genes, green indicates down-regulated genes, and black indicate genes non-significant deregulated genes.

Supporting the principal component analysis result, differential expression analysis showed that the exposure to light had a greater impact on gene expression than did the concentration of 2,4-D (Figure 2.6). A total of 11,304 and 4505 genes were deregulated in light vs dark condition with exogenous supply of 2 or 4 mg/L of 2,4-D, respectively (Figure 2.6a, 2.6b; Figure 2.7a). GO enrichment analysis showed that genes involved in, "tetrapyrrole binding", "monooxygenase activity", "oxidoreductase activity" and "response to stimulus" were up-regulated in light condition regardless of concentration of 2,4-D supplied. "Photosynthetic membrane" and "photosystem" related transcripts were up-regulated in light vs dark condition at 2, and 4 mg/L of 2,4-D, respectively. The 3401 genes up-regulated in callus grown with 4 mg/L of 2,4-D exposed to light were enriched in the "phenylpropanoid metabolic process", whereas the "phenylpropanoid catabolic process" was downregulated (Figure 2.7a).

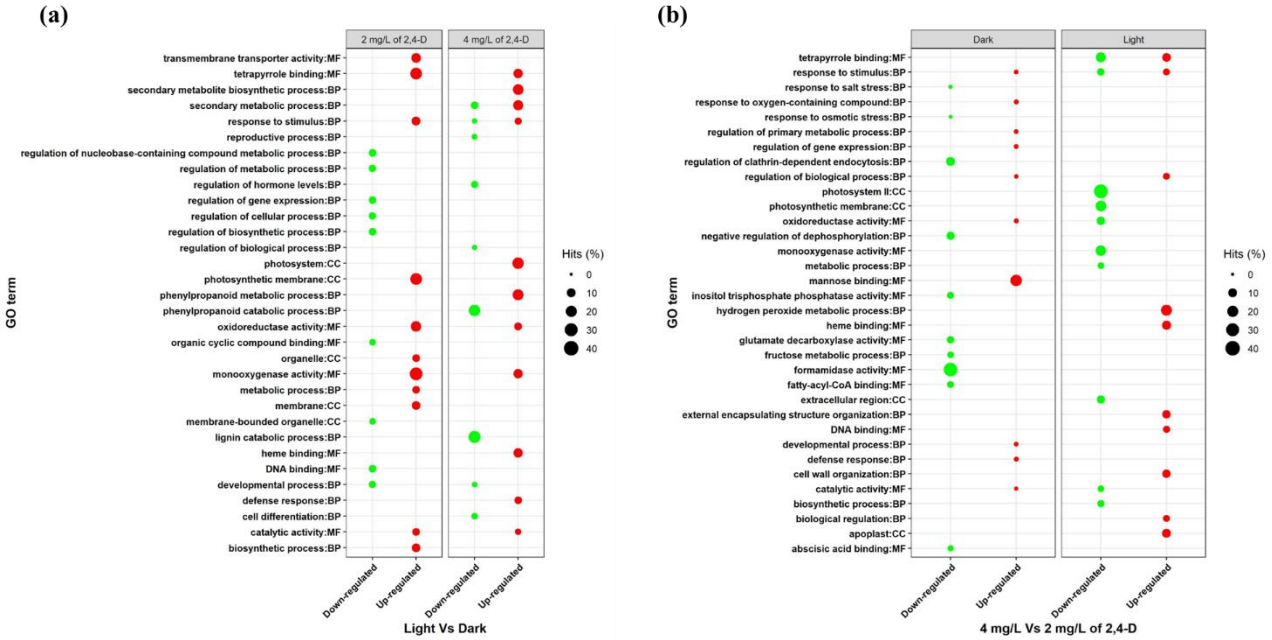

Figure 2.7 Gene Ontology analysis of differentially deregulated genes. (a) Comparison of differentially expressed genes in calli developed with in light Vs dark with supply of 2 mg/L or 4 mg/L of 2,4-D. (b). Comparison of differentially expressed genes in calli developed in 4 mg/L Vs 2 mg/L of 2,4-D in light or dark condition. Red and green colours indicate the down regulated and upregulated genes, respectively. Analysis was done with a *p*-value of 0.05. Y-axis in each figure represent the GO term and ontology (MF: molecular function, BP: Biological process, CC: cellular component).

To understand the effect of 2,4-D on *C.* x *powellii* "Album" callus transcriptome, we also performed differential gene expression analysis between calli obtained using 4 mg/L compared to 2 mg/L of 2,4-D, with and without light exposure (Figure 2.6c, 2.6d; Figure 2.7b). In light condition, 4 936 genes were up-regulated, and 4 129 gene were down-regulated in culture with 4 compared to 2 mg/L of 2,4-D (Figure 2.6d; ANNEX B Figure S7a). Compared to samples exposed to light, a smaller number of genes were differentially expressed between, with only 455 genes deregulated in dark conditions, consistent with the PCA result (ANNEX B Figure S6). When grown with 4 mg/L of 2,4-D in darkness, genes involved in "oxidoreductase activity", "defense response" and "developmental process" were up-regulated compared to the lower concentration of 2,4-D, whereas genes involved in "formamidase activity" was the most commonly down-regulated GO-category. The most enriched category among the up-regulated genes in 4 vs 2 mg/L of 2,4-D exposed to light, was the "hydrogen peroxidase metabolic process" and "tetarpyrolle binding", whereas down-regulated genes were observed in "photosystem II", "oxidoreductase activity" and "monoxygenease activity".

2.3.8 2,4-D and light affect the expression pattern of phenylpropanoids and AAs biosynthesis genes.

Candidate AAs biosynthesis genes, from the precursor shikimate pathway to AAs specific genes, were identified in *C.* x *powellii* "Album" transcriptome based on blast homology searches. We identified a total of 78 complete and partial hits to genes that are putatively involved in the shikimate, the phenylpropanoid and the AAs pathways and their gene transcript sequences were deposited in GenBank with the accession numbers listed in ANNEX B Table S5. Candidate genes involved in the AAs biosynthesis were selected based on homology and on their differential expression profile, *i.e.* only the genes that were upregulated in conditions that accumulated AAs were selected. Overall, there was significantly more transcripts in light (with 2 or 4 mg/L 2.-4D) compared to dark condition, when callus cultures were treated with 2 (p<0.001 and p=0.002, respectively, Friedman multiple comparisons test, (ANNEX B Figure S8) or 4 mg/L of 2,4-D (p=0.0102 in both cases). Specifically, light and 2,4-D both impacted specifically on the gene expression profile of *CpPAL*, *CpTYDC*, *CpC3H*, *CpHCT*, *CpOMT*, *CpNBS*, *CpNR*, *CpCYP96 and CpV11H* (ANNEX B Table S5, ANNEX B Figure. S8a and b). On the right arm of the AAs precursors biosynthetic pathway that leads to 3,4-DHBA (Figure 2.1), the exposure of callus to light led to a 3.35 to 4.55 $\log_2$ fold increase in expression of *PAL (i.e. CpPAL1)* candidate genes compared to callus grown in the dark. In this condition, candidate genes involved in the phenylpropanoid pathway, such as *CpC3H, CpC4H, CpHCT1*, were also up-regulated (ANNEX B Table S5, ANNEX B Figure S8a.). On the left arm of AAs precursors pathway leading to tyramine (Figure 2.1), *CpTYDC1* candidate genes followed a very similar profile to *CpPAL1,* greatly impacted by light, but also by 2,4-D concentration (ANNEX B Figure S8a). *CpNBS*candidates, encoding the enzyme predicted to be involved in the condensation of 3,4-DHBA and tyramine to give norbelladine, was expressed at very low levels overall, and upregulated in callus exposed to light and 4 mg/L of 2,4-D compared to dark condition (ANNEX Table S5, ANNEX Figure S8b). Furthermore, a 6.07 $\log_2$ fold increase was observed for *CpNBS1* in light condition with supply of 2 mg/L of 2,4-D. A candidate gene homologous of the norbelladine *O*-methyltransferase (*CpOMT*) was upregulated by a 2.67 $\log_2$ fold in light compared to dark condition when supplied with 4 mg/L of 2,4-D. Interestingly, although the gene encoding a cytochrome p450 monooxygenase enzyme (*CpNoroSyn2*; *CYP96T* candidate for the phenol-phenol coupling) was expressed at low levels

overall, and higher expressed in callus exposed to light (a 2.48 to 5.52 log_2 fold increase compared to dark), its expression was lower in 4 mg/L compared to 2 mg/L of 2,4-D in light conditions.

Furthermore, to understand the effect of photosynthesis-related and auxin inducible genes, we performed a WGCNA analysis. From 12526 DEGs, 1092 genes with a raw count > 10 were selected for WGCNA analysis, leading to the identification of seven modules, indicated by different colors (Figure 2.8; ANNEX B Figure. S9). Among all modules, turquoise included the highest number of genes (403 genes) while the red module contained only 30 genes (Figure 2.8). Candidate genes of AAs and phenylpropanoid biosynthesis pathways all clustered in the turquoise module, suggesting that these two pathways are interconnected. In this module that was selected for further analysis,185 genes were significantly correlated (Spearman correlation > 0.8). We identified 9 transcription factors (*i.e*. B-box zinc finger protein 24 (BBX24),NAC domain containing protein (NAC58 and NAC83), Homeobox-leucine zipper protein (HOX21), transcription factor MYB78, WRKY transcription factor (WRKY24 and WRKY75),Zinc-finger transcription factor(ZAT12), 3 genes encoding auxin inducible proteins (*i.e* (auxin responsive protein (ARFG), two SUR32 (auxin responsive protein)), and 4 genes encoding f photosynthesis related proteins (*i.e*. SGR protein STAY-GREEN homolog(SGR),photosystem II stability/ assembly factor HCF136 (P2SAF,Chromoplast-specific carotenoid-associated protein C1 (CHRC1)and Chorophyll a-b binding protein (CB2D, together with genes involved in phenylpropanoid and AAs pathway. These results show that auxin-inducible genes and photosynthesis-related genes are interconnected with specialized metabolites biosynthesis gene.

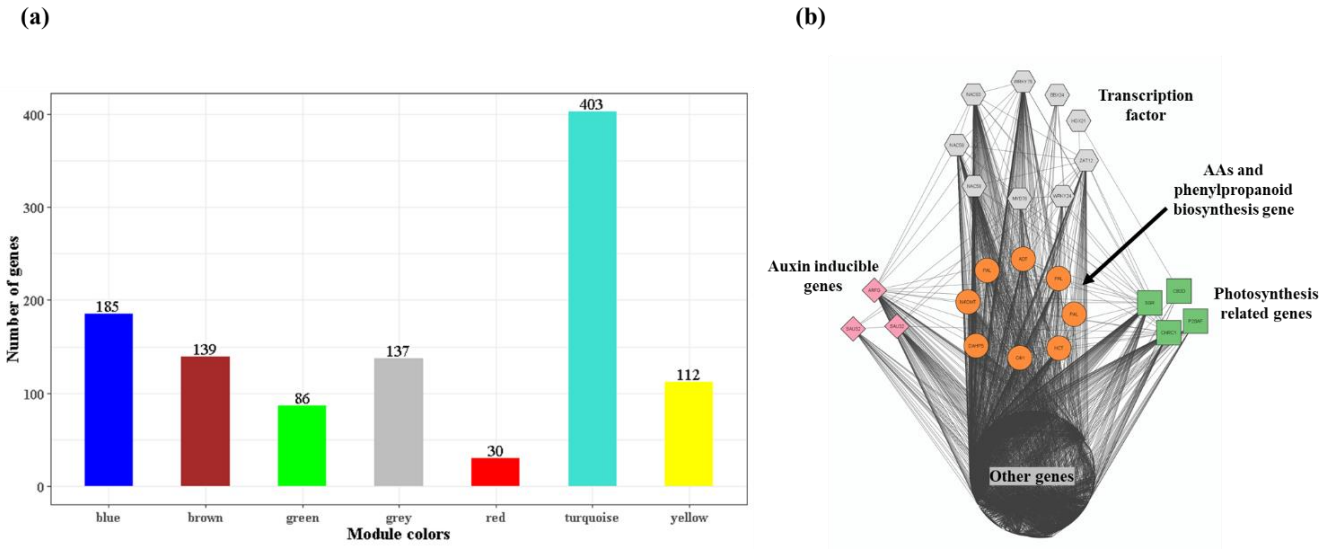

Figure 2.8 Weighted gene co-expression network analysis (WGCNA) of differentially expressed genes (DEGs) identified from four culture conditions. (a) Bar graph showing number of genes present in seven identified modules, which are shown in designated colors: "Blue", "Brown", "Greens", "Grey", "Red", "Turquoise" and "Yellow". The bar graph color of bar graph corresponds to the hierarchical cluster tree in ANNEX B Figure S9.b, each color specific to a module. (b) Co-expression network analysis of genes involved in phenylpropanoid & AAs biosynthesis (orange, circular), auxin-inducible genes (pink, lozenge), transcription factors (grey, hexagonal), photosynthesis related genes (green, rectangular) and other genes present in modules turquoise. For network analysis, gene having Spearman correlation > 0.8 and p-value < 0.05 were selected from the turquoise module.

2.4 Discussion

To boost the production of specialized metabolites *in planta* or in heterologous hosts, it is essential to uncover the conditions that trigger their production and to understand their biosynthetic route. Accumulation of AAs is affected by the type of tissue, and both, biotic and abiotic stresses. For example, light exposure affects growth and development, as well as the synthesis and accumulation of specialized metabolites in plants, as shown in studies in *Leucojum aestivum* L. and *Lycoris longituba* (Li, Xu et al. 2021, Moranska, Simlat et al. 2023). In addition, phytohormones play a critical role in tissue differentiation and growth. Auxins promote cell elongation and control a variety of functions, including organogenesis, general shoot and root architecture, responses to light and gravity, and tropic growth (Woodward and Bartel 2005, Ptak, Tahchy et al. 2013, Khadr, Wang et al. 2020). Recently, the effect of different levels of NAA on the tissue differentiation of *Narcissus pseudonarcissus* cv. Carlton was reported, and it was shown that the synthesis and accumulation of AAs vary with the type of tissue (Ferdausi, Chang et al. 2020). Indeed, these factors are easily manipulated in *in vitro* cultures, which also enable the fine-tuning of alkaloid production and related gene expression analysis (Gallego, Rojas et al. 2018). Complementarily, comparative transcriptomics and targeted metabolomics studies of *in vitro* cultures can uncover genes associated with biosynthesis of specific metabolites of interest (Kilgore, Augustin et al. 2014, Wang, Xu et al. 2016, Singh and Desgagne-Penix 2017). Because AAs profile is usually less diversified than *in planta, in vitro* cultures have the advantage to provide a template with a more focused pathway and less background noise. Therefore, as first aim in this study, we developed *in vitro* tissue culture to study the effect of light and auxin and to understand the AAs biosynthetic route in *C.* x *powellii* "Album" at both, the metabolomic and the transcriptomic levels.

C. x *powellii* "Album" shows a close relationship with the South-African clade of *Crinum* species, including *C. bulbispermum*, *C. stuhlmannii* and *C. moorei*. This phylogenetic analysis is consistent with the known origin of *C.* x *powellii* "Album" as a crossing between *C. bulbispermum* (orange river lily) and *C. moorei* (natal lily) (Meerow, Lehmiller et al. 2003). GC-MS analysis revealed that *C.* x *powellii* "Album" methanolic extracts contained lycorine, cherylline and crinine ,as reported previously (Velten, Erdelen et al. 1998, Nino, Hincapie et al. 2007), together with additional AAs. The detection of AAs of lycorine- and crinine-types suggests that AAs biosynthesis in *C.* x *powellii* "Album" follows mainly two types of phenol-oxidative coupling of 4'-*O*-methylnorbelladine, *i.e.*

‘para-para’ and ‘ortho-para’ (Figure 2.1). Indeed, AAs that follow para-ortho’ coupling reactions, such as galanthamine, were not detected. Interestingly, cherylline, an AAs more specifically isolated from *Crinum* species, was detected in all tissues except in leaves extract, suggesting that either cherylline biosynthesis does not occur in this tissue, or it may transfer to and accumulate in other parts of plant.

Since bulbs of *C.* x *powellii* “Album” contained all three ring-types of alkaloids, it was selected as an explant source for tissue culture, starting from twin scale extracted from its inner part, as previously reported (Slabbert, De Bruyn et al. 1993, Priyadharshini, Kannan et al. 2020, Trujillo-Chacon, Pastene-Navarrete et al. 2020, Aleya, Xianmin et al. 2021). The major challenge associated with the development of *in vitro* culture from explants, such as bulbs, is the presence of endophytic contamination. Although disinfection of Amaryllidaceae (*Zephyranthes grandiflora* and *N. tazetta* L.) bulbs has been performed using mercury chloride, this compound is excessively toxic. Here, we performed a heat treatment at 52°C for one hour, followed by ethanol washing and bleach treatment, and no contamination was detected following the initiation of *in vitro* culture. This indicated that our surface sterilization methodology was effective to remove endophytic microorganisms from the explant, in agreement with other reports (Langens-Gerrits, Albers et al. 1998, Ferdausi, Chang et al. 2020, Xu, Li et al. 2020). Another common challenge associated with *in vitro* culture of plants is explant browning, which occurs mainly due to accumulation and oxidation of phenolic compounds (Dixon and Paiva 1995, Ndakidemi, Mneney et al. 2014). Plants produce phenolic compounds in response to stress, such as wounding and changes in culture environment, commonly occurring during the extraction of explant and *in vitro* culture of plant tissues. In our study, browning was specifically observed in callus exposed to light and higher concentration of 2,4-D, which indicated that these conditions may be toxic for newly developing tissue. Previous reports on parental *C. moorei in vitro* culture also showed a higher ratio of explant browning in light condition (Fennell, Elgorashi et al. 2003). Following successful initiation of *in vitro* culture and survival, explants may develop into different tissue. The type of auxin supplied in the culture media impacted the type of tissue generated, and auxin addition was necessary to induce callus, conforming to previous reports (Rahimi Khonakdari, Rezadoost et al. 2020). In the presence of 2,4-D, explants grew as undifferentiated tissue, regardless of its concentration and exposure to light. For light exposed callus supplemented with 2 or 4 mg/L of NAA, shoot generation occurred within 8 weeks, whereas with 8 mg/L NAA, 14 weeks were necessary for tissue differentiation.

For callus that were not exposed to light, tissue differentiation arose on the 10th week of culture when supplied with 2 or 4 mg/L of NAA, however no shoot formation was seen with higher concentrations of NAA, in agreement with other studies on *N. pseudonarcissus* cv. Carlton tissue (Ferdausi, Chang et al. 2020). Our results show that exogenous supply of auxin and light modulate tissue differentiation during *in vitro* culture of *C.* x *powellii* "Album".

Second, we explored the metabolite profiles of different types of tissues developed during *in vitro* culture using GC-MS and LC-MS/MS. The accumulation of AAs was higher in in differentiated tissues as compared to callus, which probably relates to organ-specific biosynthesis of AAs, as reported in *L. aestivum* L. and *C. moorei,* or to the involvement of multiple tissues in AAs biosynthesis (Elgorashi, Drewes et al. 2002, Demir, Yildirim et al. 2022). Furthermore, tissue exposed to light stress were also actively involved in photosynthesis, ,providing access to higher carbon source, which could result in higher AAs accumulation in light condition (Rahimi Khonakdari, Rezadoost et al. 2020, Aleya, Xianmin et al. 2021). Detection of crinamidine, a crinine-type of AAs was surprising, as they were not detected in *in vivo* samples of *C.* x *powellii* "Album" This might indicate that metabolites analysis of native plant may not always be sufficient to reveal its SMs biosynthesis potential. Moreover, plant produce SMs as defensive response to biotic and abiotic response, therefore biosynthesis of SMs such as crinamidine could be related to plant defense response. This suggests that harsh culture condition can be utilized to induce SMs biosynthesis. Furthermore, mature plant organs often maintain their relative cell undifferentiated stage to adjust to different hormonal changes and stress (Ikeuchi, Iwase et al. 2015). Cellular differentiation results in global changes of gene expression patterns, including SMs biosynthesis genes, which is probably related to higher alkaloid content in differentiated tissue as compared to undifferentiated tissue, but also to differential alkaloid profile in newly growing *in vitro* tissue as compared to mature *in vivo* tissue (Bruex, Kainkaryam et al. 2012, Taylor-Teeples, Lin et al. 2015). AAs profile in callus was also distinct between the culture condition (light) and between the type and the concentration of the hormone used. SMs, including phenylpropanoids and AAs, accumulated at higher levels in the light condition compared to dark, regardless of the type of auxin that was used, in keeping with reports in *Agastache rugosa* (Korean mint) (Park, Yeo et al. 2020), and in Amaryllidaceae *L. aestivum* L. and *L. longituba* (Li, Xu et al. 2021, Moranska, Simlat et al. 2023). These results show that *in vitro* tissues of *C.* x *powellii* "Album" conserved a biosynthetic capability that can be manipulated by modifying the culture conditions. Expression of biosynthesis

genes are often regulated by chromatin remodeling which is indeed related to the level of cell differentiation (Ikeuchi, Iwase et al. 2015). Another important factor that can regulate differential alkaloid biosynthesis in different types of tissue is RNA post-modification such alternative splicing of genes (Lam, Wang et al. 2022). However, we observed low abundance of transcript belonging to "RNA processing and modification" as well as "chromatin structure and dynamics" in our assembled transcriptome. These processes, when measured at the proteomic levels, have been associated with increased accumulation of Amaryllidaceae alkaloids, although the mechanism is not known (Tang, Li et al. 2023). Even though, callus produced fewer types of alkaloids, they were responsive to light and 2,4-D, and so could provide a straightforward matrix to resolve the biosynthetic route of specific AAs as compared to RNA-seq data generated from *in vivo* tissues. Hence, the calli were selected as homogenous biological sample for transcriptomic study. Genes related to photosynthesis and involved in tetrapyrrole binding activity were up-regulated in calli exposed to light, regardless of 2,4-D concentration. Increased activity of tetrapyrrole binding helps the plant to adapt under different stress conditions, including excess or lack of light. Oxidoreductase activity and monooxygenase activity were also enriched GO term categories in the light condition. When calli were grown in absence of light, genes related to mannose binding, crucial for plant defense signaling during pathogen attack, were upregulated by increased concentration of 2,4-D (Hwang and Hwang 2011, Ma, Haile et al. 2023). We did not observe any contamination during this study, and to our knowledge, there is no data associating 2,4-D concentration with mannose binding gene expression. This was intriguing, as phenylpropanoids and alkaloids, which are also produced to defend the plant against external stress, accumulated as well in these conditions.

Next, based on homology search, we identified candidate genes including *TYDC*, *C3H*, *PAL*, *HCT*, *OMT*, *NR (NoroRed)*, *NBS*, and *CYP96 (NoroSyn),* which are involved in the phenylpropanoid and AAs biosynthetic pathways. High % (>75%) of amino acid sequence identity with functionally characterized homologous gene from other Amaryllidaceae plant strongly suggests that these genes encode enzymes involved AAs pathway. However, the biosynthesis route of many AAs such as methylated norbelladine, is still not uncovered, (Li, Qiao et al. 2019). We identified *CYP96* candidates in *C.* x *powellii* "Album" transcriptome together with alkaloids resulting fromdifferent phenol-phenol coupling reactions, suggesting that they are indeed involved in the proposed reactions (Kilgore, Holland et al. 2016). Further AAs biosynthesis gene mining from *C. x powelllii*

"Album" transcriptome, and their functional characterization will provide a solid understanding of AAs biosynthesis type. Candidate genes expression levels were higher in calli exposed to light compared to those grown in the dark, and was also modulated by 2,4-D addition. Thus, light and auxins led to an increase in AAs and AAs precursors at both metabolomic and transcriptomic levels. This is probably related to their protective role from the damages caused by light (Winkel-Shirley 2001, Wink 2008). In conditions of light exposure, an increased concentration of 2,4-D led to a decrease in photosynthesis related genes, and an accumulation of transcripts associated with hydrogen peroxide catabolic process and with the apoplast. These genes are related to cell death, indicating that 4 mg/L of 2,4-D in calli exposed to light may be toxic and trigger programmed cell death (Yoda, Yamaguchi et al. 2003, Gupta, Sengupta et al. 2016), in accordance with the observed lower survival of explants and with El Tahchy, Bordage et al. (2011). Alternatively, alkaloid accumulation triggered by light and 2,4-D could be the cause of this toxicity. Indeed, the expression levels of genes related to production of phenylpropanoid compounds, and AA biosynthetic pathways are interconnected with each other, together with photosynthesis-related and hormone-induced genes, linking light and auxin response to their expression. Refining the equilibrium between stress and death appears to be key to optimize alkaloid production.

2.5 Conclusion

As an alternative to native plant sources, biotechnological approaches have been developed to increase the production of plant biomass and yield a sustainable supply of plant-derived compounds, essential to fully explore their biological potential and use them as therapeutic agents (Tallini, Torras-Claveria et al. 2018, Priyadharshini, Kannan et al. 2020, Koirala, Karimzadegan et al. 2022). In this study, we developed *in vitro* cultures of *C*. x *powellii* "Album" with 2,4-D and NAA at three different concentrations, exposed or not to light. We showed that exogenous supply of auxin is necessary for callus induction in *C.* x *powellii* "Album". 2,4-D at 2 mg/L efficiently induces callus formation in this species, whereas different concentrations of NAA promote shoot formation. We detected more AAs in tissues exposed to light compared to those grown in dark, while accumulation of AAs was higher in differentiated tissues. Indeed, light condition promoted the synthesis and accumulation of alkaloids, and differentiated tissues are more suitable for AAs production from *C* x *powellii* "Album". Consistently, transcriptomic studies showed that genes related to stress are upregulated in callus exposed to light, associating the production of SMs to a

protection mechanism against light in *C.* x *powellii* "Album". With optimal selection of growth hormone and culture conditions, *in vitro* tissues can potentially be exploited for the production of AAs in *C.* x *powellii* "Album", including cherylline. The differential transcriptomic data obtained in this study also paves the way to the discovery of cherylline and lycorine pathways, required to bioengineer heterologous microbial hosts to produce these potent molecules.

2.5 Experimental

2.5.1 Plant material and chemical reagents

C. x *powellii* "Album" bulbs (Figure 2.2a) were purchased from commercial market (Phoenix perennials, Canada). Plant growth hormones (2,4-dichlorophenoxyacetic acid (2,4-D), 6-benzylaminopurine (BAP), kinetin, Phytagel, sucrose and plant preservative mixture (PPM) were all purchased from Millipore Sigma (Massachusetts, USA). Murashige and Skoog (MS) medium was from PhytoTech Labs (Kansas, USA). Standards of the alkaloids 11-hydroxyvittatine, 9-O-demethylhomolycorine, cherylline, flexinine, gigancrinine, gigantelline, gigantellinine, haemanthamine, homolycorine, obliquine, pancracine, sanguinine, tazzetine, vittatine and crinine were kindly obtained from Professors Antonio Evidente and Marco Masi (Universitario Monte Sant'Angelo, Naples, Italy). Standards of 3ˈ-*O*-methylnorbelladine, 4ˈ-*O*-methylnorbelladine, 3ˈ4ˈ-*O*-dimethylnorbelladine and norbelladine were synthetized as described in (Girard, Karimzadegan et al. 2022). Standards of 3,4-dihydroxybenzaldehyde (97%), 4-hydroxybenzaldehyde (99%), isovanillic acid (99%), isovanillin (98%) and *trans*-cinnamic acid (98%) were purchased from Acros Organics (Massachusetts, USA). Standards of 3,4-dihydroxybenzoic acid (97%), levodopa (98%), L-tyrosine (99%) and *p*-coumaric acid (98%) were purchased from Alfa Aesar (Massachusetts, USA). Standards of caffeic acid (98%), dopamine (98%), ferulic acid (99%), lycorine (98%), papaverine (98%), tyramine (99%) and vanillin (99%) were procured from Millipore Sigma (Massachusetts, USA). Standards of galanthamine (98%) and narciclasine (98%) were purchased from Tocris Bioscience (Bristol, United Kingdom). Standards of norgalanthamine, lycoramine (97%), coclaurine (95%), isoferulic acid (98%), and phenylalanine 98%) were obtained from Toronto Research Chemicals (Ontario, Canada), US Biological, Musechem (New Jersey, USA), TCI America (Oregon, USA), and MP Biomedicals (California, USA) respectively. Analytical LC-MS grade methanol was purchased from Fisher scientific (New Hampshire, USA)

2.5.2 Genotyping of plant samples

To determine the genotype of the plant sample, total genomic DNA was extracted by using the plant DNA extraction mini kit (Qiagen, Hilden, Germany), according to the manufacturer's protocol, and the quality of genomic DNA was estimated by using Implen nanophotometer (California, United states). Highly conserved internal transcribed spacer 2 (ITS2) region were amplified using gene-specific primers (*i.e* forward primer 5'-ATGCGATACTTGATGTGTGAAT -3' and reverse primer 5'-GACGCTTCTTCTCCAGACTACAAT-3')), with Q5 DNA polymerase (New England Biolab, Massachusetts, USA). The specificity of the amplified region was verified following agarose gel electrophoresis and sequenced using Sanger sequencing at Genome Quebec Innovation Centre (QC, Canada). Phylogenetic analysis was performed by using Neighbor-Joining method in Mega11 software, including ITS2 regions from 10 Crinum species. *Amaryllis belladonna* (Amaryllidaceae family) was used as outgroup(Saitou and Nei 1987, Tamura, Stecher et al. 2021).

2.5.3 Development of *in vitro* culture

Two bulbs of *C.* x *powellii* "Album"of approximately 75 grams were selected and surface sterilized according to Ferdausi *et al.* 2020, with some modifications (Ferdausi, Chang et al. 2020). Briefly, *C.* x *powellii* "Album" bulbs were kept at 4℃ for 4 weeks, and then at room temperature for 24 hours. Leaves, roots, and bulbs were separately flash frozen in liquid nitrogen and kept at -80℃ for further alkaloid analysis. Bulbs underwent a heat treatment at 52℃ for 1 hour and were then kept at room temperature overnight. For surface sterilization, dead and dry scales were removed before bulbs were washed with tap water and detergent five times and dipped into 70% ethanol for 1 minute. Then, bulbs were treated for 30 minutes with commercial bleach containing 6% of sodium hypochlorite. Afterwards, bulbs were washed with autoclaved water five times inside a biological hood. Several layers of bulb scales were removed to reach the inner part of the bulbs. Finally, ~100-120 twin-scale size explants were obtained from each bulb. Untreated bulb, surface sterilized bulb, and example of a twin scale explants are shown in ANNEX B Figure S1.

Basic media was prepared with MS supplemented with 3% of sucrose, 0.075% of PPM, 3 g/L of Phytagel, 0.5 mg/L of BAP, 0.5 mg/L of kinetin and 100 mg/L of yeast extract. The pH was adjusted to 5.7 ± 0.1 before adding phytagel and autoclaving. Plant growth hormones were added after sterilization. This basic media was used as a control to measure the effect of auxin in *C.* x *powellii*

"Album" *in vitro* culture. During the experiment, two different types of auxins, *i.e.,* 2,4-D and NAA, were used at three concentrations, *i.e.,* 2, 4, and 8 mg/L. Five explants were cultured in each plate at 23°C in light conditions (14hs:10hs light:dark, 100 µMol/m^2) or in 24h dark conditions. Explants were sub-cultured every two weeks. Then, the effects of light and auxin on explant's characteristics were recorded. To generate enough sample material, culture was continued for 6 months.

2.5.4 Metabolites extraction

Different types of tissues from native plant (young leaves, bulbs, basal plates and roots) and from *in vitro* culture tissue, *i.e*., callus and differentiated tissues, were selected for alkaloid analysis. Samples were grounded into a fine powder upon addition of liquid nitrogen using a pestle and mortar. Then, crude alkaloids were extracted with 1 mL of methanol per 100 mg of plant sample with continued shaking for 24 hs, followed by sonication for 30 min at room temperature. Extracts were centrifuged at 5000 g for 10 min, and supernatants were transferred into a new falcon tube and completely evaporated using Thermo Scientific Savant SPD1010 SpeedVac Concentrator (Massachusetts, USA). Samples were resuspended in LC-MS/MS grade methanol (100 µL per 100 mg of the initial sample) by sonication, then centrifugated at 10 000g for 10 min and filtered through 0.22 µM nylon filter.

2.5.5 Metabolites constituents analysis by GC-MS

For GC-MS analysis, *in vivo* tissues and *in vitro* samples were resuspended in LC-MS/MS grade methanol (100 µL per 100 mg of initial sample) and were directly injected into the GC-MS (Agilent Technologies 6890N GC coupled with 5973N inert MSD) in EI (Electron Ionization) mode at 70 eV. The temperature ramp was done as follows: temperature was set at 100°C for 2 min, followed by 100–180°C at 15°C min^{-1}, 180–300°C at 5°C min^{-1}, and a 10 min hold at 300°C. Injector and detector temperatures were set at 250°C and 280°C, respectively, and the flow rate of carrier gas (He) was 1 $mL.min^{-1}$. The GC column was an Agilent J&W DB-5Ms Ultra Inert Column (30 m x 0.25 mm x 0.25 µM, Agilent technology, Santa Clara, USA). A split ratio of 1:10 was applied, and the injection volume was 1 µL. Alkaloids were identified by comparison with the 2005 National Institute of Standards (NIST) database based on matching mass spectra, GC-MS spectra of authentic compounds previously isolated and identified by other spectroscopic methods in these

species, or with data obtained from the literature. All raw GC-MS experimental data were deposited in MetaboLights database (http://www.ebi.ac.uk/metabolights) (accession number: MTBLS8511) (Haug, Cochrane et al. 2020).

2.5.6 Targeted metabolite analysis by LC-MS/MS

Targeted metabolite analysis for AAs precursor molecules and AAs were performed on *in vitro* tissue. A high-performance liquid chromatography (HPLC) coupled with a tandem mass spectrometer (MS/MS) (Agilent, QC, Canada) equipped with an Agilent Jet Stream ionization source, a Kinetex EVO C18 column (150 x 4.6 mm, 5 µm, 100 Å; Phenomenex, Torrance, USA), a binary pump, an autosampler set at 4°C and a column compartment were used for the analyses. Five µl of each sample were injected into the column that was set at 30°C. A gradient made of (A) formic acid 0.1% v/v in milli-Q water and (B) methanol, with a flow rate of 0.4 mL/min, was used to achieve chromatographic separation. The HPLC elution program started with 10% solvent B; 0-10 min, isocratic conditions with 10% B; 10-20 min, linear gradient to reach 100% B; 20-25 min, isocratic conditions with 100% B; 25-26 min, linear gradient to return to initial conditions of 10% B. The total run time was 30 min per sample to allow the reconditioning of the column prior to the next injection. The parameters used for the MS/MS source to perform the analyses were set as follows: gas flow rate 10 L/min, gas temperature 300°C, nebulizer 45 psi, sheath gas flow 11 L/min, sheath gas temperature 300°C, capillary voltage 4000 V in ESI+ and 3500 V in ESI– and nozzle voltage 500 V. Agilent MassHunter Data Acquisition (version 1.2) was used to control the HPLC-MS/MS, MassHunter Qualitative Analysis (version 10.0) and MassHunter Quantitative QQQ Analysis (version 10.0) were used for data processing. MRM transitions and instrument parameters used in ESI+ for identification of target compound during LC-MS/MS analysis are included in ANNEX B Table S2.

2.5.7 Total RNA extraction, de novo transcriptomic assembly, and functional annotation

Total RNA was extracted from different plant organs (roots, bulbs, basal plate, and leaves) and from in vitro tissues (callus developed with 2 mg/L and 4 mg/L of 2,4-D in light and dark conditions). For in vitro tissues, RNA was extracted by using a Qiagen RNeasy Plant Mini kit (Hildon, Germany), using approximately 100 mg callus samples according to the manufacturer's protocol. For in vivo tissues, total RNA was extracted using the method described in Meisel,

Fonseca et al. (2005). Briefly, 1 g (fresh weight) of *in vivo* tissues were homogenized and the powder was transferred to a tube containing 5 mL of extraction buffer (20 mg/ml CTAB,100 mM of Tris-HCL pH 8, 20 mM EDTA, 1.4 M NaCl, 10 mg/ml of polyvinylpyrrodine, 100 µL of β-mercaptoethanol and 50 µl of spermidine trihydrochloride) at 65 °C. After agitation, extraction of nucleic acids was performed twice with chloroform:isoamyl alcohol 24:1. RNA was precipitated overnight with 0.25x of 10M LiCl at 4ºC. After centrifugation at 12 000 g for 35 min at room temperature, the pellet was resuspended in 0.5 mL of DEPC-treated H_2O. Another extraction was performed with chloroform:isoamyl alcohol 24:1, and after centrifugation at 14 000g for 30 min at 4ºC, RNA was precipitated in the aqueous phase by adding 1 mL of 100% ice cold ethanol and incubating for 30 min at -80ºC. After centrifugation at 14 000 g for 20 min at 4ºC, the pellet was washed with 1 mL of 75% ethanol. Finally, RNA pellet was resuspended in 50 µL of DEPC-treated H_2O. Three independent biological replicates from each sample *type were used for transcriptomic analysis,* except for callus obtained in dark conditions with 2 mg/L of 2,4-D (n=2), for which one sample was rejected due to low RNA quality.

The mRNA was converted into a cDNA library and sequenced through Illumina NovaSeq 6000, sequencing system, with paired-end reads of 100bp, at Genome Quebec Innovation Centre (Montreal, QC, Canada). Raw reads were analyzed using FastQC (v0.11.9) for quality control (Conesa, Madrigal et al. 2016) and visualized with MultiQC (v1.13). The quality trimming was performed using modified Fastp (v0.23.1) software with cut front mean quality 20, cut tail mean quality 20 and length required 50. Then *de novo* transcriptomic assembly of all the generated clean reads was performed with Trinity assembler (v2.14.0) using default parameters. The completeness of the transcriptome assembly was assessed with BUSCO (v5.2.2) using embryophyte_odb_10. The coding regions were predicted using TransDecoder (version 5.5.0) (http://transdecoder.github.io/). The longest open reading frames (ORFs) obtained were functionally annotated with Trinotate pipeline (version 2.0) (http://trinotate.github.io/) (Bryant, Johnson et al. 2017). Briefly, the assembled *C*. x *powellii* "Album" transcriptome was searched against the UniProt database (release 2022_04) using blastp and blastx (blast+ v2.12.0) with e-value threshold of 1e-5 to identify homologous proteins. Putative signal peptides were predicted with SignalP (v4.1) and conserved protein domains were identified with HMMER (v3.3.2) using Pfam-A database (v3.1b2). The gene ontology (GO) of the annotated transcripts was extracted to illustrate the ten most abundant GO terms of each category (molecular function, cellular

component, and biological process). Assigned Clusters of Orthologous Genes (COGs) id was used to identify the COG annotation using cog-20 and fun-20 (https://ftp.ncbi.nih.gov/pub/COG/COG2020/data) (Galperin, Wolf et al. 2021). Candidates annotated gene transcript sequences were deposited in GenBank with the accession numbers listed in ANNEX Table S5 (supply as excel file in original scientific article).

2.5.8 Differential gene expression analysis, putative Amaryllidaceae alkaloids gene identification and co-expression analysis

Clean reads were aligned to the assembled transcriptome, and the read count per gene was determined for each sample using RSEM software v1.3.3 (Li and Dewey 2011). The raw read counts per gene was used to analyse differential expression with the R (4.2.2) package DESeq2 (Anders and Huber 2012) using default parameters and genes $|\log_2(\text{fold change})| > 2$ at an adjusted p-value ≤ 0.05 were considered as significantly deregulated. Gene ontology enrichment analysis was further performed on differentially expressed genes (DEGs) sets.

To identify the putative genes encoding the enzymes involved in the phenylpropanoid pathways, and AAs pathways local blast search was performed. Local Blastx was performed by using from assemble transcriptome data of *C.* x *powellii* "Album" and characterized genes were used as query with blast+ version 2.13.0.

Furthermore, to understand the expression pattern of genes related to phenylpropanoid and AAs pathways, and with auxin photosynthesis, Highly co-expressed gene modules were inferred from the DEGs generated with *in vitro* and *in vivo* tissue samples using the R package WGCNA (Langfelder and Horvath 2008).. Prior to the WGCNA analysis, selected gene sets were filtered for outlier samples and for raw count value greater than 10 in 50% of sample. The soft thresholding power β of 14 was selected to make the networks exhibit an approximate scale-free topology (ANNEX B Figure S7a). Co-expression modules were identified using the blockwiseModules function and the Dynamic Tree Cut algorithm with minimum module size 30, a branch merge cut-off height of 0.25 and "signed" TOMtypes (Zhan, Thakare et al. 2015). All genes were hierarchically clustered based on TOMsimilarity, and a gene dendrogram was produced. The module that encompassed phenylpropanoid and AAs biosynthesis genes was selected for further analysis. Spearman correlation was calculated for each pair of genes present in the module of

interest. Genes having correlation > 0.8 with *p*-value 0.05 were selected for network visualization by Cytoscape 3.9.1. Genes were annotated as auxin inducible genes, photosynthesis related genes and transcription factors on the basis trinotate file generated during this study.Finally, GraphPad Prism v10.0.2 (GraphPad software LLC) was used to generate Figure 2.5, ANNEX B Figure S4, ANNEX B Figure S8 and the associated statistics.

2.6 References

Abd el Hafiz, M. A., Ramadan, M. A., Jung, M. L., Beck, J. P., Anton, R., 1991. Cytotoxic activity of Amaryllidaceae alkaloids from *Crinum augustum* and *Crinum bulbispermum*. Planta Med. 57, 437-439. https://doi.org/10.1055/s-2006-960144.

Aleya, F., Xianmin, C., Anthony, H., Meriel, J., 2021. Relative expression of putative genes involved in galanthamine and other Amaryllidaceae alkaloids biosynthesis in *Narcissus* field and in vitro tissues. Gene. 774, 145424. https://doi.org/10.1016/j.gene.2021.145424.

Anders, S., Huber, W., 2012. Differential expression of RNA-Seq data at the gene level–the DESeq package. Heidelberg, Germany: European Molecular Biology Laboratory (EMBL). 10, f1000research.

Brossi, A., Grethe, G., Teitel, S., Wildman, W. C., Bailey, D. T., 2002. Cherylline, a 4-phenyl-1,2,3,4-tetrahydroisoquinoline alkaloid. The Journal of Organic Chemistry. 35, 1100-1104. https://doi.org/10.1021/jo00829a052.

Bruex, A., Kainkaryam, R. M., Wieckowski, Y., Kang, Y. H., Bernhardt, C., Xia, Y., Zheng, X., Wang, J. Y., Lee, M. M., Benfey, P., Woolf, P. J., Schiefelbein, J., 2012. A gene regulatory network for root epidermis cell differentiation in *Arabidopsis*. PLoS Genet. 8, e1002446. https://doi.org/10.1371/journal.pgen.1002446.

Bryant, D. M., Johnson, K., DiTommaso, T., Tickle, T., Couger, M. B., Payzin-Dogru, D., Lee, T. J., Leigh, N. D., Kuo, T. H., Davis, F. G., Bateman, J., Bryant, S., Guzikowski, A. R., Tsai, S. L., Coyne, S., Ye, W. W., Freeman, R. M., Jr., Peshkin, L., Tabin, C. J., Regev, A., Haas, B. J., Whited, J. L., 2017. A Tissue-Mapped Axolotl De Novo Transcriptome Enables Identification of Limb Regeneration Factors. Cell Rep. 18, 762-776. https://doi.org/10.1016/j.celrep.2016.12.063.

Conesa, A., Madrigal, P., Tarazona, S., Gomez-Cabrero, D., Cervera, A., McPherson, A., Szczesniak, M. W., Gaffney, D. J., Elo, L. L., Zhang, X., Mortazavi, A., 2016. A survey of best practices for RNA-seq data analysis. Genome Biol. 17, 13. https://doi.org/10.1186/s13059-016-0881-8.

Demir, S. C., Yildirim, A. B., Turker, A. U., Eker, I., 2022. Seasonal variation in alkaloid content, phenolic constituent and biological activities of some *Leucojum aestivum* L. populations in Turkey. South African Journal of Botany. 147, 713-723. https://doi.org/10.1016/j.sajb.2022.03.004.

Dereeper, A., Guignon, V., Blanc, G., Audic, S., Buffet, S., Chevenet, F., Dufayard, J. F., Guindon, S., Lefort, V., Lescot, M., Claverie, J. M., Gascuel, O., 2008. Phylogeny.fr: robust phylogenetic analysis for the non-specialist. Nucleic Acids Res. 36, W465-469. https://doi.org/10.1093/nar/gkn180.

Desgagné-Penix, I., 2020. Biosynthesis of alkaloids in Amaryllidaceae plants: a review. Phytochemistry Reviews. 20, 409-431. https://doi.org/10.1007/s11101-020-09678-5.

Dewick, P. M., 2009. Medicinal natural products: a biosynthetic approach. John Wiley and Sons Ltd.

Dixon, R. A., Paiva, N. L., 1995. Stress-Induced Phenylpropanoid Metabolism. Plant Cell. 7, 1085-1097. https://doi.org/10.1105/tpc.7.7.1085.

El Tahchy, A., Bordage, S., Ptak, A., Dupire, F., Barre, E., Guillou, C., Henry, M., Chapleur, Y., Laurain-Mattar, D., 2011. Effects of sucrose and plant growth regulators on acetylcholinesterase inhibitory activity of alkaloids accumulated in shoot cultures of Amaryllidaceae. Plant Cell, Tissue and Organ Culture (PCTOC). 106, 381-390. https://doi.org/10.1007/s11240-011-9933-7.

Elgorashi, E. E., Drewes, S. E., Van Staden, J., 2002. Organ-to-organ and seasonal variation in alkaloids from *Crinum macowanii*. Fitoterapia. 73, 490-495. https://doi.org/10.1016/s0367-326x(02)00164-8.

Fennell, C. W., Elgorashi, E. E., van Staden, J., 2003. Alkaloid production in *Crinum moorei* cultures. J Nat Prod. 66, 1524-1526. https://doi.org/10.1021/np030206o.

Fennell, C. W., van Staden, J., 2001. *Crinum* species in traditional and modern medicine. J Ethnopharmacol. 78, 15-26. https://doi.org/10.1016/s0378-8741(01)00305-1.

Ferdausi, A., Chang, X., Hall, A., Jones, M., 2020. Galanthamine production in tissue culture and metabolomic study on Amaryllidaceae alkaloids in *Narcissus pseudonarcissus* cv. Carlton. Industrial Crops and Products. 144, 112058. https://doi.org/10.1016/j.indcrop.2019.112058.
Gaba, V. P., 2005. Plant growth regulators in plant tissue culture and development. Plant development and biotechnology. CRC Press Boca Raton, FL, pp. 87-99.
Gallego, A. M., Rojas, L. F., Parra, O., Rodriguez, H. A., Mazo Rivas, J. C., Urrea, A. I., Atehortua, L., Fister, A. S., Guiltinan, M. J., Maximova, S. N., Pabon-Mora, N., 2018. Transcriptomic analyses of cacao cell suspensions in light and dark provide target genes for controlled flavonoid production. Sci Rep. 8, 13575. https://doi.org/10.1038/s41598-018-31965-7.
Galperin, M. Y., Wolf, Y. I., Makarova, K. S., Vera Alvarez, R., Landsman, D., Koonin, E. V., 2021. COG database update: focus on microbial diversity, model organisms, and widespread pathogens. Nucleic Acids Res. 49, D274-D281. https://doi.org/10.1093/nar/gkaa1018.
Girard, M. P., Karimzadegan, V., Heneault, M., Cloutier, F., Berube, G., Berthoux, L., Merindol, N., Desgagne-Penix, I., 2022. Chemical Synthesis and Biological Activities of Amaryllidaceae Alkaloid Norbelladine Derivatives and Precursors. Molecules. 27, 5621. https://doi.org/10.3390/molecules27175621.
Gupta, K., Sengupta, A., Chakraborty, M., Gupta, B., 2016. Hydrogen Peroxide and Polyamines Act as Double Edged Swords in Plant Abiotic Stress Responses. Front Plant Sci. 7, 1343. https://doi.org/10.3389/fpls.2016.01343.
Haug, K., Cochrane, K., Nainala, V. C., Williams, M., Chang, J., Jayaseelan, K. V., O'Donovan, C., 2020. MetaboLights: a resource evolving in response to the needs of its scientific community. Nucleic Acids Res. 48, D440-D444. https://doi.org/10.1093/nar/gkz1019.
Hotchandani, T., de Villers, J., Desgagne-Penix, I., 2019. Developmental Regulation of the Expression of Amaryllidaceae Alkaloid Biosynthetic Genes in *Narcissus papyraceus*. Genes (Basel). 10, 594. https://doi.org/10.3390/genes10080594.
Hu, J., Li, W., Liu, Z., Zhang, G., Luo, Y., 2021. Molecular cloning and functional characterization of tyrosine decarboxylases from galanthamine-producing *Lycoris radiata*. Acta Physiologiae Plantarum. 43, 84. https://doi.org/10.1007/s11738-021-03258-6.
Hwang, I. S., Hwang, B. K., 2011. The pepper mannose-binding lectin gene CaMBL1 is required to regulate cell death and defense responses to microbial pathogens. Plant physiology. 155, 447-463.
Ieven, M., Vlietinck, A. J., Vanden Berghe, D. A., Totte, J., Dommisse, R., Esmans, E., Alderweireldt, F., 1982. Plant antiviral agents. III. Isolation of alkaloids from Clivia miniata Regel (Amaryllidaceae). J Nat Prod. 45, 564-573. https://doi.org/10.1021/np50023a009.
Ikeuchi, M., Iwase, A., Sugimoto, K., 2015. Control of plant cell differentiation by histone modification and DNA methylation. Curr Opin Plant Biol. 28, 60-67. https://doi.org/10.1016/j.pbi.2015.09.004.
Jacobowitz, J. R., Weng, J. K., 2020. Exploring Uncharted Territories of Plant Specialized Metabolism in the Postgenomic Era. Annu Rev Plant Biol. 71, 631-658. https://doi.org/10.1146/annurev-arplant-081519-035634.
Jin, Z., Yao, G., 2019. Amaryllidaceae and Sceletium alkaloids. Nat Prod Rep. 36, 1462-1488. https://doi.org/10.1039/c8np00055g.
Ka, S., Masi, M., Merindol, N., Di Lecce, R., Plourde, M. B., Seck, M., Gorecki, M., Pescitelli, G., Desgagne-Penix, I., Evidente, A., 2020. Gigantelline, gigantellinine and gigancrinine, cherylline- and crinine-type alkaloids isolated from *Crinum jagus* with anti-acetylcholinesterase activity. Phytochemistry. 175, 112390. https://doi.org/10.1016/j.phytochem.2020.112390.
Ka, S., Merindol, N., Seck, I., Ricard, S., Diop, A., Boye, C. S. B., Landelouci, K., Daoust, B., Berthoux, L., Pepin, G., Seck, M., Desgagne-Penix, I., 2021a. Biological Investigation of Amaryllidaceae Alkaloid Extracts from the Bulbs of *Pancratium trianthum* Collected in the Senegalese Flora. Molecules. 26, 7382. https://doi.org/10.3390/molecules26237382.

Ka, S., Merindol, N., Sow, A. A., Singh, A., Landelouci, K., Plourde, M. B., Pepin, G., Masi, M., Di Lecce, R., Evidente, A., Seck, M., Berthoux, L., Chatel-Chaix, L., Desgagne-Penix, I., 2021b. Amaryllidaceae Alkaloid Cherylline Inhibits the Replication of Dengue and Zika Viruses. Antimicrob Agents Chemother. 65, e0039821. https://doi.org/10.1128/AAC.00398-21.
Khadr, A., Wang, G. L., Wang, Y. H., Zhang, R. R., Wang, X. R., Xu, Z. S., Tian, Y. S., Xiong, A. S., 2020. Effects of auxin (indole-3-butyric acid) on growth characteristics, lignification, and expression profiles of genes involved in lignin biosynthesis in carrot taproot. PeerJ. 8, e10492. https://doi.org/10.7717/peerj.10492.
Kilgore, M. B., Augustin, M. M., Starks, C. M., O'Neil-Johnson, M., May, G. D., Crow, J. A., Kutchan, T. M., 2014. Cloning and characterization of a norbelladine 4'-O-methyltransferase involved in the biosynthesis of the Alzheimer's drug galanthamine in Narcissus sp. aff. pseudonarcissus. PLoS One. 9, e103223. https://doi.org/10.1371/journal.pone.0103223.
Kilgore, M. B., Holland, C. K., Jez, J. M., Kutchan, T. M., 2016. Identification of a Noroxomaritidine Reductase with Amaryllidaceae Alkaloid Biosynthesis Related Activities. J Biol Chem. 291, 16740-16752. https://doi.org/10.1074/jbc.M116.717827.
Koirala, M., Karimzadegan, V., Liyanage, N. S., Merindol, N., Desgagne-Penix, I., 2022. Biotechnological Approaches to Optimize the Production of Amaryllidaceae Alkaloids. Biomolecules. 12, 893. https://doi.org/10.3390/biom12070893.
Lam, P. Y., Wang, L., Lo, C., Zhu, F. Y., 2022. Alternative Splicing and Its Roles in Plant Metabolism. Int J Mol Sci. 23. https://doi.org/10.3390/ijms23137355.
Langens-Gerrits, M., Albers, M., De Klerk, G.-J., 1998. Hot-water treatment before tissue culture reduces initial contamination in *Lilium* and *Acer*. Plant Cell, Tissue and Organ Culture. 52, 75-77.
Langfelder, P., Horvath, S., 2008. WGCNA: an R package for weighted correlation network analysis. BMC Bioinformatics. 9, 559. https://doi.org/10.1186/1471-2105-9-559.
Lewis, J. R., 1996. Amaryllidaceae and Sceletium alkaloids. Natural Product Reports. 13, 171-176. https://doi.org/10.1039/np9961300171.
Li, B., Dewey, C. N., 2011. RSEM: accurate transcript quantification from RNA-Seq data with or without a reference genome. BMC Bioinformatics. 12, 323. https://doi.org/10.1186/1471-2105-12-323.
Li, Q., Xu, J., Yang, L., Sun, Y., Zhou, X., Zheng, Y., Zhang, Y., Cai, Y., 2021. LED Light Quality Affect Growth, Alkaloids Contents, and Expressions of Amaryllidaceae Alkaloids Biosynthetic Pathway Genes in *Lycoris longituba*. Journal of Plant Growth Regulation. 41, 257-270. https://doi.org/10.1007/s00344-021-10298-2.
Li, W., Qiao, C., Pang, J., Zhang, G., Luo, Y., 2019. The versatile O-methyltransferase LrOMT catalyzes multiple O-methylation reactions in amaryllidaceae alkaloids biosynthesis. International journal of biological macromolecules. 141, 680-692.
Lubbe, A., Gude, H., Verpoorte, R., Choi, Y. H., 2013. Seasonal accumulation of major alkaloids in organs of pharmaceutical crop *Narcissus* Carlton. Phytochemistry. 88, 43-53. https://doi.org/10.1016/j.phytochem.2012.12.008.
Ma, L., Haile, Z. M., Sabbadini, S., Mezzetti, B., Negrini, F., Baraldi, E., 2023. Functional characterization of MANNOSE-BINDING LECTIN 1, a G-type lectin gene family member, in response to fungal pathogens of strawberry. J Exp Bot. 74, 149-161. https://doi.org/10.1093/jxb/erac396.
Majhi, B. B., Gélinas, S.-E., Mérindol, N., Desgagné-Penix, I., 2022. Characterization of norbelladine synthase and noroxomaritidine/norcraugsodine reductase reveals a novel catalytic route for the biosynthesis of Amaryllidaceae alkaloids including the Alzheimer's drug galanthamine. bioRxiv. Accepted in Frontiers in Plant Sciences Manuscript ID: 1231809, 2022.2007.2030.502154. https://doi.org/10.1101/2022.07.30.502154.
Martin, S. F., 1988. The Amaryllidaceae alkaloids., The alkaloids, vol. 30. Academic Press, p. 251.

Meerow, A. W., Lehmiller, D. J., Clayton, J. R., 2003. Phylogeny and biogeography of *Crinum* L. (Amaryllidaceae) inferred from nuclear and limited plastid non-coding DNA sequences. Botanical Journal of the Linnean Society. 141, 349-363. https://doi.org/10.1046/j.1095-8339.2003.00142.x.
Meisel, L., Fonseca, B., Gonzalez, S., Baeza-Yates, R., Cambiazo, V., Campos, R., Gonzalez, M., Orellana, A., Retamales, J., Silva, H., 2005. A rapid and efficient method for purifying high quality total RNA from peaches (*Prunus persica*) for functional genomics analyses. Biol Res. 38, 83-88. https://doi.org/10.4067/s0716-97602005000100010.
Moranska, E., Simlat, M., Warchol, M., Skrzypek, E., Waligorski, P., Laurain-Mattar, D., Spina, R., Ptak, A., 2023. Phenolic Acids and Amaryllidaceae Alkaloids Profiles in *Leucojum aestivum* L. In Vitro Plants Grown under Different Light Conditions. Molecules. 28, 1525. https://doi.org/10.3390/molecules28041525.
Nair, J. J., van Staden, J., 2023. Antiviral Effects of the Plant Family Amaryllidaceae. Natural Product Communications. 18, 1934578X231162781. https://doi.org/10.1177/1934578x231162781.
Ndakidemi, C. F., Mneney, E., Ndakidemi, P. A., 2014. Effects of Ascorbic Acid in Controlling Lethal Browning in in Vitro Culture of *Brahylaena huillensis*; Using Nodal Segments. American Journal of Plant Sciences. 05, 187-191. https://doi.org/10.4236/ajps.2014.51024.
Nino, J., Hincapie, G. M., Correa, Y. M., Mosquera, O. M., 2007. Alkaloids of *Crinum x powellii* "Album" (Amaryllidaceae) and their topoisomerase inhibitory activity. Z Naturforsch C J Biosci. 62, 223-226. https://doi.org/10.1515/znc-2007-3-411.
Park, W. T., Yeo, S. K., Sathasivam, R., Park, J. S., Kim, J. K., Park, S. U., 2020. Influence of light-emitting diodes on phenylpropanoid biosynthetic gene expression and phenylpropanoid accumulation in Agastache rugosa. Applied Biological Chemistry. 63, 25. https://doi.org/10.1186/s13765-020-00510-4.
Priyadharshini, S., Kannan, N., Manokari, M., Shekhawat, M. S., 2020. In vitro regeneration using twin scales for restoration of critically endangered aquatic plant *Crinum malabaricum* Lekhak & Yadav: a promising source of galanthamine. Plant Cell, Tissue and Organ Culture (PCTOC). 141, 593-604. https://doi.org/10.1007/s11240-020-01818-1.
Ptak, A., Tahchy, A., Skrzypek, E., Wójtowicz, T., Laurain-Mattar, D., 2013. Influence of auxins on somatic embryogenesis and alkaloid accumulation in *Leucojum aestivum* callus. Open Life Sciences. 8, 591-599. https://doi.org/10.2478/s11535-013-0160-y.
Rahimi Khonakdari, M., Rezadoost, H., Heydari, R., Mirjalili, M. H., 2020. Effect of photoperiod and plant growth regulators on in vitro mass bulblet proliferation of *Narcissus tazzeta* L. (Amaryllidaceae), a potential source of galantamine. Plant Cell Tissue Organ Culture. 142, 187-199. https://doi.org/10.1007/s11240-020-01853-y.
Rates, S. M. K., 2001. Plants as source of drugs. Toxicon. 39, 603-613. https://doi.org/10.1016/s0041-0101(00)00154-9.
Refaat, J., Kamel, M. S., Ramadan, M. A., Ali, A. A., 2012. *Crinum*; an endless source of bioactive principles: a review. Part III; *Crinum* alkaloids: Belladine-, galanthamine-, lycorenine-, tazettine-type alkaloids and other minor types. International Journal of Pharmaceutical Sciences and Research. 3, 3630. https://doi.org/10.13040/IJPSR.0975-8232.3(10).3630-38.
Saitou, N., Nei, M., 1987. The neighbor-joining method: a new method for reconstructing phylogenetic trees. Mol Biol Evol. 4, 406-425. https://doi.org/10.1093/oxfordjournals.molbev.a040454.
Singh, A., Desgagne-Penix, I., 2015. Chapter 3 : Biosynthesis of Amaryllidaceae alkaloids: A biochemical outlook. In: Alkaloids: Biosynthesis, Biological Roles and Health benefits. Nova Science Publishers.
Singh, A., Desgagne-Penix, I., 2017. Transcriptome and metabolome profiling of *Narcissus pseudonarcissus* 'King Alfred' reveal components of Amaryllidaceae alkaloid metabolism. Sci Rep. 7, 17356. https://doi.org/10.1038/s41598-017-17724-0.
Singh, A., Massicotte, M. A., Garand, A., Tousignant, L., Ouellette, V., Berube, G., Desgagne-Penix, I., 2018. Cloning and characterization of norbelladine synthase catalyzing the first committed reaction in

Amaryllidaceae alkaloid biosynthesis. BMC Plant Biol. 18, 338. https://doi.org/10.1186/s12870-018-1570-4.
Slabbert, M., De Bruyn, M., Ferreira, D., Pretorius, J., 1993. Regeneration of bulblets from twin scales of *Crinum macowanii* in vitro. Plant cell, tissue and organ culture. 33, 133-141. https://doi.org/10.1007/BF01983226.
Tallini, L. R., Osorio, E. H., Santos, V. D. D., Borges, W. S., Kaiser, M., Viladomat, F., Zuanazzi, J. A. S., Bastida, J., 2017. *Hippeastrum reticulatum* (Amaryllidaceae): Alkaloid Profiling, Biological Activities and Molecular Docking. Molecules. 22, 4901. https://doi.org/10.3390/molecules22122191.
Tallini, L. R., Torras-Claveria, L., Borges, W. S., Kaiser, M., Viladomat, F., Zuanazzi, J. A. S., Bastida, J., 2018. N-oxide alkaloids from *Crinum amabile* (Amaryllidaceae). Molecules. 23, 1277. https://doi.org/10.3390/molecules23061277.
Tamura, K., Stecher, G., Kumar, S., 2021. MEGA11: Molecular Evolutionary Genetics Analysis Version 11. Mol Biol Evol. 38, 3022-3027. https://doi.org/10.1093/molbev/msab120.
Tang, M., Li, C., Zhang, C., Cai, Y., Zhang, Y., Yang, L., Chen, M., Zhu, F., Li, Q., Li, K., 2023. SWATH-MS-Based Proteomics Reveals the Regulatory Metabolism of Amaryllidaceae Alkaloids in Three *Lycoris* Species. Int J Mol Sci. 24. https://doi.org/10.3390/ijms24054495.
Taylor-Teeples, M., Lin, L., de Lucas, M., Turco, G., Toal, T. W., Gaudinier, A., Young, N. F., Trabucco, G. M., Veling, M. T., Lamothe, R., Handakumbura, P. P., Xiong, G., Wang, C., Corwin, J., Tsoukalas, A., Zhang, L., Ware, D., Pauly, M., Kliebenstein, D. J., Dehesh, K., Tagkopoulos, I., Breton, G., Pruneda-Paz, J. L., Ahnert, S. E., Kay, S. A., Hazen, S. P., Brady, S. M., 2015. An *Arabidopsis* gene regulatory network for secondary cell wall synthesis. Nature. 517, 571-575. https://doi.org/10.1038/nature14099.
Tousignant, L., Diaz-Garza, A. M., Majhi, B. B., Gelinas, S. E., Singh, A., Desgagne-Penix, I., 2022. Transcriptome analysis of *Leucojum aestivum* and identification of genes involved in norbelladine biosynthesis. Planta. 255, 30. https://doi.org/10.1007/s00425-021-03741-x.
Trujillo Chacón, L. M., Leiva, H., Zapata Vahos, I. C., Restrepo, D. C., Osorio, E., 2023. Influence of plant growth regulators on in vitro biomass production and biosynthesis of cytotoxic Amaryllidaceae alkaloids in *Caliphuria tenera* Baker. Biocatalysis and Agricultural Biotechnology. 50, 102670. https://doi.org/10.1016/j.bcab.2023.102670.
Trujillo-Chacon, L. M., Pastene-Navarrete, E. R., Bustamante, L., Baeza, M., Alarcon-Enos, J. E., Cespedes-Acuna, C. L., 2020. In vitro micropropagation and alkaloids analysis by GC-MS of Chilean Amaryllidaceae plants: *Rhodophiala pratensis*. Phytochem Anal. 31, 46-56. https://doi.org/10.1002/pca.2865.
Velten, R., Erdelen, C., Gehling, M., Göhrt, A., Gondol, D., Lenz, J., Lockhoff, O., Wachendorff, U., Wendisch, D., 1998. Cripowellin A and B, a novel type of Amaryllidaceae alkaloid from *Crinum powellii*. Tetrahedron Letters. 39, 1737-1740. https://doi.org/10.1016/S0040-4039(98)00057-4.
Wang, R., Xu, S., Wang, N., Xia, B., Jiang, Y., Wang, R., 2016. Transcriptome Analysis of Secondary Metabolism Pathway, Transcription Factors, and Transporters in Response to Methyl Jasmonate in *Lycoris aurea*. Front Plant Sci. 7, 1971. https://doi.org/10.3389/fpls.2016.01971.
Wang, W., Chen, Z.-D., 2007. Generic level phylogeny of Thalictroideae (Ranunculaceae) - implications for the taxonomic status of *Paropyrum* and petal evolution. Taxon. 56, 811-821. https://doi.org/10.2307/25065863.
Wink, M., 2008. Ecological roles of alkaloids. Wiley Online Library, pp. 3-52.
Winkel-Shirley, B., 2001. Flavonoid biosynthesis. A colorful model for genetics, biochemistry, cell biology, and biotechnology. Plant Physiol. 126, 485-493. https://doi.org/10.1104/pp.126.2.485.
Woodward, A. W., Bartel, B., 2005. Auxin: regulation, action, and interaction. Ann Bot. 95, 707-735. https://doi.org/10.1093/aob/mci083.
Xu, J., Li, Q., Yang, L., Li, X., Wang, Z., Zhang, Y., 2020. Changes in carbohydrate metabolism and endogenous hormone regulation during bulblet initiation and development in *Lycoris radiata*. BMC Plant Biol. 20, 180. https://doi.org/10.1186/s12870-020-02394-4.

Yoda, H., Yamaguchi, Y., Sano, H., 2003. Induction of hypersensitive cell death by hydrogen peroxide produced through polyamine degradation in tobacco plants. Plant Physiology. 132, 1973-1981. https://doi.org/10.1104/pp.103.024737.
Zhan, J., Thakare, D., Ma, C., Lloyd, A., Nixon, N. M., Arakaki, A. M., Burnett, W. J., Logan, K. O., Wang, D., Wang, X., Drews, G. N., Yadegari, R., 2015. RNA sequencing of laser-capture microdissected compartments of the maize kernel identifies regulatory modules associated with endosperm cell differentiation. Plant Cell. 27, 513-531. https://doi.org/10.1105/tpc.114.135657.

Chapter III contains a study that presents a functional characterization of norbelladine *O*-methyltransferase from *Narcissus papyraceus*, it includes *in vitro* biochemical characterization, *in vivo* enzymatic assay, subcellular localization, and molecular dynamics studies.

Chapter III

3. Promiscuous norbelladine *O*-methyltransferase from *Narcissus papyraceus* shows regioselective methylation of norbelladine

Manoj Koirala, Natacha Merindol, Vahid Karimzadegan, Sarah-Eve Gelinas, Nuwan Sameera Liyanage, Basanta Lamichhane, Maria Camila Gracia Tobon, Isabel Desgagné-Penix

Manuscript prepared to be submitted in journal of biological chemistry.

Contribution: Manoj Koirala, Natacha Merindol, and Isabel Desgagné-Penix designed the research project. Manoj Koirala performed cloning, enzyme purification, and enzymatic assay. LC-MS/MS was done by Sarah-Eve Gelinas. Manoj Koirala did localization and *in-vivo* enzymatic assay with the help of Vahid Karimzadegan and Basanta Lamichhane. Nuwan Sameera Liyanage provided native plant samples and extracted metabolites, Sarah-Eve Gelinas did LC-MS/MS and data visualization was done by Manoj Koirala. qRT-PCR was done by Maria Camila Gracia Tobon with the help of Nuwan Sameera Liyanage and Natacha Merindol. Natacha Merindol performed protein docking and molecular dynamic studies. Mano Koirala and Natacha Merindol wrote the manuscript. Sarah-Eve Gélinas, Natacha Merindol, and Isabel Desgagné-Penix revised the manuscript. Manoj Koirala did the experiments with supervision of Natacha Merindol and Isabel Desgagné-Penix.

3.1 Abstract

Amaryllidaceae alkaloids (AAs) are a diverse group of alkaloids exclusively reported from the Amaryllidaceae plant family. *In planta*, their biosynthesis is still not fully characterized. However, a labeling study established 4′-*O*-methylnorbelladine as the key intermediate compound of the pathway. Previous studies have characterized different *O*-methyltransferases from several species of the Amaryllidaceae plant family. Nevertheless, the formation of the different *O*-methylnorbelladine derivatives (3′-*O*-methylnorbelladine, 4′-*O*-methylnorbelladine, and 3′4′-*O*-dimethylnorbelladine), the role, and the preferred substrates of *O*-methyltransferases are not clearly understood. In this study, we characterized the norbelladine *O*-methyltransferase from *Narcissus papyraceus* (*Np*OMT) and showed that it methylates preferentially norbelladine at the 4′-OH position but also yields 3′,4′-*O*-dimethylnorbelladine as a minor product during *in vitro* enzymatic assay. In addition, *Np*OMT methylated norbelladine regioselectively at the 4′-OH position in a heterologous cellular environment. Interestingly, we show that *Np*OMT can also methylate 3,4-dihydroxybenzoylaldehyde and caffeic acid in a non-regiospecific manner to produce meta/para monomethylated products. This study reveals a novel catalytic potential of *O*-methyltransferase from the Amaryllidaceae plant and its ability to regioselectively methylate norbelladine in the heterologous host *Nicotiana benthamiana*.

3.2 Introduction

Amaryllidaceae plants are ornamentally and medicinally important perennial herbaceous plants that have been used in traditional medicine for a long time (Jin and Yao 2019). Phytochemical analysis showed the presence of various types of structurally diverse Amaryllidaceae alkaloids (AAs), many of which possess significant pharmacological value (Hotchandani and Desgagne-Penix 2017). Common AAs include galanthamine, a specific, competitive, and reversible acetylcholinesterase inhibitor used in the management and treatment of Alzheimer's disease early symptoms (Olin and Schneider 2002), and antiviral AAs lycorine and cherylline (Chen, Lao et al. 2020, Ka, Merindol et al. 2021). Although extensive research has been carried out to explore phytochemical content and medicinal potential of Amaryllidaceae plants, less information is available on AAs metabolism and regulation. A proposed AAs biosynthetic pathway has been built

based on radiolabeling studies and enzyme characterization experiments (Desgagné-Penix 2021). All AAs are derived from the aromatic amino acids L-phenylalanine and L-tyrosine, which are respectively transformed into 3,4-dihydroxybenzaldehyde (3,4-DHBA), and tyramine (Figure 3.1). The condensation and reduction of 3,4-DHBA and tyramine catalyzed by norbelladine synthase (NBS) and/or norcraugsodine reductase (NR) generates norbelladine, the universal common intermediate of AAs (Kilgore, Holland et al. 2016, Singh, Massicotte et al. 2018, Tousignant, Diaz-Garza et al. 2022, Majhi, Gélinas et al. 2023).

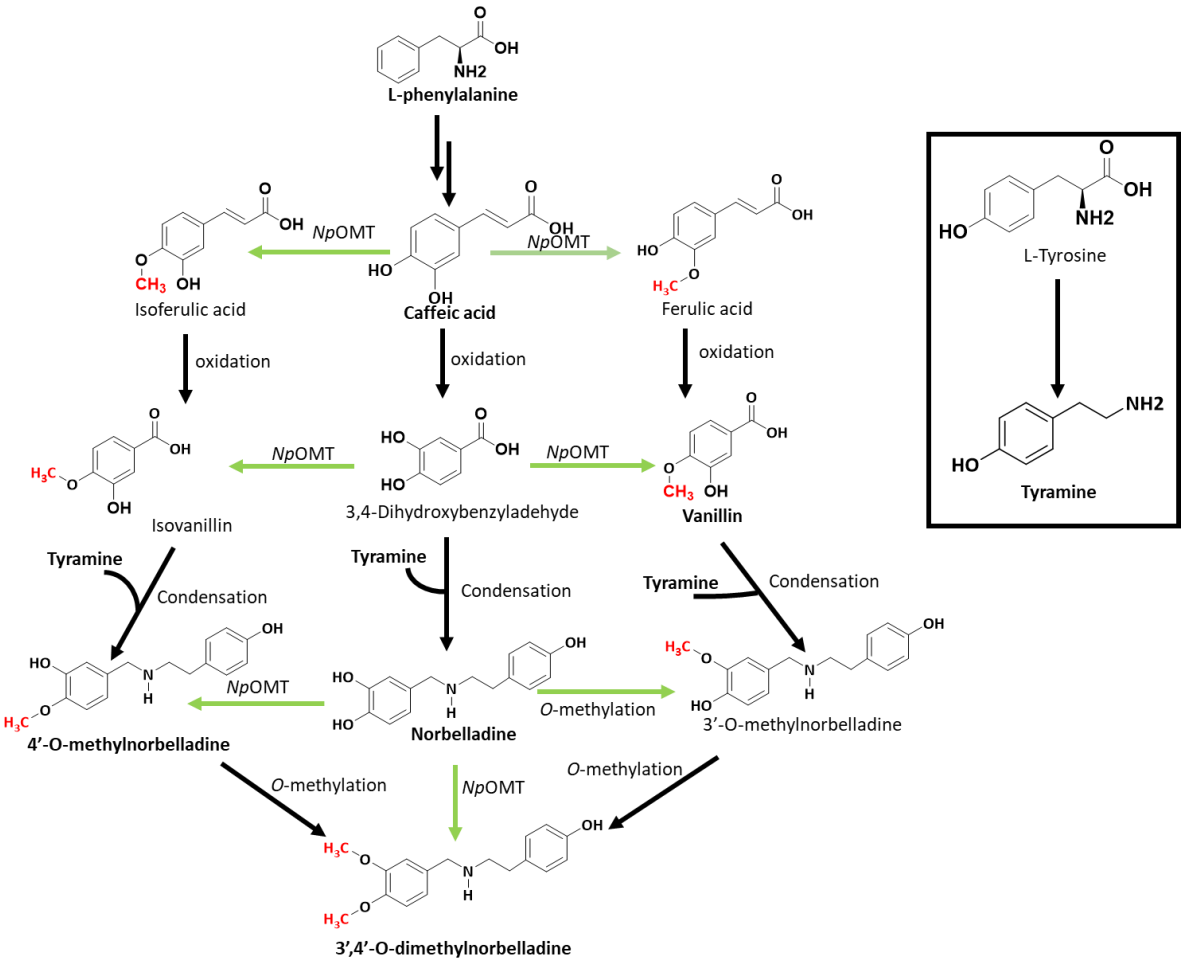

Figure 3.1 Schematic representation of the proposed pathway for methylated norbelladine formation. The compounds detected during this study from *N. papyraceus* samples are written in bold. Double arrows indicate a series of biochemical reactions whereas single arrows indicate single step reactions. Green arrows indicate the reactions characterized during this study.

Early labeling feeding studies established 4'-*O*-methylnorbelladine, as the key intermediate compound of the AAs pathway (Eichhorn, Takada et al. 1998, El Tahchy, Ptak et al. 2011). The proposed route of methylated norbelladine is shown in Figure 3.1. Central to the biosynthesis of the majority of these alkaloids is the *O*-methylation of norbelladine followed by a *C*-*C* phenol-coupling reaction, *para-para'*, *para-ortho'*, or *ortho-para'*, leading to AAs with different core ring skeletons (Ka, Koirala et al. 2020, Desgagné-Penix 2021).

In comparison to mammalian OMT, plant OMTs have attracted interest as they display high promiscuity, and the ability to generate methylated products non-regioselectively. Although a small group of plant OMTs display enzymatic specificity toward a single substrate, most plant OMTs such as OMTs involved in phenylpropanoids, flavonoids and alkaloids biosynthesis show a promiscuous behaviour, are less selective and catalyse sequential methylations of almost identical substrates (Lashley, Miller et al. 2022). In plants, *O*-methylation is catalyzed by *S*-adenosyl methionine (SAM) dependent OMTs, which transfer SAM methyl group to the free OH of an acceptor compound, such as an alkaloid (Mann, Fales et al. 1963, Kilgore, Augustin et al. 2014, Sun, Wang et al. 2018, Li, Qiao et al. 2019). Previous, studies on *Narcissus* sp. *aff. pseudonarcissus*, *Lycoris* sp., and *Galanthus elwesii* showed that the class I type of OMTs was involved in the *O*-methylation of different substrates in the AAs pathway. Interestingly, the step (*i.e*., substrate, caffeic acid or 3,4-DHBA or norbelladine) at which *O*-methylation preferentially occurs is unclear.

In 2014, Kilgore *et al* uncovered that *N. sp. aff. pseudonarcissus* norbelladine 4'-*O*-methyltransferases (*Np*N4OMT) catalyzed the regioselective transfer of a methyl group to the free 4'-OH of norbelladine and of *N*-methylnorbelladine (Kilgore, Augustin et al. 2014). Later, *Lycoris* species OMT were shown to catalyze methylation at free 4' or 3'-OH of norbelladine, but also of caffeic acid and 3,4-DHBA (Sun, Wang et al. 2018, Li, Qiao et al. 2019). These studies provided a potential alternative hypothesis for the formation of *O*-methylated norbelladine derivatives, *i.e.,* directly from methylated precursor molecules such as vanillin (methylated form of 3,4-DHBA) (Figure 3.1). Norbelladine OMT were shown to be metal-dependent working with different cations such Mg^{2+}, Co^{2+} and Mn^{2+}. Recently, *Galanthus elwesii* OMT (*Ge*OMT) was shown to methylate diverse catechols (Su, Li et al. 2022). Enzyme residues and metal ion combinations responsible for the enzyme regioselectivity were identified and confirmed by protein engineering studies.

Interestingly, although several downstream AAs are 3ˈ,4ˈ-*O*-dimethylate, there is no report on OMT that would generate 3ˈ,4ˈ-*O*-dimethylnorbelladine. Pursuing the characterization of OMT from different Amaryllidaceae species, which may display differences in substrate preference is interesting for both fundamental questions, *i.e*. unravel the sequence of the AAs pathway, and biotechnological approach, as methylations catalyzed by OMTs to generate bioactive compounds are more selective and require milder conditions compared to chemical synthesis (McKean, Hoskisson et al. 2020).

N. papyraceus is a plant native to the Mediterranean region that easily grow indoor and produces paperwhite fragrant flowers. *Narcissus* species are of great interest as a source of anti-Alzheimer's compound galanthamine (Tarakemeh, Azizi et al. 2019), and of other alkaloids with potent antiviral properties, such as lycorine, and haemanthamine. During this study, a candidate *NpOMT* transcript was identified and isolated from the transcriptome of *N. papyraceus*. Sequence and phylogenetic analysis revealed that *Np*OMT belonged to class I type, metal-dependant, plant OMT. In enzymatic reaction, *Np*OMT methylated norbelladine to yield 4ˈ-*O*-methylnorbelladine as major product and 3ˈ,4ˈ-*O*-dimethylnorbelladine as minor product, but not 3ˈ-*O*-methylnorbelladine. Furthermore, *Np*OMT methylated free 3- or 4-OH of 3,4-DHBA and caffeic acid. Interestingly, *Np*OMT had more affinity for norbelladine than for other substrates, as revealed by docking analysis and enzyme kinetics study. The enzyme promiscuity and its ability to methylate substrates in regioselective and non-regioselective manners can be exploited to design specific synthetic biological routes to rewire AAs pathway in heterologous chassis for the production targeted AAs (Khersonsky, Roodveldt et al. 2006, Rodriguez, Tashiro et al. 2014, Waki, Takahashi et al. 2021).

3.3 Results

3.3.1 *N. papyraceus* leaves are enriched in AAs while roots contain precursors.

To understand AAs biosynthetic capacity of *N. papyraceus,* we performed combined profiling of targeted metabolites and transcripts in roots, bulbs, and leaves using HPLC-MS/MS and RT-qPCR. Overall, three AAs precursor molecules (tyramine, vanillin and caffeic acid) and nine AAs (norbelladine, 4ˈ-*O*-methylnorbelladine, 3ˈ,4ˈ-*O*-dimethylnorbelladine, haemanthamine, narciclasine, pancracine, crinine, 11-hydroxyvittaine and lycorine) were detected during this study (Figure 3.2 and ANNEX C Figure S1). We observed that AAs precursor molecules were

accumulated in higher levels in root. Indeed, tyramine amounts was 1.52 and 16.16-fold higher in roots as compared to leaves and bulb respectively. Vanillin level was 8.60-fold higher in roots compared to bulbs, and not detected in leaves. Caffeic acid was only detected in roots. By contrast, AAs were accumulated at relatively higher in leaves of vegetative *N. papyraceus*. Norbelladine, 3ˈ,4ˈ-*O*-dimethylnorbelladine and crinine were only detected in leaves while 4ˈ-*O*-dimethylnorbelladine, narciclasine, pancracine, 11- hydroxyvittatine and lycorine were detected in all tissues. The accumulation of AAs in leaves of *N. papyraceus* during vegetative stage was consistent with previous reports (Hotchandani, de Villers et al. 2019).

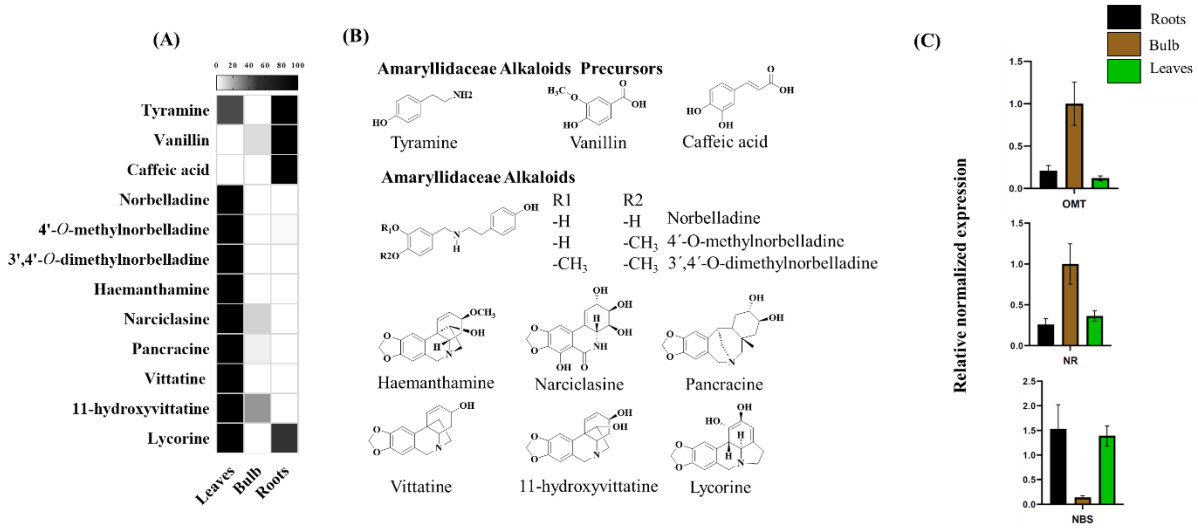

Figure 3.2 Targeted metabolites profiling and expression of Amaryllidaceae alkaloids biosynthesis genes. (A) Heat map showing the organ-specific profile of AAs in *N. papyraceus*. Relative abundance corresponds to the mean value of three independent replicates. Values were normalized to the sample with the highest level (100%) for each compound (B) Structures corresponding to detected target metabolites (AAs precursors and AAs). (C) RT-qPCR analysis of *NpOMT*, *NpNR* and *NpOMT* in leaves, bulb, and roots *of N. papyraceus*. *Histone3* specific primers were used as base for relative expression. Three biological and two technical replicates were considered for each gene evaluated.

Next, we determined the expression profile of transcripts encoding OMT, NBS and NR in *N. papyraceus* (*i.e NpOMT*, *NpNBS* and *NpNR*) leaves, bulb and roots tissues (Figure 3.2). Interestingly, gene expression was similar for *NpOMT* and *NpNR*, which presented a higher expression in bulbs, and comparatively low expression in leaves and roots. The expression pattern was inversed in the case of *NpNBS,* with low transcripts level in bulbs, and high in roots, which

contained also more precursors, and in leaves which contained most of the alkaloids including norbelladine and 4'-*O*-methylnorbelladine.

3.3.2 *N. papyraceus O*-methyltransferase candidate is a class I type metal-dependent OMT.

Next, we used *N. papyraceus* transcript encoding putative OMT (*NpOMT)* by using previously characterized OMTs from *N.* sp. *aff. pseudonarcissus* as bait (Hotchandani, de Villers et al. 2019). The candidate *Np*OMT has 720 nucleotides and translation products displayed an expected molecular mass of 27.16 kDa with 239 amino acids and a predicted isoelectric point of 4.87. Phylogenetic analysis shows that *Np*OMT clusters together with other Amaryllidaceae alkaloid OMT (AAOMT) in a single clade of class I type of metal dependent OMT, and closely related caffeoyl-CoA OMT (CCoAOMT) from *Vanillin planifolia* (*Vp*OMT) (Figure 3.3A). This result was consistent with characterized norbelladine OMT from *Narcissus* and *Lycoris* (Kilgore, Augustin et al. 2014, Sun, Wang et al. 2018, Li, Qiao et al. 2019). Multiple sequence alignment revealed that *Np*OMT shared 96.49%, 97.49% and 92.89 % amino acid sequence identity with characterized norbelladine OMT from *N. aff. pseudonarcissus* (*Np*N4OMT), *L. radiata* (*Lr*OMT) and *L. aurea* (*La*OMT) (ANNEX C Table S2, Figure 3.3B). *Np*OMT shows high amino acid sequence identity with other functionally characterized norbelladine OMT and conserved amino acid sequences involved in SAM binding (in red), metal binding (in yellow), and methyl transferase catalysis (in green) (Figure 3.3B).

To study the 3D structure of *Np*OMT, we used AlphaFold to predict its folding. The enzyme resembles other catechol-OMT (CatOMT). It comprises 7 β-sheets in its core, mostly constituted by hydrophobic residues, surrounded by a succession of α-helices and loops on the surface of the protein (Figure 3.3C and D). *Np*OMT like other CatOMT, contains a single catalytic domain, consisting of a Rossman-like fold for binding cofactor SAM. SAM and Mg^{2+} were included in the predicted structure upon pocket superimposition with reported CatOMT crystal structures (Figure 3C). Mg^{2+} interacted with Asp155 (n=2), Asp181, Asn182, while SAM formed hydrophobic bond with Tyr81, H-bonds with Val55, Tyr81, Tyr84, Ser85, Asp103, (n=2), Val104, Ala132, Asp155, Asp157 (n=2) and a salt bridge with Asp155 (ANNEX C Table S3), consistently with the identified conserved residues of class I CCoAOMT (Figure 3B). Interestingly, characterized *Lr*OMT predicted folding closely matched (RMSD = 0.074) to *Np*OMT, with an apparent difference in the

bending of the N-terminal alpha-helices (Figure 3D). Thus, the structure analysis confirms that *Np*OMT resembles enzyme that can catalyze metal-dependent *O*-methylation of substrates.

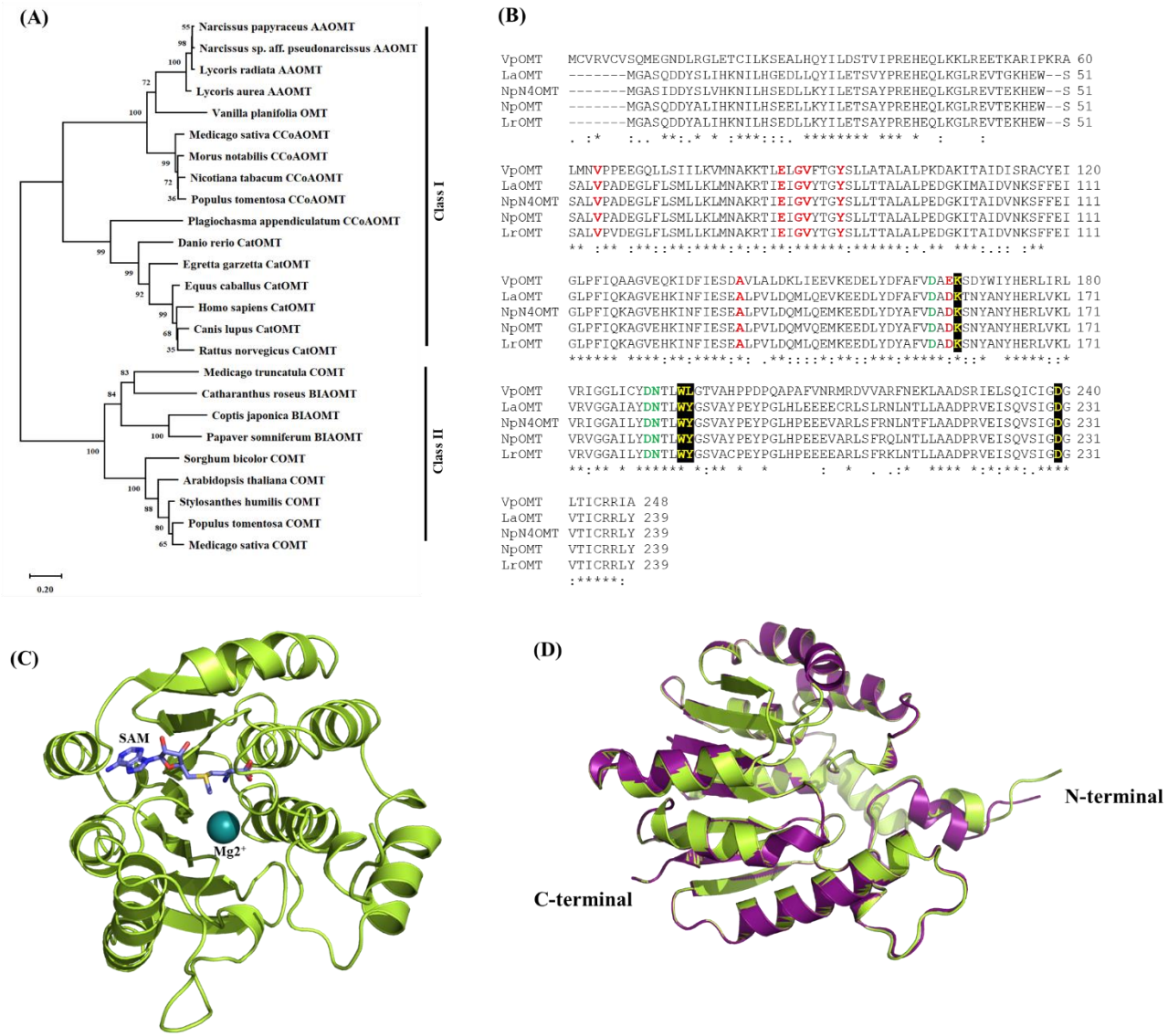

Figure 3.3 Phylogenetic analysis, multiple sequence alignment and predicted 3D structure of *Np*OMT. (A) The phylogenetic tree was constructed using the MEGA 6.0 software package and neighbor-joining program (http://www.megasoftware.net) with 1000 bootstrapped values support. The amino acid residue sequences of the plant OMTs were obtained by using the National Center for Biotechnology Information (NCBI) search engine (http://www.ncbi.nlm.nih.gov/protein/). The accession number of used amino acids are provided in ANNEX C Table S3. Amino acid sequence of *L. aurea* AAOMT (*La*OMT) was taken from reference (Sun, Wang et al. 2018). The scale indicates evolutionary distance. Abbreviation: AAOMT: Amaryllidaceae Alkaloid *O*-

methyltransferase, CCoAOMT: caffeoyl CoA *O*-methyltransferase, CatOMT: catechol *O*-methyltransferase, COMT: caffeic acid *O*-methyltransferase, and BIAOMT: Benzylisoquinoline *O*-methyltransferase. (B) Multiple amino acid residue sequences alignment was performed with *Np*OMT, *L. radiata* OMT (*Lr*OMT), *La*OMT, *N.* sp. aff *pseudonarcissus* OMT (*Np*N4OMT) and *Vanilla panifolia* OMT (*Vp*OMT) by using cluster omega online tool (https://www.ebi.ac.uk/Tools/msa/clustalo/). The highly conserved amino acids involved in interactions with SAM are highlighted in red. The highly conserved amino acids that contribute to metal ion binding are marked in green, and the amino acids involved in the catalysis of the methyl transfer are highlighted in yellow. (C) Predicted *Np*OMT folding with SAM and Mg^{2+} binding pocket. (D) Superimposition of *Np*OMT (in light green) and *Lr*OMT (in deep purple).

3.3.3 *Np*OMT is a norbelladine 4'-*O*-methyl and 3'4'-*O*-dimethyltransferase

To gain insight into enzyme function and regioselectivity, recombinant *Np*OMT activity was screened using norbelladine as substrate. Targeted open reading frame of *NpOMT* transcript was amplified from bulb cDNA. Recombinant N-terminal-MBP-tagged *Np*OMT enzyme was expressed in *E. coli* and purified using amylose-resin chromatography. The purity of *Np*OMT was assessed using SDS-PAGE (ANNEX C Figure S2). The molecular weight of the purified protein and the predicted translation products were similar (approximately 72 kDa with MBP-tag).

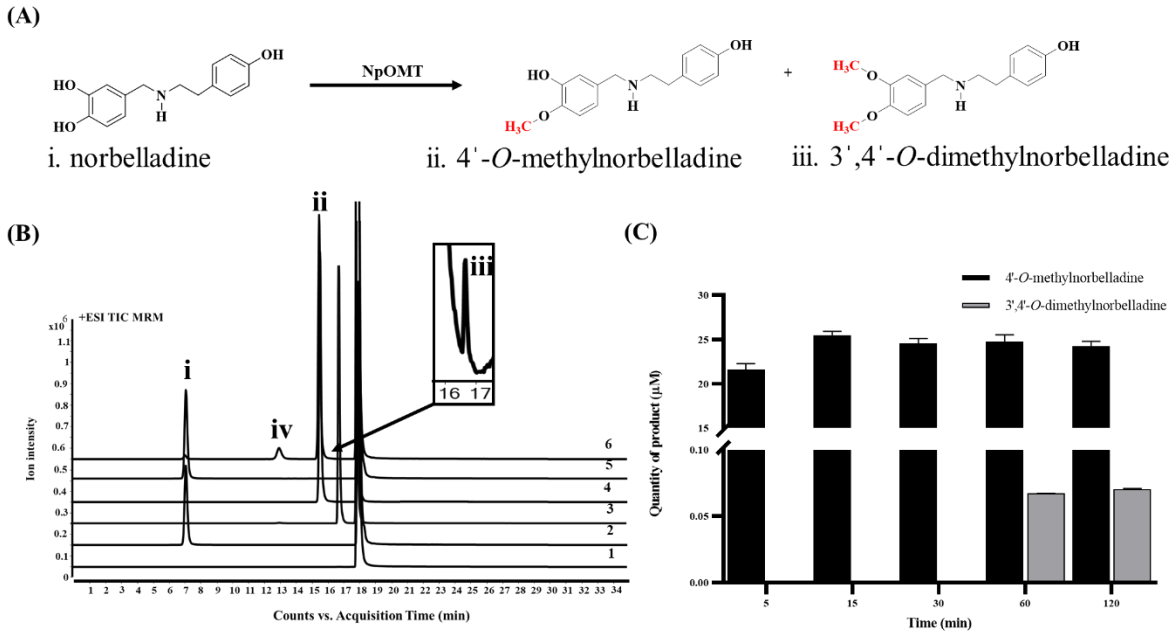

Figure 3.4 LC-MS/MS analysis of *in vitro* enzymatic assay with norbelladine. (A) Schematic conversion of (i) norbelladine into (ii) 4'-*O*-methylnorbelladine and (iii) 3',4'-*O*-dimethylnorbelladine. (B) +ESI TIC MRM chromatogram with detection of assay products in MRM mode, iv represent the unknown peak detected. (1) No substrate, (2) No SAM, (3) standard 3'-*O*-methylnorbelladine, (4) standard 4'-*O*-methylnorbelladine, (5) enzymatic assay with heat

deactivated *Np*OMT and (6) enzymatic assay with *Np*OMT. (C) Enzymatic assay of *Np*OMT with norbelladine at different time course. Experiment was performed for 5, 15, 30, 60 and 120 min. All experimental values represent the means of three replicates.

Norbelladine displays 3 free OH-groups associated with a benzene ring at C4', C3', and C4 positions that could theoretically be *O*-methylated. The LC-MS/MS analysis reveals the presence of three new product peaks *i.e.,* ii. 4'-*O*-methylnorbelladine, iii. 3',4'-*O*-dimethylnorbelladine and iv. unknown product (Figure 3.4B). The product peaks were measured with an increase of 14 Da for (ii) and (iv), and of 28 Da for (iii) with respect to norbelladine molecular mass. This suggested that mono- and di-methylated products of norbelladine were formed. Peak (ii) was confirmed to be 4'-*O*-methylnorbelladine ($[M+H]^+$ ion m/z 274) as major product, and peak (iii) as 3',4'-*O*-dimethylnorbelladine ($[M+H]^+$ ion m/z 288) by comparison with available authentic standards. Peak (iv) displayed an $[M+H]^+$ ion m/z 274 but its fragmentation pattern and parent ions did not match neither 4'-*O*- nor 3'-*O*-methylated norbelladine (Figure 3.4B and ANNEX C Figure S3). To understand the formation of 3',4'-*O*-dimethylnorbelladine, we incubated *Np*OMT with norbelladine in 5-120 minutes time series (Figure 4C). This showed exclusive formation of 4'-*O*-methylnorbelladine for the first 30 minutes, followed by concomitant detection of the latter, and 3',4'-*O*-dimethylnorbelladine from 60 to 120 minutes, albeit at much lower levels. Further enzymatic reactions were performed using 4'-*O*- and 3'-*O*-methylnorbelladine as substrates, and surprisingly, this did not lead to the synthesis of the 3',4'-*O*-dimethylnorbelladine. These results confirm that the candidate *Np*OMT catalyzes 4'-*O*-methylation of norbelladine (Table 3.1) and shows for the first time that *Np*OMT can also catalyze the formation of 3'4'-*O*-dimethylnorbelladine in 1h incubation.

3.3.4 *Np*OMT also accepts AAs precursors as substrates.

Next, we sought to measure the enzyme ability to methylate AAs precursor compounds 3,4-DHBA and caffeic acid. 3,4-DHBA and caffeic acid have two free hydroxyl groups associated with a benzene ring at C3 and C4 positions, and tyramine has a free hydroxyl group at C4 position. Upon *Np*OMT reactions with 3,4-DHBA or caffeic acid as substrates, two new peaks appeared (Figure 5), with an increased mass of 14 Da relative to each substrate. This indicated that methylation happened in single position for both 3,4-DHBA or caffeic acid. With 3,4-DHBA as substrate, the products were confirmed as isovanillin ($[M+H]^+$ m/z 153, peak vi) and vanillin ($[M+H]^+$ ion m/z 153, peak vii) by comparison with authentic standards. In the case of caffeic acid, products were confirmed as ferulic acid ($[M+H]^+$ m/z 195, peak ix) and isoferulic acid ($[M+H]^+$ ion m/z 195, peak x).

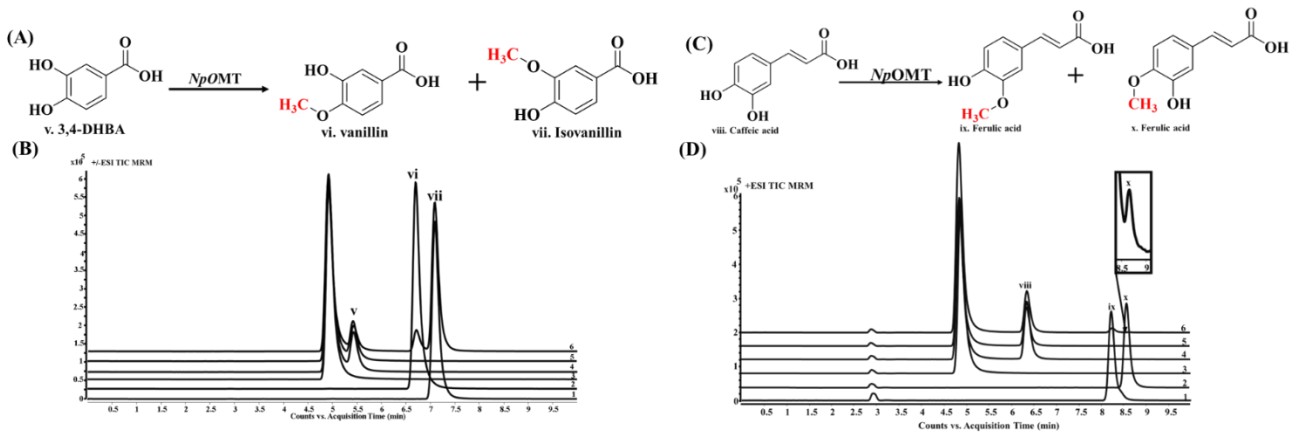

Figure 3.5 LC-MS/MS analysis of *Np*OMT enzymatic assay with 3,4-DHBA and caffeic acid. (A) Schematic diagram of *Np*OMT catalysed enzymatic reaction with 3,4-DHBA (v). Diagram shows the formation of isovanillin (vi) and vanillin (vii). (B) +ESI TIC MRM chromatograms of NpOMT enzymatic reaction with 3,4-DHBA. (1) No 3,4-DHBA (2) No SAM, (3) Standard isovanillin (4) Standard vanillin, (5) no protein enzymatic reaction (6) enzymatic assay with 3,4-DHBA. (C) Schematic diagram of *Np*OMT catalysed enzymatic reaction with caffeic acid (viii). Diagram shows the formation of ferulic acid (ix) and isoferulic acid (x). (D) +ESI TIC MRM chromatograpms of *Np*OMT enzymatic assay with caffeic acid. (1) No caffeic acid (2) No SAM, (3) standard ferulic acid (4) standard isoferulic acid, (5) no protein enzymatic reaction (6) enzymatic assay with caffeic acid.

To further study the substrate promiscuity of *Np*OMT, enzymatic reactions were carried out using ferulic acid, isoferulic acid, vanillin, isovanillin or tyramine as substrates. These substrates display only one free hydroxyl on their benzene ring. Interestingly, no new product peak was detected in the enzymatic reactions using *Np*OMT with any of these substrates (Table 3.1). Altogether, these

results suggest that *Np*OMT accepts norbelladine and its phenylpropanoid precursors as substrates. They also support a requirement for two vicinal free hydroxy groups on the benzene ring of the substrate to enable *O*-methylation catalysis, as reported in *Lr*OMT (Li, Qiao et al. 2019).

Table 3.1. Enzyme promiscuity of *Np*OMT with different types of substrates.

Substrate	Major product	Minor product
Norbelladine*	4ˈ-O methyl Norbelladine	3ˈ,4ˈ-O-dimethylnorbelladine
Caffeic acid	Ferulic acid	Isoferulic acid
3,4-DHBA	Vanillin	Isovanillin
4′-O-methylnorbelladine	Npd	Npd
3′-O-methylnorbelladine	Npd	Npd
Tyramine	Npd	Npd
Ferulic acid	Npd	Npd
Isoferulic acid	Npd	Npd
Vanillin	Npd	Npd
Isovanillin	Npd	Npd

*An additional unknown peak was detected on the reaction mixture. Npd: no new product detected.

3.3.5 Enzyme kinetic study of *Np*OMT with 3,4-DHBA and norbelladine

The optimal temperature and pH for enzymatic reaction of *Np*OMT was determined by incubating *Np*OMT with 3,4-DHBA at a temperature ranging from 20-60 ℃ and a pH ranging from 4.5 to 13. Vanillin and isovanillin production were optimal at temperature of 45℃ and pH 7.4 (ANNEX C Figure S4). Class I OMT are metal dependent, and metal ions have been shown to impact on enzyme regioselectivity (Su, Li et al. 2022). To determine the effect of different divalent metal ions on the rate of reaction, we compared product formation in presence of Mg^{2+}, Zn^{2+}, Ni^{2+}, Co^{2+}, Ca^{2+}, and Mn^{2+} using norbelladine and 3,4-DHBA as substrates. In presence of EDTA, the reaction rate was decreased to barely detectable levels, as expected (ANNEX C Figure S5 (A, B and C)). The reaction rate increased in presence of metal ions compared to no salt control, except for Ca^{2+}, in which case, the rate of reaction decreased. These results indicate that *Np*OMT requires metal divalent ions for catalysis of *O*-methylation reaction. The higher rate of reaction for the formation

of isovanillin was observed with Ni^{2+} (ANNEX C Figure S5B), and higher vanillin formation was observed with Zn^{2+} , although the difference was not statistically significant compared to other metal ion *i.e* Mg^{2+} ,Ni^{2+}, Co^{2+} and Mn^{2+}. These results suggests that the metal ion impacted the regioselective methylation of 3,4-DHBA. We further performed a kinetic study of *Np*OMT using two different metal ions Zn^{2+} and Ni^{2+} for 3,4 DHBA, and Mg^{2+} for norbelladine, as there was no difference in product formation compared to other metals. For the formation of vanillin, *Np*OMT lowest K_m value (491.37 ± 51.31 µM) was observed with Zn^{2+}, whereas for isovanillin, the lowest K_m value (626.83 ± 76.70 µM) was observed with Ni^{2+}. V_{max} and K_{cat} values related to the synthesis of both vanillin and isovanillin favored the presence of Ni^{2+}, as compared to Zn^{2+} (Table 3.2). To prevent the formation of dimethylated product and concentrate the kinetic study on 4'-*O*-methylnorbelladine as product, *Np*OMT was incubated with norbelladine and metal ions for 30 min and the reaction was quenched. *Np*OMT catalyzed *O*-methylation of norbelladine followed the Michaelis-Menten kinetic with K_m value of 169.17 ± 19.27 µM and K_{cat} value of 2.17 min^{-1}. The V_{max} and K_{cat}/K_m value were 10.86 ± 1.25 µM min^{-1} and 12.82 mM^{-1} min^{-1}, respectively (Table 3.2 and ANNEX B Figure S7). These results suggest that *Np*OMT preferentially 4'-*O*-methylate norbelladine, favors 3-*O*-methylation of 3,4-DHBA over its 4-*O*-methylation, and that metal species influence reaction rates and reaction type.

Table 3.2 Kinetic parameters of *Np*OMT catalysed methylation of norbelladine and 3,4-DHBA

Substrate	Norbelladine	3,4-DHBA			
Product	4'-*O*-methylnorbelladine	Vanillin		Isovanillin	
	Mg^{2+}	Zn^{2+}	Ni^{2+}	Zn^{2+}	Ni^{2+}
K_{cat} (min^{-1})	2.17 ± 0.24	3.82 ± 0.15	4.48 ± 0.16	0.21 ± 0.01	0.35 ± 0.02
K_m (µM)	169.17 ± 19.27	491.37± 51.31	544.2 ± 57.73	868.7± 129.99	626.83± 76.70
V_{max} (µM min^{-1})	10.86 ± 1.25	19.09 ± 0.75	22.41 ± 0.81	1.07 ± 0.07	1.77 ± 0.08
K_{cat}/K_m (mM^{-1} min^{-1})	12.82	7.81	8.30	0.24	0.56

3.3.6 *Np*OMT localizes in the cytoplasm and nucleus and methylates norbelladine *in planta.*

To determine the subcellular localization of *Np*OMT, we used N- and C-terminal GFP-tagged *Np*OMT. The fusion proteins were identically expressed under the control of the 35S promoter in *N. benthamiana* epidermal leaf cells, with RFP and DAPI as positive controls for the cytosol, and nucleus markers. GFP-tag-*Np*OMT localization followed a similar pattern to the RFP marker (cytosolic and nucleic). DAPI staining of *N. benthamiana* leaf also confirmed localization of N-terminal GFP-tag-*Np*OMT (GFP-*Np*OMT) in nucleus (Figure 3.6). The expression patterns of C-terminal GFP-tagged NpOMT (*Np*OMT-GFP) were similar with GFP-*Np*OMT (ANNEX C Figure S6A). The correct expression of the full-length GFP-tagged *Np*OMT fusion proteins in the *Agrobacterium*-infiltrated *N. benthamiana* leaves was further confirmed by Western blot analysis with GFP antibodies (ANNEX C Figure S6B).

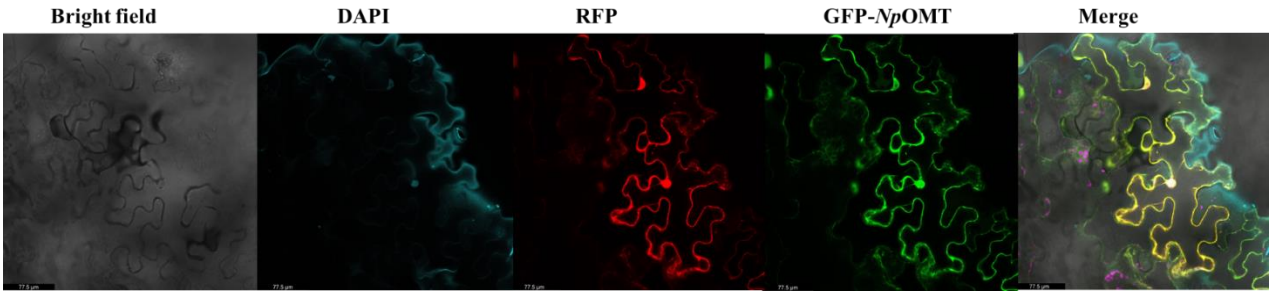

Figure 3.6. Cellular localization of N-terminal GFP-tagged *Np*OMT (GFP-*Np*OMT). N-terminal GFP fusion *Np*OMT was co-expressed with red fluorescent protein (RFP) in epidermal cell of *N. benthamiana* leaves, and images were taken after 48 hrs with confocal microscopy. DAPI was used as positive control for nucleus marker. Bright field, DAPI, RFP, GFP-*Np*OMT and merge image are shown. Scale bars in image represent 77.5 µM

To characterize the enzymatic potential of *Np*OMT in an *in vivo* system, norbelladine was infiltrated into *N. benthamiana* leave, which displayeds transient expression of GFP-*Np*OMT as confirmed by confocal microscopy. LC-MS/MS analysis of infiltrated leaves methanolic extracts confirmed the presence of methylated norbelladine ($[M+H]^+$m/z 274) (ANNEX C Figure S7). Furthermore, a comparison with authenticated standards confirmed the methylated product to be 4'-*O*-methylnorbelladine, consistently with our *in vitro* experiments. However, we did not detect a dimethylated product during *in vivo* enzymatic assay. This indicated ability of *Np*OMT to regioselectivitely methylate the norbelladine in heterologous cellular environment.

3.3.7 Differential positioning for 3ˈand 4ˈ-*O*-methylation were predicted *in silico.*

To get insight into *Np*OMT promiscuity and specificity, 3,4-DHBA, caffeic acid, norbelladine and 4ˈ-*O*-methylnorbelladine were docked in the *Np*OMT active site. CatOMT catalyzes a direct nucleophilic attack of one of the hydroxyl groups of catechol on the methyl carbon of SAM through an S_N2-like transition state, assisted by Mg^{2+} and Lys144 (Woodard, Tsai et al. 1980). During the reaction, SAM binds first to the CatOMT followed by the metal ion and finally the substrate (Tsao, Diatchenko et al. 2011). Hence, SAM and Mg^{2+} were first positioned into the predicted *Np*OMT active site using CatOMT crystalized structures (1H1D and 3A7E) as references. Following docking, all tested ligands were highly coordinated in the enzyme active site by multiple interactions (ANNEX C Table S4), and they superimposed nicely with the catechol's placement in the original crystals. First, for both 4ˈ and 3ˈ-*O*-methylation reactions, norbelladine oriented their 3ˈand 4ˈ-OH group on each side of Mg^{2+} (Figure 3.7A, B and C). The docking scores were -11.34 and -10.77 kCal/mol for norbelladine in position of 4ˈ and 3ˈ-*O*-methylation, respectively, and -10.24 kCal/mol for 4'-*O*-methylnorbelladine in the position for 3ˈ-*O*-dimethylation. The ligand acceptor oxygen atom that was close to the methyl group of SAM donor sulphur atom was stabilized by H-bond with Lys158 and Mg^{2+} (Figure 3.7B, C, for 3'- and 4'-*O*-methylation), while the other OH interacted with Asn182, Ser52, and Mg^{2+}. Hydrophobic interactions with Leu197, π-stacking with Trp185 and Tyr186, and H-bonds with Ser188 and Tyr194 steadied norbelladine phenol ring methylation in a hydrophobic pocket when in position for 4ˈ-*O*- (Figure 3.7(A and B), ANNEX C Table S4). The position favorable to 3ˈ-*O*-dimethylation of 4ˈ-*O*-methylnorbelladine also lead to a parallel π-stack interaction between Tyr186 and the ligand phenol rings, further stabilized by Trp185 and Leu197 (Figure 3.7 (B and D)). By contrast, the catechol group sled to expose its 3ˈ-OH towards the methyl donor, binding to Mg^{2+}, Lys158 and Asn182, while Ser52 stabilized the amine group (Figure 3.7 (D), ANNEX C Table S4). However, the weaker docking score (-10.24 kcal/mol; ANNEX C Table S4) of 4ˈ-*O*-methylnorbelladine by comparison to norbelladine, suggests that this reaction is less favorable. In poses favorable to 3ˈ-*O*-methylation, norbelladine laid more parallel to SAM (Figure 3.7C) (compared to transverse norbelladine in Figure 3.7A and B), stabilizing interactions with Trp185, Tyr186, Ser188, Leu197, were lacking,

while hydrophobic interactions with Asp157, Lys158, and Ala204 and an H-bond with Ser159 steadied its side chain and opposite ring.

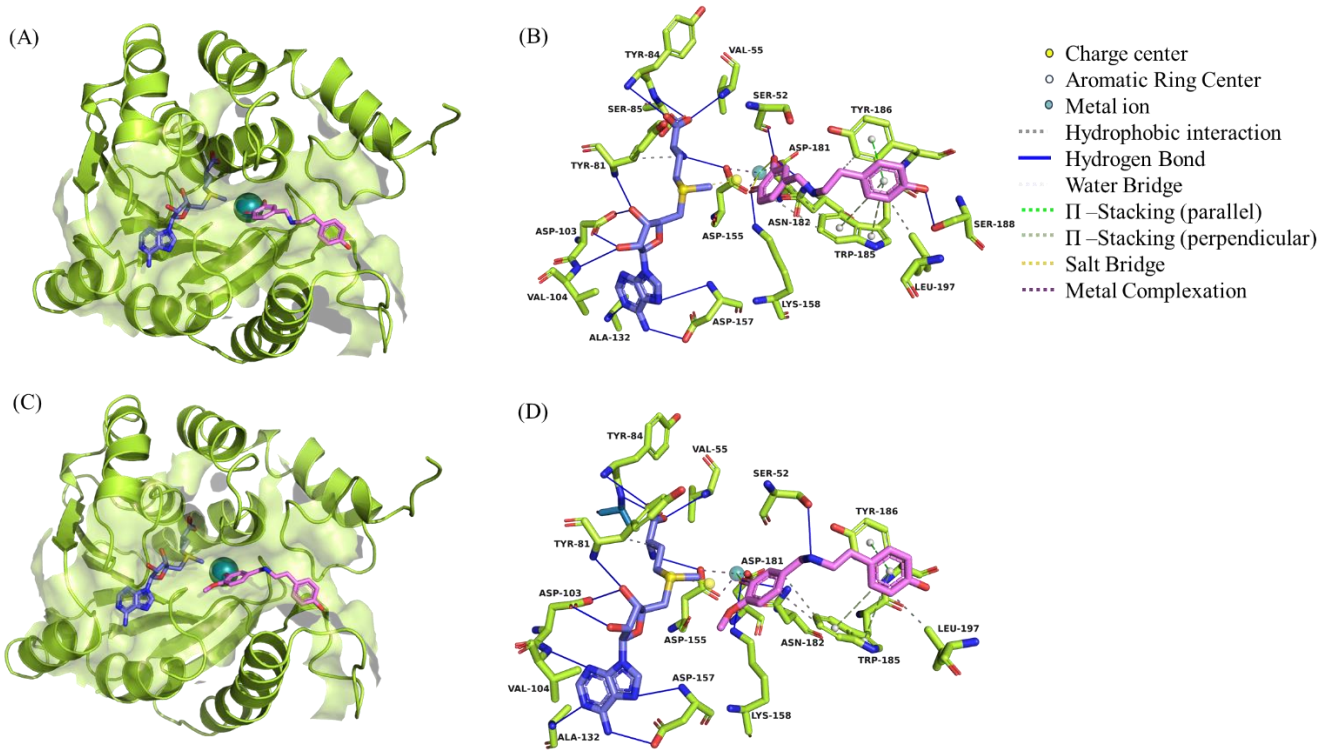

Figure 3.7 Molecular docking study of *Np*OMT with Norbelladine and 4'-O-methylnorbelladine. (A) *Np*OMT (in ribbon structure) interacting with norbelladine (light pink sticks) in presence of Mg^{2+}(blue sphere) and SAM (purple sticks). B. Docked norbelladine in position for 4'-*O*-methylation, SAM and Mg^{2+} interacting with *Np*OMT residues (light green) C. Docked norbelladine in position for 3'-*O*-methylation, SAM and Mg^{2+} interacting with *Np*OMT residues (light green). (D) Docked 4'-*O*-methylnorbelladine in position for 3'-*O*-dimethylation, SAM and Mg^{2+} interacting with *Np*OMT residues (light green).

For the phenylpropanoid pathway ligands, docked 3,4-DHBA laid in a favorable positioning for a nucleophilic attack of its 4-OH with a score of -10.03 kCal/mol, and of its 3-OH group with a score of -9.44 kCal/mol (ANNEX C Figure S8, ANNEX C Table S4). Caffeic acid also positioned favorably for methylation of its 4-OH with a score of -9.67 kCal/mol while, its 3-OH positioned with a score of -9.62 kCal/mol (ANNEX C Figure S9, ANNEX C Table S4). In poses coherent with 3-*O*-methylation catalysis, ligands laid parallel to SAM, while in the case of 4-*O*-methylation, they laid nearly perpendicular. This was consistent with norbelladine docking results. The similar scores between the reactions and the ligands (<1 kCal/mol differences) suggest that both 3 and 4-*O*-methylation of these two ligands can occur. Overall, the intricate array of conserved binding interactions of the tested ligands with *Np*OMT collectively anchor the substrate molecules such

that the reactive oxygen atom (at position 3 or 4) forms favorable interactions with the enzyme's catalytic residues and the SAM methyl donor.

3.3.8 Molecular dynamic simulation predicts a shift of norbelladine towards 4'-*O*-methylation positioning.

To further understand the mechanisms involved in the selectivity of 4'-*O*-methylation catalysis by *Np*OMT, we performed a molecular dynamics simulation of docked norbelladine in the position of 3' *vs.* 4'-*O*-methylation in Alphafold predicted *Np*OMT (from Figure 3.7). The trajectory was followed for 25 ns with a 500 ps checkpoint time. The overall positioning of SAM and norbelladine, the root-mean-square deviation (RMSD) of pocket residues and ligands, and the distance with the metal ion and methyl group were analyzed (Figure 3.8 and 9). Over 25 ns, norbelladine 4'-OH progressed from 3.1 to 4.6 Å from the methyl group (Figure 3.8A). RMSD analysis of the backbone deviation revealed that pocket residues and ligands were stable for 15 ns (0-3.5 Å). Norbelladine RMSD was stable for 5 ns (~1 Å) and then increased at 2 Å for the rest of the simulation (Figure 3.8B). In the two other replicates, norbelladine RMSD values steadied around 1 Å for the 25 ns. Such RMSD values indicate a stable interaction of norbelladine with the active site. SAM was even more stably bound to the enzymes, with values varying between 1 and 1.5 for the 20 last ns of the simulation. In comparison, pocket residues varied more across the simulation period, reaching 2.5 to 3.5 Å following the first 7 ns (Figure 3.8B). The distance between the norbelladine catechol ring hydroxyl groups and the metal ion remained quite constant for the first 4 ns, then the 4'OH moved closer to the Mg^{2+} while the 3'OH remained overall at a constant larger distance (Figure 3.8C). This appeared to occur concomitantly to the RMSD increase of pocket residues (Figure 8B). Throughout the simulation, the 4'OH group stayed in proximity to the methyl donor too, with change in distance between 3 to 5 Å, while the distance to the 3'OH varied between 3.5 to 7 Å (Figure 3.8D).

When norbelladine was docked in position for 3'-*O*-methylation, norbelladine deviated more from its original position. Norbelladine was steady for 9 ns (~0.5 Å), at which time it deviated of ~2 Å from its original position and stabilized for the rest of the trajectory (Figure 3.9B). In other replicates, norbelladine position deviated ~3-3.5 Å compared to its original position. The evolution of the interactions between the ligand, the methyl donor and the metal ion were also different (Figure 3.9A). For the first 9 ns, the distances between Mg^{2+} and the 3'OH or 4'OH declined

steadily after its initial increase. Intriguingly, from 10 ns to the end of the trajectory norbelladine 4'OH got closer to the metal ion compared to its 3'OH (Figure 3.9C). Similarly, while at the beginning of the simulation, the 3'OH was closest to SAM methyl group, after 9 ns, norbelladine shifted to bring its 4'OH in proximity to the cofactor (Figure 3.9A and D). For both SAM and Mg^{2+}, the curves of distance with 3'OH and 4'OH inverted after 9 ns, corresponding to the moment of norbelladine deviation from its original position. Overall, these results suggest that norbelladine shifts to a position favoring 4'-*O*-methylation over the simulation period.

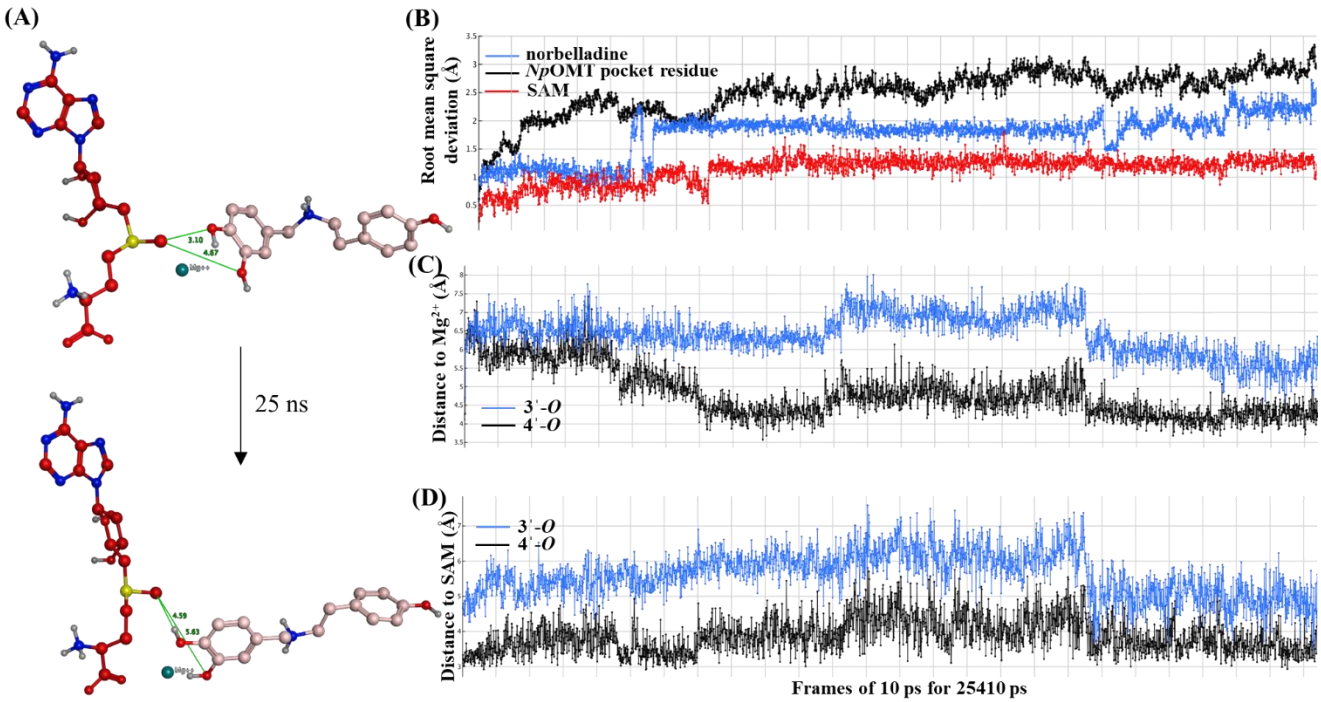

Figure 3.8 25 ns trajectory analysis of norbelladine in position for 4'-O-methylation. (A) Initial and final distance positioning between SAM and 3'/4' oxygen of norbelladine following a 25 ns trajectory. (B) Root mean square deviation (RMSD) of norbelladine (blue), SAM (red) and enzyme pocket residue surrounding norbelladine (black) over 2541 frames of 10 ps. (C) Distance between Mg^{2+} and 3'(blue)/4'(black) oxygen over the 25410 ps trajectory. (D) Distance between SAM and 3'(blue)/4'(black) oxygen over the 25410 ps trajectory. These results are representative of 3 independent trajectory of 25 ns.

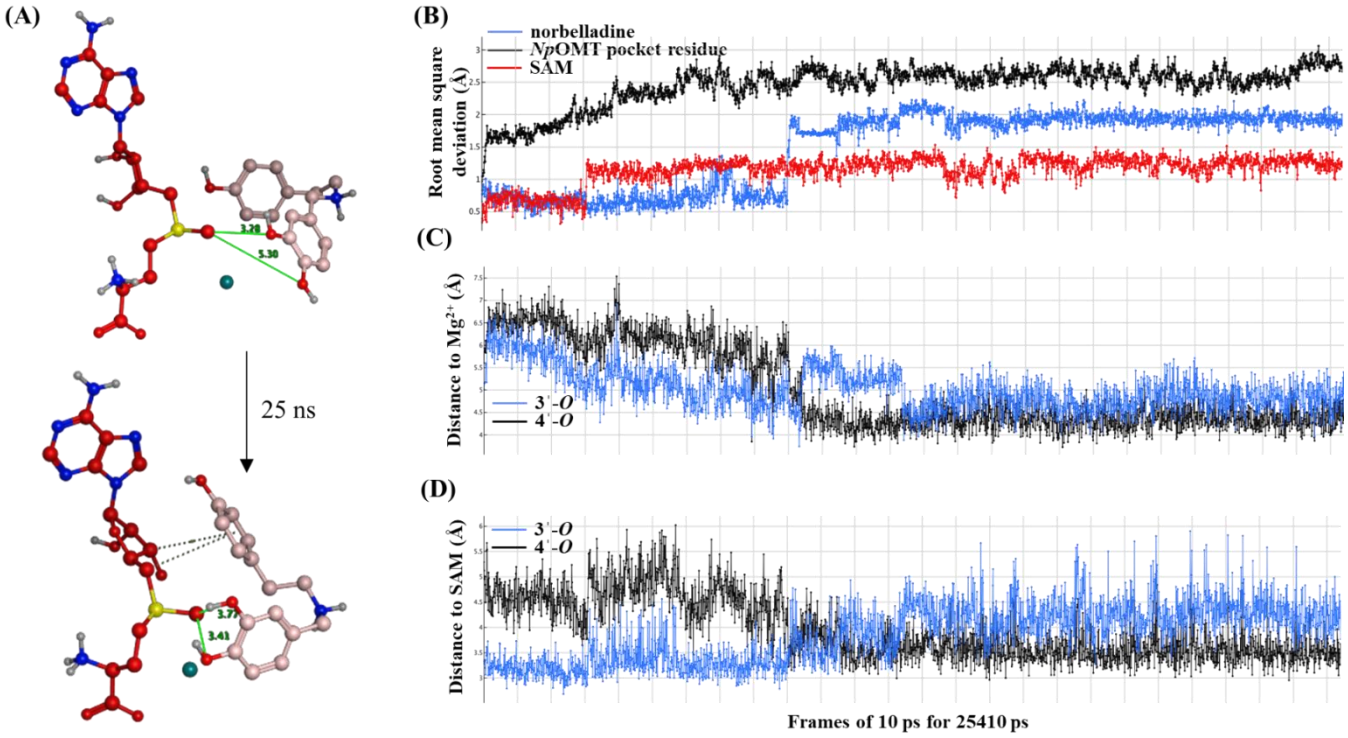

Figure 3.9 25 ns analysis trajectory of norbelladine in position for 3'-*O*-methylation. (A) Initial and final distance positioning between SAM and 3'/4' oxygen of norbelladine following a 25 ns trajectory. (B) Root-mean-square deviation (RMSD) of norbelladine (blue), SAM (red) and enzyme pocket residue surrounding norbelladine (black) over 2541 frames of 10 ps. (C) Distance between Mg^{2+} and 3'(blue)/4'(black) oxygen over the 25410 ps trajectory. (D) Distance between SAM and 3'(blue)/4'(black) oxygen over the 25410 ps trajectory. These results are representative of 3 independent trajectory of 25 ns.

3.4 Discussion

Although AAs are known for their diverse biological properties and wide range of structural diversity, their biosynthetic route is still not clear. The proposed biosynthesis considers norbelladine as a first common intermediate compound of this pathway, in which regioselectively methylated norbelladine such as 3'-*O*-methylnorbelladine, 4'-*O*-methylnorbelladine and 3',4'-*O*-dimethylnorbelladine could determine end product of AAs metabolic pathway (Desgagné-Penix 2021). Different labeling studies shows 4'-*O*-methylnorbelladine as a precursor intermediate involved in the biosynthesis of different types of AAs, including galanthamine and lycorine (Eichhorn, Takada et al. 1998, El Tahchy, Ptak et al. 2011), while dimethylation is observed in the cherylline types of AAs. Here, we performed the targeted metabolites analysis of *N. papyraceus,*

which is well known to accumulate various types of AAs, including galanthamine. Interestingly, targeted metabolites analysis of *N. papyraceus* shows the presence of norbelladine, 4'-*O*-methylnorbelladine, and 3',4'-*O*-dimethylnorbelladine.

Previous reports have shown different results regarding the regioselectivity and substrate specificity of AAOMT, but none has been shown to produce dimethylated products before. Norbelladine *O*-methyltransferase from *N*. sp *aff. pseudonarsissus* (*Np*N4OMT) was shown to be regioselective, methylating norbelladine and *N*-methylnorbelladine at 4'-OH position. *Np*N4OMT enzyme did not accept AAs precursor molecules as substrate (Kilgore, Augustin et al. 2014). By contrast, norbelladine methyltransferase from *Lycoris* species and *Galanthus elwesii* were non-regioselective, methylating norbelladine at 3'or 4'-OH position (Sun, Wang et al. 2018, Li, Qiao et al. 2019, Su, Li et al. 2022) with a broad range of substrates promiscuity. As we detected 4'-*O*-methylnorbelladine and 3',4'-*O*-methylnorbelladine in *N. papyraceus*, we decided to characterize its norbelladine OMT. We first assessed its expression levels by RT-qPCR. While our candidate *NpOMT* transcript was expressed at higher levels in bulbs, AAs mostly accumulated in leaves, together with NR and NBS, the enzymes required to produce norbelladine from 3,4-DHBA and tyramine. The uncorrelated patterns of AAs and biosynthesis enzyme transcripts suggest that enzymes and/or alkaloids may be transported to different tissues after synthesis and accumulated in specific tissue.

*Np*OMT candidate was highly similar in sequence and in predicted folding to other characterized norbelladine OMT, defined as class I OMT. *Ab initio* modeling by AlphaFold showed that *Np*OMT adopted the Rossmann-like fold with an αβα sandwich structure at its core, a domain required for SAM binding (Chatterjee, Kudlinzki et al. 2015). Class I OMT catalytic activity depends on the presence of a divalent metal ion, like Mg^{2+}, in the vicinity of SAM donor sulfur atom. The metal ion stabilizes and interacts directly with conserved active site residues Asp155, Asp181 and Asn182, and with the substrate (Liscombe, Louie et al. 2012, Lee, Kang et al. 2019). On the outside of the protein, the N-terminal α-helices and loops play a significant role in oligomerization and modulation of the substrate specificity (Kozbial and Mushegian 2005). Interestingly, some variations were observed between *LrO*MT and *Np*OMT, suggesting that they may differ in catalytic potential.

During this study, we cloned and produced recombinant *Np*OMT enzymes and performed the enzymatic assay. Our results show that *Np*OMT preferably methylates norbelladine at 4'-OH position with a lower K_m value and higher efficiency than reported homologous norbelladine OMT from *Lycoris* species (Li, Qiao et al. 2019). Unlike *Np*N4OMT (Kilgore, Augustin et al. 2014), but similar to *Lr*OMT, *Np*OMT can methylate caffeic acid and 3,4-DHBA to produce monomethylated products at both 3 or 4-OH positions. Unlike any other reported AAOMT, *Np*OMT can produce a dimethylated product form of norbelladine. In addition, when using norbelladine as substrate, we observed an additional reaction product at a retention time of 13.1 min with a mass of $[M+H]^+$ ion m/z 274 corresponding to a monomethylated norbelladine. However, the fragmentation pattern of the product peak at 13.1 min (peak iv) did not match with neither 4'-*O*- nor 3'-*O*-methylnorbelladine. It is possible that *Np*OMT can methylate at the 4-OH position of norbelladine, but we could not confirm it, as we lack 4-*O*-methylnorbelladine as standard.

*Np*OMT enzymatic assays were consistent with metal dependency to promote the *O*-methylation reaction. Furthermore, docking analysis supports 3-*O* (3' in the case of norbelladine) and 4-*O* (4') methylation catalysis of the tested ligands by *Np*OMT. An intricate array of binding interactions with *Np*OMT collectively anchors the substrate molecules such that the reactive oxygen atom (at position 3 or 4) forms favorable interactions with the enzyme's catalytic groups and the SAM methyl donor. Lys158 and Mg^{2+} bound with the oxygen to be methylated, and Asn182 interacted with the other hydroxyl group of the catechol ring, emphasizing their key role in the catalytic process (Brandt, Manke et al. 2015). While a previous report on *Galanthus elwesii Ge*OMT suggested that Tyr186 was important for meta (3) methylated products (Su, Li et al. 2022), in the case of *Np*OMT it interacted mostly with ligands (3,4-DHBA, caffeic acid and norbelladine) in position for 4/4'-*O*-methylation. Interestingly, Tyr186 also interacted with 4'-*O*-methylnorbelladine in position for its 3'-*O*-methylation. Regioselectivity was indeed reported to be dependent on key residues, ligand structure, and metal species (Subrizi, Wang et al. 2021). Other studies have described Trp185 as an important amino acid (Brandt, Manke et al. 2015); here, it stabilized the larger alkaloid ligand, and two additional π-stacking interactions were detected for norbelladine in position for 4'-*O*-methylation compared to 3'-*O*-methylation. The latter also missed a hydrophobic interaction with Leu197. Ala53 and Trp50 seemed to stabilize norbelladine consistently with (Su, Li et al. 2022), Ala53 supported norbelladine in the position of 4'-*O*-methylation and Trp50 interacted with norbelladine in position for 3'-*O*-methylation during

simulation, while interactions with Asp230 were not detected. Experimental evidence has shown that a water molecules vicinal to the metal ion were primordial for deprotonation of the hydroxyl group to enable methyl transfer of the sulfur cation of SAM to the acceptor oxygen (Liscombe, Louie et al. 2012). In our study, adding of water molecules in the active site during docking did not yield consistent ligand positioning, but deprotonation of ligand hydroxyl group (as predicted protomers) to be methylate led to correctly positioned ligands. In a nutshell, docking models suggest that *Np*OMT can perform both 3- or 4-OH methylation of caffeic acid, 3,4-DHBA and prefers 4'-*O*-methylation of norbelladine. A conserved group of binding interactions between ligands and *Np*OMT collectively anchor the substrate molecules such that the reactive oxygen atom (at position 3 or 4) forms favorable interactions with the enzyme's catalytic groups and the SAM methyl donor. Overall, the differences in interacting residues and in docking scores hinted that *Np*OMT catalysis of 3'-*O*-methylation of norbelladine was less favorable than its 4'-*O*-methylation. Molecular dynamics further supports these predictions, showing that when norbelladine was positioned for 3'-*O*-methylation, it shifted towards a 4'-*O*-methylation position over the simulation period.

This study reveals that *Np*OMT is a promiscuous enzyme that can accept AAs and precursor molecules. This study provides further support to an alternative hypothesis to generate methylated norbelladine from the condensation of methylated precursor molecules. Nonethelss, our study on *N. benthamiana* also shows that *Np*OMT can catalyze the regioselective formation of 4'-*O*-methylation *in vivo,* with a better docking score and a lower determined K_m value, suggesting that this is the favored reaction in the natural host.

3.5 Conclusion

Overall, this study reveals the novel catalytic potential of norbelladine *O*-methyltransferase from *N. papyraceus*. 4'-*O*-methylnorbelladine was the main product formed by *Np*OMT and, interesting 3',4'-*O*-dimethylnorbelladine was also formed. Studies on important amino acids involved in the interactions with the substrate will be helpful to understand the promiscuous behaviour of AAOMT. As regioselective methylation is important in the context of metabolite fate of norbelladine, deeper understanding of underlined reaction mechanism of norbelladine OMT will be beneficial to develop tool for synthetic biology for production of targeted types of AAs in heterologous host.

3.6 Methodology

3.6.1 Chemical reagents

Caffeic acid (98%), ferulic acid (99%) and papaverine (98%) standards were purchased from Sigma-Aldrich (city, ON, Canada). 3,4-dihydroxybenzaldehyde and isovanillin (98%) standards were bought from Acros Organics (City, Massachusetts, USA). Standards of 3ˈ-*O*-methylnorbelladine, 4ˈ-*O*-methylnorbelladine, 3ˈ4ˈ-*O*-dimethylnorbelladine, and norbelladine were synthetized, as described in (Girard, Karimzadegan et al. 2022). Standards of the alkaloids 11-hydroxyvittatine, haemanthamine, homolycorine, obliquine, pancracine, sanguinine, tazzetine, and crinine were kindly obtained from Professors Antonio Evidente and Marco Masi (Universitario Monte Sant'Angelo, Naples, Italy). S-adenosylmethionine (SAM) was purchased from New England Biolab Inc. (Massachusetts, USA). Standards of lycorine (98%), papaverine (98%), tyramine (99%) and vanillin (99%) were procured from Millipore Sigma (Massachusetts, USA). Standards of galanthamine (98%) was purchased from Tocris Bioscience (Bristol, United Kingdom). Analytical LC-MS grade methanol (99.9%) and formic acid (99%) were purchased from Fisher Scientific (Ontario, Canada).

3.6.2 Plant sample and metabolites extraction

N. papyraceus bulbs were purchased from Florissa, Canada (https://florissa.com) and were planted in autoclaved soil (ARGO MIX G6 potting soil) (Quebec, Canada). The plants were grown in room temperature with 14:10, light: dark condition for 18 months and were watered when necessary. Different tissues (leaves, bulbs, and roots) were harvested at the vegetative stage of plant, flash frozen under the liquid nitrogen and at -80 ˚C.

The frozen tissues (leaves, roots, and bulbs) of *N. papyraceus* were ground into powder using mortar and pestle with the aid of liquid nitrogen, and 100 mg of homogenized tissues were used for metabolite extraction. Crude metabolites extraction was done by adding 1 ml of 90% methanol then kept in the sonication bath for one hour followed by two hours in a 60˚C water bath. Then the extracts were filtered using 0.2 μm syringe filters. Presence of targeted metabolites was detected and identified by HPLC-MS/MS.

3.6.3 Identification of *Np*OMT and phylogenic analysis

To identify potential OMT transcript, we performed a local blast in *N. papyraceus* transcriptome by using blast 2+ software, using characterized norbelladine-*O*-methyltransferase from *N. aff. pseudonarcissus* (*Np*N4OMT) (KJ584561) as query sequence (Hotchandani, de Villers et al. 2019). This yielded one potential OMT candidate from *N. papyraceus* (*Np*OMT) (MF979869). Protein molecular weight and pI predictions were made using the expasy tool (https://web.expasy.org/compute_pi/). Further blastx was performed in the NCBI database to compare with similar OMT. Amino acid sequence alignments were performed using the default parameters of cluster Omega (https://www.ebi.ac.uk/Tools/msa/clustalo/). Evolutionary analyses were conducted in MEGA11 (Tamura, Stecher et al. 2021). The evolutionary history was inferred using the Neighbor-Joining method (Saitou and Nei 1987). The tree is drawn to scale, with branch lengths in the same units as those of the evolutionary distances used to infer the phylogenetic tree. The evolutionary distances were computed using the Poisson correction method (Zuckerkandl and Pauling 1965) and are in the units of the number of amino acid substitutions per site. This analysis involved 25 amino acid sequences belongs to Amaryllidaceae alkaloid *O*-methyltransfrease (AAOMT), caffeoyl coenzyme A *O*-methyltransferase (CCoOMT), benzylisoquinoline alkaloid *O*-methyltransferase (BIAOMT) and catechol *O*-methyltransferase (CatOMT). All positions containing gaps and missing data were eliminated (complete deletion option).

3.6.4 RNA extraction, cDNA synthesis and qPCR analysis

Total RNA was extracted from homogenized tissues of *N. papyraceus* (*i.e.*, leaves, bulbs and roots) using TRIzol reagent (Invitrogen). Briefly, for 100 mg of homogenized tissues 1 ml of TRIzol reagent was added. The liquid was transferred to a microcentrifuge tube, incubated 5 min at room temperature and extracted with 200 µL chloroform. Following centrifugation at 12,000g for 15 min at 4°C, the upper phase containing RNA was transferred to a fresh tube. The RNA was precipitated with 500 µL of isopropanol (ThermoFisher) for 10 min at room temperature and centrifuged at 12,000g for 10 min at 4°C. The RNA pellet was washed twice with 1 mL of 75% ethanol (with DEPC water) and centrifuged at 7500g for 5 min at 4°C. Finally, RNA pellet was air dried and suspended in 40 µL of DEPC-treated water. The quality and quantity of RNA extracted from different tissues were verified on NanoPhotometer (Implen) and 1.5% (w/v) agarose gel electrophoresis. RNA samples (1 µg) were reverse transcribed using SensiFAST cDNA synthesis

kit (Bioline) according to manufacturer's protocol. Afterwards, qPCR was performed using Luna® Universal qPCR Master Mix (New England Biolabs) with 1 µL of cDNA and 0.25 µM of gene-specific primers (ANNEX C Table S1) to test 4 genes expression: *NpOMT* coding for norbelladine-*O*-methyltransferase, *NpNBS* coding for norbelladine synthase, *NpNR* coding for noroxomaritidine/norcraugsodine reductase and *histone3* as endogenous reference to calculate relative expression using the $2^{-\Delta Ct}$ method.

3.6.5 Heterologous expression, and purification of *Np*OMT

The open reading frame (ORF) of full-length *NpOMT* was amplified from *N. papyraceus* bulbs cDNA using PrimeStar GXL premix (TaKaRa Bio) in 50 µL reaction with 0.3 µM of gene-specific primer having BamHI and HindIII in forward and reverse primer. PCR program parameters: 2 min 98 °C 1 cycle, 10 s 98 °C, 20 s 55 °C, 1 min 72 °C for 35 cycles, 5 min 72 °C 1 cycle, and final infinite hold at 4 °C. Then amplified region of cDNA was digested with BamHI and HindIII, then cleaned up with GenepHlow Gel/PCR kit (Geneaid). The digested PCR product was cloned into a pMAL-c2X vector by using T_4 DNA ligase (New England Biolabs). The recombinant plasmids were transformed into chemically competent *Escherichia coli* DH5α cells by heat shock and colonies were selected on LB agar plates containing ampicillin (100 µg/mL, Fisher Scientifics). The further presence of the target gene was confirmed by colony PCR and the identity of the nucleotide was confirmed by sequencing.

For heterologous expression of the *Np*OMT protein, the recombinant plasmid was transformed in *E. coli* Rosetta (DE3) pLysS (EMD Millipore, MA) strain and single colonies were used to inoculate 50 ml of LB medium supplemented with 100 g/ml of ampicillin and 35 g/ml of chloramphenicol. Cultures were grown at 37 °C with orbital shaking at 200 rpm for overnight and used to inoculate 1 liter of LB media (100 g/ml of ampicillin and 35 g/ml of chloramphenicol to a starting OD_{600} 0.1. Cultures were grown at 37 °C until OD_{600} 0.6, cooled on ice for 5 minutes and the production of recombinant protein was induced by the addition of isopropyl-D-thiogalactoside (IPTG) to a final concentration of 0.5 mM. Cultures were kept at 18 °C with shaking at 200 rpm for 16 h, and cells were harvested by centrifugation at 5,000 *g* for 10 min at 4 °C. Cell pellets were resuspended in 50 ml of protein extraction buffer (30mM Tris-HCl, pH 8, 150mM NaCl,1 mM EDTA, 10% (v/v) glycerol) incubated for 30 min in ice and sonicated on ice for 5 min (10-s on, 10-s off). The crude lysate was centrifuged at 16,000 *g* for 30 min at 4 °C to remove cellular debris.

The cleared supernatant was incubated with 1 ml of amylose resin beads (New England Biolabs) and incubated at 4 °C with constant shaking. After 1 hour, the mixture was centrifuged at 1000 g and the supernatant was discarded and washed with 20 ml of washing buffer (same composition of lysis buffer) 2 times. Purified *Np*OMT protein was eluted by using elution buffer (same composition of lysis buffer with addition of 25 mM of freshly prepared maltose) and subsequently concentrated and desalted by repeated ultrafiltration on an Amicon Ultra 30K column (EMD Millipore,MA) in storage buffer (30 mMTris-HCl,pH8, 10% (v/v) glycerol). Purified MBP-tagged protein concentration was determined using the Bradford reagent according to the manufacturer's protocol (Thermo Fisher), with BSA as standard. Protein purity was assessed by 10% (w/v) SDS-PAGE gel.

3.6.6 Enzymatic assay of *Np*OMT

An initial enzymatic assay of *Np*OMT was performed according to *Kilgore et al* procedure (Kilgore, Augustin et al. 2014). First, 3 potential substrates (*i.e.* norbelladine, 3,4-DHBA, and caffeic acid) were screened for the enzymatic assay. Briefly, an enzymatic reaction was carried out in a 50 µl reaction volume containing substrate of interest (norbelladine 0.1mM, 3,4-DHBA 1mM or caffeic acid 1 mM), 2 mM of SAM (methyl donor), 20 µM of purified MBP-tagged *Np*OMT, and 30 mM sodium glycine buffer (pH 9). The reaction mixture was incubated at 37 ℃ for 1 hour. The enzymatic reaction was quenched by 100 µL of LC-MS/MS grade methanol and 1000 mg/L of papaverine was added as internal standard and centrifuged at 12000 rpm for 5 min. The product(s) formation was carried out by LC-MS/MS.

3.6.7 HPLC-MS/MS analysis

Targeted metabolite analysis for AAs precursor molecules and AAs were performed on roots, bulb and leaves tissue. A high-performance liquid chromatograph (HPLC) coupled with a tandem mass spectrometer (MS/MS) (Agilent, QC, Canada) equipped with an Agilent Jet Stream ionization source, a Kinetex EVO C18 column (150 x 4.6 mm, 5 µm, 100 Å; Phenomenex, Torrance, USA), a binary pump, an autosampler set at 4°C and a column compartment were used for the analyses. 5 µl of each sample were injected into the column that was set at 30°C. A gradient made of (A) formic acid 0.1% v/v in milli-Q water and (B) formic acid 0.1% v/v in methanol, with a flow rate of 0.4 mL/min, was used to achieve chromatographic separation. The HPLC elution program started with 10% solvent B; 0-10 min, isocratic conditions with 10% B; 10-20 min, linear gradient

to reach 100% B; 20-25 min, isocratic conditions with 100% B; 25-26 min, linear gradient to return to initial conditions of 10% B. The total run time was 30 min per sample to allow the reconditioning of the column prior to the next injection. The parameters used for the MS/MS source to perform the analyses were set as follows: gas flow rate 10 L/min, gas temperature 300°C, nebulizer 45 psi, sheath gas flow 11 L/min, sheath gas temperature 300°C, capillary voltage 4000 V in ESI+ and nozzle voltage 500 V. Agilent MassHunter Data Acquisition (version 1.2) software was used to control the HPLC-MS/MS. MassHunter Qualitative Analysis (version 10.0) and MassHunter Quantitative QQQ Analysis (version 10.0) softwares were used for data processing. Compounds identifications were made using authentic standards and analytical parameters presented in ANNEX C Table S5. Internal standard papaverine was added to each sample at a final concentration of 1000 mg/L to allow normalization of each detected signal obtained by HPLC-MS/MS. To obtain Accurate relative quantification of targeted metabolites was achieved using area ratios where the peak area of each analyte was divided by the peak area of papaverine.

For enzymatic assays, HPLC-MS/MS analysis were conducted similarly as described previously except the HPLC gradients which were different depending of the analytes to be analysed in the enzymatic assays. Enzymatic assays performed with 3,4-dihydroxybenzaldehyde and caffeic acid as substrates were analyzed with the following HPLC elution program: 0 min, 35% B; 5.0 min, 50% B; 8.0 min, 60% B; 8.1 min, 35% B. The total run time was 10 min per sample to allow the reconditioning of the column prior to the next injection. Enzymatic assays made with norbelladine as substrate were analyzed with the following gradient:0 min, 10% B; 10.0 min, 10% B; 20.0 min, 100% B; 25 min, 100% B; 30 min, 90% B. The total run time was 35 min per sample to allow the reconditioning of the column prior the next injection. Data processing and identifications were made with the same software described previously and using authentic standards. ANNEX C Table S5 present analytical acquisition parameters used on HPLC-MS/MS for each enzymatic assay.

3.6.8 Optimization of *Np*OMT enzymatic reaction and determination kinetic parameters

To determine the catalytic properties of *Np*OMT, the enzymatic reaction was optimized for temperature and pH range using 3,4-DHBA as substrate. The reaction was carried out at a temperature range of 20-60 °C. To determine the optimal pH for *Np*OMT enzymatic reaction, reaction mixture was incubated with sodium citrate buffer (pH 4.5), sodium phosphate buffer (pH 6, 7, and 7.4), Tris-HCl buffer (pH 8), sodium glycine buffer (pH 9**),** Na_2HPO_4-NaOH buffer (pH

11.0), and KCl-NaOH buffer (pH 13.0). The optimal temperature and pH were then selected for further study. The metal dependency of *Np*OMT was determined by using divalent metal ions, such as Mg^{+2}, Zn^{+2}, Ni^{+2}, Co^{+2}, and Ca^{+2} at a final concentration of 1 mM in the reaction performed with 1 mM of 3,4-DHBA or 0.1 mM of norbelladine as substrate. Depending upon the effect of metal on the rate of reaction, specific divalent metal ions were selected for further study. Enzyme kinetic parameters of *Np*OMT with 3,4-DHBA were determined with substrate concentration range of 25-2000 µM and 5 µM of purified MBP-tagged *Np*OMT at optimized condition. Enzyme kinetic parameters of *Np*OMT with norbelladine were determined with substrate concentration range of 7.62-250 µM and 5 µM of purified MBP-tagged *Np*OMT at optimized condition. All analysis were done with LC-MS/MS as described above. Kinetic parameters of *Np*OMT with different substrates were determined by using non-linear regression from GraphPad Prism 8.0.1.

3.6.9 Sub-cellular localization of *Np*OMT and *in vivo* enzymatic assay with norbelladine

For the sub-cellular localization study, *Np*OMT from *N. papyraceus* was amplified from bulb cDNA. The PCR reaction was performed in 25 µl reaction volume with 200 µM of dNTP, 0.5 µl of high fidelity Q5 DNA polymerase, and 0.2 µM of forward and reverse primers. PCR parameter was 98 °C for 30 sec-1 cycle, 98 °C for 10 sec, 72 °C for 30 sec, 72 °C for 1 min - 30 cycles and 72 °C for 2 mins. AttB-flanked PCR products of *Np*OMT were purified by using Gel/PCR DNA fragment purification kit (Geneaid, NEW Taipei city, Taiwan). BP reaction was performed with pDONR^{TM}221 vector to generate the entry clone which was transformed into *E. coli* DH5α strain and positive clone selected on LB agar plate containing 50 µl of kanamycin. Further sequence identity was confirmed by sequencing. Then LR reaction of entry clone was performed with pB7FWG2 (C-terminal GFP) or pB7WG2F (N-terminal GFP) vector and transformed into *E. coli* DH5α. A positive colony was selected on LB agar plate containing 50µl of streptomycin. pB7FWG2 or pB7WG2F having full open reading frame of *Np*OMT was transformed into *Agrobacterium tumefaciens* strain GB3101 by electroporation and a positive colony was selected on LB agar plate containing rifampicin, streptomycin and gentamycin at 28°C. Single positive colonies of Agrobacteria harboring pB7FWG2:*Np*OMT or pB7WG2F:*Np*OMT were selected and plated on LB media containing rifampicin, streptomycin and gentamycin overnight. Agrobacteria cells were harvested by using a sterile loop and washed twice with induction buffer (10 mM $MgCl_2$, 10 mM MES-buffer pH-5.6, and 200 µM acetosyrigone). Then, *A. tumefaciens* culture was diluted to $O.D._{600}$ 0.5 and incubated in induction buffer for 2 hours at room temperature. Finally,

Agrobacterium culture was infiltered into 4-weeks old young leaves of *Nicotiana benthamiana* plant. Infiltrated *N. benthamiana* plant was cultured for 48 hours. For co-expression analysis, pB7FWG2:*Np*OMT or pB7WG2F:*Np*OMT were co-infiltered with RFP (nucleo-cytosolic marker), and mCherry (with signal peptide to endoplasmic reticulum marker (ER)). 4',6-diamidino-2-phenylindole (DAPI) was used to stain *N. benthamiana* leaves as a nucleus marker.

48 hours post-infiltration, the abaxial epidermis of leaves was placed in a water drop containing DAPI at final concentration of 1 µg/ml, covered by a slip, and imaged immediately. Images were captured with a Leica TCS SP8 confocal laser scanning microscope (Leica Microsystems) with a 40×1.30 oil immersion objective. The GFP excitation wavelength used was 488 nm and the emission of fluorescence signals was detected from 500 to 525 nm. Chlorophyll auto-fluorescence was observed with an excitation wavelength of 552 nm and the emission of fluorescence signals was detected from 630 to 670 nm. The mCherry excitation used was 587 nm and emission of fluorescence signals was 619 nm and that for DAPI was 358 nm and 461 nm. The images were first processed in the Las AF Lite software and the combined images were generated using the Las X program from leica microsystem (Morrisville, USA).

To confirm the potential of *Np*OMT to methylate norbelladine in a heterologous *in vivo* system, 50 µl of norbelladine were infiltrated into the *Np*OMT-expressed leaves and incubated for 24 hours in a growth chamber. 100 mg of Norbelladine infiltered leaves were harvested and homogenized under the liquid nitrogen and then extracted with 100 µl of LC-MS grade methanol. Methanol extraction of *Np*OMT-expressing leaves with norbelladine were centrifuged at 10000 rpm for 5 min, supernatant was filtered using a 0.2 µm Nylon PTEE filter and analyzed by LC-MS/MS as described above for enzymatic assays of norbelladine.

3.6.10 Western blot analysis

To confirm the integrity of GFP-tagged *Np*OMT, we performed western blotting. A leave disc of 1 cm diameter of GFP-tagged *Np*OMT, GFP alone and non-infiltrated *N. benthamiana* were harvested and ground under liquid nitrogen. Crude protein was extracted by using 100 µl of protein sample loading buffer and boil at 95 °C for 5 mins. Plant debris was sedimented by brief centrifugation, and supernatant was fractionated by using 10% SDS page. Then, migrated proteins were transfered into a polyvinylidene difluoride (PVDF) membrane by using Turbo transfer system (Bio-Rad). Then PVDF membrane was equilibrated with Tris-buffer saline (TBS) for 5 mins and

blocking was done with 10 ml TBST (TBS with 0.02% of tween 20) containing 5 % of commercial skim milk powder for 1 hour at room temperature. PVDF membrane was incubated with TBST containing 3% BSA and 1:1000 diluted mouse anti-GFP monoclonal antibody (Cedarlane (CLH106AP)) overnight at 4 °C. Then the membrane was washed 5 times with TBST, each lasting 5 mins and further incubated with TBST containing 5% skim milk and 1:10000 diluted anti-mouse horse peroxidase antibody. The PVDF membrane was washed 6 times each for 5 mins with TBST and developed clarity ECL substrate and visualized by Bio rad gel doc XR system.

3.6.11 Protein structure prediction and docking study.

The predicted models of norbelladine 4'-*O*-methyltransferase of *Np*OMT and *L. radiata* (*Lr*OMT) were downloaded from the AlphaFold protein database (AF-A0A346TLF5-F1; AF-AOA5BP8H727, respectively). Models were visualized and superimposed using Pymol (Shrödinger). MOE2022.09 software (Chemical Computing Group) was further used to analyze the resulting models conformation, and prepare receptors for docking, as described in (Majhi, Gélinas et al. 2023). SAM and Mg^{+2} were positioned into *Np*OMT structure following superimposition of the pocket residues with the crystal structure of *Rattus norvegicus* and *H. sapiens* CatOMT (PDB:1H1D (Bonifácio, Archer et al. 2002) and 3A7E, respectively) in MOE. The receptor was then prepared using Structure preparation, which consists of correcting issues, capping, charging termini, selecting appropriate alternate, and calculating optimal hydrogen position and charges using Protonate 3D. Dummies atoms were added to the receptor using Site Finder, and Quickprep was then applied. This included an energy minimization step with tethered active site residues and fixed SAM and Mg^{2+}.

Ligands (3,4-DHBA, norbelladine, caffeic acid, and 4'-*O*-methylnorbelladine) isomeric smiles codes were retrieved from PubChem when available and submitted to the ZINC15 database to download 3D data files (Irwin, Sterling et al. 2012, Sterling and Irwin 2015). Ligands were further prepared in MOE, and all protomers predicted at pH=7.5 were included as possible ligands. The MMFF94× force field was used. Receptor docking site included dummy atoms, Mg^{+2} and SAM. Triangle Matcher was used as placement method for 200 poses, and tethered induced fit as refinement to perform flexible docking, yielding 10 best poses. Docking poses were analyzed by comparison with crystalized catechol OMT-ligand complex (1H1D, 3A7E), and the first pose (with the best docking score) coherent with crystalized OMT and catalyzed reaction was selected for

each ligand. This corresponded to one of the first two best predictions of one of the two most abundant protomers by MOE. PLIP was used to analyze the interactions between ligands and receptor residues (Adasme, Linnemann et al. 2021) , the images were further processed using PyMOL (Shrödinger). PyMOL was also used to predict H-bonds between the metal ion and the docked ligand.

3.6.12 Molecular dynamics simulation

The docked AlphaFold structure were used as template for the simulation. MOE was used to set the parameters, bisualize and analyze the results. The protonation state of norbelladine and *S*-adenosyl l-methionine (SAM) was verified. Amber10: EHT was used as forcefield. The docked receptor was prepared, incorrect topology, protonation and charges were adjusted with the structure preparation tool. Then the system was energy minimized. The system was solvated with water and 0.1mol/L NaCl. The system consisted of 329 amino acids, SAM, Mg2+, norbelladine, 40 NaCl, and 1850 water molecules. NAMD was used to execute the simulation in a periodic system with free atoms, light bonds constrain and rigid wrapped waters. Particle Mesh Ewald (PME) was used for long range interactions. The time step was 2 fs and checkpoint was 500 ps. An initial minimization step lasted 10 ps, followed by heating from 10 to 300K for 100 ps, then temperature equibration (nvt) for 100 ps at 300 K, followed by equilibration of pressure and density (npt) for 200 ps at 300 K and 100 kPa. The production phase was carried out for 25 ns at 300 K and 100 kPa. This process was performed in triplicates for the two positioning of norbelladine. The simulations were performed on Digital Research Alliance of Canada servers.

3.7 References

Adasme, M. F., K. L. Linnemann, S. N. Bolz, F. Kaiser, S. Salentin, V. J. Haupt and M. Schroeder (2021). "PLIP 2021: Expanding the scope of the protein–ligand interaction profiler to DNA and RNA." Nucleic acids research **49**(W1): W530-W534.

Bonifácio, M. J., M. Archer, M. L. Rodrigues, P. M. Matias, D. A. Learmonth, M. A. Carrondo and P. c. Soares-da-Silva (2002). "Kinetics and crystal structure of catechol-o-methyltransferase complex with co-substrate and a novel inhibitor with potential therapeutic application." Molecular pharmacology **62**(4): 795-805.

Brandt, W., K. Manke and T. Vogt (2015). "A catalytic triad--Lys-Asn-Asp--Is essential for the catalysis of the methyl transfer in plant cation-dependent O-methyltransferases." Phytochemistry **113**: 130-139.

Chatterjee, D., D. Kudlinzki, V. Linhard, K. Saxena, U. Schieborr, S. L. Gande, J. P. Wurm, J. Wohnert, R. Abele, V. V. Rogov, V. Dotsch, H. D. Osiewacz, S. Sreeramulu and H. Schwalbe (2015). "Structure and Biophysical Characterization of the S-Adenosylmethionine-dependent O-Methyltransferase PaMTH1, a Putative Enzyme Accumulating during Senescence of Podospora anserina." J Biol Chem **290**(26): 16415-16430.

Chen, H., Z. Lao, J. Xu, Z. Li, H. Long, D. Li, L. Lin, X. Liu, L. Yu, W. Liu, G. Li and J. Wu (2020). "Antiviral activity of lycorine against Zika virus in vivo and in vitro." Virology **546**: 88-97.

Desgagné-Penix, I. (2021). "Biosynthesis of alkaloids in Amaryllidaceae plants: A review." Phytochemistry Reviews **20**(2): 409-431.

Eichhorn, J., T. Takada, Y. Kita and M. H. Zenk (1998). "Biosynthesis of the Amaryllidaceae alkaloid galanthamine." Phytochemistry **49**(4): 1037-1047.

El Tahchy, A., A. Ptak, M. Boisbrun, E. Barre, C. Guillou, F. o. Dupire, F. o. Chrétien, M. Henry, Y. Chapleur and D. Laurain-Mattar (2011). "Kinetic study of the rearrangement of deuterium-labeled 4′-O-methylnorbelladine in Leucojum aestivum shoot cultures by mass spectrometry. Influence of precursor feeding on Amaryllidaceae alkaloid accumulation." Journal of natural products **74**(11): 2356-2361.

Girard, M. P., V. Karimzadegan, M. Heneault, F. Cloutier, G. Berube, L. Berthoux, N. Merindol and I. Desgagne-Penix (2022). "Chemical Synthesis and Biological Activities of Amaryllidaceae Alkaloid Norbelladine Derivatives and Precursors." Molecules **27**(17).

Hotchandani, T., J. de Villers and I. Desgagné-Penix (2019). "Developmental regulation of the expression of Amaryllidaceae alkaloid biosynthetic genes in Narcissus papyraceus." Genes **10**(8): 594.

Hotchandani, T. and I. Desgagne-Penix (2017). "Heterocyclic Amaryllidaceae Alkaloids: Biosynthesis and Pharmacological Applications." Current Topics in Medicinal Chemistry **17**(4): 418-427.

Irwin, J. J., T. Sterling, M. M. Mysinger, E. S. Bolstad and R. G. Coleman (2012). "ZINC: a free tool to discover chemistry for biology." Journal of chemical information and modeling **52**(7): 1757-1768.

Jin, Z. and G. Yao (2019). "Amaryllidaceae and Sceletium alkaloids." Natural Product Reports **36**(10): 1462-1488.

Ka, S., M. Koirala, N. Mérindol and I. Desgagné-Penix (2020). "Biosynthesis and biological activities of newly discovered Amaryllidaceae alkaloids." Molecules **25**(21): 4901.

Ka, S., N. Merindol, A. A. Sow, A. Singh, K. Landelouci, M. B. Plourde, G. Pépin, M. Masi, R. Di Lecce, A. Evidente, M. Seck, L. Berthoux, L. Chatel-Chaix and I. Desgagné-Penix (2021). "Amaryllidaceae Alkaloid Cherylline Inhibits the Replication of Dengue and Zika Viruses." Antimicrob Agents Chemother **65**(9): e0039821.

Khersonsky, O., C. Roodveldt and D. S. Tawfik (2006). "Enzyme promiscuity: evolutionary and mechanistic aspects." Current opinion in chemical biology **10**(5): 498-508.

Kilgore, M. B., M. M. Augustin, G. D. May, J. A. Crow and T. M. Kutchan (2016). "CYP96T1 of Narcissus sp. aff. pseudonarcissus Catalyzes Formation of the Para-Para' C-C Phenol Couple in the Amaryllidaceae Alkaloids." Front Plant Sci **7**: 225.
Kilgore, M. B., M. M. Augustin, C. M. Starks, M. O'Neil-Johnson, G. D. May, J. A. Crow and T. M. Kutchan (2014). "Cloning and characterization of a norbelladine 4'-O-methyltransferase involved in the biosynthesis of the Alzheimer's drug galanthamine in Narcissus sp. aff. pseudonarcissus." PLoS One **9**(7): e103223.
Kilgore, M. B., M. M. Augustin, C. M. Starks, M. O'Neil-Johnson, G. D. May, J. A. Crow and T. M. Kutchan (2014). "Cloning and characterization of a norbelladine 4'-O-methyltransferase involved in the biosynthesis of the Alzheimer's drug galanthamine in Narcissus sp. aff. pseudonarcissus." PloS one **9**(7): e103223.
Kilgore, M. B., C. K. Holland, J. M. Jez and T. M. Kutchan (2016). "Identification of a Noroxomaritidine Reductase with Amaryllidaceae Alkaloid Biosynthesis Related Activities *." Journal of Biological Chemistry **291**(32): 16740-16752.
Kozbial, P. Z. and A. R. Mushegian (2005). "Natural history of S-adenosylmethionine-binding proteins." BMC Struct Biol **5**: 19.
Lashley, A., R. Miller, S. Provenzano, S.-A. Jarecki, P. Erba and V. Salim (2022). "Functional diversification and structural origins of plant natural product methyltransferases." Molecules **28**(1): 43.
Lee, S., J. Kang and J. Kim (2019). "Structural and biochemical characterization of Rv0187, an O-methyltransferase from Mycobacterium tuberculosis." Sci Rep **9**(1): 8059.
Li, W., C. Qiao, J. Pang, G. Zhang and Y. Luo (2019). "The versatile O-methyltransferase LrOMT catalyzes multiple O-methylation reactions in amaryllidaceae alkaloids biosynthesis." International journal of biological macromolecules **141**: 680-692.
Liscombe, D. K., G. V. Louie and J. P. Noel (2012). "Architectures, mechanisms and molecular evolution of natural product methyltransferases." Nat Prod Rep **29**(10): 1238-1250.
Majhi, B. B., S.-E. Gélinas, N. Mérindol, S. Ricard and I. Desgagné-Penix (2023). "Characterization of norbelladine synthase and noroxomaritidine/norcraugsodine reductase reveals a novel catalytic route for the biosynthesis of Amaryllidaceae alkaloids including the Alzheimer's drug galanthamine." Frontiers in Plant Science **14**.
Mann, J. D., H. M. Fales and S. H. Mudd (1963). "Alkaloids and Plant Metabolism: VI. O-methylation in vitro of norbelladine, a precursor of amaryllidaceae alkaloids." Journal of Biological Chemistry **238**(11): 3820-3823.
McKean, I. J. W., P. A. Hoskisson and G. A. Burley (2020). "Biocatalytic Alkylation Cascades: Recent Advances and Future Opportunities for Late-Stage Functionalization." Chembiochem **21**(20): 2890-2897.
Olin, J. and L. Schneider (2002). "Galantamine for Alzheimer's disease." Cochrane Database Syst Rev(3): CD001747.
Rodriguez, G. M., Y. Tashiro and S. Atsumi (2014). "Expanding ester biosynthesis in Escherichia coli." Nature chemical biology **10**(4): 259-265.
Saitou, N. and M. Nei (1987). "The neighbor-joining method: a new method for reconstructing phylogenetic trees." Molecular biology and evolution **4**(4): 406-425.
Singh, A., M.-A. Massicotte, A. Garand, L. Tousignant, V. Ouellette, G. Bérubé and I. Desgagné-Penix (2018). "Cloning and characterization of norbelladine synthase catalyzing the first committed reaction in Amaryllidaceae alkaloid biosynthesis." BMC plant biology **18**(1): 1-12.
Sterling, T. and J. J. Irwin (2015). "ZINC 15–ligand discovery for everyone." Journal of chemical information and modeling **55**(11): 2324-2337.
Su, Y., H.-P. Li, M. Zhang, X.-W. Ding, J.-H. Xu, Q. Chen and G.-W. Zheng (2022). "Regioselectivity Inversion of an O-Methyltransferase via Semi-rational Mutagenesis Combined with Metal Ion Substitution." ChemCatChem **14**(23): e202200844.

Subrizi, F., Y. Wang, B. Thair, D. Mendez-Sanchez, R. Roddan, M. Cardenas-Fernandez, J. Siegrist, M. Richter, J. N. Andexer, J. M. Ward and H. C. Hailes (2021). "Multienzyme One-Pot Cascades Incorporating Methyltransferases for the Strategic Diversification of Tetrahydroisoquinoline Alkaloids." Angew Chem Int Ed Engl **60**(34): 18673-18679.
Sun, B., P. Wang, R. Wang, Y. Li and S. Xu (2018). "Molecular Cloning and Characterization of a meta/para-O-Methyltransferase from Lycoris aurea." International journal of molecular sciences **19**(7): 1911.
Tamura, K., G. Stecher and S. Kumar (2021). "MEGA11: molecular evolutionary genetics analysis version 11." Molecular biology and evolution **38**(7): 3022-3027.
Tarakemeh, A., M. Azizi, V. Rowshan, H. Salehi, R. Spina, F. Dupire, H. Arouie and D. Laurain-Mattar (2019). "Screening of Amaryllidaceae alkaloids in bulbs and tissue cultures of Narcissus papyraceus and four varieties of N. tazetta." J Pharm Biomed Anal **172**: 230-237.
Tousignant, L., A. M. Diaz-Garza, B. B. Majhi, S.-E. Gélinas, A. Singh and I. Desgagne-Penix (2022). "Transcriptome analysis of Leucojum aestivum and identification of genes involved in norbelladine biosynthesis." Planta **255**(2): 30.
Tsao, D., L. Diatchenko and N. V. Dokholyan (2011). "Structural mechanism of S-adenosyl methionine binding to catechol O-methyltransferase." PLoS One **6**(8): e24287.
Waki, T., S. Takahashi and T. Nakayama (2021). "Managing enzyme promiscuity in plant specialized metabolism: A lesson from flavonoid biosynthesis: Mission of a “body double” protein clarified." BioEssays **43**(3): 2000164.
Woodard, R. W., M. D. Tsai, H. G. Floss, P. A. Crooks and J. K. Coward (1980). "Stereochemical course of the transmethylation catalyzed by catechol O-methyltransferase." J Biol Chem **255**(19): 9124-9127.
Zuckerkandl, E. and L. Pauling (1965). Evolutionary divergence and convergence in proteins. Evolving genes and proteins, Elsevier**:** 97-166.

Chapter IV contains a discussion that presents a combine result and discussion section from chapter II and chapter III, together with its future perspective.

Chapter IV

4. Conclusion

4.1 Discussion

To minimize over-harvesting of native plants, biotechnological approaches such as *in vitro* culture of plant or plant's tissue, and genetic engineering can be utilized as a sustainable source of AAs. The molecular understanding of the effect of different factors on the biosynthesis of AAs may improve their production from *in vitro* tissue and provide essential genetic knowledge (Park, Yeo et al. 2020, Rahimi Khonakdari, Rezadoost et al. 2020, Li, Xu et al. 2021). Exploring the genetic and enzymatic basis of AAs biosynthesis routes can open the door for more advanced technique, such as genetic engineering approach to rewire the chassis of heterologous hosts and bypass the dependency of the supply chain of AAs on plants (Diamond and Desgagné-Penix 2016). To develop the tools for sustainable production of AAs, we initially aimed to develop *in vitro* culture of Amaryllidaceae plant and later focused on a comparative transcriptomic study between alkaloid-producing and non-producing tissues, and finally we performed a functional characterization of a candidate biosynthetic genes.

Several studies reported species-specific AAs profiles. Previous transcriptomic studies on *Narcissus* sp, *Lycoris* sp, and *Leucojum* sp., well known to accumulate galanthamine-type and lycorine-type AAs, have provided insight into AAs biosynthesis genes (Aleya, Xianmin et al. 2021, Li, Xu et al. 2021, Tousignant, Diaz-Garza et al. 2022). Here, we focused our efforts on a cherylline-type producing species (*Crinum* x *powellii* "Album"). We performed initial metabolite screening of *C.* x *powellii* "Album" that confirmed the presence of cherylline-type of AAs together with lycorine- and crinine-types, as previously reported (Niño, Hincapié et al. 2007). Phylogenetic analysis of ITS2 region verified that *C.* x *powellii* "Album" belong to the South-African clade of *Crinum* species, including *C. bulbispermum*, *C. stuhlmannii* and *C. moorei*. The unique AAs profile of *C.* x *powellii* "Album", and the unexplored transcriptome of plant belonging to *Crinum* genera, made of *C.* x *powellii* "Album" a good candidate for further study.

In *in vitro* cultures, modifications of physical and chemical parameters enable the finetuning of tissue differentiation, organogenesis and ultimately alkaloid production (Gallego, Rojas et al. 2018). Phytohormones, such as auxins, play a vital role in plant development, promote cell

elongation and control a variety of functions, including organogenesis, general shoot and root architecture, responses to light and gravity, and tropical growth (Woodward and Bartel 2005, Ptak, Tahchy et al. 2013, Khadr, Wang et al. 2020). A study on *Narcissus pseudonarcissus* cv. Carlton shows that the concentration of NAA, a type of auxin, impacts on the types of tissue that develop, and eventually on the AAs accumulation (Ferdausi, Chang et al. 2020). Therefore, as first objective of our study, we studied the effect of light and auxin on *in vitro* tissue culture.

It is often challenging to initiate *in vitro* culture from underground tissue such as bulbs which are in direct contact with soil microorganism. The presence of endophytic contamination is a major challenge associated with the initiation of *in vitro* culture form ground plant tissue. Effective ways of mild surface sterilization that include cold and heat treatment were used to remove endophytic contamination from Amaryllidaceae plant in previous studies (Ferdausi, Chang et al. 2020). We adapted our surface sterilization technique to include heat treatment at 52°C for one hour, followed by ethanol rinsing and bleaching for 30 min of bulbs, then *in vitro* culture was initiated from twin scale explant extracted from bulb inner part, as previously reported (Slabbert, De Bruyn et al. 1993, Priyadharshini, Kannan et al. 2020, Trujillo-Chacon, Pastene-Navarrete et al. 2020, Aleya, Xianmin et al. 2021). No contamination was detected during initiation of *in vitro* culture, which indicates that our surface sterilization methodology was effective enough to remove surface contamination as well as endophytic microorganism from explants extracted from bulb. During this initiation period, plants often release phenolic compounds in response to stress, such as wounding or changing culture condition. Oxidation of phenolic compounds can be toxic for newly growing plants (Dixon and Paiva 1995, Ndakidemi, Mneney et al. 2014). During our study, a higher ratio of explant browning in light condition was observed, which eventually lead to death of the explants. This indicated that light conditions were harsher as compared to dark. Previous reports on parental *C. moorei in vitro* culture also showed a higher ratio of explant browning in light condition (Fennell, Elgorashi et al. 2003).

To understand the effect of exogenous supply of auxin and growth condition, we monitored growth of tissue for 6 months. During our study we observed that exogenous auxin impacted both the type of tissue that develop and its survival rate. Direct organogenesis only occurred on explant that were not supplied with exogenous auxin. This confirms that endogenous auxin level is sufficient for growth of tissue at initial phase. However, exogenous auxin was essential to induce callus

conforming to previous reports (Rahimi Khonakdari, Rezadoost et al. 2020). In the presence of 2,4-D, explants grew as undifferentiated tissue*, i.e.*, callus, regardless of its concentration and of exposure to light. Our results show that exogenous supply of auxin and light modulate tissue differentiation during *in vitro* culture of *C.* x *powellii* "Album".

We explored the AAs profiles of different types of tissues developed during *in vitro* culture using GC-MS and LC-MS/MS. The accumulation of AAs was more important in light compared to dark condition, and in differentiated tissues as compared to unorganized tissue (callus), in keeping with reports in *Agastache rugosa* (Korean mint) (Park, Yeo et al. 2020), and in Amaryllidaceae *L. aestivum* L. and *L. longituba* (Li, Xu et al. 2021, Morańska, Simlat et al. 2023). Higher accumulation of AAs in tissues exposed to light condition is probably related to the availability of carbon source, as these tissues are actively involved in photosynthesis (Ferdausi, Chang et al. 2020). Alternatively, light stress could trigger the synthesis of SMs in *C.* x *powellii* "Album" as defensive response. In native plants, there is a tissue-specific accumulation of AAs, which could be related to the involvement of multiple tissue in AAs metabolism. As tissue survival rate in dark condition is higher, but differentiated and light-exposed tissues produce more alkaloids, future research could be focused on initial development of differentiated tissue for production of AAs in dark condition, and later shift to light condition to induce AAs biosynthesis with better tissue survival rate.

As our study was the first to generate transcriptomic data of plants belonging to *Crinum* genus, there was no reference transcriptome available for this non-model plant. To generate more reliable reference transcriptome from RNA-seq data of *C.* x *powellii* "Album", we performed the *de novo* transcriptomic assembly by including RNA-seq data generated from both *in vivo* and *in vitro* tissues. Our assembled transcriptome of *C.* x *powellii* "Album" generated 785 475 trinity genes with 90.70% complete orthologs as compared to embryophyte database, and an N50 of 1 033, with mean and median contig lengths of 364 and 658.04 respectively. This revealed that we generated reliable transcriptome data for *C.* x *powellii* "Album" which can be used as reference transcriptome for our study, as well as for other plants belonging to *Crinum* genus.

In our assembled transcriptome containing both *in vivo* and *in vitro* samples, we observed a low abundance of transcripts belonging to "RNA processing and modification" as well as "chromatin structure and dynamics". Often, the expression of genes varies in between tissues, depending on

their developmental stage, a process related to remodeling of chromatin (Jarillo, Piñeiro et al. 2009, Ojolo, Cao et al. 2018). RNA post-transcriptional modifications such as alternative splicing can also regulate the level of alkaloid biosynthesis. Increase in these regulatory processes, when measured at the proteomic levels, have been associated with increased accumulation of AAs, although the mechanism is not known (Tang, Li et al. 2023). Even though calluses produced fewer alkaloids as compared to differentiated tissue, a variation was observed in alkaloid profile in tissue grown in light and dark condition with different level of 2,4-D. In addition, in our study of *N. papyraceus* plant tissues, the relative expression of putative biosynthetic genes such as *NpNBS*, *NpNR* and *NpOMT* did not correlate with the alkaloid profile. This indicated that the site of metabolite synthesis and their storage may be different, as reported in case of nicotine in *Nicotiana* plant (Katoh, Ohki et al. 2005). In such case, corelating metabolite level with gene expression between different tissue types may not be reliable (Delli-Ponti, Shivhare et al. 2021). Samples containing homogenous cells such as callus provide an alternative strategy for performing such correlation. Therefore, they were selected for in depth transcriptomic analysis for their homogeneity, (similar kind of tissue) and because they provide a straightforward matrix to understand AAs biosynthesis.

As expected in light condition, genes related to photosynthesis and those involved in tetrapyrrole binding activity were up-regulated in callus, regardless of 2,4-D concentration. Increased activity of tetrapyrrole binding helps the plant to adapt under different abiotic stress conditions, including excess or lack of light. We observed higher accumulation of AAs in light, together with up-regulation of genes category involved in the adaptation to light stress condition. It is conceivable that Amaryllidaceae produce alkaloids in a defensive response to light stress. In line with this hypothesis, oxidoreductase and monooxygenase activity were also enriched GO term categories in the light condition.

When callus were grown in absence of light, genes related to mannose binding, crucial for plant defense signaling during pathogen attack, were upregulated by increased concentration of 2,4-D (Hwang and Hwang 2011, Ma, Haile et al. 2023). We did not observe any contamination during this study, and to our knowledge, there is no data associating 2,4-D concentration with mannose binding gene expression. This was intriguing, as phenylpropanoids and alkaloids, which are also

produced to defend the plant against external stress, accumulated as well in higher concentration of 2,4-D in dark conditions.

AAs biosynthetic genes such as *TYDC*, *C3H*, *PAL*, *HCT*, *OMT*, *NorRed*, *NBS*, and *CYP96* were identified and characterized from other Amaryllidaceae. We identified putative AAs biosynthesis gene from *C.* x *powellii* "Album" transcriptome based on homology search and a high % (*i.e.* >75%) of amino acids sequence identity. Expression levels of *TYDC*, *C3H*, *PAL*, *HCT*, *OMT*, *NorRed, NBS*, and *CYP96* were higher in callus exposed to light compared to those grown in the dark. Their expression was also modulated by 2,4-D concentration. Light and auxins led to an increase in AAs and its precursors at both metabolomic and transcriptomic levels. This is probably related to their protective role from the damages caused by light (Winkel-Shirley 2001, Wink 2008). In conditions of light exposure, an increased concentration of 2,4-D led to a decrease in photosynthesis related genes, and an accumulation of transcripts associated with hydrogen peroxide catabolic process and apoplast. These genes are related to cell death, indicating that 4 mg/L of 2,4-D in callus exposed to light may be toxic and trigger programmed cell death (Yoda, Yamaguchi et al. 2003, Gupta, Sengupta et al. 2016), in accordance with the observed lower survival of explants and with El Tahchy, Bordage et al. (2011). Alternatively, alkaloid synthesis induced by light and 2,4-D could be the cause of this toxicityTo understand the pattern of genes related to AAs metabolism in *C.* x *powellii*, we performed co-expression analysis. Often genes which are involved in similar kind of biological function are co-expressed, and during the co-expression analysis these genes are present in a same module (Delli-Ponti, Shivhare et al. 2021). Therefore, we performed a detailed analysis of modules in which AAs biosynthesis gene were identified. The expression levels of genes related to production of phenylpropanoid compounds, and AAs biosynthetic pathways were interconnected with each other, together with photosynthesis-related and hormone-induced genes, linking light and auxin response to their expression. A balance between stress and death appears to be key to optimize AAs production in plant.

Although, AAs can be produced from *in vitro* tissue without being affected by external environmental factors, accumulation of AAs was low as compared to *in vivo* tissue (Ferdausi, Chang et al. 2020). Therefore, knowledge base discovery of biosynthesis genes and functional characterization of biosynthesis genes is essential to jump into more advanced biotechnological approach, such as genetic engineering of native plant or of heterologous organism. During this

Ph.D. project, as a second objective, we functionally characterized homologous norbelladine *O*-methyltransferase (OMT) proposed to be involved in the *O*-methylation of norbelladine. Initially, we aimed at characterizing this enzyme from *Crinum x. powelli*, but because of delays in the project due to COVID-related restrictions, the slow growth rate of callus, and the time required for transcriptomic analysis, we functionally characterised *N. papyraceus O*-methyltransferase instead. Moreover, *Np*OMT shows 82.01% amino acid sequence identity with putative norbelladine *O*-methyltransferase from *C.* x *powellii* "Album".

There were differences in the metabolic profile of *C.* x *powellii* "Album" and *N. papyraceus*. However, both contain ED the proposed AAs route, that considers norbelladine as a first common intermediate compound undergoing regioselective *O*-methylation (Desgagné-Penix 2021). AAs such as lycorine are reported from both *Crinum.* sp and *Narcissus.* sp, and labelling studies have shown that lycorine is derived from 4'-*O*-methylnorbelladine (Eichhorn, Takada et al. 1998, El Tahchy, Ptak et al. 2011). In addition to AAs derived 3'-*O* or 4'-*O*-methylnorbelladine, AAs such as belladine are supposed to be derived from 3',4'-*O*-dimethylnorbelladine (Desgagné-Penix 2021). Norbelladine *O*-methyltransferase from *N*. sp *aff. pseudonarsissus* (*Np*N4OMT) was shown to be regioselective*,* methylating norbelladine and *N*-methylnorbelladine at 4'-OH position, nut not AAs precursor molecules (Kilgore, Augustin et al. 2014). By contrast, norbelladine methyltransferase from *Lycoris* species and *Galanthus elwesii* were reported to be non-regioselective, methylating norbelladine at 3'or 4'-OH position (Sun, Wang et al. 2018, Li, Qiao et al. 2019, Su, Li et al. 2022) and a broad range of other substrates. Upon analysis of *N. papyraceus* metabolome, we detected AAs such as 3',4'-dimethylnorbelladine and 4'- *O*-methylnorbelladine, but not 3'-*O*-methylnorbelladine, making norbelladine *O*-methyltransferase from *N. papyraceus* a good candidate for our study.

*Np*OMT catalytic activity was consistent with metal dependent *O*-methylation. The enzyme preferably methylated norbelladine at 4'-OH position with lower K_m value and higher efficiency, than reported with homologous norbelladine OMT from *Lycoris* species (Li, Qiao et al. 2019). *In vivo* studies with *N. benthamiana*, confirmed that *Np*OMT can catalyze the regio-selective formation of 4'-*O*-methylation in *in vivo* system. Unlike *Np*N4OMT (Kilgore, Augustin et al. 2014), but similarly to *Lr*OMT, it also methylated caffeic acid and 3,4-DHBA to produce monomethylated product at both 3 or 4-OH position. *Np*OMT is a promiscuous enzyme that accepts both AAs and AAs precursor molecules. Such behavior has previously reported for other AAOMT,

leading to alternative hypothesis methylated norbelladine synthesis, which could occur from the condensation of methylated precursor molecules (such as vanillin or isovanillin). The ability of NBS to accept and methylated precursor molecules then transform them into methylated norbelladine must be tested to confirm this hypothesis.

Distinct to any other reported AAOMT, *Np*OMT also yielded a dimethylated form of norbelladine. We hypothesized that 3',4'-*O*-dimethylnorbelladine could be formed by methylation of monomethylated norbelladine. However, *Np*OMT did not accept 3' nor 4'-*O*-methylnorbelladine as substrate. Although the reaction mechanism of 3', 4'-*O*-dimethylnorbelladine difficult to predict, our study revealed a novel catalytic potential of *Np*OMT.

In addition, when norbelladine was used as substrate, we observed an additional reaction product at 13.45 min with a mass of $[M+H]^+$ ion m/z 274 corresponding to a monomethylated norbelladine during both *in vitro* and *in vivo* enzymatic assy. Previously such product equivalent to monomethylated norbelladine was reported when norbelladine was incubated with homologous norbelladine *O*-methyltransferase from *L. aurea* and considered as 3'-*O*-methylnorbelladine without any spectral evidence (Sun, Wang et al. 2018). While in our study, retention time and fragmentation pattern of product peak at 13.45 min (peak iv) did not match with neither 4'-*O*- and 3'-*O*-methylnorbelladine. We hypothesize that *Np*OMT could also methylate norbelladine at 4-OH position. As we lack 4-*O*-methylnorbelladine as standard molecule, we could not further confirm and considered it as unknown peak.

Even though we did not detect 3'-*O*-methylnorbelladine, docking analysis supported 3-*O* (3' in the case of norbelladine) and 4-*O* (4') methylation catalysis of the tested ligands by *Np*OMT. An intricate array of binding interactions with *Np*OMT collectively anchor the substrate molecules such that the reactive oxygen atom (at position 3 or 4) forms favorable interactions with the enzyme's catalytic groups and SAM methyl donor. Lys158 and Mg^{2+} bound with the oxygen to be methylated, and Asn182 interacted with the other hydroxyl group of the catechol ring, emphasizing their key role in the catalytic process (Brandt et al., 2015). While a previous report on *Galanthus elwesii Ge*OMT suggested that Tyr186 was important for meta (3-OH) methylated products (Su et al., 2022), in the case of *Np*OMT it interacted mostly with ligands (3,4-DHBA, caffeic acid and norbelladine) in position for 4/4'-*O*-methylation. Interestingly, Tyr186 also interacted with 4'-*O*-methylnorbelladine in position for its 3'-*O*-methylation. Regio-selectivity was indeed reported to

be dependent on key residues, ligand structure and metal species (Subrizi et al., 2021). Other studies have described Trp185 as an important amino acid (Brandt et al., 2015), here, it stabilized larger alkaloid ligand. Docking has its limitation, especially since we used a modeled protein, and the prediction did not provide an explanation to the observed absence of catalysis of 3ˈ-*O*-methylation of norbelladine in *in vitro* assay, although the docking score was indeed lower. At the same time alphafold predicted protein model have enough atomic accuracy to support the further investigation of protein and substrate (Jumper, Evans et al. 2021). We investigated further *Np*OMT methylation process by two different orientations of 3ˈ-OH and 4ˈ-OH using molecular dynamics. During molecular dynamic study, we can investigate how every atoms of a protein moved over time to interact with substrate, and it can provide understanding at the atomic level (Hollingsworth and Dror 2018). Three trajectory of 25 ns were analysed for each position (4ˈand 3ˈ-*O*-methylation) of norbelladine. When simulation was performed with norbelladine in 4ˈ-OH orientation towards the methyl donor, 4ˈ-OH remained closer to SAM and Mg^{2+} compared to the 3ˈOH. In this orientation, SAM and norbelladine deviated little over the trajectory period suggesting that the complex was stable. Distance to the possible base-acting residue Lys158 remained stable over the trajectory course. When simulation was performed with norbelladine in 3ˈ-OH orientation, the ligand deviated more significantly from its initial trajectory. An inversion of the -OH group occurred in all cases to bring norbelladine 4ˈOH in proximity to the cofactor and to the metal. Distance with Lys158 also increased over time. Together, kinetic parameters of *Np*OMT with norbelladine and *in vivo* enzymatic assay, this simulation study supports that methylation of 4ˈOH of norbelladine is favored by *Np*OMT.

Studies on important amino acids interacting with the substrate involved in changing orientation of norbelladine will be helpful to understand the promiscuous behaviour of AAOMT. As regio-selective methylation is important for the metabolite fate of norbelladine, a deeper understanding of the underlined reaction mechanism will be beneficial to develop tools for synthetic biology for production of targeted types of AAs in heterologous host.

4.2 Overall Conclusion

In conclusion, our study involved the development of *in vitro* culture, comparative transcriptomic study between alkaloid producing and non-producing tissues, and functional characterization of a biosynthetic enzyme. As reported in other Amaryllidaceae plant, we observed higher accumulation

of AAs in differentiated as compared to undifferentiated tissues, and light induced the synthesis of AAs. *In vitro* culture of differentiated tissues, such as bulb in light condition could be an effective way to produce the AA. Our study reveals that higher concentration of auxin such as 2,4-D promotes the AAs synthesis but can be toxic to tissue in light condition. Transcriptomic study on tissue grown with different levels of auxin and lightshows that balancing stress and death will yield to the optimal condition to produce alkaloid in a sustainable manner. In addition, our study on catalytic potential of *Np*OMT shows its possible promiscuous behaviour in AAs biosynthesis pathway. Understanding the detailed reaction mechanism is important to orient the AAs pathway towards regio-specific methylated norbelladine.

4.3 Future perspectives

As a first objective of this Ph.D. research project, we develop *in vitro* culture and performed transcriptomic study on alkaloid producing and non-producing *in vitro* tissue of *C.* x *powellii* "Album", a non-model medicinal plant. The demand for medicinal compounds from plant source is increasing, and *in vitro* tissue propagation can serve as wonderful platform to produce them. Therefore, our research on initiation and development of *in vitro* culture can be referenced to develop *in vitro* culture from other non-model bulbous. During the initiation of *in vitro,* we observed that survival of tissue was higher in dark condition with low concentration of auxin, however accumulation of AAs was higher in light condition. Hence, further research should be performed by initiating *in vitro* culture in dark condition and then shifting tissue culture to light condition which is more favourable AAs synthesis. A study on the effect of different light intensity on callus will help to determine optimum light intensity for alkaloid production. Transcriptomic study on these calli will provide an understanding of the regulatory factors for alkaloid production. We performed the transcriptomic study on 12 samples generated from *in vitro* culture. Structural base blast (DeepBLAST) of low sequence similarity protein can increase functional annotation of existing data, which can help to identify novel genes encoding enzymes putatively involved in AAs biosynthesis (Hamamsy, Morton et al. 2023). Our study reveals the co-expression pattern of different AAs production genes, photosynthesis related genes and auxin induce genes. Uncovering the relationship between different biosynthetic genes and other regulatory genes can be further used in metabolic engineering approaches. Further research on auxin will also contribute to determine its optimal ratio to develop specific types of tissue for alkaloid production.

During this Ph.D. project, we functionally characterized the *O*-methyltransferase possibly involved in diversification of AAs. Our study shows that homologous norbelladine OMT from *N. papyraceus* is highly promiscuous. We observed a novel catalytic potential of *Np*OMT, to transform norbelladine into 3',4'-*O*-dimethylnorbelladine. Future research could focus on comparative analysis between different plant OMT and their catalytic behaviour.

Finally, the knowledge developed during this study is beneficial to the development of sustainable platforms to produce AAs through biotechnological approaches.

Reference

Abd el Hafiz, M. A., Ramadan, M. A., Jung, M. L., Beck, J. P., & Anton, R. (1991). Cytotoxic activity of Amaryllidaceae alkaloids from *Crinum augustum* and *Crinum bulbispermum*. *Planta Med, 57* (5), 437-439.

Aleya, F., Xianmin, C., Anthony, H., & Meriel, J. (2021). Relative expression of putative genes involved in galanthamine and other Amaryllidaceae alkaloids biosynthesis in *Narcissus* field and in vitro tissues. *Gene, 774*, 145424.

Anders, S., & Huber, W. (2012). Differential expression of RNA-Seq data at the gene level–the DESeq package. *Heidelberg, Germany: European Molecular Biology Laboratory (EMBL), 10*, f1000research.

Ausländer, S., Ausländer, D., & Fussenegger, M. (2017). Synthetic biology—the synthesis of biology. *Angewandte Chemie International Edition, 56* (23), 6396-6419.

Banwell, M. G., Edwards, A. J., Jolliffe, K. A., & Kemmler, M. (2001). An operationally simple and fully regiocontrolled formal total synthesis of the montanine-type Amaryllidaceae alkaloid (±)-pancracine. *Journal of the Chemical Society, Perkin Transactions 1* (12), 1345-1348.

Bergoñón, S., Codina, C., Bastida, J., Viladomat, F., & Melé, E. (1996). Galanthamine production in "shoot-clump" cultures of Narcissus confusus in liquid-shake medium. *Plant cell, tissue and organ culture, 45* (3), 191-199.

Berkov, S., Georgieva, L., Sidjimova, B., Nikolova, M., Stanilova, M., & Bastida, J. (2021). In vitro propagation and biosynthesis of Sceletium-type alkaloids in Narcissus pallidulus andNarcissus cv. Hawera. *South African Journal of Botany, 136*, 190-194.

Berkov, S., Osorio, E., Viladomat, F., & Bastida, J. (2020). Chemodiversity, chemotaxonomy and chemoecology of Amaryllidaceae alkaloids. *The Alkaloids: Chemistry and Biology, 83*, 113-185.

Berkov, S., Pavlov, A., Georgiev, V., Bastida, J., Burrus, M., Ilieva, M., et al. (2009). Alkaloid synthesis and accumulation in Leucojum aestivum in vitro cultures. *Natural product communications, 4* (3), 1934578X0900400328.

Bourgaud, F., Gravot, A., Milesi, S., & Gontier, E. (2001). Production of plant secondary metabolites: a historical perspective. *Plant Science, 161* (5), 839-851.

Brossi, A., Grethe, G., Teitel, S., Wildman, W. C., & Bailey, D. T. (1970). Cherylline, a 4-phenyl-1, 2, 3, 4-tetrahydroisoquinoline alkaloid. *The Journal of Organic Chemistry, 35* (4), 1100-1104.

Bruex, A., Kainkaryam, R. M., Wieckowski, Y., Kang, Y. H., Bernhardt, C., Xia, Y., et al. (2012). A gene regulatory network for root epidermis cell differentiation in *Arabidopsis*. *PLoS Genet, 8* (1), e1002446.

Brusotti, G., Cesari, I., Dentamaro, A., Caccialanza, G., & Massolini, G. (2014). Isolation and characterization of bioactive compounds from plant resources: The role of analysis in the ethnopharmacological approach. *Journal of pharmaceutical and biomedical analysis, 87*, 218-228.

Bryant, D. M., Johnson, K., DiTommaso, T., Tickle, T., Couger, M. B., Payzin-Dogru, D., et al. (2017). A Tissue-Mapped Axolotl De Novo Transcriptome Enables Identification of Limb Regeneration Factors. *Cell Rep, 18* (3), 762-776.

Cahlíková, L., Kawano, I., Řezáčová, M., Blunden, G., Hulcová, D., & Havelek, R. (2021). The Amaryllidaceae alkaloids haemanthamine, haemanthidine and their semisynthetic derivatives as potential drugs. *Phytochemistry Reviews, 20*, 303-323.

Cao, M., Gao, M., Suastegui, M., Mei, Y., & Shao, Z. (2020). Building microbial factories for the production of aromatic amino acid pathway derivatives: from commodity chemicals to plant-sourced natural products. *Metabolic engineering, 58*, 94-132.

Carbone, F., Preuss, A., De Vos, R. C., D'Amico, E., Perrotta, G., Bovy, A. G., et al. (2009). Developmental, genetic and environmental factors affect the expression of flavonoid genes, enzymes and metabolites in strawberry fruits. *Plant Cell Environ, 32* (8), 1117-1131.

Casciaro, B., Mangiardi, L., Cappiello, F., Romeo, I., Loffredo, M. R., Iazzetti, A., et al. (2020). Naturally-occurring alkaloids of plant origin as potential antimicrobials against antibiotic-resistant infections. *Molecules, 25* (16), 3619.

Chan, J. L. A. (1973). *BIOSYNTHESIS OF CHERYLLINE USING DOUBLY-LABELED NORBELLADINE-TYPE PRECURSORS*: Iowa State University.

Chase, M. W., Reveal, J. L., & Fay, M. F. (2009). A subfamilial classification for the expanded asparagalean families Amaryllidaceae, Asparagaceae and Xanthorrhoeaceae. *Botanical Journal of the Linnean Society, 161* (2), 132-136.

Colque, R., Viladomat, F., Bastida, J., & Codina, C. (2002). Micropropagation of the rare Eucrosia stricklandii (Amaryllidaceae) by twin-scaling and shake liquid culture. *The Journal of Horticultural Science and Biotechnology, 77* (6), 739-743.

Colque, R., Viladomat, F., Bastida, J., & Codina, C. (2004). Improved production of galanthamine and related alkaloids by methyl jasmonate in Narcissus confusus shoot-clumps. *Planta medica, 70* (12), 1180-1188.

Conesa, A., Madrigal, P., Tarazona, S., Gomez-Cabrero, D., Cervera, A., McPherson, A., et al. (2016). A survey of best practices for RNA-seq data analysis. *Genome Biol, 17* (1), 13.

Cordell, G. A., Quinn-Beattie, M. L., & Farnsworth, N. R. (2001). The potential of alkaloids in drug discovery. *Phytotherapy Research: An International Journal Devoted to Pharmacological and Toxicological Evaluation of Natural Product Derivatives, 15* (3), 183-205.

Cushnie, T. T., Cushnie, B., & Lamb, A. J. (2014). Alkaloids: An overview of their antibacterial, antibiotic-enhancing and antivirulence activities. *International journal of antimicrobial agents, 44* (5), 377-386.

Dasari, R., Banuls, L. M. Y., Masi, M., Pelly, S. C., Mathieu, V., Green, I. R., et al. (2014). C1, C2-ether derivatives of the Amaryllidaceae alkaloid lycorine: Retention of activity of highly lipophilic analogues against cancer cells. *Bioorganic & medicinal chemistry letters, 24* (3), 923-927.

De Smet, P. A. (1997). The role of plant-derived drugs and herbal medicines in healthcare. *Drugs, 54*, 801-840.

Delli-Ponti, R., Shivhare, D., & Mutwil, M. (2021). Using gene expression to study specialized metabolism—a practical guide. *Frontiers in Plant Science, 11*, 625035.

Demir, S. C., Yildirim, A. B., Turker, A. U., & Eker, I. (2022). Seasonal variation in alkaloid content, phenolic constituent and biological activities of some Leucojum aestivum L. populations in Turkey. *South African Journal of Botany, 147*, 713-723.

Desgagné-Penix, I. (2021). Biosynthesis of alkaloids in Amaryllidaceae plants: A review. *Phytochemistry Reviews, 20* (2), 409-431.

Dewick, P. M. (2009). *Medicinal natural products: a biosynthetic approach.* (3rd ed.): John Wiley and Sons Ltd.

Diamond, A., & Desgagné-Penix, I. (2016). Metabolic engineering for the production of plant isoquinoline alkaloids. *Plant biotechnology journal, 14* (6), 1319-1328.

Ding, Y., Qu, D., Zhang, K.-M., Cang, X.-X., Kou, Z.-N., Xiao, W., et al. (2017). Phytochemical and biological investigations of Amaryllidaceae alkaloids: a review. *Journal of Asian natural products research, 19* (1), 53-100.

Diop, M., Hehn, A., Ptak, A., Chrétien, F., Doerper, S., Gontier, E., et al. (2007). Hairy root and tissue cultures of Leucojum aestivum L.—relationships to galanthamine content. *Phytochemistry reviews, 6*, 137-141.

Dixon, R. A., & Paiva, N. L. (1995). Stress-induced phenylpropanoid metabolism. *The plant cell, 7* (7), 1085.

Dixon, R. A., & Paiva, N. L. (1995). Stress-Induced Phenylpropanoid Metabolism. *Plant Cell, 7* (7), 1085-1097.

Dostál, J. (2000). Two faces of alkaloids. *Journal of Chemical Education, 77* (8), 993.

Eichhorn, J., Takada, T., Kita, Y., & Zenk, M. H. (1998). Biosynthesis of the Amaryllidaceae alkaloid galanthamine. *Phytochemistry, 49* (4), 1037-1047.

El Tahchy, A., Bordage, S., Ptak, A., Dupire, F., Barre, E., Guillou, C., et al. (2011a). Effects of sucrose and plant growth regulators on acetylcholinesterase inhibitory activity of alkaloids accumulated in shoot cultures of Amaryllidaceae. *Plant Cell, Tissue and Organ Culture (PCTOC), 106* (3), 381-390.

El Tahchy, A., Ptak, A., Boisbrun, M., Barre, E., Guillou, C., Dupire, F. o., et al. (2011). Kinetic study of the rearrangement of deuterium-labeled 4'-O-methylnorbelladine in Leucojum aestivum shoot cultures by mass spectrometry. Influence of precursor feeding on Amaryllidaceae alkaloid accumulation. *Journal of natural products, 74* (11), 2356-2361.

Elgorashi, E. E., Drewes, S. E., Morris, C., & van Staden, J. (2003). Variation among three Crinum species in alkaloid content. *Biochemical Systematics and Ecology, 31* (6), 601-615.

Elgorashi, E. E., Drewes, S. E., & Van Staden, J. (2002). Organ-to-organ and seasonal variation in alkaloids from *Crinum macowanii*. *Fitoterapia, 73* (6), 490-495.

Espinosa-Leal, C. A., Mora-Vásquez, S., Puente-Garza, C. A., Alvarez-Sosa, D. S., & García-Lara, S. (2022). Recent advances on the use of abiotic stress (water, UV radiation, atmospheric gases, and temperature stress) for the enhanced production of secondary metabolites on in vitro plant tissue culture. *Plant Growth Regulation, 97* (1), 1-20.

Evans, W. C. (2009). *Trease and Evans' pharmacognosy*: Elsevier Health Sciences.

Facchini, P. J., Bohlmann, J., Covello, P. S., De Luca, V., Mahadevan, R., Page, J. E., et al. (2012). Synthetic biosystems for the production of high-value plant metabolites. *Trends in biotechnology, 30* (3), 127-131.

Facchini, P. J., & De Luca, V. (2008). Opium poppy and Madagascar periwinkle: model non-model systems to investigate alkaloid biosynthesis in plants. *The Plant Journal, 54* (4), 763-784.

Farhi, M., Marhevka, E., Ben-Ari, J., Algamas-Dimantov, A., Liang, Z., Zeevi, V., et al. (2011). Generation of the potent anti-malarial drug artemisinin in tobacco. *Nature biotechnology, 29* (12), 1072-1074.

Fennell, C. W., Elgorashi, E. E., & van Staden, J. (2003). Alkaloid production in *Crinum moorei* cultures. *J Nat Prod, 66* (11), 1524-1526.

Fennell, C. W., & van Staden, J. (2001). *Crinum* species in traditional and modern medicine. *J Ethnopharmacol, 78* (1), 15-26.

Ferdausi, A., Chang, X., Hall, A., & Jones, M. (2020a). Galanthamine production in tissue culture and metabolomic study on Amaryllidaceae alkaloids in *Narcissus pseudonarcissus* cv. Carlton. *Industrial Crops and Products, 144*, 112058.

Ferdausi, A., Chang, X., & Jones, M. (2021a). Enhancement of galanthamine production through elicitation and NMR-based metabolite profiling in Narcissus pseudonarcissus cv. Carlton in vitro callus cultures. *In Vitro Cellular & Developmental Biology-Plant, 57* (3), 435-446.

Ferdausi, A., Chang, X., & Jones, M. (2021b). Transcriptomic analysis for differential expression of genes involved in secondary metabolite production in Narcissus pseudonarcissus field derived bulb and in vitro callus. *Industrial Crops and Products, 168*, 113615.

Fossati, E., Narcross, L., Ekins, A., Falgueyret, J.-P., & Martin, V. J. (2015). Synthesis of morphinan alkaloids in Saccharomyces cerevisiae. *PLoS One, 10* (4).

Gaba, V. P. (2005). Plant growth regulators in plant tissue culture and development. Dans *Plant development and biotechnology* (pp. 87-99): CRC Press Boca Raton, FL.

Gallego, A. M., Rojas, L. F., Parra, O., Rodriguez, H. A., Mazo Rivas, J. C., Urrea, A. I., et al. (2018a). Transcriptomic analyses of cacao cell suspensions in light and dark provide target genes for controlled flavonoid production. *Scientific reports, 8* (1), 13575.

Galperin, M. Y., Wolf, Y. I., Makarova, K. S., Vera Alvarez, R., Landsman, D., & Koonin, E. V. (2021). COG database update: focus on microbial diversity, model organiSM, and widespread pathogens. *Nucleic Acids Res, 49* (D1), D274-D281.

Gaspar, T., Kevers, C., Penel, C., Greppin, H., Reid, D. M., & Thorpe, T. A. (1996). Plant hormones and plant growth regulators in plant tissue culture. *In vitro Cellular & Developmental Biology-Plant, 32* (4), 272-289.

Georgiev, V., Ivanov, I., Berkov, S., Ilieva, M., Georgiev, M., Gocheva, T., et al. (2012). Galanthamine production byLeucojum aestivumL. shoot culture in a modified bubble column bioreactor with internal sections. *Engineering in Life Sciences, 12* (5), 534-543.

Girard, M.-P., Karimzadegan, V., Héneault, M., Cloutier, F., Bérubé, G., Berthoux, L., et al. (2022). Chemical Synthesis and Biological Activities of Amaryllidaceae Alkaloid Norbelladine Derivatives and Precursors. *Molecules, 27* (17), 5621.

Group, A. P., Chase, M. W., Christenhusz, M. J., Fay, M. F., Byng, J., Judd, W., et al. (2016). An update of the Angiosperm Phylogeny Group classification for the orders and families of flowering plants: APG IV. *Botanical journal of the Linnean Society, 181* (1), 1-20.

Gupta, K., Sengupta, A., Chakraborty, M., & Gupta, B. (2016). Hydrogen peroxide and polyamines act as double edged swords in plant abiotic stress responses. *Frontiers in plant science, 7*, 1343.

Gupta, K., Sengupta, A., Chakraborty, M., & Gupta, B. (2016). Hydrogen Peroxide and Polyamines Act as Double Edged Swords in Plant Abiotic Stress Responses. *Front Plant Sci, 7*, 1343.

Hagel, J. M., & Facchini, P. J. (2013). Benzylisoquinoline alkaloid metabolism: a century of discovery and a brave new world. *Plant and Cell Physiology, 54* (5), 647-672.

Hamamsy, T., Morton, J. T., Blackwell, R., Berenberg, D., Carriero, N., Gligorijevic, V., et al. (2023). Protein remote homology detection and structural alignment using deep learning. *Nature Biotechnology*, 1-11.

Haug, K., Cochrane, K., Nainala, V. C., Williams, M., Chang, J., Jayaseelan, K. V., et al. (2020). MetaboLights: a resource evolving in response to the needs of its scientific community. *Nucleic Acids Res, 48* (D1), D440-D444.

He, M., Qu, C., Gao, O., Hu, X., & Hong, X. (2015). Biological and pharmacological activities of Amaryllidaceae alkaloids. *Rsc advances, 5* (21), 16562-16574.

Hollingsworth, S. A., & Dror, R. O. (2018). Molecular dynamics simulation for all. *Neuron, 99* (6), 1129-1143.

Hotchandani, T., de Villers, J., & Desgagne-Penix, I. (2019). Developmental Regulation of the Expression of Amaryllidaceae Alkaloid Biosynthetic Genes in *Narcissus papyraceus*. *Genes (Basel), 10* (8), 594.

Houghton, P. J., Agbedahunsi, J. M., & Adegbulugbe, A. (2004). Choline esterase inhibitory properties of alkaloids from two Nigerian Crinum species. *Phytochemistry, 65* (21), 2893-2896.

Houghton, P. J., Ren, Y., & Howes, M.-J. (2006). Acetylcholinesterase inhibitors from plants and fungi. *Natural product reports, 23* (2), 181-199.

Howes, M.-J. R., & Perry, E. (2011). The role of phytochemicals in the treatment and prevention of dementia. *Drugs & aging, 28*, 439-468.

Hu, J., Li, W., Liu, Z., Zhang, G., & Luo, Y. (2021a). Molecular cloning and functional characterization of tyrosine decarboxylases from galanthamine-producing Lycoris radiata. *Acta Physiologiae Plantarum, 43* (6), 1-12.

Hwang, I. S., & Hwang, B. K. (2011). The pepper mannose-binding lectin gene CaMBL1 is required to regulate cell death and defense responses to microbial pathogens. *Plant physiology, 155* (1), 447-463.

Ibrahim, R. K., Bruneau, A., & Bantignies, B. (1998). Plant O-methyltransferases: molecular analysis, common signature and classification. *Plant molecular biology, 36*, 1-10.

Idu, M., Obaruyi, G., & Erhabor, J. (2008). Ethnobotanical uses of plants among the binis in the treatment of ophthalmic and ENT (ear, nose and throat) ailments. *Ethnobotanical leaflets, 2009* (4), 9.

Ieven, M., Vlietinck, A. J., Vanden Berghe, D. A., Totte, J., Dommisse, R., Esmans, E., et al. (1982). Plant antiviral agents. III. Isolation of alkaloids from Clivia miniata Regel (Amaryllidaceae). *J Nat Prod, 45* (5), 564-573.

Ikeuchi, M., Iwase, A., & Sugimoto, K. (2015). Control of plant cell differentiation by histone modification and DNA methylation. *Curr Opin Plant Biol, 28*, 60-67.

Ivanov, I., Georgiev, V., Berkov, S., & Pavlov, A. (2012). Alkaloid patterns in Leucojum aestivum shoot culture cultivated at temporary immersion conditions. *J Plant Physiol, 169* (2), 206-211.

Ivanov, I., Georgiev, V., Georgiev, M., Ilieva, M., & Pavlov, A. (2011). Galanthamine and related alkaloids production by Leucojum aestivum L. shoot culture using a temporary immersion technology. *Appl Biochem Biotechnol, 163* (2), 268-277.

Ivanov, I., Georgiev, V., & Pavlov, A. (2013). Elicitation of galanthamine biosynthesis by Leucojum aestivum liquid shoot cultures. *Journal of plant physiology, 170* (12), 1122-1129.

Jacobowitz, J. R., & Weng, J.-K. (2020). Exploring uncharted territories of plant specialized metabolism in the postgenomic era. *Annual review of plant biology, 71*, 631-658.

Jarillo, J. A., Piñeiro, M., Cubas Domínguez, P., & Martínez-Zapater, J. M. (2009). Chromatin remodeling in plant development.

Jiang, Y., Xia, N., Li, X., Shen, W., Liang, L., Wang, C., et al. (2011). Molecular cloning and characterization of a phenylalanine ammonia-lyase gene (LrPAL) from Lycoris radiata. *Molecular biology reports, 38*, 1935-1940.

Jin, Z., & Yao, G. (2019). Amaryllidaceae and Sceletium alkaloids. [10.1039/C8NP00055G] *Nat Prod Rep, 36* (10), 1462-1488.

Juan-Vicedo, J., Pavlov, A., Ríos, S., & Casas, J. L. (2019). In vitro culture and micropropagation of the Baetic-Moroccan endemic plant Lapiedra martinezii Lag. (Amaryllidaceae). *In Vitro Cellular & Developmental Biology - Plant, 55* (6), 725-732.

Jumper, J., Evans, R., Pritzel, A., Green, T., Figurnov, M., Ronneberger, O., et al. (2021). Highly accurate protein structure prediction with AlphaFold. *Nature, 596* (7873), 583-589.

Ka, S., Koirala, M., Merindol, N., & Desgagne-Penix, I. (2020). Biosynthesis and Biological Activities of Newly Discovered Amaryllidaceae Alkaloids. *Molecules, 25* (21).

Ka, S., Koirala, M., Mérindol, N., & Desgagné-Penix, I. (2020). Biosynthesis and biological activities of newly discovered Amaryllidaceae alkaloids. *Molecules, 25* (21), 4901.

Ka, S., Masi, M., Merindol, N., Di Lecce, R., Plourde, M. B., Seck, M., et al. (2020). Gigantelline, gigantellinine and gigancrinine, cherylline- and crinine-type alkaloids isolated from *Crinum jagus* with anti-acetylcholinesterase activity. *Phytochemistry, 175*, 112390.

Ka, S., Merindol, N., Seck, I., Ricard, S., Diop, A., Boye, C. S. B., et al. (2021). Biological Investigation of Amaryllidaceae Alkaloid Extracts from the Bulbs of *Pancratium trianthum* Collected in the Senegalese Flora. *Molecules, 26* (23), 7382.

Ka, S., Merindol, N., Sow, A. A., Singh, A., Landelouci, K., Plourde, M. B., et al. (2021). Amaryllidaceae alkaloid cherylline inhibits the replication of dengue and Zika viruses. *Antimicrobial Agents and Chemotherapy, 65* (9), e00398-00321.

Kallscheuer, N., Classen, T., Drepper, T., & Marienhagen, J. (2019). Production of plant metabolites with applications in the food industry using engineered microorganiSM. *Current opinion in biotechnology, 56*, 7-17.

Kathe, W., Honnef, S., & Heym, A. (2003). Medicinal and aromatic plants in Albania, Bosnia-Herzegovina, Bulgaria, Croatia and Romania: a study of the collection of and trade in medicinal and aromatic plants (MAPs), relevant legislation and the potential of MAP use for financing nature conservation and protected areas.

Katoh, A., Ohki, H., Inai, K., & Hashimoto, T. (2005). Molecular regulation of nicotine biosynthesis. *Plant Biotechnology, 22* (5), 389-392.

Kenrick, P., & Crane, P. R. (1997). The origin and early evolution of plants on land. *Nature, 389* (6646), 33-39.

Khadr, A., Wang, G.-L., Wang, Y.-H., Zhang, R.-R., Wang, X.-R., Xu, Z.-S., et al. (2020). Effects of auxin (indole-3-butyric acid) on growth characteristics, lignification, and expression profiles of genes involved in lignin biosynthesis in carrot taproot. *PeerJ, 8*, e10492.

Kilgore, M. B., Augustin, M. M., May, G. D., Crow, J. A., & Kutchan, T. M. (2016). CYP96T1 of Narcissus sp. aff. pseudonarcissus Catalyzes Formation of the Para-Para' C-C Phenol Couple in the Amaryllidaceae Alkaloids. *Front Plant Sci, 7*, 225.

Kilgore, M. B., Augustin, M. M., Starks, C. M., O'Neil-Johnson, M., May, G. D., Crow, J. A., et al. (2014). Cloning and characterization of a norbelladine 4'-O-methyltransferase involved in the biosynthesis of the Alzheimer's drug galanthamine in Narcissus sp. aff. pseudonarcissus. *PLoS One, 9* (7), e103223.

Kilgore, M. B., Holland, C. K., Jez, J. M., & Kutchan, T. M. (2016). Identification of a Noroxomaritidine Reductase with Amaryllidaceae Alkaloid Biosynthesis Related Activities. *J Biol Chem, 291* (32), 16740-16752.

Kitney, R., & Freemont, P. (2012). Synthetic biology–the state of play. *FEBS letters, 586* (15), 2029-2036.

Koirala, M., Karimzadegan, V., Liyanage, N. S., Merindol, N., & Desgagne-Penix, I. (2022). Biotechnological Approaches to Optimize the Production of Amaryllidaceae Alkaloids. *Biomolecules, 12* (7), 893.

Kornienko, A., & Evidente, A. (2008). Chemistry, biology, and medicinal potential of narciclasine and its congeners. *Chemical reviews, 108* (6), 1982-2014.

Krug, E., & Proksch, P. (1993). Influence of dietary alkaloids on survival and growth of Spodoptera littoralis. *Biochemical systematics and ecology, 21* (8), 749-756.

Kurek, J. (2019). *Alkaloids: their importance in nature and human life*: BoD–Books on Demand.

Lam, P. Y., Wang, L., Lo, C., & Zhu, F. Y. (2022). Alternative Splicing and Its Roles in Plant Metabolism. *Int J Mol Sci, 23* (13).

Langens-Gerrits, M., Albers, M., & De Klerk, G.-J. (1998). Hot-water treatment before tissue culture reduces initial contamination in *Lilium* and *Acer*. *Plant Cell, Tissue and Organ Culture, 52* (1), 75-77.

Langfelder, P., & Horvath, S. (2008). WGCNA: an R package for weighted correlation network analysis. *BMC Bioinformatics, 9* (1), 559

Laurain-Mattar, D., & Ptak, A. (2018). Amaryllidaceae alkaloid accumulation by plant in vitro systems.

Lebrun, S., Couture, A., Deniau, E., & Grandclaudon, P. (2003). A new synthesis of (+)-and (−)-cherylline. *Organic & biomolecular chemistry, 1* (10), 1701-1706.

Lewis, J. R. (1996). Amaryllidaceae and Sceletium alkaloids. [10.1039/NP9961300171] *Natural Product Reports, 13* (2), 171-176.

Li, B., & Dewey, C. N. (2011). RSEM: accurate transcript quantification from RNA-Seq data with or without a reference genome. *BMC Bioinformatics, 12*, 323.

Li, Q., Xu, J., Yang, L., Sun, Y., Zhou, X., Zheng, Y., et al. (2021a). LED light quality affect growth, alkaloids contents, and expressions of amaryllidaceae alkaloids biosynthetic pathway genes in Lycoris longituba. *Journal of Plant Growth Regulation*, 1-14.

Li, Q., Xu, J., Zheng, Y., Zhang, Y., & Cai, Y. (2021). Transcriptomic and Metabolomic Analyses Reveals That Exogenous Methyl Jasmonate Regulates Galanthamine Biosynthesis in Lycoris longituba Seedlings. *Frontiers in plant science*, 1933.

Li, W., Qiao, C., Pang, J., Zhang, G., & Luo, Y. (2019). The versatile O-methyltransferase LrOMT catalyzes multiple O-methylation reactions in amaryllidaceae alkaloids biosynthesis. *International journal of biological macromolecules, 141*, 680-692.

Li, Y., Li, J., Qian, B., Cheng, L., Xu, S., & Wang, R. (2018). De novo biosynthesis of p-coumaric acid in E. coli with a trans-cinnamic acid 4-hydroxylase from the Amaryllidaceae plant Lycoris aurea. *Molecules, 23* (12), 3185.

Li, Y., Li, S., Thodey, K., Trenchard, I., Cravens, A., & Smolke, C. D. (2018). Complete biosynthesis of noscapine and halogenated alkaloids in yeast. *Proceedings of the National Academy of Sciences, 115* (17), E3922-E3931.

Liu, Z., Zhou, J., Li, Y., Wen, J., & Wang, R. (2020). Bacterial endophytes from Lycoris radiata promote the accumulation of Amaryllidaceae alkaloids. *Microbiological Research, 239*, 126501.

Lubbe, A., Gude, H., Verpoorte, R., & Choi, Y. H. (2013). Seasonal accumulation of major alkaloids in organs of pharmaceutical crop *Narcissus* Carlton. *Phytochemistry, 88*, 43-53.

Ma, L., Haile, Z. M., Sabbadini, S., Mezzetti, B., Negrini, F., & Baraldi, E. (2023). Functional characterization of MANNOSE-BINDING LECTIN 1, a G-type lectin gene family member, in response to fungal pathogens of strawberry. *Journal of Experimental Botany, 74* (1), 149-161.

Maafi, N. (2023). Amaryllidaceae alkaloids of montanine type and their derivatives as potential drugs.

Majhi, B. B., Gélinas, S.-E., Mérindol, N., & Desgagné-Penix, I. (2022a). Characterization of norbelladine synthase and noroxomaritidine/norcraugsodine reductase reveals a novel catalytic route for the biosynthesis of Amaryllidaceae alkaloids including the Alzheimer's drug galanthamine. *bioRxiv, Accepted in Frontiers in Plant Sciences Manuscript ID: 1231809*, 2022.2007.2030.502154.

Mann, J., & Mudd, S. H. (1963). In vitro alkaloid biosynthesis in the Amaryllidaceae; Norbelladine O-Methylpherase. *Journal of the American Chemical Society, 85* (13), 2025-2026.

Manolov, S. P., Atanasova, S. N., Ghate, M., & Ivanov, I. I. (2015). A brief review of Cherylline synthesis.

Marco-Contelles, J., Rodríguez, C., & García, A. G. (2005). Chemical synthesis of galantamine, an acetylcholinesterase inhibitor for treatment of Alzheimer's disease. *Expert opinion on therapeutic patents, 15* (5), 575-587.

Martin, S. F. (1988). The Amaryllidaceae alkaloids. Dans *The alkaloids* (Brossi A. éd., Vol. 30, pp. 251): Academic Press.

Meerow, A. W., Lehmiller, D. J., & Clayton, J. R. (2003). Phylogeny and biogeography of *Crinum* L. (Amaryllidaceae) inferred from nuclear and limited plastid non-coding DNA sequences. *Botanical Journal of the Linnean Society, 141* (3), 349-363.

Meisel, L., Fonseca, B., Gonzalez, S., Baeza-Yates, R., Cambiazo, V., Campos, R., et al. (2005). A rapid and efficient method for purifying high quality total RNA from peaches (*Prunus persica*) for functional genomics analyses. *Biol Res, 38* (1), 83-88.

Miller, I. R., McLean, N. J., Moustafa, G. A., Ajavakom, V., Kemp, S. C., Bellingham, R. K., et al. (2022). Transition-metal-mediated chemo-and stereoselective total synthesis of (−)-galanthamine. *The Journal of Organic Chemistry, 87* (2), 1325-1334.

Moranska, E., Simlat, M., Warchol, M., Skrzypek, E., Waligorski, P., Laurain-Mattar, D., et al. (2023). Phenolic Acids and Amaryllidaceae Alkaloids Profiles in *Leucojum aestivum* L. In Vitro Plants Grown under Different Light Conditions. *Molecules, 28* (4), 1525.

Mu, H.-m., Wang, R., Li, X.-d., Jiang, Y.-m., Wang, C.-y., Quan, J.-p., et al. (2009). Effect of abiotic and biotic elicitors on growth and alkaloid accumulation of Lycoris chinensis seedlings. *Zeitschrift für Naturforschung C, 64* (7-8), 541-550.

Nair, J. J., & van Staden, J. (2023). Antiviral Effects of the Plant Family Amaryllidaceae. *Natural Product Communications, 18* (3), 1934578X231162781.

Ncube, B., Nair, J., Rárová, L., Strnad, M., Finnie, J., & Van Staden, J. (2015). Seasonal pharmacological properties and alkaloid content in Cyrtanthus contractus NE Br. *South African Journal of Botany, 97*, 69-76.

Ndakidemi, C. F., Mneney, E., & Ndakidemi, P. A. (2014a). Effects of ascorbic acid in controlling lethal browning in in vitro culture of Brahylaena huillensis using nodal segments. *American Journal of Plant Sciences, 2014*.

Nino, J., Hincapie, G. M., Correa, Y. M., & Mosquera, O. M. (2007). Alkaloids of *Crinum x powellii* "Album" (Amaryllidaceae) and their topoisomerase inhibitory activity. *Z Naturforsch C J Biosci, 62* (3-4), 223-226.

Nonn, M., Binder, A., Volk, B., & Kiss, L. (2020). Stereo-and regiocontrolled synthesis of highly functionalized cyclopentanes with multiple chiral centers. *Synthetic Communications, 50* (8), 1199-1209.

Ojolo, S. P., Cao, S., Priyadarshani, S., Li, W., Yan, M., Aslam, M., et al. (2018). Regulation of plant growth and development: a review from a chromatin remodeling perspective. *Frontiers in plant science, 9*, 1232.

Othman, L., Sleiman, A., & Abdel-Massih, R. M. (2019). Antimicrobial activity of polyphenols and alkaloids in middle eastern plants. *Frontiers in microbiology, 10*, 911.

Parc, G., Canaguier, A., Landré, P., Hocquemiller, R., Chriqui, D., & Meyer, M. (2002). Production of taxoids with biological activity by plants and callus culture from selected Taxus genotypes. *Phytochemistry, 59* (7), 725-730.

Park, C. H., Yeo, H. J., Park, Y. E., Baek, S.-A., Kim, J. K., & Park, S. U. (2019). Transcriptome analysis and metabolic profiling of Lycoris radiata. *Biology, 8* (3), 63.

Park, W. T., Yeo, S. K., Sathasivam, R., Park, J. S., Kim, J. K., & Park, S. U. (2020a). Influence of light-emitting diodes on phenylpropanoid biosynthetic gene expression and phenylpropanoid accumulation in Agastache rugosa. *Applied Biological Chemistry, 63* (1), 1-9.

Patnaik, R., Zolandz, R. R., Green, D. A., & Kraynie, D. F. (2008). l-Tyrosine production by recombinant Escherichia coli: Fermentation optimization and recovery. *Biotechnology and bioengineering, 99* (4), 741-752.

Pavlov, A., Berkov, S., Courot, E., Gocheva, T., Tuneva, D., Pandova, B., et al. (2007). Galanthamine production by Leucojum aestivum in vitro systems. *Process Biochemistry, 42* (4), 734-739.

Priyadharshini, S., Kannan, N., Manokari, M., & Shekhawat, M. S. (2020). In vitro regeneration using twin scales for restoration of critically endangered aquatic plant Crinum malabaricum Lekhak & Yadav: a promising source of galanthamine. *Plant Cell, Tissue and Organ Culture (PCTOC), 141* (3), 593-604.

Ptak, A., Morańska, E., Saliba, S., Zieliński, A., Simlat, M., & Laurain-Mattar, D. (2017). Elicitation of galanthamine and lycorine biosynthesis by Leucojum aestivum L. and L. aestivum 'Gravety Giant'plants cultured in bioreactor RITA®. *Plant Cell, Tissue and Organ Culture (PCTOC), 128* (2), 335-345.

Ptak, A., Morańska, E., Skrzypek, E., Warchoł, M., Spina, R., Laurain-Mattar, D., et al. (2020). Carbohydrates stimulated Amaryllidaceae alkaloids biosynthesis in Leucojum aestivum L. plants cultured in RITA® bioreactor. *PeerJ, 8*, e8688.

Ptak, A., Morańska, E., Warchoł, M., Gurgul, A., Skrzypek, E., Dziurka, M., et al. (2022). Endophytic bacteria from in vitro culture of Leucojum aestivum L. a new source of galanthamine and elicitor of alkaloid biosynthesis. *Scientific Reports, 12* (1), 13700.

Ptak, A., Simlat, M., Morańska, E., Skrzypek, E., Warchoł, M., Tarakemeh, A., et al. (2019). Exogenous melatonin stimulated Amaryllidaceae alkaloid biosynthesis in in vitro cultures of Leucojum aestivum L. *Industrial Crops and Products, 138*, 111458.

Ptak, A., Simlat, M., Morańska, E., Spina, R., Dupire, F., Kozaczka, S., et al. (2019). Potential of the Leucojum aestivum L. endophytic bacteria to promote Amaryllidaceae alkaloids biosynthesis. *Acta Biol. Cracov, 62*, 30.

Ptak, A., Tahchy, A., Skrzypek, E., Wójtowicz, T., & Laurain-Mattar, D. (2013). Influence of auxins on somatic embryogenesis and alkaloid accumulation in Leucojum aestivum callus. *Open life sciences, 8* (6), 591-599.

Pyne, M. E., Narcross, L., & Martin, V. J. (2019). Engineering plant secondary metabolism in microbial systems. *Plant physiology, 179* (3), 844-861.

Rahimi Khonakdari, M., Rezadoost, H., Heydari, R., & Mirjalili, M. H. (2020a). Effect of photoperiod and plant growth regulators on in vitro mass bulblet proliferation of *Narcissus tazzeta* L. (Amaryllidaceae), a potential source of galantamine. *Plant Cell Tissue Organ Culture, 142* (1), 187-199.

Rates, S. M. K. (2001). Plants as source of drugs. *Toxicon, 39* (5), 603-613.

Refaat, J., Kamel, M. S., Ramadan, M. A., & Ali, A. A. (2012). Crinum; an endless source of bioactive principles: a review. Part III; crinum alkaloids: Belladine-, galanthamine-, lycorenine-, tazettine-type alkaloids and other minor types. *International Journal of Pharmaceutical Sciences and Research, 3* (10), 3630.

Ren, Z., Lin, Y., Lv, X., Zhang, J., Zhang, D., Gao, C., et al. (2021). Clonal bulblet regeneration and endophytic communities profiling of Lycoris sprengeri, an economically valuable bulbous plant of pharmaceutical and ornamental value. *Scientia Horticulturae, 279*, 109856.

Saitou, N., & Nei, M. (1987). The neighbor-joining method: a new method for reconstructing phylogenetic trees. *Mol Biol Evol, 4* (4), 406-425.

Santos, A., Fidalgo, F., Santos, I., & Salema, R. (2002). In vitro bulb formation of Narcissus asturiensis, a threatened species of the Amaryllidaceae. *The Journal of Horticultural Science and Biotechnology, 77* (2), 149-152.

Sato, F., & Yamada, Y. (1984). High berberine-producing cultures of Coptis japonica cells. *Phytochemistry, 23* (2), 281-285.

Schumann, A., Torras-Claveria, L., Berkov, S., Claus, D., Gerth, A., Bastida, J., et al. (2013). Elicitation of galanthamine production by Leucojum aestivum shoots grown in temporary immersion system. *Biotechnology progress, 29* (2), 311-318.

Sellés, M., Bergoñón, S., Viladomat, F., Bastida, J., & Codina, C. (1997). Effect of sucrose on growth and galanthamine production in shoot-clump cultures of Narcissus confusus in liquid-shake medium. *Plant cell, tissue and organ culture, 49* (2), 129-136.

Shawky, E., Abou-Donia, A. H., Darwish, F. A., Toaima, S. M., Takla, S. S., Pigni, N. B., et al. (2015). HPTLC and GC/MS study of Amaryllidaceae alkaloids of two Narcissus species. *Chemistry & biodiversity, 12* (8), 1184-1199.

Shimomura, K., Sudo, H., Saga, H., & Kamada, H. (1991). Shikonin production and secretion by hairy root cultures of Lithospermum erythrorhizon. *Plant Cell Reports, 10*, 282-285.

Shin, H.-S., Jung, Y.-G., Cho, H.-K., Park, Y.-G., & Cho, C.-G. (2014). Total synthesis of (±)-lycorine from the endo-cycloadduct of 3, 5-dibromo-2-pyrone and (E)-β-borylstyrene. *Organic letters, 16* (21), 5718-5720.

Singh, A., & Desgagne-Penix, I. (2015). *Chapter 3 : Biosynthesis of Amaryllidaceae alkaloids: A biochemical outlook. In: Alkaloids: Biosynthesis, Biological Roles and Health benefits.*: Nova Science Publishers.

Singh, A., & Desgagne-Penix, I. (2017). Transcriptome and metabolome profiling of *Narcissus pseudonarcissus* 'King Alfred' reveal components of Amaryllidaceae alkaloid metabolism. *Sci Rep, 7* (1), 17356.

Singh, A., & Desgagné-Penix, I. (2017). Transcriptome and metabolome profiling of Narcissus pseudonarcissus 'King Alfred'reveal components of Amaryllidaceae alkaloid metabolism. *Scientific reports, 7* (1), 17356.

Singh, A., Massicotte, M. A., Garand, A., Tousignant, L., Ouellette, V., Berube, G., et al. (2018). Cloning and characterization of norbelladine synthase catalyzing the first committed reaction in Amaryllidaceae alkaloid biosynthesis. *BMC Plant Biol, 18* (1), 338.

Slabbert, M., De Bruyn, M., Ferreira, D., & Pretorius, J. (1993a). Regeneration of bulblets from twin scales of *Crinum macowanii* in vitro. *Plant cell, tissue and organ culture, 33* (2), 133-141.

Slattery, S. S., Diamond, A., Wang, H., Therrien, J. A., Lant, J. T., Jazey, T., et al. (2018). An expanded plasmid-based genetic toolbox enables Cas9 genome editing and stable maintenance of synthetic pathways in Phaeodactylum tricornutum. *ACS synthetic biology, 7* (2), 328-338.

Su, Y., Li, H.-P., Zhang, M., Ding, X.-W., Xu, J.-H., Chen, Q., et al. (2022). Regioselectivity Inversion of an O-Methyltransferase via Semi-rational Mutagenesis Combined with Metal Ion Substitution. *ChemCatChem, 14* (23), e202200844.

Sun, B., Wang, P., Wang, R., Li, Y., & Xu, S. (2018). Molecular Cloning and Characterization of a meta/para-O-Methyltransferase from Lycoris aurea. *International journal of molecular sciences, 19* (7), 1911.

Tallini, L. R., Osorio, E. H., Santos, V. D. D., Borges, W. S., Kaiser, M., Viladomat, F., et al. (2017). *Hippeastrum reticulatum* (Amaryllidaceae): Alkaloid Profiling, Biological Activities and Molecular Docking. *Molecules, 22* (12), 4901.

Tallini, L. R., Torras-Claveria, L., Borges, W. S., Kaiser, M., Viladomat, F., Zuanazzi, J. A. S., et al. (2018). N-oxide alkaloids from *Crinum amabile* (Amaryllidaceae). *Molecules, 23* (6), 1277.

Tamura, K., Stecher, G., & Kumar, S. (2021). MEGA11: Molecular Evolutionary Genetics Analysis Version 11. *Mol Biol Evol, 38* (7), 3022-3027.

Tang, M., Li, C., Zhang, C., Cai, Y., Zhang, Y., Yang, L., et al. (2023). SWATH-MS-Based Proteomics Reveals the Regulatory Metabolism of Amaryllidaceae Alkaloids in Three *Lycoris* Species. *Int J Mol Sci, 24* (5).

Tarakemeh, A., Azizi, M., Rowshan, V., Salehi, H., Spina, R., Dupire, F., et al. (2019). Screening of Amaryllidaceae alkaloids in bulbs and tissue cultures of Narcissus papyraceus and four varieties of N. tazetta. *J Pharm Biomed Anal, 172*, 230-237.

Taylor-Teeples, M., Lin, L., de Lucas, M., Turco, G., Toal, T. W., Gaudinier, A., et al. (2015). An *Arabidopsis* gene regulatory network for secondary cell wall synthesis. *Nature, 517* (7536), 571-575.

Tousignant, L., Diaz-Garza, A. M., Majhi, B. B., Gélinas, S.-E., Singh, A., & Desgagne-Penix, I. (2022a). Transcriptome analysis of Leucojum aestivum and identification of genes involved in norbelladine biosynthesis. *Planta, 255* (2), 30.

aestivum and identification of genes involved in norbelladine biosynthesis. *Planta, 255* (2), 30.

Trujillo-Chacon, L. M., Pastene-Navarrete, E. R., Bustamante, L., Baeza, M., Alarcon-Enos, J. E., & Cespedes-Acuna, C. L. (2020). In vitro micropropagation and alkaloids analysis by GC-MS of Chilean Amaryllidaceae plants: *Rhodophiala pratensis*. *Phytochem Anal, 31* (1), 46-56.

Trujillo-Chacón, L. M., Pastene-Navarrete, E. R., Bustamante, L., Baeza, M., Alarcón-Enos, J. E., & Cespedes-Acuña, C. L. (2020). In vitro micropropagation and alkaloids analysis by GC–MS of Chilean Amaryllidaceae plants: Rhodophiala pratensis. *Phytochemical Analysis, 31* (1), 46-56.

Trujillo Chacón, L. M., Leiva, H., Zapata Vahos, I. C., Restrepo, D. C., & Osorio, E. (2023). Influence of plant growth regulators on in vitro biomass production and biosynthesis of cytotoxic Amaryllidaceae alkaloids in *Caliphuria tenera* Baker. *Biocatalysis and Agricultural Biotechnology, 50*, 102670.

Tu, Y. (2016). Nobel lecture: Artemisinin—a gift from traditional Chinese medicine to the world. *Angew. Chem. Int. Ed. Engl, 55* (35), 10210-10226.

Velten, R., Erdelen, C., Gehling, M., Göhrt, A., Gondol, D., Lenz, J., et al. (1998). Cripowellin A and B, a novel type of Amaryllidaceae alkaloid from Crinum powellii. *Tetrahedron Letters, 39* (13), 1737-1740.

Wang, R., Xu, S., Wang, N., Xia, B., Jiang, Y., & Wang, R. (2016). Transcriptome Analysis of Secondary Metabolism Pathway, Transcription Factors, and Transporters in Response to Methyl Jasmonate in *Lycoris aurea*. *Front Plant Sci, 7*, 1971.

Wang, S., Alseekh, S., Fernie, A. R., & Luo, J. (2019). The structure and function of major plant metabolite modifications. *Molecular Plant, 12* (7), 899-919.

Wang, W., & Chen, Z.-D. (2007). Generic level phylogeny of Thalictroideae (Ranunculaceae) - implications for the taxonomic status of *Paropyrum* and petal evolution. *Taxon, 56* (3), 811-821.

Wink, M. (2008). Ecological roles of alkaloids (pp. 3-52): Wiley Online Library.

Wink, M. (2011). *Annual plant reviews, biochemistry of plant secondary metabolism*: John Wiley & Sons.

Winkel-Shirley, B. (2001). Flavonoid biosynthesis. A colorful model for genetics, biochemistry, cell biology, and biotechnology. *Plant Physiol, 126* (2), 485-493.

Woodward, A. W., & Bartel, B. (2005). Auxin: regulation, action, and interaction. *Ann Bot, 95* (5), 707-735.

Xu, J., Li, Q., Yang, L., Li, X., Wang, Z., & Zhang, Y. (2020). Changes in carbohydrate metabolism and endogenous hormone regulation during bulblet initiation and development in *Lycoris radiata*. *BMC Plant Biol, 20* (1), 180.

Xu, P., Bhan, N., & Koffas, M. A. (2013). Engineering plant metabolism into microbes: from systems biology to synthetic biology. *Current opinion in biotechnology, 24* (2), 291-299.

Yoda, H., Yamaguchi, Y., & Sano, H. (2003). Induction of hypersensitive cell death by hydrogen peroxide produced through polyamine degradation in tobacco plants. *Plant Physiology, 132* (4), 1973-1981.

Zhan, J., Thakare, D., Ma, C., Lloyd, A., Nixon, N. M., Arakaki, A. M., et al. (2015). RNA sequencing of laser-capture microdissected compartments of the maize kernel identifies regulatory modules associated with endosperm cell differentiation. *Plant Cell, 27* (3), 513-531.

Zhou, J., Liu, Z., Wang, S., Li, J., Li, Y., Chen, W. K., et al. (2020). Fungal endophytes promote the accumulation of Amaryllidaceae alkaloids in Lycoris radiata. *Environmental Microbiology*.

ANNEX A

The following, published in biomolecules entitle Biotechnological approaches to optimize the production of Amaryllidaceae alkaloids.

Review

Biotechnological approaches to optimize the production of Amaryllidaceae alkaloids

Manoj Koirala[1], Vahid Karimzadegan[1], Nuwan Sameera Liyanage[1], Natacha Mérindol[1], and Isabel Desgagné-Penix [1,2,*]

[1] Department of Chemistry, Biochemistry and Physics, Université du Québec à Trois-Rivières, 3351, boul. des Forges, C.P. 500, Trois-Rivières, Québec, Canada G9A 5H7; Manoj.Koirala@uqtr.ca (M.K.); Natacha.Merindol@uqtr.ca (N.M.); Isabel.Desgagne-Penix@uqtr.ca (I.D-P.)

[2] Groupe de Recherche en Biologie Végétale, Université du Québec à Trois-Rivières, 3351, boul. des Forges, C.P. 500, Trois-Rivières, Québec, Canada G9A 5H7; Isabel.Desgagne-Penix@uqtr.ca (I.D-P.)

***** Correspondence: Isabel.Desgagne-Penix@uqtr.ca

Citation: Lastname, F.; Lastname, F.; Lastname, F. Title. *Biomolecules* **2022**, *12*, x. https://doi.org/10.3390/xxxxx

Academic Editor: Firstname Lastname

Received: date
Accepted: date
Published: date

Publisher's Note: MDPI stays neutral with regard to jurisdictional claims in published maps and institutional affiliations.

Abstract: Amaryllidaceae alkaloids (AA) are plant specialized metabolites with therapeutic properties exclusively produced by the Amaryllidaceae plant family. The two most studied representatives of the family are galanthamine, an acetylcholinesterase inhibitor used as a treatment of Alzheimer's disease, and lycorine displaying potent *in vitro* and *in vivo* cytotoxic and antiviral properties. Unfortunately, the variable level of AA' production *in planta* restricts most of the pharmaceutical applications. Several biotechnological alternatives, such as *in vitro* culture or synthetic biology, are being developed to enhance the production and fulfil the increasing demand for these AA plant-derived drugs. In this review, current biotechnological approaches to produce different types of bioactive AA are discussed.

Keywords: Amaryllidaceae alkaloids; bioactive molecules; biotechnological approach; biosynthesis; *in vitro* cultures; synthetic biology

A.1. Current challenges in the production of Amaryllidaceae alkaloids

Amaryllidaceae alkaloids (AA) are isoquinoline alkaloids exclusively isolated from the Amaryllidaceae plant family. AA are structurally diverse biomolecules classified into different types (or groups) based on their structure, biogenetic origin, or chemical nature (Martin 1987, He, Qu et al. 2015, Berkov, Osorio et al. 2020, Desgagné-Penix 2020). They can be divided into nine groups: norbelladine, cherylline, galanthamine, lycorine, homolycorine, crinine, pancratistatin, pretazettine and montanine, according to their ring type and biosynthetic origin (Ka, Koirala et al. 2020). Among all the AA, the reversible acetylcholinesterase inhibitor galanthamine is yet the only one to be approved for medicinal purposes to treat early symptoms of Alzheimer's disease in humans (Houghton, Ren et al. 2006). Although the mechanism of action is still not fully understood, two main speculations have been proposed.

Galanthamine reversibly, competitively, and selectively inhibits acetylcholinesterase, an enzyme known for acetylcholine degradation, so that the neurotransmitter associated with memory formation and learning, will be available for longer time in the synaptic cleft of cholinergic neurons to transfer neuro signals (Razay and Wilcock 2008, Kalola and Nguyen 2022). In addition, galanthamine allosterically binds to nicotinic acetylcholine receptors of the central nervous system that control the release of different types of neurotransmitters, altering their conformation leading to an increase in neurotransmitters secretion (Kalola and Nguyen 2022). AChEs inhibitory action of galanthamine also decreases the level of reactive oxygens (Tsvetkova, Obreshkova et al. 2013), oxidative stress being a common adverse effect of many human diseases such as Alzheimer's, Parkinson's, Down syndrome, cancer, etc, this hints towards a neuro-protective effect.

Up to now, galanthamine production mainly has relied on natural resource exploitation from species such as *Galanthus*, *Leucojum*, *Narcissus*, etc. Providing galanthamine to the 55 millions of people living with dementia cannot solely rely on plant source, and in the case of some species like *Leucojum*, it has already endangered biodiversity of wild population in the past years (Santos, Sinoti et al. 2020). As an alternative strategy, chemical synthesis of galanthamine has been attempted (Trost and Tang 2002, Marco-Contelles, do Carmo Carreiras et al. 2006). However, multi-step synthesis of structurally complex compounds such as galanthamine is not economically competitive compared to extraction from native plants due to the low final yield (Takos and Rook 2013).

Lycorine, another prominent AA, exhibits a broad spectrum of biological activities, including anti-viral, anti-bacterial, anti-parasitic and anti-inflammatory properties, and it has been particularly studied for its anticancer activity (Roy, Liang et al. 2018). Lycorine's antitumor potency involves several pathways, such as induction of apoptosis and necrotic cell death, inhibition of cell cycle, of autophagy, and of metastasis, probably aiming at multiple molecular targets (Roy, Liang et al. 2018). Its high cytotoxic potency at low concentrations makes lycorine's structure an interesting leading molecule for the design of new anticancer drugs. Recently, the less abundant AA cherylline was also shown to possess antiflaviviral potential, inhibiting both dengue and Zika viruses at the viral RNA replication step, with EC_{50} of 8.8μM and 20.3μM respectively (Ka, Merindol et al. 2021). In fact, novel AA with anti-acetylcholinesterase, anti-viral, cytotoxic, anticonvulsant, antitumor, hypotensive and anti-inflammatory properties are continuously discovered (He, Qu et al. 2015, Ding, Qu et al. 2017, Ka, Koirala et al. 2020, Ka, Merindol et al. 2021). Their pharmacological potential depends on their complex chemical structure, including their region-specific functionalization and chirality (Nonn, Binder et al. 2020). Consequently, it is often challenging and not always cost-effective nor ecological to chemically synthetize intact structures of AA. Although there are some reports on successful chemical synthesis of AA such as galanthamine, lycorine or cherylline, the multiple steps involved lead to a low overall yield while the end products may contain a mixture of *R* and *S* enantiomers (Lebrun, Couture et al. 2003, Marco-Contelles, Rodríguez et al. 2005, Satcharoen, McLean et al. 2007, Yamada, Yamashita et al. 2009, Shin, Jung et al. 2014, Manolov, Nikolova et al. 2015, Miller, McLean et al. 2022).

Currently, plants are the main source of AA. Even though, many AA with interesting pharmacological potentials were identified, clinical application and further research are restricted mainly because of the variable and low production levels *in planta*. For example, cherylline-type AA are rare because they are specifically recovered from few species of *Crinum* (0.004% crude alkaline solution in *C. powelli*) and in about twenty ornamental cultivars of *Narcissus* (extraction from the leaves of jonquilla and apodanthus daffodil cultivar "sundial") (Brossi, Grethe et al. 2002, Torras-Claveria, Berkov et al. 2014). Furthermore, the synthesis and accumulation of AA in plants vary with environmental and seasonal changes throughout the year. For example, the alkaloid content of *Cyrtanthus contractus* changes from 667.4 to 1020.6 μg/g between months of the same year (Ncube, Nair et al. 2015). In addition, massive harvesting for the extraction of alkaloids decreases the number of Amaryllidaceae in nature and have led some species to become endangered, such as *Narcissus asturiensis* (Santos, Fidalgo et al. 2015).

Therefore, intensive research on sustainable alternative techniques is carried out to achieve economical and eco-responsible production of pharmacologically active AA (Diop, Hehn et al. 2007, Pavlov, Berkov et al. 2007, Berkov, Pavlov et al. 2009, Georgiev, Berkov et al. 2009). In recent years, a book chapter by Laurrain-Mattar *et al*, and two reviews well describing such techniques were published, emphasizing the growing interest on this matter (Laurain-Mattar and Ptak 2018, Georgiev, Ivanov et al. 2020, Kaur, Chahal et al. 2022). As an alternative to native source harvesting or chemical synthesis, biotechnological strategies offer many advantages to sustainably produce AA (Figure 1). This includes cultivation of plant and plant parts in artificial systems, or synthetic biology (metabolic engineering) of heterologous host for AA production (Figure 1). In addition, different approaches have been reported to optimize AA yield in plants and *in vitro* cultures. In this review, we discuss recent progress on the biotechnological approaches and overall factors affecting their efficiency, together with future perspective to boost the synthesis and accumulation of AA.

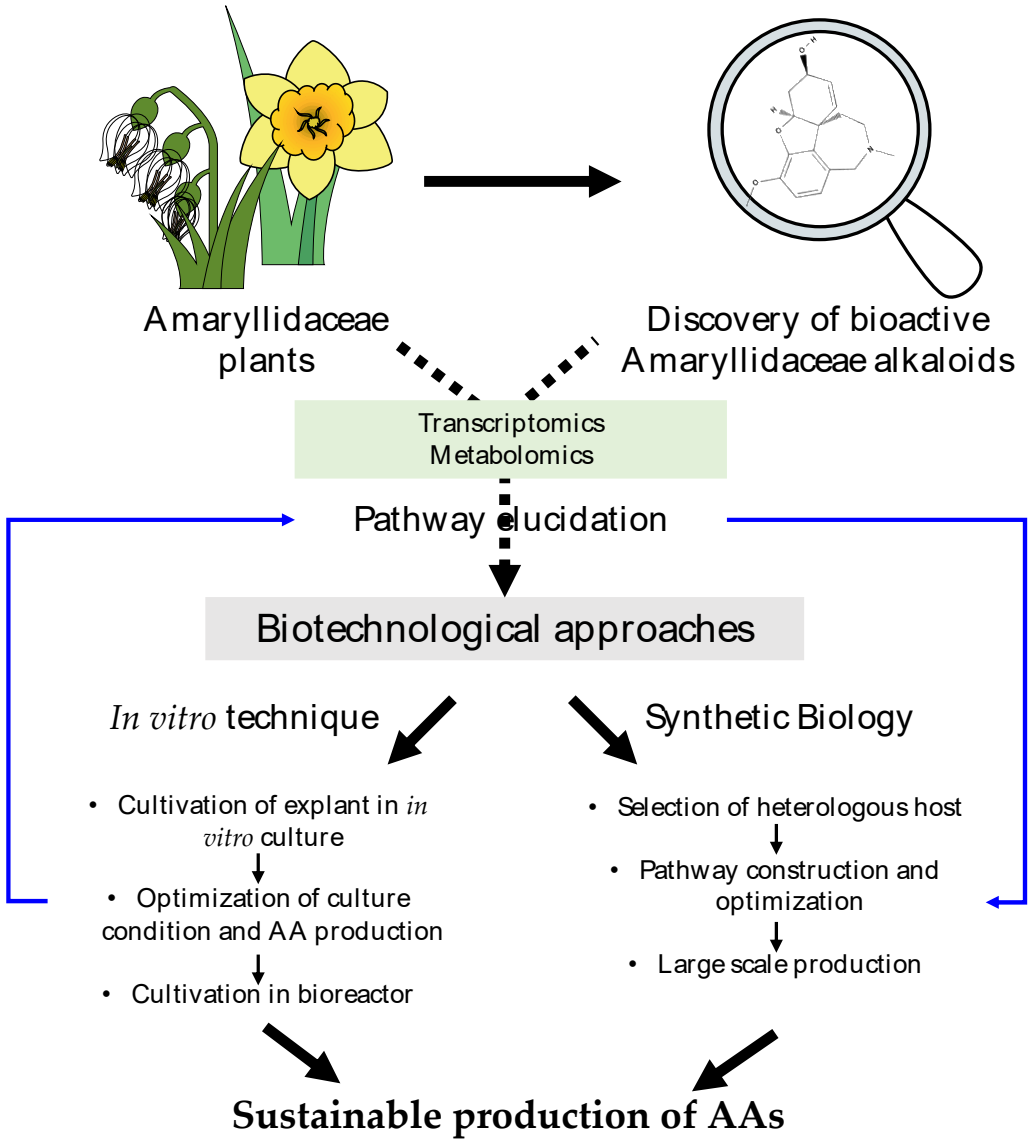

Figure 1: Current and future biotechnological approaches to produce Amaryllidaceae alkaloids.

A.2. *In vitro* techniques to produce Amaryllidaceae alkaloids

In vitro systems hold the beneficial ability to continuously produce plant specialized metabolites in a sustainable way. They also enable the control of environmental factors, a complicated task in nature, providing the opportunity to analyze the effect of different variables in the production of specialized metabolites (Carbone, Preuss et al. 2009). Several therapeutic and marketed metabolites have been produced using *in vitro* cultures, such as the anti-bacterial and anti-inflammatory naphtoquinone shikonin from *Lithospermum erythrorhizon*, the chemotherapeutic agent paclitaxel from *Taxus baccata, the antioxidant* saponins from *Panax ginseng* cells, the bioactive alkaloids berberine and sanguinarine from *Coptis japonica* and *Papaver somniferum cultures, respectively, as reviewed in* (Bourgaud, Gravot et al. 2001) and (Singh and Sharma 2018). Thus, reports on many other plant families have shown that *in vitro* cell culture techniques can be a fantastic platform to produce specialized molecules and to understand their biosynthesis (Gallego, Rojas et al. 2018, Ka, Koirala et al. 2020). The specific interest in Amaryllidaceae *in vitro* cultures as a mean to produce alkaloids was first reported in 1963 by Fales *et al.* (Mann and Mudd 1963) and has been since intensively and continuously studied.

In vitro techniques involve the transfer of healthy sterile explants into artificial condition using suitable growth media. It can be applied to grow whole plants, plant parts or undifferentiated tissues. Micropropagation, a technique that enables rapid vegetative/clonal multiplication of plants from limited or small size plants, has been successfully applied with Amaryllidaceae species such as *Rhodophiala pratensis*, *Lapiedra martinezii*, *Eucrosia stricklandii*, and *Lycoris sprengeri* leading to plant development with similar morphometric traits (Colque, Viladomat et al. 2015, Santos, Fidalgo et al. 2015, Juan-Vicedo, Pavlov et al. 2019, Trujillo-Chacon, Pastene-Navarrete et al. 2020, Ren, Lin et al. 2021). Other cultivation methods of plant material *in vitro* (bulblets, seedlings, plantlets, shoots, roots, shoot-clump, callus) also provide an interesting opportunity to produce AA, being effective for both conservation, long term growth and industrial purpose. Specifically, callus induction is defined as the growth of undifferentiated tissues from any plant parts. Because different plant parts produce different amount and types of alkaloids, the obtained type of callus and its metabolite content may be related to the type of tissue used as a starting material (Hotchandani, de Villers et al. 2019). The production of uncommon but interesting AA such as cherylline, tazettine, haemanthamine, mesembrenone was reported in various studies of *in vitro* propagation of Amaryllidaceae species (Table 1). For example, up to 6.9 mg/100 g DW of anti-acetylcholinesterase and anti-viral cherylline (Ka, Masi et al. 2020, Ka, Merindol et al. 2021) was observed in bulblets cultures of *Crinum moorei* cultivated in presence of charcoal (Fennell, Elgorashi et al. 2003).

Table 1. Yields of uncommon AA of therapeutical interest in *in vitro* cultures.

Target metabolites	Species	Tissue type	Maximum yield	Ref
Cherylline	*Crinum moorei*	Bulblets	6.9 mg/100 g DW	(Fennell, Elgorashi et al. 2003)
Haemanthamine	*Rhodophiala pratensis*	Callus	6.9 μg/mg Ext	(Trujillo-Chacon, Pastene-Navarrete et al. 2020)
	Narcissus cv. Hawera	Plants	25.5 μg/100 mg Ext	(Berkov, Georgieva et al. 2021)
Powelline	*Crinum moorei*	Bulblets	46.84 mg/100 g DW	(Fennell, Elgorashi et al. 2003)
Tazettine	*Rhodophiala pratensis*	Callus	2.68 μg/mg Ext	(Trujillo-Chacon, Pastene-Navarrete et al. 2020)
	Narcissus confuses	Shoot-clump culture	0.043 % DW	(Sellés, Bergoñón et al. 1997)

Mesembrenone	*Narcissus pallidulus*	Plants	337.6 μg/100 mg Ext	(Berkov, Georgieva et al. 2021)
	N. cv. Hawera	Plants	214.8 μg/100 mg Ext	(Berkov, Georgieva et al. 2021)

DW = Dry weight, Ext: Extract

Additionally, the production of well-known bioactive AA has been investigated in *in vitro* cultures (Table 2). Although undifferentiated tissues do not always yield to high amounts of alkaloid, elicitation helps increase the yield of various AA in *in vitro* cultures (Table 2) (Tarakemeh, Azizi et al. 2019, Ferdausi, Chang et al. 2020). Still this technique is advantageous because it can maintain growth for long periods of time, and callus can be used as a gateway for micropropagation, plant cell suspension cultures, or other *in vitro* systems to produce alkaloids. Indeed, because of somaclonal variations, shoots grown from callus displayed galanthamine production in some studies (Ferdausi, Chang et al. 2020).

Table 2: Production of Amaryllidaceae alkaloids in *in vitro* cultures following elictor treatment.

Species	**Culture condition (tissue type)**	**Amaryllidaceae alkaloid**	**Yield and type of condition**	**Elicitor and yield**	**Ref**
Narcissus confuses	Liquid-shaked culture (shoot clumps)	Galanthamine	ut. 2-2.5 mg / culture	MeJa (3.8 X)	(Colque, Viladomat et al. 2004)
N. pseudonarcissus cv. Carlton	Callus	Galanthamine	ut. 7.88 μg/g FW	MeJa (5.6 X) Chitosan (3 X)	(Ferdausi, Chang et al. 2021)
Lycoris longituba	Liquid medium (seedling)	Galanthamine	ut. n.a.	MeJa (2.71 X)	(Li, Xu et al. 2021)
		Lycorine	ut. n.a.	MeJa (2.01 X)	
		Lycoramine	ut.n.a.	MeJa (2.85 X)	
	Seedling (culture in tray)	Galanthamine	white light n.a.	Blue light (2.45X)	(Li, Xu et al. 2021)
		Lycorine	white light n.a.	Blue light (1.74 X)	
		Lycoramine	white light n.a.	Blue light (1.92 X)	
Lycoris chinensis	seedling	Galanthamine	ut. n.a.	MeJa (1.49 X) YE (1.62 X) SNP (1.72 X)	(Mu, Wang et al. 2009)
		Lycorine	ut. n.a.	MeJA (1.37 X) YE (1.38 X)	

L. aestivum	*In vitro* plants	Galanthamine	ut. n.a.	Melatonin (58.6X)	(Ptak, Simlat et al. 2019)
		Lycorine	ut. n.a.	Melatonin (1.5 X)	
	Liquid shoot culture	Galanthamine	ut. n.a.	JA (1.36 X)	(Ivanov, Georgiev et al. 2013)
		Lycorine	ut. n.a.	JA (1.40-1.67 X) MeJa (1.3 X)	
		Norgalanthamine	ut. n.a.	JA (2X) MeJa (2X)	
	temporary immersion system (bulblets, leaves)	Galanthamine	ut. 372.2-1719.6 µg/g DW	MeJa (468.6-2202.5 µg/g DW)	(Schumann, Torras-Claveria et al. 2013)
L. aestivum L.	RITA Bioreactor	Galanthamine	ut. n.a.	MeJa (0.1 mg /g DW) ACC (0.10 mg/ g DW)	(Ptak, Morańska et al. 2017)
		Lycorine	ut. 0.2-0.25 mg /g DW	MeJa (0.6 mg /g DW) SA (1 mg /g DW) Ethephon (0.46 mg /g DW)	
L. aestivum Gravety Giant	RITA Bioreactor	Galanthamine	ut. 0.08-0.1 mg/g DW	MeJa (0.4 mg/g 5X DW) SA (8x) ACC (0.60 mg/g)	(Ptak, Morańska et al. 2017)
		Lycorine	ut. 0.15 - 0.62 mg/g DW	MeJa (1.15 mg/g DW 1.85X) SA (5X) ACC (0.54mg/g DW, 3.6X)	

Abbreviations; n.a.: not available; ut: untreated, basal condition, MJ: methyl jasmonate, JA: jasmonic acid; SA: salicylic acid; ACC: 1-aminocyclopropane-1-carboxylic acid; FW: Fresh weight; DW : Dry weight; X: fold change; YE: yeast elicitor; SNP: sodium nitroprusside; Ref: reference.

In addition to a proper selection of tissue and *in vitro* propagation technique, many other factors affect the growth and the efficiency of alkaloid production. In natural conditions, the growth of Amaryllidaceae plants and their ability to synthesize different types of alkaloids vary throughout the year and are influenced by biotic and abiotic environmental factors that affect the synthesis and accumulation of AA

(Mu, Wang et al. 2009, Ncube, Nair et al. 2015, Zhou, Liu et al. 2020). Therefore, understanding and controlling both the effects of growth conditions and the plant defense response mechaniSM would be helpful to increase biomass production with higher yields of specialized metabolites such as AA. Remarkably, these factors can be monitored and optimized using *in vitro* methods, Studies have shown that Amaryllidaceae plants grow differently under distinctive artificial conditions. The overall goal of all culture techniques is to provide optimal growth conditions and boost the production of alkaloids. The main focus of the majority of the published research was the production of galanthamine, while there is also abundant data on lycorine production optimization. Table 2 illustrates the impact of different conditions of elicitation on AA production in *in vitro* systems. Bergoñón *et al* achieved a total production of 2.50 mg of galanthamine per culture by cultivating shoot-clumps in shaking-liquid media which is the highest amount of *in vitro* production of galanthamine ever reported to date (Bergoñón, Codina et al. 1996).

In the following section, we briefly discuss the effect of the different physical and chemical parameters used in the studies summarized here, that may be applied on the *in vitro* system and eventually affect growth and development of Amaryllidaceae plant tissue culture, as well as the synthesis and accumulation of alkaloids.

2.1 Physical parameters

Different cultivation methods have been tested to optimize the *in vitro* growth of Amaryllidaceae plants, this includes solid media culture, shaken-flask submerged condition, and temporary immersion or fully-submersive techniques in RITA® bioreactor (Table 1 and 2) (Bergoñón, Codina et al. 1996, Ivanov, Georgiev et al. 2011, Colque, Viladomat et al. 2015). Pavlov *et al* grew *Leucojum aestivum* 80 shoot culture in shaken-flasks following induction from callus, and monitored their growth-index. They observed that the maximum biomass was obtained at day 35 and that AA biosynthesis intensified at late exponential to early stationary growth phases (Pavlov, Berkov et al. 2007). In a following study, to optimize production of target metabolites (mostly galanthamine), *L. aestivum* 80 shoots were cultivated in temporary immersion RITA system with a higher growth index (i.e. 2.98) compared to shaken-flasks culture. The main advantage of the temporary immersion system was that cultivated shoots increased significantly, while shoot generated from meristematic cell (Ivanov, Georgiev et al. 2011). The system was further improved for *L. aestivum* 80 shoot culture using advanced modified gas column bioreactor with a 1.7 mg/L maximum production of galanthamine (Georgiev, Ivanov et al. 2012). *L. aestivum* shoot cultures show balanced growth at all tested regimes in this bubble-column bioreactor. Similar techniques using twin scale from bulbs as starting materials have shown that *Narcissus confuses* shoot-clump culture in liquid-shake medium lead to an efficient micropropagation system to produce galanthamine (2.50 mg per culture in day long photoperiod) (Bergoñón, Codina et al. 1996).

In addition to the type of *in vitro* cultivation system, temperature is a key factor that modulate both growth and alkaloid production in Amaryllidaceae species. Some studies have shown that among different culture temperature (*i.e.* 18°C, 22°C, 26°C, and 30°C), the maximum yield of galanthamine was achieved at 26°C whereas the best combination of highest amount of dry mass (20.8 g/L) and galanthamine content (1.7 g/L) was achieved at 22°C when shoot culture were grown under 18 L/(L·h) flow rate of inlet air (Ivanov, Georgiev et al. 2011, Georgiev, Ivanov et al. 2012, Ivanov, Georgiev et al. 2012). Others have been more successful at lower temperatures. *Ivanov et al* obtained 18 different AA from shoot culture of *L. aestivum* 80, and reported that lower temperature (18°C) favored the production of galanthamine, while inhibiting the production of lycorine- and haemanthamine-types of alkaloid. They concluded that temperature possibly alters the activity of the enzymes catalyzing pheno-oxidative coupling reaction of 4'-*O* methylnorbelladine (Ivanov, Georgiev et al. 2012).

Light is another important factor that can boost the production of AA in *in vitro* cultures. In general, studies suggest that light has a positive impact on alkaloid production in Amaryllidaceae tissues (Bergoñón, Codina et al. 1996, Pavlov, Berkov et al. 2007, Berkov, Pavlov et al. 2009, Rahimi Khonakdari, Rezadoost et al. 2020). In shoot cultures of *N. confuses*, light affected both morphology and alkaloid content (Bergoñón, Codina et al. 1996). In *N. tazetta L.*, bulblets and leaves proliferation per explant was higher in light condition light/dark photoperiod (16/8h), as compared to a 24h dark condition. Also, regenerated bulblets contained 40 μg/g dry weight of galanthamine under exposed photoperiod compared to 20 μg/g dry weight for 24 h dark condition (Rahimi Khonakdari, Rezadoost et al. 2020). Not only the light condition, but also its quality have been studied in relation to the production of AA. For example, it was observed that, increases in the production of galanthamine (2.45 times), lycorine (1.74 times) and lycoramine (1.92 times) were generated by blue light condition compared to white light in *in vitro* plantlets of *Lycoris longituba* (Li, Xu et al. 2021). Altogether, these studies demonstrate that a complex combination of physical parameters impact alkaloid production, and that cultivation system, light and temperature should be optimized in each system, and may vary in between species.

2.2. Chemical factors

Plants require diverse types of micro- and macro-elements for their growth and development. Generally, the type of media and the addition of growth factors, hormones or other regulators such as charcoal affect both the growth and the production of metabolites (Fridborg, Pedersen et al. 1978). Activated charcoal is known to promote plant cells and callus differentiation, possibly through the induction of genes from the phenylpropanoid biosynthesis pathway, which could lead to an increase alkaloid production (Fridborg, Pedersen et al. 1978, Fennell, Elgorashi et al. 2003, Dong, Lv et al. 2020). The quantity of carbon and nitrogen in the media affects both growth the production of specialized metabolites Studies have shown that the type and the concentration of different carbon source play an important role in plant tissue culture. In plant tissue culture research, sucrose is widely used as carbon source. The effect of its concentration on *N. confuses* culture was measured following growth in liquid-shaked medium by Sellés *et al* (1997) (Sellés, Bergoñón et al. 1997). They showed that sucrose concentration affects biomass production, as well as galanthamine synthesis. Assessing the effects of concentrations ranging between 3% - 18% of sucrose, optimal combination of growth and galanthamine production was achieved with 9% (Sellés, Bergoñón et al. 1997). In 2020, Ptak *et al*. showed that both the concentration and the type of carbohydrate are critical for synthesis of AA. Similar to Sellés study, they demonstrate that the highest amount of *L. aestivum* biomass was obtained with 9% sucrose when cultivated in RITA® bioreactor. However, they also show that the use of other types of sugar can increase the success of AA synthesis, as the highest amount of galanthamine was recorded with 3% fructose (Ptak, Moranska et al. 2020).

The type of phytohormones and their concentration play a key role in tissue survival and differentiation, including in organogenesis and eventually in the synthesis of AA. Auxins, abscisic acid, cytokinins, ethylene, and gibberellins are commonly recognized as the five main classes of naturally occurring plant hormones. The isolated or combined effect of auxin or cytokinin on *in vitro* cultures' nutrient uptake and metabolism was demonstrated (Gaspar, Kevers et al. 1996). In 2011, Tahchy *et al.* observed that an increment of auxin (2,4-dicholophenoxyacetic acid or 2,4-D) in growth media reduced the survival of *in vitro* cultured tissues of *N. pseudonarcissus, Galanthus elwesii* and *L. aestivum*, whereas an increment of cytokinin (6-benzylaminopurine, BAP) increased it (El Tahchy, Bordage et al. 2011). The concentration and the type of phytohormones also influence the type of tissue that will develop, which eventually affects the alkaloid profile. Hence, the alkaloid profile of *L. aestivum* and *N. pseudonarcissus cv. Carlton* obtained from *in vitro* system revealed that differentiated cells are more suitable for production of AA, as compared to undifferentiated cells (callus) in which alkaloid contents was lower (Pavlov, Berkov et al. 2007, Ferdausi, Chang et al. 2020). A study completed on different varieties of *Narcissus* showed that undifferentiated calli

development was induced following treatment with auxin concentrations of 25 μM of 1-napthaleneacetic acid (NAA), 50 μM of 2,4-D and picloram, whereas organogenesis only happened on calli treated with NAA, or using higher concentration of picloram. Interestingly, AA demethylmaritidine and tazettine were only detected on the differentiated callus (Tarakemeh, Azizi et al. 2019). Most studies have confirmed that the amount and the type of auxin correlated with the alkaloid profile and with tissue differentiation during *in vitro* culture (Tarakemeh, Azizi et al. 2019, Ferdausi, Chang et al. 2020), although no consensual combination can be clearly defined at this point.

Although, the eco-physiological role of many plants specialized metabolites is not clear, studies demonstrated that different biotic and abiotic factors or signaling agents (elicitors) can boost the production of AA (Mu, Wang et al. 2009, Ptak, Simlat et al. 2019, Liu, Zhou et al. 2020, Zhou, Liu et al. 2020). Different types of elicitors such as fungal elicitors, methyl jasmonate, jasmonic acid, salicylic acid, and melatonin have been used to enhance the synthesis of AA in *in vitro* culture (Table 2). The induction of AA using methyl jasmonate treatment on seedling of *Lycoris aurea* was well studied by Wang *et al.* (2017) (Wang, Xu et al. 2016). Others have deciphered that methyl jasmonate and jasmonic acid increased the production of AA in *L. aestivum.* shoot cultures cultivated in submerged condition by stimulating two enzymes involved in the formation of AA precursors (Ivanov, Georgiev et al. 2013). Melatonin addition (10 μM) during *in vitro* culture of *L. aestivum L.* reduced the negative effect of NaCl (*i.e.* salt stress) and enhanced the biomass production together with an increased accumulation of galanthamine and lycorine by 58.6 and 1.5 folds, respectively (Table 2) (Ptak, Simlat et al. 2019). In conclusion, the optimization of media components and of elicitor type in *in vitro* culture of Amaryllidaceae provides an alternative and sustainable source of AA.

3. Genetic engineering of heterologous host for alternative production of AA

Bioengineered microbial hosts that grow rapidly can produce plant target specialized metabolites faster as compared to whole plant systems. In addition, the production of plant metabolites in heterologous hosts can reduce downstream extraction process, which eventually becomes more economically sustainable. For the successful synthesis of plant metabolites such as AA, heterologous hosts require the introduction of reconstructed biosynthetic pathway, requiring key enzymes. This requires comprehensive knowledge of the enzymatic reactions involved in the biosynthesis of the compound of interest in the native host organiSM (*i.e.* plants).

3.1 Molecular understanding of Amaryllidaceae alkaloids biosynthesis

Even though the pharmacological aspect of AA has extensively been explored, the full understanding of the AA biosynthetic pathway and the characterization of enzymes responsible for catalyzing the different biosynthetic reactions demand more efforts. This knowledge would enable the establishment of improved systems or sustainable platforms for the production of these valuable biologically active compounds. Combined application of early labeling study followed by latest omics strategies have accelerated the discovery of AA biosynthetic enzymes (Kilgore and Kutchan 2016, Desgagné-Penix 2020). After the proposition of the biosynthetic route of different intermediates, several biosynthetic enzymes were predicted based on the nature of the biochemical reaction and by homology with enzymes involved in alkaloid biosynthesis of other plant families. Databases generated from transcriptomic and metabolic analysis of different species of Amaryllidaceae support the presence of different enzyme families involved in AA pathway (Kilgore, Augustin et al. 2014, Singh and Desgagne-Penix 2017, Hotchandani, de Villers et al. 2019, Park, Yeo et al. 2019, Li, Xu et al. 2020, Li, Xu et al. 2021, Tousignant, Diaz-Garza et al. 2022).

The AA biosynthetic pathway utilizes two common amino acids, namely L-tyrosine and L-phenylalanine, building blocks to produce a vast range of alkaloids with diverse biological activities. The first reactions of AA biosynthesis involve the formation of the 'precursors' from the phenylpropanoid and tyramine pathways (Figure 2). As such, L-tyrosine is decarboxylated by the enzyme tyrosine decarboxylase

(TYDC) to yield tyramine while the production of the second building block, 3,4-dihydroxybenzaldehyde (3,4- DHBA), is achieved via the phenylpropanoid pathway by the action of enzymes such as phenylalanine ammonia-lyase (PAL), cinnamate 4-hydoxylase (C4H), *p*-coumarate 3-hydroxylase (C3H), to name but a few. TYDC was characterized from *Lycoris radiata*, a galanthamine producing Amaryllidaceae plant (Hu, Li et al. 2021). The functional characterization of PAL and C4H in *L. radiata* was reported using heterologous expression in bacteria (Singh, Massicotte et al. 2018).

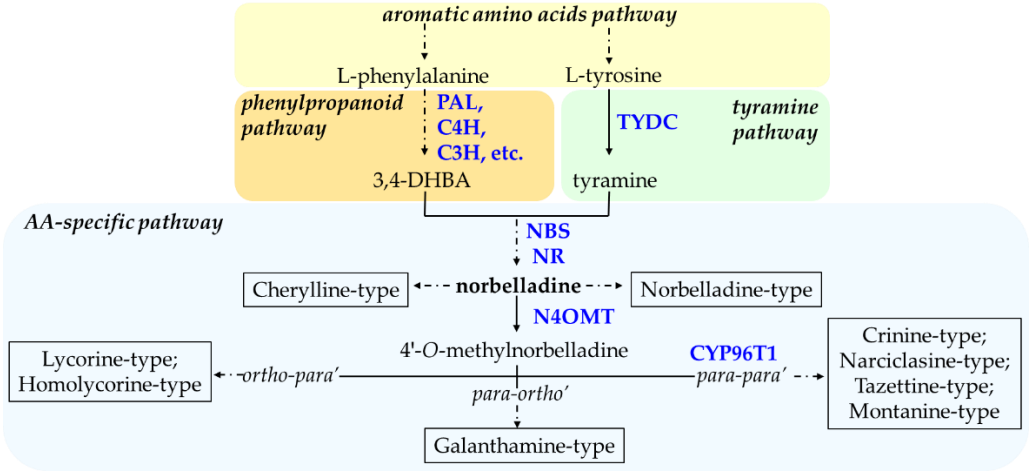

Figure 2. Biosynthetic routes to main types (boxed) of Amaryllidaceae alkaloid (AA). Arrows without labeling reflect chemical reactions where no enzyme was characterized. Enzymes that have been identified are labeled in blue. A solid arrow shows one enzymatic step whereas a broken arrow symbolizes multiple enzymatic reactions. Following 4'*O*-methylnorbelladine, the regioselective *phenol-phenol'* coupling reaction is indicated in the broken arrow leading to various AA-types. Enzyme abbreviations: 3,4-DHBA, 3,4-dihydroxybenzaldehyde; PAL, phenylalanine ammonia-lyase; C4H, cinnamate 4-hydroxylase; C3H, coumarate 3-hydroxylase; TYDC, tyrosine decarboxylase; NBS, norbelladine synthase; NR, noroxomaritidine/norcraugsodine reductase; N4OMT, norbelladine 4'-*O*-methyltransferase; CYP96T1, cytochrome P450 monooxygenase 96T1.

Despite having a remarkable diversity in structure and biological activity, all AA are derived from a common intermediate, norbelladine. The condensation of tyramine and 3,4-DHBA yields norbelladine and was shown to be catalyzed either by norbelladine synthase (NBS) or by noroxomaritidine/norcraugsodine reductase (NR), in both cases with low yield (Kilgore, Holland et al. 2016, Singh, Massicotte et al. 2018, Tousignant, Diaz-Garza et al. 2022). NBS was characterized from *N. pseudonarcisus* king Alfred and *L. aestivum* (Singh, Massicotte et al. 2018, Tousignant, Diaz-Garza et al. 2022). GFP-tagged *La*NBS and CFP-tagged NR showed that both enzymes are localized to the cytosol, which suggests that the first committed step of AA biosynthesis probably occurs in the cytosol (Majhi, Gélinas et al. 2022, Tousignant, Diaz-Garza et al. 2022).

Norbelladine can either be utilized directly to generate norbelladine- and cherylline-type AA, or be further methylated by norbelladine 4'-*O*-methyltransferase (N4OMT) to give 4'-*O*-methylnorbelladine (Figure 2). The structural feature of cherylline-type of AA suggests the occurrence of 3'-*O*-methylation during the biosynthesis of these types of AA, although it remains to be proven. In addition to a norbelladine 3'-O-methyltransferase (N3OMT), cherylline biosynthesis would require steps catalyzed by 3'-O-methylnorbelladine N-methyltransferase (MNB-NMT) and 3'-O,N-dimethylnorbelladine 2-hydroxylase (DMNB-2H) or a cherylline synthase (CherySyn.) (Figure 3). The specific synthesis of both 3'-*O*-methylated

and 4'-*O*-methylated AA suggest that regioselective methylation is important to determine the types of the end product of AA biosynthesis route. The characterization of norbelladine OMT from *Narcissus sp. aff. pseudonarsissus* suggests that methylation by *Np*N4OMT happens specifically at 4'-*O* position of norbelladine (Kilgore, Augustin et al. 2014). However, later studies on *L. radiata* OMT (*Lr*OMT) proposes that methylation can occur either in the 3'-*O* or 4'-*O* position of norbelladine, 3,4-DHBA, or caffeic acid. Kinetic study of *Lr*OMT indicates that it has a higher affinity for 3,4-DHBA as substrate compared to norbelladine. The methylated forms of 3,4-DHBA (*i.e.* vanillin and isovanillin) could also be condensed with tyramine to generate 3' or 4'-*O*-methylnorbelladine. However, up to now, none of the possible methylated forms of 3, 4-DHBA were tested as a substrate for NBS.

One step deeper in the AA pathway and depending on the type of phenol-coupling reaction, the 4'-*O*-methylnorbelladine can be directed to 1) galanthamine-type through *para-ortho'*, 2) lycorine-type AA by *ortho-para'* and 3) crinine-type of AA by *para-para'* phenol coupling reactions (Figure 2). These types of C-C phenol-coupling reactions are putatively catalyzed by members of the cytochrome P450 enzyme family. For example, *Np*CYP96T1 was shown to catalyze the *para-para'* oxidative reaction of 4'-*O*-methylnorbelladine into noroxomaritidine and was also shown to catalyzed formation of the *para-ortho'* phenol coupled product, *N*-demethylnarwedine as less than 1% of the total product (Kilgore, Augustin et al. 2016). Aside from CYP96T1 and NR, there are no other steps (genes or enzymes) that have been identified in the formation of phenol-coupled AA-types to date (Figure 2). In a nutshell, galanthamine production could be catalyzed by para-ortho' phenol oxidative coupling of 4'-O-methylnorbelladine to yield nornarwedine by nornarwedine synthase (NNS); then a nornarwedine reductase (NNR) and finally a norgalanthamine N-methyltransferase (NG-NMT) (Figure 3).

Plants synthesize specialized metabolites by using complex biosynthetic routes that derive from primary metabolic pathways. AA biosynthesis is a multifaceted process that involves different regulatory elements and gene functions. The expression of certain genes involved in plant metabolism also changes with different climatic and environmental factors (Ncube, Nair et al. 2015). Furthermore, it also varies within different developmental stage of plant (Hotchandani, de Villers et al. 2019). It remains challenging to correlate gene expression and metabolite accumulation *in planta*, as the site of metabolite synthesis may differ from the site of accumulation. For example, nicotine biosynthesis occurs in root of tobacco but accumulate in the aerial part of the plant (Katoh, Ohki et al. 2005) whereas morphine biosynthesis starts in sieve elements of the phloem but accumulates in adjacent laticifers cells in opium poppy (Onoyovwe, Hagel et al. 2013). As such, *in vitro* cultures have been an essential tool to decipher the alkaloid biosynthesis pathway. In 2011, Tahchy *et al* used deuterium-labeled precursors fed to *in vitro* cultures of *L. aestivum*. In this study, the authors followed the transfer of labeled precursor 4'-*O*-methyl-d_3-norbelladine from media into shoot and then its metabolization into lycorine and galanthamine. This study demonstrated that 4'-*O*-methylated-norbelladine was a key intermediate AA (El Tahchy, Ptak et al. 2011). Until now, AA specific genes such as *NBS, N4OMT, CYP96T1,* and *NR* have been characterized and confirmed from *Leucojum sp., Narcissus sp*., *Lycoris sp.* cultures [44-47], however, our molecular understanding regarding this complex biosynthesis route of AA and its regulation is still unclear. Furthermore, the pattern of relative expression of putative AA biosynthetic genes (in fields versus *in vitro* and in differentiated *versus* undifferentiated tissues of *Narcissus* development) added some clear knowledge regarding their role in alkaloid biosynthesis (Aleya, Xianmin et al. 2021). A study performed on callus culture of *L. radiata* showed how different factors, such as temperature (cold treatment), osmotic pressure (PEG treatment) or elicitor treatment (methyl jasmonate) can influence *Lr*OMT gene expression pattern (Sun, Wang et al. 2018). Thus, *in vitro* system cultures are a powerful tool to uncover AA biosynthesis and gene regulation that should be thoroughly exploited.

3.2. Synthetic biology for AA biosynthesis

Although, the complete biosynthetic pathway of AA is not resolved, and up to now the AA demand is not sufficiently fulfilled by plant source, synthetic biological approach could be a powerful approach to produce AA. Recent achievement in synthetic biological approaches includes the production of complex biomolecules such as noscapine (a benzylisoquinoline alkaloid from opium poppy) and its halogenated derivatives (anticancer) in *Saccharomyces cerevisiae*, assembling 30 biosynthetic enzymes from plant, bacteria and mammal and yeast itself including seven plant endoplasmic reticulum localized genes (Li, Li et al. 2018). This success rises the hope to produce complex biomolecules such as AA by using synthetic biological approach.

Proper selection of host organism is the starting point of synthetic biological approach. The chosen organism should be producing (or easily modified to produce) enough core metabolites such as aromatic amino acids L-phenylalanine and L-tyrosine, precursors needed for the biosynthesis of target specialized metabolite such as AA. Selection of host species will also rely on prior knowledge of their ease of engineering, established cloning tools, culture techniques, and possibility to scale up to industrial requirements. Due to rapid growth and easy handling, microbial hosts such as yeast (*Saccharomyces cerevisiae*) and to a lesser extent *Escherichia coli*, were used to produce plant derived high value alkaloids, like morphinan alkaloids (Facchini, Bohlmann et al. 2012, Fossati, Narcross et al. 2015, Diamond and Desgagne-Penix 2016). Furthermore, the production of aromatic amino acid (precursor for AA) and associated upstream gene/enzyme were well studies in these hosts (Cao, Gao et al. 2020). Precursors such as L-tyrosine and *p*-coumaric have been already produced in *E. coli* (Patnaik, Zolandz et al. 2008, Li, Li et al. 2018). Recently unicellular photosynthetic organiSM, such as microalgae and cyanobacteria became interesting research platforms because of their unicellular physiology together with their photosynthetic, heterotrophic, and mixotrophic lifestyles (Slattery, Diamond et al. 2018). Moreover, plant based genetic engineering technique is also emerging in model plant such as *Nicotiana tabacum* and *N. benthamiana* (Farhi, Marhevka et al. 2011).

Once a host organism is selected, availability of precursor molecules can be enhanced by modifications to its metabolic pathway, such as gene deletions, swapping of endogenous enzymes with more active homologues, or overexpression of endogenous metabolic genes. Then, a route to the desired specialized metabolites can be planned and implemented. A candidate pathway is first outlined through selection of stepwise chemical intermediates leading from host metabolism to the target compound, followed by selection of enzymes to carry out each specified reaction (Kitney and Freemont 2012, Auslander, Auslander et al. 2017). Even though, the lack of knowledge in the AA biosynthetic pathway hinders this approach as of yet, it could be partially overcome by creating libraries of gap-filling genes candidate generated from huge plant transcriptomic database, as available for thousands of plants or as part of the PhytoMetaSyn project (Matasci, Hung et al. 2014). In addition, the decrease in the cost of DNA synthesis helps accelerate gene characterization from its native source and ultimately facilitate the production of complex biomolecules like AA (Xiao, Zhang et al. 2013, Matasci, Hung et al. 2014, Pyne, Narcross et al. 2019). Such work was done to produce polyketides. Soon, platform of synthetic approach will not only provide techniques to produce AA but also help in biosynthesis of novel AA derivatives with improved biological and physiological properties. In example, once we have completed identification of methyltransferases, reductases and other enzymes required for the biosynthesis of galanthamine, we can add one more gene in the transgenic construct that will increase glycosylation, shifting the polarity of parent molecule and eventually improving drug uptake by human body.

4. Conclusions

Studies on the production of AA using *in vitro* systems have mainly focused on the commercially available galanthamine and the abundant lycorine. Nowadays, the demand for natural therapeutic metabolites obtained from plants is growing fast, however, overexploitation of the native plants to meet this demand will be insufficient and endanger biodiversity of wild populations. Alternative chemical

synthesis requires a multi-step process to produce intact complex compounds. Fortunately, biotechnological approaches including *in vitro* platforms or synthetic biology are promising strategies to establish a more reliable, economic and environmentally friendly system for the production of plant-derived metabolites. Currently, the production of AA from *in vitro* systems does not achieve the levels produced by wild type plants. However, they have several advantages, i.e. they enable the production of target metabolites independently from environmental factors affecting the production yield, biodiversity concerns and land usage; they facilitate the discovery of biosynthetic pathway and the understanding of its regulation in a short period of time. Currently established platforms of *in vitro* systems can be used to determine the effect of different variables on plants in a controlled environment with stable chemical and physical parameters. Notable effects of biotic and abiotic stresses on AA biosynthesis and accumulation in *in vitro* system can be used as a basis platform for transcriptomic and metabolomic level studies, which generate a huge amount of data not only regarding production of AA but also on their regulation *in planta*. This generated data can serve as fundamental units for the synthetic biological approach. It can be utilized to: 1) to establish an *in vitro* production system with optimized parameters economically comparable to extraction from natural sources yet sustainable, decreasing the need for native plants harvesting; 2) be linked to other branches of science such as bioinformatics, cell biology, biochemistry, 3) to produce metabolites in a fast growing heterologous organism such as yeast, bacteria and new emerging platforms like microalgae.

In this way, research combining biologists, biochemist, bioengineers, physicists, and computer scientists will enhance deep understanding on AA metabolism and thereby enable for their (re)design in selected heterologous host such as bacteria or yeast systems.

Author Contributions: Conceptualization, M.K., N.M. and I.D-P.; writing—original draft preparation, M.K., V.K. and N.S.L.; writing—review and editing, M.K., V.K., N.S.L., N.M. and I.D-P.; visualization, M.K., N.M. and I.D-P.; supervision, N.M. and I.D-P.; project administration, N.M. and I.D-P.; funding acquisition, N.M. and I.D-P. All authors have read and agreed to the published version of the manuscript.

Funding: This work was funded by the Natural Sciences and Engineering Research Council of Canada – Discovery Grants Program Award No RGPIN-2021-03218 to I.D-P and by the Canada Research Chair on Plant Specialized Metabolism Award No 950-232164 to Isabel Desgagne-Penix. Many thanks are extended to the Canadian taxpayers and to the Canadian government for supporting the Discovery and the Canada Research Chairs Program.

Acknowledgments: The authors wish to acknowledge and dedicate this review to Professor Antonio Evidente. His achievements in natural product research, covering the chemistry, biology and medicinal potential of Amaryllidaceae alkaloids are inspiring.

Conflicts of Interest: The authors declare no conflict of interest.

References

Abd el Hafiz, M. A., M. A. Ramadan, M. L. Jung, J. P. Beck and R. Anton (1991). "Cytotoxic activity of Amaryllidaceae alkaloids from *Crinum augustum* and *Crinum bulbispermum*." Planta Med **57**(5): 437-439.

Adasme, M. F., K. L. Linnemann, S. N. Bolz, F. Kaiser, S. Salentin, V. J. Haupt and M. Schroeder (2021). "PLIP 2021: Expanding the scope of the protein–ligand interaction profiler to DNA and RNA." Nucleic acids research **49**(W1): W530-W534.

Aleya, F., C. Xianmin, H. Anthony and J. Meriel (2021). "Relative expression of putative genes involved in galanthamine and other Amaryllidaceae alkaloids biosynthesis in Narcissus field and in vitro tissues." Gene **774**: 145424.
Anders, S. and W. Huber (2012). "Differential expression of RNA-Seq data at the gene level–the DESeq package." Heidelberg, Germany: European Molecular Biology Laboratory (EMBL) **10**: f1000research.
Auslander, S., D. Auslander and M. Fussenegger (2017). "Synthetic Biology-The Synthesis of Biology." Angew Chem Int Ed Engl **56**(23): 6396-6419.
Ausländer, S., D. Ausländer and M. Fussenegger (2017). "Synthetic biology—the synthesis of biology." Angewandte Chemie International Edition **56**(23): 6396-6419.
Banwell, M. G., A. J. Edwards, K. A. Jolliffe and M. Kemmler (2001). "An operationally simple and fully regiocontrolled formal total synthesis of the montanine-type Amaryllidaceae alkaloid (±)-pancracine." Journal of the Chemical Society, Perkin Transactions 1(12): 1345-1348.
Bergoñón, S., C. Codina, J. Bastida, F. Viladomat and E. Melé (1996). "Galanthamine production in "shoot-clump" cultures of Narcissus confusus in liquid-shake medium." Plant cell, tissue and organ culture **45**(3): 191-199.
Berkov, S., L. Georgieva, B. Sidjimova, M. Nikolova, M. Stanilova and J. Bastida (2021). "In vitro propagation and biosynthesis of Sceletium-type alkaloids in Narcissus pallidulus andNarcissus cv. Hawera." South African Journal of Botany **136**: 190-194.
Berkov, S., E. Osorio, F. Viladomat and J. Bastida (2020). "Chemodiversity, chemotaxonomy and chemoecology of Amaryllidaceae alkaloids." Alkaloids Chem Biol **83**: 113-185.
Berkov, S., E. Osorio, F. Viladomat and J. Bastida (2020). "Chemodiversity, chemotaxonomy and chemoecology of Amaryllidaceae alkaloids." The Alkaloids: Chemistry and Biology **83**: 113-185.
Berkov, S., A. Pavlov, V. Georgiev, J. Bastida, M. Burrus, M. Ilieva and C. Codina (2009). "Alkaloid synthesis and accumulation in Leucojum aestivum in vitro cultures." Nat Prod Commun **4**(3): 359-364.
Berkov, S., A. Pavlov, V. Georgiev, J. Bastida, M. Burrus, M. Ilieva and C. Codina (2009). "Alkaloid synthesis and accumulation in Leucojum aestivum in vitro cultures." Natural product communications **4**(3): 1934578X0900400328.
Bonifácio, M. J., M. Archer, M. L. Rodrigues, P. M. Matias, D. A. Learmonth, M. A. Carrondo and P. c. Soares-da-Silva (2002). "Kinetics and crystal structure of catechol-o-methyltransferase complex with co-substrate and a novel inhibitor with potential therapeutic application." Molecular pharmacology **62**(4): 795-805.
Bourgaud, F., A. Gravot, S. Milesi and E. Gontier (2001). "Production of plant secondary metabolites: a historical perspective." Plant Science **161**(5): 839-851.
Brandt, W., K. Manke and T. Vogt (2015). "A catalytic triad--Lys-Asn-Asp--Is essential for the catalysis of the methyl transfer in plant cation-dependent O-methyltransferases." Phytochemistry **113**: 130-139.
Brossi, A., G. Grethe, S. Teitel, W. C. Wildman and D. T. Bailey (1970). "Cherylline, a 4-phenyl-1, 2, 3, 4-tetrahydroisoquinoline alkaloid." The Journal of Organic Chemistry **35**(4): 1100-1104.
Brossi, A., G. Grethe, S. Teitel, W. C. Wildman and D. T. Bailey (2002). "Cherylline, a 4-phenyl-1,2,3,4-tetrahydroisoquinoline alkaloid." The Journal of Organic Chemistry **35**(4): 1100-1104.
Bruex, A., R. M. Kainkaryam, Y. Wieckowski, Y. H. Kang, C. Bernhardt, Y. Xia, X. Zheng, J. Y. Wang, M. M. Lee, P. Benfey, P. J. Woolf and J. Schiefelbein (2012). "A gene regulatory network for root epidermis cell differentiation in *Arabidopsis*." PLoS Genet **8**(1): e1002446.
Brusotti, G., I. Cesari, A. Dentamaro, G. Caccialanza and G. Massolini (2014). "Isolation and characterization of bioactive compounds from plant resources: The role of analysis in the ethnopharmacological approach." Journal of pharmaceutical and biomedical analysis **87**: 218-228.
Bryant, D. M., K. Johnson, T. DiTommaso, T. Tickle, M. B. Couger, D. Payzin-Dogru, T. J. Lee, N. D. Leigh, T. H. Kuo, F. G. Davis, J. Bateman, S. Bryant, A. R. Guzikowski, S. L. Tsai, S. Coyne, W. W. Ye, R. M. Freeman,

Jr., L. Peshkin, C. J. Tabin, A. Regev, B. J. Haas and J. L. Whited (2017). "A Tissue-Mapped Axolotl De Novo Transcriptome Enables Identification of Limb Regeneration Factors." Cell Rep **18**(3): 762-776.
Cahlíková, L., I. Kawano, M. Řezáčová, G. Blunden, D. Hulcová and R. Havelek (2021). "The Amaryllidaceae alkaloids haemanthamine, haemanthidine and their semisynthetic derivatives as potential drugs." Phytochemistry Reviews **20**: 303-323.
Cao, M., M. Gao, M. Suastegui, Y. Mei and Z. Shao (2020). "Building microbial factories for the production of aromatic amino acid pathway derivatives: from commodity chemicals to plant-sourced natural products." Metabolic engineering **58**: 94-132.
Cao, M., M. Gao, M. Suastegui, Y. Mei and Z. Shao (2020). "Building microbial factories for the production of aromatic amino acid pathway derivatives: From commodity chemicals to plant-sourced natural products." Metab Eng **58**: 94-132.
Carbone, F., A. Preuss, R. C. De Vos, E. D'Amico, G. Perrotta, A. G. Bovy, S. Martens and C. Rosati (2009). "Developmental, genetic and environmental factors affect the expression of flavonoid genes, enzymes and metabolites in strawberry fruits." Plant Cell Environ **32**(8): 1117-1131.
Casciaro, B., L. Mangiardi, F. Cappiello, I. Romeo, M. R. Loffredo, A. Iazzetti, A. Calcaterra, A. Goggiamani, F. Ghirga and M. L. Mangoni (2020). "Naturally-occurring alkaloids of plant origin as potential antimicrobials against antibiotic-resistant infections." Molecules **25**(16): 3619.
Chan, J. L. A. (1973). BIOSYNTHESIS OF CHERYLLINE USING DOUBLY-LABELED NORBELLADINE-TYPE PRECURSORS, Iowa State University.
Chase, M. W., J. L. Reveal and M. F. Fay (2009). "A subfamilial classification for the expanded asparagalean families Amaryllidaceae, Asparagaceae and Xanthorrhoeaceae." Botanical Journal of the Linnean Society **161**(2): 132-136.
Chatterjee, D., D. Kudlinzki, V. Linhard, K. Saxena, U. Schieborr, S. L. Gande, J. P. Wurm, J. Wohnert, R. Abele, V. V. Rogov, V. Dotsch, H. D. Osiewacz, S. Sreeramulu and H. Schwalbe (2015). "Structure and Biophysical Characterization of the S-Adenosylmethionine-dependent O-Methyltransferase PaMTH1, a Putative Enzyme Accumulating during Senescence of Podospora anserina." J Biol Chem **290**(26): 16415-16430.
Chen, H., Z. Lao, J. Xu, Z. Li, H. Long, D. Li, L. Lin, X. Liu, L. Yu, W. Liu, G. Li and J. Wu (2020). "Antiviral activity of lycorine against Zika virus in vivo and in vitro." Virology **546**: 88-97.
Colque, R., F. Viladomat, J. Bastida and C. Codina (2002). "Micropropagation of the rare Eucrosia stricklandii (Amaryllidaceae) by twin-scaling and shake liquid culture." The Journal of Horticultural Science and Biotechnology **77**(6): 739-743.
Colque, R., F. Viladomat, J. Bastida and C. Codina (2004). "Improved production of galanthamine and related alkaloids by methyl jasmonate in Narcissus confusus shoot-clumps." Planta medica **70**(12): 1180-1188.
Colque, R., F. Viladomat, J. Bastida and C. Codina (2015). "Micropropagation of the rareEucrosia stricklandii(Amaryllidaceae) by twin-scaling and shake liquid culture." The Journal of Horticultural Science and Biotechnology **77**(6): 739-743.
Conesa, A., P. Madrigal, S. Tarazona, D. Gomez-Cabrero, A. Cervera, A. McPherson, M. W. Szczesniak, D. J. Gaffney, L. L. Elo, X. Zhang and A. Mortazavi (2016). "A survey of best practices for RNA-seq data analysis." Genome Biol **17**(1): 13.
Cordell, G. A., M. L. Quinn-Beattie and N. R. Farnsworth (2001). "The potential of alkaloids in drug discovery." Phytotherapy Research: An International Journal Devoted to Pharmacological and Toxicological Evaluation of Natural Product Derivatives **15**(3): 183-205.
Cushnie, T. T., B. Cushnie and A. J. Lamb (2014). "Alkaloids: An overview of their antibacterial, antibiotic-enhancing and antivirulence activities." International journal of antimicrobial agents **44**(5): 377-386.
Dasari, R., L. M. Y. Banuls, M. Masi, S. C. Pelly, V. Mathieu, I. R. Green, W. A. van Otterlo, A. Evidente, R. Kiss and A. Kornienko (2014). "C1, C2-ether derivatives of the Amaryllidaceae alkaloid lycorine: Retention

of activity of highly lipophilic analogues against cancer cells." Bioorganic & medicinal chemistry letters **24**(3): 923-927.
De Smet, P. A. (1997). "The role of plant-derived drugs and herbal medicines in healthcare." Drugs **54**: 801-840.
Delli-Ponti, R., D. Shivhare and M. Mutwil (2021). "Using gene expression to study specialized metabolism—a practical guide." Frontiers in Plant Science **11**: 625035.
Demir, S. C., A. B. Yildirim, A. U. Turker and I. Eker (2022). "Seasonal variation in alkaloid content, phenolic constituent and biological activities of some *Leucojum aestivum* L. populations in Turkey." South African Journal of Botany **147**: 713-723.
Desgagné-Penix, I. (2020). "Biosynthesis of alkaloids in Amaryllidaceae plants: a review." Phytochemistry Reviews **20**(2): 409-431.
Desgagné-Penix, I. (2021). "Biosynthesis of alkaloids in Amaryllidaceae plants: A review." Phytochemistry Reviews **20**(2): 409-431.
Dewick, P. M. (2009). Medicinal natural products: a biosynthetic approach., John Wiley and Sons Ltd.
Diamond, A. and I. Desgagne-Penix (2016). "Metabolic engineering for the production of plant isoquinoline alkaloids." Plant Biotechnol J **14**(6): 1319-1328.
Diamond, A. and I. Desgagné-Penix (2016). "Metabolic engineering for the production of plant isoquinoline alkaloids." Plant biotechnology journal **14**(6): 1319-1328.
Ding, Y., D. Qu, K.-M. Zhang, X.-X. Cang, Z.-N. Kou, W. Xiao and J.-B. Zhu (2017). "Phytochemical and biological investigations of Amaryllidaceae alkaloids: a review." Journal of Asian natural products research **19**(1): 53-100.
Ding, Y., D. Qu, K. M. Zhang, X. X. Cang, Z. N. Kou, W. Xiao and J. B. Zhu (2017). "Phytochemical and biological investigations of Amaryllidaceae alkaloids: a review." J Asian Nat Prod Res **19**(1): 53-100.
Diop, M., A. Hehn, A. Ptak, F. Chrétien, S. Doerper, E. Gontier, F. Bourgaud, M. Henry, Y. Chapleur and D. Laurain-Mattar (2007). "Hairy root and tissue cultures of Leucojum aestivum L.—relationships to galanthamine content." Phytochemistry reviews **6**(1): 137-141.
Diop, M., A. Hehn, A. Ptak, F. Chrétien, S. Doerper, E. Gontier, F. Bourgaud, M. Henry, Y. Chapleur and D. Laurain-Mattar (2007). "Hairy root and tissue cultures of Leucojum aestivum L.—relationships to galanthamine content." Phytochemistry reviews **6**: 137-141.
Dixon, R. A. and N. L. Paiva (1995). "Stress-Induced Phenylpropanoid Metabolism." Plant Cell **7**(7): 1085-1097.
Dixon, R. A. and N. L. Paiva (1995). "Stress-induced phenylpropanoid metabolism." The plant cell **7**(7): 1085.
Dong, F. S., M. Y. Lv, J. P. Wang, X. P. Shi, X. X. Liang, Y. W. Liu, F. Yang, H. Zhao, J. F. Chai and S. Zhou (2020). "Transcriptome analysis of activated charcoal-induced growth promotion of wheat seedlings in tissue culture." BMC Genet **21**(1): 69.
Dostál, J. (2000). "Two faces of alkaloids." Journal of Chemical Education **77**(8): 993.
Eichhorn, J., T. Takada, Y. Kita and M. H. Zenk (1998). "Biosynthesis of the Amaryllidaceae alkaloid galanthamine." Phytochemistry **49**(4): 1037-1047.
El Tahchy, A., S. Bordage, A. Ptak, F. Dupire, E. Barre, C. Guillou, M. Henry, Y. Chapleur and D. Laurain-Mattar (2011). "Effects of sucrose and plant growth regulators on acetylcholinesterase inhibitory activity of alkaloids accumulated in shoot cultures of Amaryllidaceae." Plant Cell, Tissue and Organ Culture (PCTOC) **106**: 381-390.
El Tahchy, A., S. Bordage, A. Ptak, F. Dupire, E. Barre, C. Guillou, M. Henry, Y. Chapleur and D. Laurain-Mattar (2011). "Effects of sucrose and plant growth regulators on acetylcholinesterase inhibitory activity of alkaloids accumulated in shoot cultures of Amaryllidaceae." Plant Cell, Tissue and Organ Culture (PCTOC) **106**(3): 381-390.

El Tahchy, A., A. Ptak, M. Boisbrun, E. Barre, C. Guillou, F. Dupire, F. Chretien, M. Henry, Y. Chapleur and D. Laurain-Mattar (2011). "Kinetic study of the rearrangement of deuterium-labeled 4'-O-methylnorbelladine in Leucojum aestivum shoot cultures by mass spectrometry. Influence of precursor feeding on amaryllidaceae alkaloid accumulation." J Nat Prod **74**(11): 2356-2361.
El Tahchy, A., A. Ptak, M. Boisbrun, E. Barre, C. Guillou, F. o. Dupire, F. o. Chrétien, M. Henry, Y. Chapleur and D. Laurain-Mattar (2011). "Kinetic study of the rearrangement of deuterium-labeled 4'-O-methylnorbelladine in Leucojum aestivum shoot cultures by mass spectrometry. Influence of precursor feeding on Amaryllidaceae alkaloid accumulation." Journal of natural products **74**(11): 2356-2361.
Elgorashi, E. E., S. E. Drewes, C. Morris and J. van Staden (2003). "Variation among three Crinum species in alkaloid content." Biochemical Systematics and Ecology **31**(6): 601-615.
Elgorashi, E. E., S. E. Drewes and J. Van Staden (2002). "Organ-to-organ and seasonal variation in alkaloids from *Crinum macowanii*." Fitoterapia **73**(6): 490-495.
Espinosa-Leal, C. A., S. Mora-Vásquez, C. A. Puente-Garza, D. S. Alvarez-Sosa and S. García-Lara (2022). "Recent advances on the use of abiotic stress (water, UV radiation, atmospheric gases, and temperature stress) for the enhanced production of secondary metabolites on in vitro plant tissue culture." Plant Growth Regulation **97**(1): 1-20.
Evans, W. C. (2009). Trease and Evans' pharmacognosy, Elsevier Health Sciences.
Facchini, P. J., J. Bohlmann, P. S. Covello, V. De Luca, R. Mahadevan, J. E. Page, D.-K. Ro, C. W. Sensen, R. Storms and V. J. Martin (2012). "Synthetic biosystems for the production of high-value plant metabolites." Trends in biotechnology **30**(3): 127-131.
Facchini, P. J., J. Bohlmann, P. S. Covello, V. De Luca, R. Mahadevan, J. E. Page, D. K. Ro, C. W. Sensen, R. Storms and V. J. Martin (2012). "Synthetic biosystems for the production of high-value plant metabolites." Trends Biotechnol **30**(3): 127-131.
Facchini, P. J. and V. De Luca (2008). "Opium poppy and Madagascar periwinkle: model non-model systems to investigate alkaloid biosynthesis in plants." The Plant Journal **54**(4): 763-784.
Farhi, M., E. Marhevka, J. Ben-Ari, A. Algamas-Dimantov, Z. Liang, V. Zeevi, O. Edelbaum, B. Spitzer-Rimon, H. Abeliovich and B. Schwartz (2011). "Generation of the potent anti-malarial drug artemisinin in tobacco." Nature biotechnology **29**(12): 1072-1074.
Farhi, M., E. Marhevka, J. Ben-Ari, A. Algamas-Dimantov, Z. Liang, V. Zeevi, O. Edelbaum, B. Spitzer-Rimon, H. Abeliovich, B. Schwartz, T. Tzfira and A. Vainstein (2011). "Generation of the potent anti-malarial drug artemisinin in tobacco." Nat Biotechnol **29**(12): 1072-1074.
Fennell, C., E. Elgorashi and J. Van Staden (2003). "Alkaloid production in Crinum moorei cultures." Journal of natural products **66**(11): 1524-1526.
Fennell, C. and J. Van Staden (2001). "Crinum species in traditional and modern medicine." Journal of ethnopharmacology **78**(1): 15-26.
Fennell, C. W., E. E. Elgorashi and J. van Staden (2003). "Alkaloid production in *Crinum moorei* cultures." J Nat Prod **66**(11): 1524-1526.
Fennell, C. W. and J. van Staden (2001). "*Crinum* species in traditional and modern medicine." J Ethnopharmacol **78**(1): 15-26.
Ferdausi, A., X. Chang, A. Hall and M. Jones (2020). "Galanthamine production in tissue culture and metabolomic study on Amaryllidaceae alkaloids in *Narcissus pseudonarcissus* cv. Carlton." Industrial Crops and Products **144**: 112058.
Ferdausi, A., X. Chang, A. Hall and M. Jones (2020). "Galanthamine production in tissue culture and metabolomic study on Amaryllidaceae alkaloids in Narcissus pseudonarcissus cv. Carlton." Industrial Crops and Products **144**.
Ferdausi, A., X. Chang and M. Jones (2021). "Enhancement of galanthamine production through elicitation and NMR-based metabolite profiling in Narcissus pseudonarcissus cv. Carlton in vitro callus cultures." In Vitro Cellular & Developmental Biology-Plant **57**(3): 435-446.

Ferdausi, A., X. Chang and M. Jones (2021). "Transcriptomic analysis for differential expression of genes involved in secondary metabolite production in Narcissus pseudonarcissus field derived bulb and in vitro callus." Industrial Crops and Products **168**: 113615.
Fossati, E., L. Narcross, A. Ekins, J.-P. Falgueyret and V. J. Martin (2015). "Synthesis of morphinan alkaloids in Saccharomyces cerevisiae." PLoS One **10**(4).
Fossati, E., L. Narcross, A. Ekins, J. P. Falgueyret and V. J. Martin (2015). "Synthesis of Morphinan Alkaloids in Saccharomyces cerevisiae." PLoS One **10**(4): e0124459.
Fridborg, G., M. K. Pedersen, L. Landström and T. R. Eriksson (1978). "The Effect of Activated Charcoal on Tissue Cultures: Adsorption of Metabolites Inhibiting Morphogenesis." Physiologia Plantarum **43**: 104-106.
Gaba, V. P. (2005). Plant growth regulators in plant tissue culture and development. Plant development and biotechnology, CRC Press Boca Raton, FL**:** 87-99.
Gallego, A. M., L. F. Rojas, O. Parra, H. A. Rodriguez, J. C. Mazo Rivas, A. I. Urrea, L. Atehortúa, A. S. Fister, M. J. Guiltinan and S. N. Maximova (2018). "Transcriptomic analyses of cacao cell suspensions in light and dark provide target genes for controlled flavonoid production." Scientific reports **8**(1): 13575.
Gallego, A. M., L. F. Rojas, O. Parra, H. A. Rodriguez, J. C. Mazo Rivas, A. I. Urrea, L. Atehortua, A. S. Fister, M. J. Guiltinan, S. N. Maximova and N. Pabon-Mora (2018). "Transcriptomic analyses of cacao cell suspensions in light and dark provide target genes for controlled flavonoid production." Sci Rep **8**(1): 13575.
Gallego, A. M., L. F. Rojas, O. Parra, H. A. Rodriguez, J. C. M. Rivas, A. I. Urrea, L. Atehortúa, A. S. Fister, M. J. Guiltinan and S. N. Maximova (2018). "Transcriptomic analyses of cacao cell suspensions in light and dark provide target genes for controlled flavonoid production." Scientific reports **8**(1): 1-14.
Galperin, M. Y., Y. I. Wolf, K. S. Makarova, R. Vera Alvarez, D. Landsman and E. V. Koonin (2021). "COG database update: focus on microbial diversity, model organisms, and widespread pathogens." Nucleic Acids Res **49**(D1): D274-D281.
Gaspar, T., C. Kevers, C. Penel, H. Greppin, D. M. Reid and T. A. Thorpe (1996). "Plant hormones and plant growth regulators in plant tissue culture." In Vitro Cellular & Developmental Biology-Plant **32**(4): 272-289.
Georgiev, V., S. Berkov, M. Georgiev, M. Burrus, C. Codina, J. Bastida, M. Ilieva and A. Pavlov (2009). "Optimized nutrient medium for galanthamine production in Leucojum aestivum L. in vitro shoot system." Z Naturforsch C J Biosci **64**(3-4): 219-224.
Georgiev, V., I. Ivanov, S. Berkov, M. Ilieva, M. Georgiev, T. Gocheva and A. Pavlov (2012). "Galanthamine production byLeucojum aestivumL. shoot culture in a modified bubble column bioreactor with internal sections." Engineering in Life Sciences **12**(5): 534-543.
Georgiev, V., I. Ivanov and A. Pavlov (2020). "Recent Progress in Amaryllidaceae Biotechnology." Molecules **25**(20).
Girard, M.-P., V. Karimzadegan, M. Héneault, F. Cloutier, G. Bérubé, L. Berthoux, N. Mérindol and I. Desgagné-Penix (2022). "Chemical Synthesis and Biological Activities of Amaryllidaceae Alkaloid Norbelladine Derivatives and Precursors." Molecules **27**(17): 5621.
Girard, M. P., V. Karimzadegan, M. Heneault, F. Cloutier, G. Berube, L. Berthoux, N. Merindol and I. Desgagne-Penix (2022). "Chemical Synthesis and Biological Activities of Amaryllidaceae Alkaloid Norbelladine Derivatives and Precursors." Molecules **27**(17): 5621.
Girard, M. P., V. Karimzadegan, M. Heneault, F. Cloutier, G. Berube, L. Berthoux, N. Merindol and I. Desgagne-Penix (2022). "Chemical Synthesis and Biological Activities of Amaryllidaceae Alkaloid Norbelladine Derivatives and Precursors." Molecules **27**(17).
Group, A. P., M. W. Chase, M. J. Christenhusz, M. F. Fay, J. Byng, W. Judd, D. Soltis, D. Mabberley, A. Sennikov and P. Soltis (2016). "An update of the Angiosperm Phylogeny Group classification for the orders and families of flowering plants: APG IV." Botanical journal of the Linnean Society **181**(1): 1-20.

Gupta, K., A. Sengupta, M. Chakraborty and B. Gupta (2016). "Hydrogen Peroxide and Polyamines Act as Double Edged Swords in Plant Abiotic Stress Responses." Front Plant Sci **7**: 1343.
Gupta, K., A. Sengupta, M. Chakraborty and B. Gupta (2016). "Hydrogen peroxide and polyamines act as double edged swords in plant abiotic stress responses." Frontiers in plant science **7**: 1343.
Hagel, J. M. and P. J. Facchini (2013). "Benzylisoquinoline alkaloid metabolism: a century of discovery and a brave new world." Plant and Cell Physiology **54**(5): 647-672.
Hamamsy, T., J. T. Morton, R. Blackwell, D. Berenberg, N. Carriero, V. Gligorijevic, C. E. Strauss, J. K. Leman, K. Cho and R. Bonneau (2023). "Protein remote homology detection and structural alignment using deep learning." Nature Biotechnology: 1-11.
Haug, K., K. Cochrane, V. C. Nainala, M. Williams, J. Chang, K. V. Jayaseelan and C. O'Donovan (2020). "MetaboLights: a resource evolving in response to the needs of its scientific community." Nucleic Acids Res **48**(D1): D440-D444.
He, M., C. Qu, O. Gao, X. Hu and X. Hong (2015). "Biological and pharmacological activities of amaryllidaceae alkaloids." RSC Advances **5**(21): 16562-16574.
Hollingsworth, S. A. and R. O. Dror (2018). "Molecular dynamics simulation for all." Neuron **99**(6): 1129-1143.
Hotchandani, T., J. de Villers and I. Desgagne-Penix (2019). "Developmental Regulation of the Expression of Amaryllidaceae Alkaloid Biosynthetic Genes in *Narcissus papyraceus*." Genes (Basel) **10**(8): 594.
Hotchandani, T., J. de Villers and I. Desgagné-Penix (2019). "Developmental regulation of the expression of Amaryllidaceae alkaloid biosynthetic genes in Narcissus papyraceus." Genes **10**(8): 594.
Hotchandani, T., J. de Villers and I. Desgagné-Penix (2019). "Developmental Regulation of the Expression of Amaryllidaceae Alkaloid Biosynthetic Genes in Narcissus papyraceus." Genes **10**(8).
Hotchandani, T. and I. Desgagne-Penix (2017). "Heterocyclic Amaryllidaceae Alkaloids: Biosynthesis and Pharmacological Applications." Current Topics in Medicinal Chemistry **17**(4): 418-427.
Houghton, P. J., J. M. Agbedahunsi and A. Adegbulugbe (2004). "Choline esterase inhibitory properties of alkaloids from two Nigerian Crinum species." Phytochemistry **65**(21): 2893-2896.
Houghton, P. J., Y. Ren and M.-J. Howes (2006). "Acetylcholinesterase inhibitors from plants and fungi." Natural product reports **23**(2): 181-199.
Houghton, P. J., Y. Ren and M. J. Howes (2006). "Acetylcholinesterase inhibitors from plants and fungi." Nat Prod Rep **23**(2): 181-199.
Howes, M.-J. R. and E. Perry (2011). "The role of phytochemicals in the treatment and prevention of dementia." Drugs & aging **28**: 439-468.
Hu, J., W. Li, Z. Liu, G. Zhang and Y. Luo (2021). "Molecular cloning and functional characterization of tyrosine decarboxylases from galanthamine-producing Lycoris radiata." Acta Physiologiae Plantarum **43**(6): 84.
Hu, J., W. Li, Z. Liu, G. Zhang and Y. Luo (2021). "Molecular cloning and functional characterization of tyrosine decarboxylases from galanthamine-producing Lycoris radiata." Acta Physiologiae Plantarum **43**(6): 1-12.
Hwang, I. S. and B. K. Hwang (2011). "The pepper mannose-binding lectin gene CaMBL1 is required to regulate cell death and defense responses to microbial pathogens." Plant physiology **155**(1): 447-463.
Ibrahim, R. K., A. Bruneau and B. Bantignies (1998). "Plant O-methyltransferases: molecular analysis, common signature and classification." Plant molecular biology **36**: 1-10.
Idu, M., G. Obaruyi and J. Erhabor (2008). "Ethnobotanical uses of plants among the binis in the treatment of ophthalmic and ENT (ear, nose and throat) ailments." Ethnobotanical leaflets **2009**(4): 9.
Ieven, M., A. J. Vlietinck, D. A. Vanden Berghe, J. Totte, R. Dommisse, E. Esmans and F. Alderweireldt (1982). "Plant antiviral agents. III. Isolation of alkaloids from Clivia miniata Regel (Amaryllidaceae)." J Nat Prod **45**(5): 564-573.

Ikeuchi, M., A. Iwase and K. Sugimoto (2015). "Control of plant cell differentiation by histone modification and DNA methylation." Curr Opin Plant Biol **28**: 60-67.
Irwin, J. J., T. Sterling, M. M. Mysinger, E. S. Bolstad and R. G. Coleman (2012). "ZINC: a free tool to discover chemistry for biology." Journal of chemical information and modeling **52**(7): 1757-1768.
Ivanov, I., V. Georgiev, S. Berkov and A. Pavlov (2012). "Alkaloid patterns in Leucojum aestivum shoot culture cultivated at temporary immersion conditions." J Plant Physiol **169**(2): 206-211.
Ivanov, I., V. Georgiev, M. Georgiev, M. Ilieva and A. Pavlov (2011). "Galanthamine and related alkaloids production by Leucojum aestivum L. shoot culture using a temporary immersion technology." Appl Biochem Biotechnol **163**(2): 268-277.
Ivanov, I., V. Georgiev and A. Pavlov (2013). "Elicitation of galanthamine biosynthesis by Leucojum aestivum liquid shoot cultures." Journal of plant physiology **170**(12): 1122-1129.
Ivanov, I., V. Georgiev and A. Pavlov (2013). "Elicitation of galanthamine biosynthesis by Leucojum aestivum liquid shoot cultures." J Plant Physiol **170**(12): 1122-1129.
Jacobowitz, J. R. and J.-K. Weng (2020). "Exploring uncharted territories of plant specialized metabolism in the postgenomic era." Annual review of plant biology **71**: 631-658.
Jacobowitz, J. R. and J. K. Weng (2020). "Exploring Uncharted Territories of Plant Specialized Metabolism in the Postgenomic Era." Annu Rev Plant Biol **71**: 631-658.
Jarillo, J. A., M. Piñeiro, P. Cubas Domínguez and J. M. Martínez-Zapater (2009). "Chromatin remodeling in plant development."
Jiang, Y., N. Xia, X. Li, W. Shen, L. Liang, C. Wang, R. Wang, F. Peng and B. Xia (2011). "Molecular cloning and characterization of a phenylalanine ammonia-lyase gene (LrPAL) from Lycoris radiata." Molecular biology reports **38**: 1935-1940.
Jin, Z. and G. Yao (2019). "Amaryllidaceae and Sceletium alkaloids." Natural Product Reports **36**(10): 1462-1488.
Jin, Z. and G. Yao (2019). "Amaryllidaceae and Sceletium alkaloids." Nat Prod Rep **36**(10): 1462-1488.
Juan-Vicedo, J., A. Pavlov, S. Ríos and J. L. Casas (2019). "In vitro culture and micropropagation of the Baetic-Moroccan endemic plant Lapiedra martinezii Lag. (Amaryllidaceae)." In Vitro Cellular & Developmental Biology - Plant **55**(6): 725-732.
Jumper, J., R. Evans, A. Pritzel, T. Green, M. Figurnov, O. Ronneberger, K. Tunyasuvunakool, R. Bates, A. Žídek and A. Potapenko (2021). "Highly accurate protein structure prediction with AlphaFold." Nature **596**(7873): 583-589.
Ka, S., M. Koirala, N. Merindol and I. Desgagne-Penix (2020). "Biosynthesis and Biological Activities of Newly Discovered Amaryllidaceae Alkaloids." Molecules **25**(21).
Ka, S., M. Koirala, N. Mérindol and I. Desgagné-Penix (2020). "Biosynthesis and biological activities of newly discovered Amaryllidaceae alkaloids." Molecules **25**(21): 4901.
Ka, S., M. Masi, N. Merindol, R. Di Lecce, M. B. Plourde, M. Seck, M. Gorecki, G. Pescitelli, I. Desgagne-Penix and A. Evidente (2020). "Gigantelline, gigantellinine and gigancrinine, cherylline- and crinine-type alkaloids isolated from *Crinum jagus* with anti-acetylcholinesterase activity." Phytochemistry **175**: 112390.
Ka, S., N. Merindol, I. Seck, S. Ricard, A. Diop, C. S. B. Boye, K. Landelouci, B. Daoust, L. Berthoux, G. Pepin, M. Seck and I. Desgagne-Penix (2021). "Biological Investigation of Amaryllidaceae Alkaloid Extracts from the Bulbs of *Pancratium trianthum* Collected in the Senegalese Flora." Molecules **26**(23): 7382.
Ka, S., N. Merindol, A. A. Sow, A. Singh, K. Landelouci, M. B. Plourde, G. Pépin, M. Masi, R. Di Lecce and A. Evidente (2021). "Amaryllidaceae alkaloid cherylline inhibits the replication of dengue and Zika viruses." Antimicrobial Agents and Chemotherapy **65**(9): e00398-00321.
Ka, S., N. Merindol, A. A. Sow, A. Singh, K. Landelouci, M. B. Plourde, G. Pepin, M. Masi, R. Di Lecce, A. Evidente, M. Seck, L. Berthoux, L. Chatel-Chaix and I. Desgagne-Penix (2021). "Amaryllidaceae Alkaloid

Cherylline Inhibits the Replication of Dengue and Zika Viruses." Antimicrob Agents Chemother **65**(9): e0039821.
Kallscheuer, N., T. Classen, T. Drepper and J. Marienhagen (2019). "Production of plant metabolites with applications in the food industry using engineered microorganisms." Current opinion in biotechnology **56**: 7-17.
Kalola, U. K. and H. Nguyen (2022). Galantamine. StatPearls. Treasure Island (FL).
Kathe, W., S. Honnef and A. Heym (2003). "Medicinal and aromatic plants in Albania, Bosnia-Herzegovina, Bulgaria, Croatia and Romania: a study of the collection of and trade in medicinal and aromatic plants (MAPs), relevant legislation and the potential of MAP use for financing nature conservation and protected areas."
Katoh, A., H. Ohki, K. Inai and T. Hashimoto (2005). "Molecular regulation of nicotine biosynthesis." Plant Biotechnology **22**(5): 389-392.
Kaur, H., S. Chahal, P. Jha, M. M. Lekhak, M. S. Shekhawat, D. Naidoo, A. D. Arencibia, S. J. Ochatt and V. Kumar (2022). "Harnessing plant biotechnology-based strategies for in vitro galanthamine (GAL) biosynthesis: a potent drug against Alzheimer's disease." Plant Cell, Tissue and Organ Culture (PCTOC) **149**(1-2): 81-103.
Kenrick, P. and P. R. Crane (1997). "The origin and early evolution of plants on land." Nature **389**(6646): 33-39.
Khadr, A., G.-L. Wang, Y.-H. Wang, R.-R. Zhang, X.-R. Wang, Z.-S. Xu, Y.-S. Tian and A.-S. Xiong (2020). "Effects of auxin (indole-3-butyric acid) on growth characteristics, lignification, and expression profiles of genes involved in lignin biosynthesis in carrot taproot." PeerJ **8**: e10492.
Khadr, A., G. L. Wang, Y. H. Wang, R. R. Zhang, X. R. Wang, Z. S. Xu, Y. S. Tian and A. S. Xiong (2020). "Effects of auxin (indole-3-butyric acid) on growth characteristics, lignification, and expression profiles of genes involved in lignin biosynthesis in carrot taproot." PeerJ **8**: e10492.
Khersonsky, O., C. Roodveldt and D. S. Tawfik (2006). "Enzyme promiscuity: evolutionary and mechanistic aspects." Current opinion in chemical biology **10**(5): 498-508.
Kilgore, M. B., M. M. Augustin, G. D. May, J. A. Crow and T. M. Kutchan (2016). "CYP96T1 of Narcissus sp. aff. pseudonarcissus Catalyzes Formation of the Para-Para' C-C Phenol Couple in the Amaryllidaceae Alkaloids." Front Plant Sci **7**: 225.
Kilgore, M. B., M. M. Augustin, C. M. Starks, M. O'Neil-Johnson, G. D. May, J. A. Crow and T. M. Kutchan (2014). "Cloning and characterization of a norbelladine 4'-O-methyltransferase involved in the biosynthesis of the Alzheimer's drug galanthamine in Narcissus sp. aff. pseudonarcissus." PLoS One **9**(7): e103223.
Kilgore, M. B., M. M. Augustin, C. M. Starks, M. O'Neil-Johnson, G. D. May, J. A. Crow and T. M. Kutchan (2014). "Cloning and characterization of a norbelladine 4'-O-methyltransferase involved in the biosynthesis of the Alzheimer's drug galanthamine in Narcissus sp. aff. pseudonarcissus." PloS one **9**(7): e103223.
Kilgore, M. B., C. K. Holland, J. M. Jez and T. M. Kutchan (2016). "Identification of a Noroxomaritidine Reductase with Amaryllidaceae Alkaloid Biosynthesis Related Activities." J Biol Chem **291**(32): 16740-16752.
Kilgore, M. B., C. K. Holland, J. M. Jez and T. M. Kutchan (2016). "Identification of a Noroxomaritidine Reductase with Amaryllidaceae Alkaloid Biosynthesis Related Activities *." Journal of Biological Chemistry **291**(32): 16740-16752.
Kilgore, M. B. and T. M. Kutchan (2016). "The Amaryllidaceae alkaloids: biosynthesis and methods for enzyme discovery." Phytochem Rev **15**(3): 317-337.
Kitney, R. and P. Freemont (2012). "Synthetic biology–the state of play." FEBS letters **586**(15): 2029-2036.
Kitney, R. and P. Freemont (2012). "Synthetic biology - the state of play." FEBS Lett **586**(15): 2029-2036.

Koirala, M., V. Karimzadegan, N. S. Liyanage, N. Merindol and I. Desgagne-Penix (2022). "Biotechnological Approaches to Optimize the Production of Amaryllidaceae Alkaloids." Biomolecules **12**(7): 893.
Koirala, M., V. Karimzadegan, N. S. Liyanage, N. Mérindol and I. Desgagné-Penix (2022). "Biotechnological Approaches to Optimize the Production of Amaryllidaceae Alkaloids." Biomolecules **12**(7): 893.
Kornienko, A. and A. Evidente (2008). "Chemistry, biology, and medicinal potential of narciclasine and its congeners." Chemical reviews **108**(6): 1982-2014.
Kozbial, P. Z. and A. R. Mushegian (2005). "Natural history of S-adenosylmethionine-binding proteins." BMC Struct Biol **5**: 19.
Krug, E. and P. Proksch (1993). "Influence of dietary alkaloids on survival and growth of Spodoptera littoralis." Biochemical systematics and ecology **21**(8): 749-756.
Kurek, J. (2019). Alkaloids: their importance in nature and human life, BoD–Books on Demand.
Lam, P. Y., L. Wang, C. Lo and F. Y. Zhu (2022). "Alternative Splicing and Its Roles in Plant Metabolism." Int J Mol Sci **23**(13).
Langens-Gerrits, M., M. Albers and G.-J. De Klerk (1998). "Hot-water treatment before tissue culture reduces initial contamination in *Lilium* and *Acer*." Plant Cell, Tissue and Organ Culture **52**(1): 75-77.
Langfelder, P. and S. Horvath (2008). "WGCNA: an R package for weighted correlation network analysis." BMC Bioinformatics **9**(1): 559.
Lashley, A., R. Miller, S. Provenzano, S.-A. Jarecki, P. Erba and V. Salim (2022). "Functional diversification and structural origins of plant natural product methyltransferases." Molecules **28**(1): 43.
Laurain-Mattar, D. and A. Ptak (2018). Amaryllidaceae Alkaloid Accumulation by Plant In Vitro Systems. Bioprocessing of Plant In Vitro Systems. A. Pavlov and T. Bley. Cham, Springer International Publishing**:** 203-223.
Laurain-Mattar, D. and A. Ptak (2018). Amaryllidaceae alkaloid accumulation by plant in vitro systems.
Lebrun, S., A. Couture, E. Deniau and P. Grandclaudon (2003). "A new synthesis of (+)- and (-)-cherylline." Org Biomol Chem **1**(10): 1701-1706.
Lebrun, S., A. Couture, E. Deniau and P. Grandclaudon (2003). "A new synthesis of (+)-and (−)-cherylline." Organic & biomolecular chemistry **1**(10): 1701-1706.
Lee, S., J. Kang and J. Kim (2019). "Structural and biochemical characterization of Rv0187, an O-methyltransferase from Mycobacterium tuberculosis." Sci Rep **9**(1): 8059.
Lewis, J. R. (1996). "Amaryllidaceae and Sceletium alkaloids." Natural Product Reports **13**(2): 171-176.
Li, B. and C. N. Dewey (2011). "RSEM: accurate transcript quantification from RNA-Seq data with or without a reference genome." BMC Bioinformatics **12**: 323.
Li, Q., J. Xu, L. Yang, Y. Sun, X. Zhou, Y. Zheng, Y. Zhang and Y. Cai (2021). "LED Light Quality Affect Growth, Alkaloids Contents, and Expressions of Amaryllidaceae Alkaloids Biosynthetic Pathway Genes in *Lycoris longituba*." Journal of Plant Growth Regulation **41**(1): 257-270.
Li, Q., J. Xu, L. Yang, Y. Sun, X. Zhou, Y. Zheng, Y. Zhang and Y. Cai (2021). "LED light quality affect growth, alkaloids contents, and expressions of amaryllidaceae alkaloids biosynthetic pathway genes in Lycoris longituba." Journal of Plant Growth Regulation: 1-14.
Li, Q., J. Xu, L. Yang, Y. Sun, X. Zhou, Y. Zheng, Y. Zhang and Y. Cai (2021). "LED Light Quality Affect Growth, Alkaloids Contents, and Expressions of Amaryllidaceae Alkaloids Biosynthetic Pathway Genes in Lycoris longituba." Journal of Plant Growth Regulation.
Li, Q., J. Xu, L. Yang, X. Zhou, Y. Cai and Y. Zhang (2020). "Transcriptome Analysis of Different Tissues Reveals Key Genes Associated With Galanthamine Biosynthesis in Lycoris longituba." Front Plant Sci **11**(1444): 519752.
Li, Q., J. Xu, Y. Zheng, Y. Zhang and Y. Cai (2021). "Transcriptomic and Metabolomic Analyses Reveals That Exogenous Methyl Jasmonate Regulates Galanthamine Biosynthesis in Lycoris longituba Seedlings." Frontiers in plant science: 1933.

Li, Q., J. Xu, Y. Zheng, Y. Zhang and Y. Cai (2021). "Transcriptomic and Metabolomic Analyses Reveals That Exogenous Methyl Jasmonate Regulates Galanthamine Biosynthesis in Lycoris longituba Seedlings." Frontiers in Plant Science **12**(1933).
Li, W., C. Qiao, J. Pang, G. Zhang and Y. Luo (2019). "The versatile O-methyltransferase LrOMT catalyzes multiple O-methylation reactions in amaryllidaceae alkaloids biosynthesis." International journal of biological macromolecules **141**: 680-692.
Li, Y., J. Li, B. Qian, L. Cheng, S. Xu and R. Wang (2018). "De novo biosynthesis of p-coumaric acid in E. coli with a trans-cinnamic acid 4-hydroxylase from the Amaryllidaceae plant Lycoris aurea." Molecules **23**(12): 3185.
Li, Y., S. Li, K. Thodey, I. Trenchard, A. Cravens and C. D. Smolke (2018). "Complete biosynthesis of noscapine and halogenated alkaloids in yeast." Proceedings of the National Academy of Sciences **115**(17): E3922-E3931.
Li, Y., S. Li, K. Thodey, I. Trenchard, A. Cravens and C. D. Smolke (2018). "Complete biosynthesis of noscapine and halogenated alkaloids in yeast." Proc Natl Acad Sci U S A **115**(17): E3922-E3931.
Liscombe, D. K., G. V. Louie and J. P. Noel (2012). "Architectures, mechanisms and molecular evolution of natural product methyltransferases." Nat Prod Rep **29**(10): 1238-1250.
Liu, Z., J. Zhou, Y. Li, J. Wen and R. Wang (2020). "Bacterial endophytes from Lycoris radiata promote the accumulation of Amaryllidaceae alkaloids." Microbiological Research **239**: 126501.
Liu, Z., J. Zhou, Y. Li, J. Wen and R. Wang (2020). "Bacterial endophytes from Lycoris radiata promote the accumulation of Amaryllidaceae alkaloids." Microbiol Res **239**: 126501.
Lubbe, A., H. Gude, R. Verpoorte and Y. H. Choi (2013). "Seasonal accumulation of major alkaloids in organs of pharmaceutical crop *Narcissus* Carlton." Phytochemistry **88**: 43-53.
Ma, L., Z. M. Haile, S. Sabbadini, B. Mezzetti, F. Negrini and E. Baraldi (2023). "Functional characterization of MANNOSE-BINDING LECTIN 1, a G-type lectin gene family member, in response to fungal pathogens of strawberry." J Exp Bot **74**(1): 149-161.
Ma, L., Z. M. Haile, S. Sabbadini, B. Mezzetti, F. Negrini and E. Baraldi (2023). "Functional characterization of MANNOSE-BINDING LECTIN 1, a G-type lectin gene family member, in response to fungal pathogens of strawberry." Journal of Experimental Botany **74**(1): 149-161.
Maafi, N. (2023). "Amaryllidaceae alkaloids of montanine type and their derivatives as potential drugs."
Majhi, B. B., S.-E. Gélinas, N. Mérindol and I. Desgagne-Penix (2022). "Characterization of norbelladine synthase and noroxomaritidine/norcraugsodine reductase reveals a novel catalytic route for the biosynthesis of Amaryllidaceae alkaloids including the Alzheimer's drug galanthamine." The Plant Journal **submitted**.
Majhi, B. B., S.-E. Gélinas, N. Mérindol and I. Desgagné-Penix (2022). "Characterization of norbelladine synthase and noroxomaritidine/norcraugsodine reductase reveals a novel catalytic route for the biosynthesis of Amaryllidaceae alkaloids including the Alzheimer's drug galanthamine." bioRxiv **Accepted in Frontiers in Plant Sciences Manuscript ID: 1231809**: 2022.2007.2030.502154.
Majhi, B. B., S.-E. Gélinas, N. Mérindol and I. Desgagné-Penix (2022). "Characterization of norbelladine synthase and noroxomaritidine/norcraugsodine reductase reveals a novel catalytic route for the biosynthesis of Amaryllidaceae alkaloids including the Alzheimer's drug galanthamine." bioRxiv: 2022.2007. 2030.502154.
Majhi, B. B., S.-E. Gélinas, N. Mérindol, S. Ricard and I. Desgagné-Penix (2023). "Characterization of norbelladine synthase and noroxomaritidine/norcraugsodine reductase reveals a novel catalytic route for the biosynthesis of Amaryllidaceae alkaloids including the Alzheimer's drug galanthamine." Frontiers in Plant Science **14**.
Mann, J. and S. H. Mudd (1963). "In vitro alkaloid biosynthesis in the Amaryllidaceae; Norbelladine O-Methylpherase." Journal of the American Chemical Society **85**(13): 2025-2026.

Mann, J. D., H. M. Fales and S. H. Mudd (1963). "Alkaloids and Plant Metabolism: VI. O-methylation in vitro of norbelladine, a precursor of amaryllidaceae alkaloids." Journal of Biological Chemistry **238**(11): 3820-3823.
Manolov, S., S. Nikolova, M. Ghate and I. Ivanov (2015). "A brief review of Cherylline synthesis." Indian Journal of Chemistry Section B **54B**: 1301-1320.
Manolov, S. P., S. N. Atanasova, M. Ghate and I. I. Ivanov (2015). "A brief review of Cherylline synthesis."
Marco-Contelles, J., M. do Carmo Carreiras, C. Rodriguez, M. Villarroya and A. G. Garcia (2006). "Synthesis and pharmacology of galantamine." Chem Rev **106**(1): 116-133.
Marco-Contelles, J., C. Rodríguez and A. G. García (2005). "Chemical synthesis of galantamine, an acetylcholinesterase inhibitor for treatment of Alzheimer's disease." Expert opinion on therapeutic patents **15**(5): 575-587.
Martin, S. F. (1987). The amaryllidaceae alkaloids. The Alkaloids: Chemistry and Pharmacology, Elsevier. **30:** 251-376.
Martin, S. F. (1988). The Amaryllidaceae alkaloids. The alkaloids, Academic Press. **30:** 251.
Matasci, N., L. H. Hung, Z. Yan, E. J. Carpenter, N. J. Wickett, S. Mirarab, N. Nguyen, T. Warnow, S. Ayyampalayam, M. Barker, J. G. Burleigh, M. A. Gitzendanner, E. Wafula, J. P. Der, C. W. dePamphilis, B. Roure, H. Philippe, B. R. Ruhfel, N. W. Miles, S. W. Graham, S. Mathews, B. Surek, M. Melkonian, D. E. Soltis, P. S. Soltis, C. Rothfels, L. Pokorny, J. A. Shaw, L. DeGironimo, D. W. Stevenson, J. C. Villarreal, T. Chen, T. M. Kutchan, M. Rolf, R. S. Baucom, M. K. Deyholos, R. Samudrala, Z. Tian, X. Wu, X. Sun, Y. Zhang, J. Wang, J. Leebens-Mack and G. K. Wong (2014). "Data access for the 1,000 Plants (1KP) project." Gigascience **3**(1): 17.
McKean, I. J. W., P. A. Hoskisson and G. A. Burley (2020). "Biocatalytic Alkylation Cascades: Recent Advances and Future Opportunities for Late-Stage Functionalization." Chembiochem **21**(20): 2890-2897.
Meerow, A. W., D. J. Lehmiller and J. R. Clayton (2003). "Phylogeny and biogeography of *Crinum* L. (Amaryllidaceae) inferred from nuclear and limited plastid non-coding DNA sequences." Botanical Journal of the Linnean Society **141**(3): 349-363.
Meisel, L., B. Fonseca, S. Gonzalez, R. Baeza-Yates, V. Cambiazo, R. Campos, M. Gonzalez, A. Orellana, J. Retamales and H. Silva (2005). "A rapid and efficient method for purifying high quality total RNA from peaches (*Prunus persica*) for functional genomics analyses." Biol Res **38**(1): 83-88.
Miller, I. R., N. J. McLean, G. A. Moustafa, V. Ajavakom, S. C. Kemp, R. K. Bellingham, N. P. Camp and R. C. Brown (2022). "Transition-metal-mediated chemo-and stereoselective total synthesis of (−)-galanthamine." The Journal of Organic Chemistry **87**(2): 1325-1334.
Miller, I. R., N. J. McLean, G. A. I. Moustafa, V. Ajavakom, S. C. Kemp, R. K. Bellingham, N. P. Camp and R. C. D. Brown (2022). "Transition-Metal-Mediated Chemo- and Stereoselective Total Synthesis of (-)-Galanthamine." J Org Chem **87**(2): 1325-1334.
Moranska, E., M. Simlat, M. Warchol, E. Skrzypek, P. Waligorski, D. Laurain-Mattar, R. Spina and A. Ptak (2023). "Phenolic Acids and Amaryllidaceae Alkaloids Profiles in *Leucojum aestivum* L. In Vitro Plants Grown under Different Light Conditions." Molecules **28**(4): 1525.
Morańska, E., M. Simlat, M. Warchoł, E. Skrzypek, P. Waligórski, D. Laurain-Mattar, R. Spina and A. Ptak (2023). "Phenolic Acids and Amaryllidaceae Alkaloids Profiles in Leucojum aestivum L. In Vitro Plants Grown under Different Light Conditions." Molecules **28**(4): 1525.
Mu, H.-m., R. Wang, X.-d. Li, Y.-m. Jiang, C.-y. Wang, J.-p. Quan, F. Peng and B. Xia (2009). "Effect of abiotic and biotic elicitors on growth and alkaloid accumulation of Lycoris chinensis seedlings." Zeitschrift für Naturforschung C **64**(7-8): 541-550.
Mu, H. M., R. Wang, X. D. Li, Y. M. Jiang, C. Y. Wang, J. P. Quan, F. Peng and B. Xia (2009). "Effect of abiotic and biotic elicitors on growth and alkaloid accumulation of Lycoris chinensis seedlings." Z Naturforsch C J Biosci **64**(7-8): 541-550.

Nair, J. J. and J. van Staden (2023). "Antiviral Effects of the Plant Family Amaryllidaceae." Natural Product Communications **18**(3): 1934578X231162781.
Ncube, B., J. Nair, L. Rárová, M. Strnad, J. Finnie and J. Van Staden (2015). "Seasonal pharmacological properties and alkaloid content in Cyrtanthus contractus NE Br." South African Journal of Botany **97**: 69-76.
Ncube, B., J. J. Nair, L. Rárová, M. Strnad, J. F. Finnie and J. Van Staden (2015). "Seasonal pharmacological properties and alkaloid content in Cyrtanthus contractus N.E. Br." South African Journal of Botany **97**: 69-76.
Ndakidemi, C. F., E. Mneney and P. A. Ndakidemi (2014). "Effects of ascorbic acid in controlling lethal browning in in vitro culture of Brahylaena huillensis using nodal segments." American Journal of Plant Sciences **2014**.
Ndakidemi, C. F., E. Mneney and P. A. Ndakidemi (2014). "Effects of Ascorbic Acid in Controlling Lethal Browning in in Vitro Culture of *Brahylaena huillensis*; Using Nodal Segments." American Journal of Plant Sciences **05**(01): 187-191.
Nino, J., G. M. Hincapie, Y. M. Correa and O. M. Mosquera (2007). "Alkaloids of *Crinum x powellii* "Album" (Amaryllidaceae) and their topoisomerase inhibitory activity." Z Naturforsch C J Biosci **62**(3-4): 223-226.
Niño, J., G. M. Hincapié, Y. M. Correa and O. M. Mosquera (2007). "Alkaloids of Crinum x powellii "Album"(Amaryllidaceae) and their topoisomerase inhibitory activity." Zeitschrift für Naturforschung C **62**(3-4): 223-226.
Nonn, M., A. Binder, B. Volk and L. Kiss (2020). "Stereo- and regiocontrolled synthesis of highly functionalized cyclopentanes with multiple chiral centers." Synthetic Communications **50**(8): 1199-1209.
Nonn, M., A. Binder, B. Volk and L. Kiss (2020). "Stereo-and regiocontrolled synthesis of highly functionalized cyclopentanes with multiple chiral centers." Synthetic Communications **50**(8): 1199-1209.
Ojolo, S. P., S. Cao, S. Priyadarshani, W. Li, M. Yan, M. Aslam, H. Zhao and Y. Qin (2018). "Regulation of plant growth and development: a review from a chromatin remodeling perspective." Frontiers in plant science **9**: 1232.
Olin, J. and L. Schneider (2002). "Galantamine for Alzheimer's disease." Cochrane Database Syst Rev(3): CD001747.
Onoyovwe, A., J. M. Hagel, X. Chen, M. F. Khan, D. C. Schriemer and P. J. Facchini (2013). "Morphine biosynthesis in opium poppy involves two cell types: sieve elements and laticifers." Plant Cell **25**(10): 4110-4122.
Othman, L., A. Sleiman and R. M. Abdel-Massih (2019). "Antimicrobial activity of polyphenols and alkaloids in middle eastern plants." Frontiers in microbiology **10**: 911.
Parc, G., A. Canaguier, P. Landré, R. Hocquemiller, D. Chriqui and M. Meyer (2002). "Production of taxoids with biological activity by plants and callus culture from selected Taxus genotypes." Phytochemistry **59**(7): 725-730.
Park, C. H., H. J. Yeo, Y. E. Park, S.-A. Baek, J. K. Kim and S. U. Park (2019). "Transcriptome analysis and metabolic profiling of Lycoris radiata." Biology **8**(3): 63.
Park, C. H., H. J. Yeo, Y. E. Park, S. A. Baek, J. K. Kim and S. U. Park (2019). "Transcriptome Analysis and Metabolic Profiling of Lycoris Radiata." Biology (Basel) **8**(3).
Park, W. T., S. K. Yeo, R. Sathasivam, J. S. Park, J. K. Kim and S. U. Park (2020). "Influence of light-emitting diodes on phenylpropanoid biosynthetic gene expression and phenylpropanoid accumulation in Agastache rugosa." Applied Biological Chemistry **63**(1): 1-9.
Park, W. T., S. K. Yeo, R. Sathasivam, J. S. Park, J. K. Kim and S. U. Park (2020). "Influence of light-emitting diodes on phenylpropanoid biosynthetic gene expression and phenylpropanoid accumulation in Agastache rugosa." Applied Biological Chemistry **63**(1): 25.
Patnaik, R., R. R. Zolandz, D. A. Green and D. F. Kraynie (2008). "L-tyrosine production by recombinant Escherichia coli: fermentation optimization and recovery." Biotechnol Bioeng **99**(4): 741-752.

Patnaik, R., R. R. Zolandz, D. A. Green and D. F. Kraynie (2008). "l-Tyrosine production by recombinant Escherichia coli: Fermentation optimization and recovery." Biotechnology and bioengineering **99**(4): 741-752.
Pavlov, A., S. Berkov, E. Courot, T. Gocheva, D. Tuneva, B. Pandova, M. Georgiev, V. Georgiev, S. Yanev and M. Burrus (2007). "Galanthamine production by Leucojum aestivum in vitro systems." Process Biochemistry **42**(4): 734-739.
Pavlov, A., S. Berkov, E. Courot, T. Gocheva, D. Tuneva, B. Pandova, M. Georgiev, V. Georgiev, S. Yanev, M. Burrus and M. Ilieva (2007). "Galanthamine production by Leucojum aestivum in vitro systems." Process Biochemistry **42**(4): 734-739.
Priyadharshini, S., N. Kannan, M. Manokari and M. S. Shekhawat (2020). "In vitro regeneration using twin scales for restoration of critically endangered aquatic plant *Crinum malabaricum* Lekhak & Yadav: a promising source of galanthamine." Plant Cell, Tissue and Organ Culture (PCTOC) **141**(3): 593-604.
Ptak, A., E. Morańska, S. Saliba, A. Zieliński, M. Simlat and D. Laurain-Mattar (2017). "Elicitation of galanthamine and lycorine biosynthesis by Leucojum aestivum L. and L. aestivum 'Gravety Giant'plants cultured in bioreactor RITA®." Plant Cell, Tissue and Organ Culture (PCTOC) **128**(2): 335-345.
Ptak, A., E. Moranska, E. Skrzypek, M. Warchol, R. Spina, D. Laurain-Mattar and M. Simlat (2020). "Carbohydrates stimulated Amaryllidaceae alkaloids biosynthesis in Leucojum aestivum L. plants cultured in RITA((R)) bioreactor." PeerJ **8**: e8688.
Ptak, A., E. Morańska, E. Skrzypek, M. Warchoł, R. Spina, D. Laurain-Mattar and M. Simlat (2020). "Carbohydrates stimulated Amaryllidaceae alkaloids biosynthesis in Leucojum aestivum L. plants cultured in RITA® bioreactor." PeerJ **8**: e8688.
Ptak, A., E. Morańska, M. Warchoł, A. Gurgul, E. Skrzypek, M. Dziurka, D. Laurain-Mattar, R. Spina, A. Jaglarz and M. Simlat (2022). "Endophytic bacteria from in vitro culture of Leucojum aestivum L. a new source of galanthamine and elicitor of alkaloid biosynthesis." Scientific Reports **12**(1): 13700.
Ptak, A., M. Simlat, E. Morańska, E. Skrzypek, M. Warchoł, A. Tarakemeh and D. Laurain-Mattar (2019). "Exogenous melatonin stimulated Amaryllidaceae alkaloid biosynthesis in in vitro cultures of Leucojum aestivum L." Industrial Crops and Products **138**: 111458.
Ptak, A., M. Simlat, E. Morańska, R. Spina, F. Dupire, S. Kozaczka and D. Laurain-Mattar (2019). "Potential of the Leucojum aestivum L. endophytic bacteria to promote Amaryllidaceae alkaloids biosynthesis." Acta Biol. Cracov **62**: 30.
Ptak, A., A. Tahchy, E. Skrzypek, T. Wójtowicz and D. Laurain-Mattar (2013). "Influence of auxins on somatic embryogenesis and alkaloid accumulation in Leucojum aestivum callus." Open life sciences **8**(6): 591-599.
Pyne, M. E., L. Narcross and V. J. Martin (2019). "Engineering plant secondary metabolism in microbial systems." Plant physiology **179**(3): 844-861.
Pyne, M. E., L. Narcross and V. J. J. Martin (2019). "Engineering Plant Secondary Metabolism in Microbial Systems." Plant Physiol **179**(3): 844-861.
Rahimi Khonakdari, M., H. Rezadoost, R. Heydari and M. H. Mirjalili (2020). "Effect of photoperiod and plant growth regulators on in vitro mass bulblet proliferation of Narcissus tazzeta L. (Amaryllidaceae), a potential source of galantamine." Plant Cell Tissue Organ Cult **142**(1): 1-13.
Rahimi Khonakdari, M., H. Rezadoost, R. Heydari and M. H. Mirjalili (2020). "Effect of photoperiod and plant growth regulators on in vitro mass bulblet proliferation of Narcissus tazzeta L. (Amaryllidaceae), a potential source of galantamine." Plant Cell Tissue Organ Cult: 1-13.
Rahimi Khonakdari, M., H. Rezadoost, R. Heydari and M. H. Mirjalili (2020). "Effect of photoperiod and plant growth regulators on in vitro mass bulblet proliferation of *Narcissus tazzeta* L. (Amaryllidaceae), a potential source of galantamine." Plant Cell Tissue Organ Culture **142**(1): 187-199.

Rahimi Khonakdari, M., H. Rezadoost, R. Heydari and M. H. Mirjalili (2020). "Effect of photoperiod and plant growth regulators on in vitro mass bulblet proliferation of Narcissus tazzeta L. (Amaryllidaceae), a potential source of galantamine." Plant Cell, Tissue and Organ Culture (PCTOC) **142**(1): 187-199.
Rahimi Khonakdari, M., H. Rezadoost, R. Heydari and M. H. Mirjalili (2020). "Effect of photoperiod and plant growth regulators on in vitro mass bulblet proliferation of Narcissus tazzeta L.(Amaryllidaceae), a potential source of galantamine." Plant Cell, Tissue and Organ Culture (PCTOC) **142**: 187-199.
Rates, S. M. K. (2001). "Plants as source of drugs." Toxicon **39**(5): 603-613.
Razay, G. and G. K. Wilcock (2008). "Galantamine in Alzheimer's disease." Expert Rev Neurother **8**(1): 9-17.
Refaat, J., M. S. Kamel, M. A. Ramadan and A. A. Ali (2012). "Crinum; an endless source of bioactive principles: a review. Part III; crinum alkaloids: Belladine-, galanthamine-, lycorenine-, tazettine-type alkaloids and other minor types." International Journal of Pharmaceutical Sciences and Research **3**(10): 3630.
Ren, Z., Y. Lin, X. Lv, J. Zhang, D. Zhang, C. Gao, Y. Wu and Y. Xia (2021). "Clonal bulblet regeneration and endophytic communities profiling of Lycoris sprengeri, an economically valuable bulbous plant of pharmaceutical and ornamental value." Scientia Horticulturae **279**: 109856.
Rodriguez, G. M., Y. Tashiro and S. Atsumi (2014). "Expanding ester biosynthesis in Escherichia coli." Nature chemical biology **10**(4): 259-265.
Roy, M., L. Liang, X. Xiao, P. Feng, M. Ye and J. Liu (2018). "Lycorine: A prospective natural lead for anticancer drug discovery." Biomed Pharmacother **107**: 615-624.
Saitou, N. and M. Nei (1987). "The neighbor-joining method: a new method for reconstructing phylogenetic trees." Molecular biology and evolution **4**(4): 406-425.
Saitou, N. and M. Nei (1987). "The neighbor-joining method: a new method for reconstructing phylogenetic trees." Mol Biol Evol **4**(4): 406-425.
Santos, A., F. Fidalgo, I. Santos and R. Salema (2002). "In vitro bulb formation of Narcissus asturiensis, a threatened species of the Amaryllidaceae." The Journal of Horticultural Science and Biotechnology **77**(2): 149-152.
Santos, A., F. Fidalgo, I. Santos and R. Salema (2015). "In vitrobulb formation ofNarcissus asturiensis, a threatened species of theAmaryllidaceae." The Journal of Horticultural Science and Biotechnology **77**(2): 149-152.
Santos, G. S., S. B. P. Sinoti, F. T. C. de Almeida, D. Silveira, L. A. Simeoni and K. K. P. Gomes-Copeland (2020). "Use of galantamine in the treatment of Alzheimer's disease and strategies to optimize its biosynthesis using the in vitro culture technique." Plant Cell, Tissue and Organ Culture (PCTOC) **143**(1): 13-29.
Satcharoen, V., N. J. McLean, S. C. Kemp, N. P. Camp and R. C. Brown (2007). "Stereocontrolled synthesis of (-)-galanthamine." Org Lett **9**(10): 1867-1869.
Sato, F. and Y. Yamada (1984). "High berberine-producing cultures of Coptis japonica cells." Phytochemistry **23**(2): 281-285.
Schumann, A., L. Torras-Claveria, S. Berkov, D. Claus, A. Gerth, J. Bastida and C. Codina (2013). "Elicitation of galanthamine production by Leucojum aestivum shoots grown in temporary immersion system." Biotechnology progress **29**(2): 311-318.
Sellés, M., S. Bergoñón, F. Viladomat, J. Bastida and C. Codina (1997). "Effect of sucrose on growth and galanthamine production in shoot-clump cultures of Narcissus confusus in liquid-shake medium." Plant cell, tissue and organ culture **49**(2): 129-136.
Shawky, E., A. H. Abou-Donia, F. A. Darwish, S. M. Toaima, S. S. Takla, N. B. Pigni and J. Bastida (2015). "HPTLC and GC/MS study of Amaryllidaceae alkaloids of two Narcissus species." Chemistry & biodiversity **12**(8): 1184-1199.

Shimomura, K., H. Sudo, H. Saga and H. Kamada (1991). "Shikonin production and secretion by hairy root cultures of Lithospermum erythrorhizon." Plant Cell Reports **10**: 282-285.
Shin, H.-S., Y.-G. Jung, H.-K. Cho, Y.-G. Park and C.-G. Cho (2014). "Total synthesis of (±)-lycorine from the endo-cycloadduct of 3, 5-dibromo-2-pyrone and (E)-β-borylstyrene." Organic letters **16**(21): 5718-5720.
Shin, H. S., Y. G. Jung, H. K. Cho, Y. G. Park and C. G. Cho (2014). "Total synthesis of (+/-)-lycorine from the endo-cycloadduct of 3,5-dibromo-2-pyrone and (E)-beta-borylstyrene." Org Lett **16**(21): 5718-5720.
Singh, A. and I. Desgagne-Penix (2015). Chapter 3 : Biosynthesis of Amaryllidaceae alkaloids: A biochemical outlook. In: Alkaloids: Biosynthesis, Biological Roles and Health benefits., Nova Science Publishers.
Singh, A. and I. Desgagne-Penix (2017). "Transcriptome and metabolome profiling of *Narcissus pseudonarcissus* 'King Alfred' reveal components of Amaryllidaceae alkaloid metabolism." Sci Rep **7**(1): 17356.
Singh, A. and I. Desgagné-Penix (2017). "Transcriptome and metabolome profiling of Narcissus pseudonarcissus 'King Alfred'reveal components of Amaryllidaceae alkaloid metabolism." Scientific reports **7**(1): 17356.
Singh, A., M.-A. Massicotte, A. Garand, L. Tousignant, V. Ouellette, G. Bérubé and I. Desgagné-Penix (2018). "Cloning and characterization of norbelladine synthase catalyzing the first committed reaction in Amaryllidaceae alkaloid biosynthesis." BMC plant biology **18**(1): 1-12.
Singh, A., M. A. Massicotte, A. Garand, L. Tousignant, V. Ouellette, G. Berube and I. Desgagne-Penix (2018). "Cloning and characterization of norbelladine synthase catalyzing the first committed reaction in Amaryllidaceae alkaloid biosynthesis." BMC Plant Biol **18**(1): 338.
Singh, N. and B. Sharma (2018). "Toxicological Effects of Berberine and Sanguinarine." Front Mol Biosci **5**: 21.
Slabbert, M., M. De Bruyn, D. Ferreira and J. Pretorius (1993). "Regeneration of bulblets from twin scales of *Crinum macowanii* in vitro." Plant cell, tissue and organ culture **33**(2): 133-141.
Slabbert, M., M. De Bruyn, D. Ferreira and J. Pretorius (1993). "Regeneration of bulblets from twin scales ofCrinum macowanii in vitro." Plant cell, tissue and organ culture **33**(2): 133-141.
Slattery, S. S., A. Diamond, H. Wang, J. A. Therrien, J. T. Lant, T. Jazey, K. Lee, Z. Klassen, I. Desgagné-Penix and B. J. Karas (2018). "An expanded plasmid-based genetic toolbox enables Cas9 genome editing and stable maintenance of synthetic pathways in Phaeodactylum tricornutum." ACS synthetic biology **7**(2): 328-338.
Slattery, S. S., A. Diamond, H. Wang, J. A. Therrien, J. T. Lant, T. Jazey, K. Lee, Z. Klassen, I. Desgagne-Penix, B. J. Karas and D. R. Edgell (2018). "An Expanded Plasmid-Based Genetic Toolbox Enables Cas9 Genome Editing and Stable Maintenance of Synthetic Pathways in Phaeodactylum tricornutum." ACS Synth Biol **7**(2): 328-338.
Sterling, T. and J. J. Irwin (2015). "ZINC 15–ligand discovery for everyone." Journal of chemical information and modeling **55**(11): 2324-2337.
Su, Y., H.-P. Li, M. Zhang, X.-W. Ding, J.-H. Xu, Q. Chen and G.-W. Zheng (2022). "Regioselectivity Inversion of an O-Methyltransferase via Semi-rational Mutagenesis Combined with Metal Ion Substitution." ChemCatChem **14**(23): e202200844.
Subrizi, F., Y. Wang, B. Thair, D. Mendez-Sanchez, R. Roddan, M. Cardenas-Fernandez, J. Siegrist, M. Richter, J. N. Andexer, J. M. Ward and H. C. Hailes (2021). "Multienzyme One-Pot Cascades Incorporating Methyltransferases for the Strategic Diversification of Tetrahydroisoquinoline Alkaloids." Angew Chem Int Ed Engl **60**(34): 18673-18679.
Sun, B., P. Wang, R. Wang, Y. Li and S. Xu (2018). "Molecular Cloning and Characterization of a meta/para-O-Methyltransferase from Lycoris aurea." Int J Mol Sci **19**(7): 1911.
Sun, B., P. Wang, R. Wang, Y. Li and S. Xu (2018). "Molecular Cloning and Characterization of a meta/para-O-Methyltransferase from Lycoris aurea." International journal of molecular sciences **19**(7): 1911.

Takos, A. M. and F. Rook (2013). "Towards a molecular understanding of the biosynthesis of amaryllidaceae alkaloids in support of their expanding medical use." Int J Mol Sci **14**(6): 11713-11741.
Tallini, L. R., E. H. Osorio, V. D. D. Santos, W. S. Borges, M. Kaiser, F. Viladomat, J. A. S. Zuanazzi and J. Bastida (2017). "*Hippeastrum reticulatum* (Amaryllidaceae): Alkaloid Profiling, Biological Activities and Molecular Docking." Molecules **22**(12): 4901.
Tallini, L. R., L. Torras-Claveria, W. S. Borges, M. Kaiser, F. Viladomat, J. A. S. Zuanazzi and J. Bastida (2018). "N-oxide alkaloids from *Crinum amabile* (Amaryllidaceae)." Molecules **23**(6): 1277.
Tamura, K., G. Stecher and S. Kumar (2021). "MEGA11: molecular evolutionary genetics analysis version 11." Molecular biology and evolution **38**(7): 3022-3027.
Tamura, K., G. Stecher and S. Kumar (2021). "MEGA11: Molecular Evolutionary Genetics Analysis Version 11." Mol Biol Evol **38**(7): 3022-3027.
Tang, M., C. Li, C. Zhang, Y. Cai, Y. Zhang, L. Yang, M. Chen, F. Zhu, Q. Li and K. Li (2023). "SWATH-MS-Based Proteomics Reveals the Regulatory Metabolism of Amaryllidaceae Alkaloids in Three *Lycoris* Species." Int J Mol Sci **24**(5).
Tang, M., C. Li, C. Zhang, Y. Cai, Y. Zhang, L. Yang, M. Chen, F. Zhu, Q. Li and K. Li (2023). "SWATH-MS-Based Proteomics Reveals the Regulatory Metabolism of Amaryllidaceae Alkaloids in Three Lycoris Species." International Journal of Molecular Sciences **24**(5): 4495.
Tarakemeh, A., M. Azizi, V. Rowshan, H. Salehi, R. Spina, F. Dupire, H. Arouie and D. Laurain-Mattar (2019). "Screening of Amaryllidaceae alkaloids in bulbs and tissue cultures of Narcissus papyraceus and four varieties of N. tazetta." Journal of Pharmaceutical and Biomedical Analysis **172**: 230-237.
Tarakemeh, A., M. Azizi, V. Rowshan, H. Salehi, R. Spina, F. Dupire, H. Arouie and D. Laurain-Mattar (2019). "Screening of Amaryllidaceae alkaloids in bulbs and tissue cultures of Narcissus papyraceus and four varieties of N. tazetta." J Pharm Biomed Anal **172**: 230-237.
Taylor-Teeples, M., L. Lin, M. de Lucas, G. Turco, T. W. Toal, A. Gaudinier, N. F. Young, G. M. Trabucco, M. T. Veling, R. Lamothe, P. P. Handakumbura, G. Xiong, C. Wang, J. Corwin, A. Tsoukalas, L. Zhang, D. Ware, M. Pauly, D. J. Kliebenstein, K. Dehesh, I. Tagkopoulos, G. Breton, J. L. Pruneda-Paz, S. E. Ahnert, S. A. Kay, S. P. Hazen and S. M. Brady (2015). "An *Arabidopsis* gene regulatory network for secondary cell wall synthesis." Nature **517**(7536): 571-575.
Torras-Claveria, L., S. Berkov, C. Codina, F. Viladomat and J. Bastida (2014). "Metabolomic analysis of bioactive Amaryllidaceae alkaloids of ornamental varieties of Narcissus by GC–MS combined with k-means cluster analysis." Industrial Crops and Products **56**: 211-222.
Tousignant, L., A. M. Diaz-Garza, B. B. Majhi, S.-E. Gélinas, A. Singh and I. Desgagne-Penix (2022). "Transcriptome analysis of Leucojum aestivum and identification of genes involved in norbelladine biosynthesis." Planta **255**(2): 1-23.
Tousignant, L., A. M. Diaz-Garza, B. B. Majhi, S.-E. Gélinas, A. Singh and I. Desgagne-Penix (2022). "Transcriptome analysis of Leucojum aestivum and identification of genes involved in norbelladine biosynthesis." Planta **255**(2): 30.
Tousignant, L., A. M. Diaz-Garza, B. B. Majhi, S. E. Gelinas, A. Singh and I. Desgagne-Penix (2022). "Transcriptome analysis of *Leucojum aestivum* and identification of genes involved in norbelladine biosynthesis." Planta **255**(2): 30.
Trost, B. M. and W. Tang (2002). "An efficient enantioselective synthesis of (-)-galanthamine." Angew Chem Int Ed Engl **41**(15): 2795-2797.
Trujillo-Chacon, L. M., E. R. Pastene-Navarrete, L. Bustamante, M. Baeza, J. E. Alarcon-Enos and C. L. Cespedes-Acuna (2020). "In vitro micropropagation and alkaloids analysis by GC-MS of Chilean Amaryllidaceae plants: *Rhodophiala pratensis*." Phytochem Anal **31**(1): 46-56.
Trujillo-Chacón, L. M., E. R. Pastene-Navarrete, L. Bustamante, M. Baeza, J. E. Alarcón-Enos and C. L. Cespedes-Acuña (2020). "In vitro micropropagation and alkaloids analysis by GC–MS of Chilean Amaryllidaceae plants: Rhodophiala pratensis." Phytochemical Analysis **31**(1): 46-56.

Trujillo Chacón, L. M., H. Leiva, I. C. Zapata Vahos, D. C. Restrepo and E. Osorio (2023). "Influence of plant growth regulators on in vitro biomass production and biosynthesis of cytotoxic Amaryllidaceae alkaloids in *Caliphuria tenera* Baker." Biocatalysis and Agricultural Biotechnology **50**: 102670.
Tsao, D., L. Diatchenko and N. V. Dokholyan (2011). "Structural mechanism of S-adenosyl methionine binding to catechol O-methyltransferase." PLoS One **6**(8): e24287.
Tsvetkova, D., D. Obreshkova, D. Zheleva-Dimitrova and L. Saso (2013). "Antioxidant activity of galantamine and some of its derivatives." Curr Med Chem **20**(36): 4595-4608.
Tu, Y. (2016). "Nobel lecture: Artemisinin—a gift from traditional Chinese medicine to the world." Angew. Chem. Int. Ed. Engl **55**(35): 10210-10226.
Velten, R., C. Erdelen, M. Gehling, A. Göhrt, D. Gondol, J. Lenz, O. Lockhoff, U. Wachendorff and D. Wendisch (1998). "Cripowellin A and B, a novel type of Amaryllidaceae alkaloid from Crinum powellii." Tetrahedron Letters **39**(13): 1737-1740.
Waki, T., S. Takahashi and T. Nakayama (2021). "Managing enzyme promiscuity in plant specialized metabolism: A lesson from flavonoid biosynthesis: Mission of a “body double” protein clarified." BioEssays **43**(3): 2000164.
Wang, R., S. Xu, N. Wang, B. Xia, Y. Jiang and R. Wang (2016). "Transcriptome Analysis of Secondary Metabolism Pathway, Transcription Factors, and Transporters in Response to Methyl Jasmonate in *Lycoris aurea*." Front Plant Sci **7**: 1971.
Wang, R., S. Xu, N. Wang, B. Xia, Y. Jiang and R. Wang (2017). "Transcriptome analysis of secondary metabolism pathway, transcription factors, and transporters in response to methyl jasmonate in Lycoris aurea." Frontiers in plant science **7**: 1971.
Wang, S., S. Alseekh, A. R. Fernie and J. Luo (2019). "The structure and function of major plant metabolite modifications." Molecular Plant **12**(7): 899-919.
Wang, W. and Z.-D. Chen (2007). "Generic level phylogeny of Thalictroideae (Ranunculaceae) - implications for the taxonomic status of *Paropyrum* and petal evolution." Taxon **56**(3): 811-821.
Wink, M. (2008). Ecological roles of alkaloids, Wiley Online Library**:** 3-52.
Wink, M. (2011). Annual plant reviews, biochemistry of plant secondary metabolism, John Wiley & Sons.
Winkel-Shirley, B. (2001). "Flavonoid biosynthesis. A colorful model for genetics, biochemistry, cell biology, and biotechnology." Plant Physiol **126**(2): 485-493.
Winkel-Shirley, B. (2001). "Flavonoid biosynthesis. A colorful model for genetics, biochemistry, cell biology, and biotechnology." Plant physiology **126**(2): 485-493.
Woodard, R. W., M. D. Tsai, H. G. Floss, P. A. Crooks and J. K. Coward (1980). "Stereochemical course of the transmethylation catalyzed by catechol O-methyltransferase." J Biol Chem **255**(19): 9124-9127.
Woodward, A. W. and B. Bartel (2005). "Auxin: regulation, action, and interaction." Ann Bot **95**(5): 707-735.
Woodward, A. W. and B. Bartel (2005). "Auxin: regulation, action, and interaction." Annals of botany **95**(5): 707-735.
Xiao, M., Y. Zhang, X. Chen, E. J. Lee, C. J. Barber, R. Chakrabarty, I. Desgagne-Penix, T. M. Haslam, Y. B. Kim, E. Liu, G. MacNevin, S. Masada-Atsumi, D. W. Reed, J. M. Stout, P. Zerbe, Y. Zhang, J. Bohlmann, P. S. Covello, V. De Luca, J. E. Page, D. K. Ro, V. J. Martin, P. J. Facchini and C. W. Sensen (2013). "Transcriptome analysis based on next-generation sequencing of non-model plants producing specialized metabolites of biotechnological interest." J Biotechnol **166**(3): 122-134.
Xu, J., Q. Li, L. Yang, X. Li, Z. Wang and Y. Zhang (2020). "Changes in carbohydrate metabolism and endogenous hormone regulation during bulblet initiation and development in *Lycoris radiata*." BMC Plant Biol **20**(1): 180.
Xu, P., N. Bhan and M. A. Koffas (2013). "Engineering plant metabolism into microbes: from systems biology to synthetic biology." Current opinion in biotechnology **24**(2): 291-299.

Yamada, K., M. Yamashita, T. Sumiyoshi, K. Nishimura and K. Tomioka (2009). "Total synthesis of (-)-lycorine and (-)-2-epi-lycorine by asymmetric conjugate addition cascade." Org Lett **11**(7): 1631-1633.
Yoda, H., Y. Yamaguchi and H. Sano (2003). "Induction of hypersensitive cell death by hydrogen peroxide produced through polyamine degradation in tobacco plants." Plant Physiology **132**(4): 1973-1981.
Zhan, J., D. Thakare, C. Ma, A. Lloyd, N. M. Nixon, A. M. Arakaki, W. J. Burnett, K. O. Logan, D. Wang, X. Wang, G. N. Drews and R. Yadegari (2015). "RNA sequencing of laser-capture microdissected compartments of the maize kernel identifies regulatory modules associated with endosperm cell differentiation." Plant Cell **27**(3): 513-531.
Zhou, J., Z. Liu, S. Wang, J. Li, Y. Li, W. K. Chen and R. Wang (2020). "Fungal endophytes promote the accumulation of Amaryllidaceae alkaloids in Lycoris radiata." Environ Microbiol **22**(4): 1421-1434.
Zhou, J., Z. Liu, S. Wang, J. Li, Y. Li, W. K. Chen and R. Wang (2020). "Fungal endophytes promote the accumulation of Amaryllidaceae alkaloids in Lycoris radiata." Environmental Microbiology.
Zuckerkandl, E. and L. Pauling (1965). Evolutionary divergence and convergence in proteins. Evolving genes and proteins, Elsevier**:** 97-166.

ANNEX B

Supplementary data for CHAPTER II

Annex B Table S1 Fragmentation pattern of detected Amaryllidaceae alkaloids. Amaryllidaceae alkaloids were identified by comparison with the 2005 National Institute of Standards (NIST) database.

* Indicates the small peaks that suffer more interference from the background, thus leading to poor matches with the databank. The peak number corresponds to Fig. S2.

Amaryllidaceae Alkaloid	Retention time	Peak number	M+	Fragmentation pattern	Match Percentage
Crinan-3-ol, 1,2-didehydro(3-alpha)	22.02	**1**	271	271, 254, 242, 228, 214, 199, 187	90-99%
Crinan-3-ol, 1,2-didehydro(3-beta)	22.30	**2**	271	271, 254, 242, 228, 214, 199, 187	98-99%
Cherylline	23.25	**3**	285	285, 242, 241, 225, 211, 181	97-99%
Crinine acetate	23.33	**4**	313	313, 270, 254, 225, 216	92-99%
Powelline	24.73	**5**	301	301, 284, 272, 258, 229, 217, 203, 190	98-99%
Epipowelline	24.92	**6**	301	301, 284, 272, 258, 229, 217, 203, 190	90%
Lycorine O-acetyl	25.49	**7**	329	329, 268, 250, 248, 227, 226, 207	97%
Lycorine	26.06	**8**	287	287, 286, 268, 250, 227, 226, 147	70*-98%
Crinamidine	27.27	**9**	317	317, 288, 272, 258, 244, 230, 217, 203, 189, 173	94-99%

Annex Table S2. MRM transitions and instrumental parameters used in ESI+ for HPLC MS/MS identifications.

Compound name	Retention time (min)	Precursor (m/z)	Product (m/z)	Fragmentor (V)	Collision energy (V)	Polarity
3'-O-methylnorbelladine	17.0	274	**137**	105	18	Positive
			121		15	
			109		40	
4'-O-methylnorbelladine	15.9	274	**137**	105	18	Positive
			122		40	
			94		40	
3',4'-O-dimethylnorbelladine	16.8	288	**151**	100	10	Positive
			135		40	
			107		40	
Caffeic acid	18.4	181	**163**	76	5	Positive
			135		10	
			117		21	
Cherylline	7.6	286	**243**	103	18	Positive
			165		40	
			137		18	
Coclaurine	16.2	286	269	115	14	Positive
			175		20	
			107		30	
Dopamine	3.3	154	**137**	78	10	Positive
			119		18	
			91		26	
Ferulic acid	19.6	195	**177**	81	5	Positive
			145		20	
			117		21	

			270		14	
Galanthamine	4.8	288	225	120	18	Positive
			213		22	
			257		20	
Gigantelline	15.6	300	194	135	20	Positive
			107		40	
			273		20	
Gigantellinine	13.5	316	192	135	20	Positive
			137		20	
			177		5	
Isoferulic acid	19.8	195	145	81	20	Positive
			117		21	
			151		10	
Isovanillic acid	18.4	169	125	81	5	Positive
			93		9	
			125		10	
Isovanillin	18.6	153	**93**	86	13	Positive
			65		25	
			181		10	
Levodopa	3.9	198	**152**	78	10	Positive
			139		14	
			165		10	
L-Tyrosine	4.4	182	**136**	83	10	Positive
			123		14	
			233		20	
Lycoramine	5.0	290	215	99	20	Positive
			189		24	
Lycorine	4.0	288	270	92	20	Positive

			177		20	
			147		28	
			119		40	
			248		28	
Narciclasine	18.4	308	218	82	36	Positive
			202		40	
			138		5	
Norbelladine	7.6	260	123	86	20	Positive
			121		17	
			231		14	
Norgalanthamine	4.4	274	**213**	115	18	Positive
			198		40	
			324		40	
Papaverine	18.0	340	**202**	165	27	Positive
			171		40	
			147		5	
p-coumaric acid	19.4	165	119	76	17	Positive
			91		20	
			121		5	
Tyramine	3.5	138	91	81	20	Positive
			77		20	
			125		10	
Vanillin	18.8	153	**93**	86	13	Positive
			65		25	

Notes: Quantifier ion for each compound is bold and qualifier ions are not.

Annex B Table S3 Type of tissue generated from 6 months old in vitro culture of *C.* x *powellii* **"Album"**.

Auxin type and concentration		**Time of callus initiation**		**Type of tissue generation in 6 months**	
		Light	**Dark**	**Light**	**Dark**
Without Auxin		n.r.	n.r.	Direct organogenesis (Shoot formation)	Direct organogenesis (Shoot formation)
2,4-D	**2 mg/L**	3 weeks	4 weeks	Brownish callus	White callus
	4 mg/L	3 weeks	4 weeks	Brownish callus	White callus
	8 mg/L	3 weeks	3 weeks	Brownish callus	White callus
NAA	**2mg/L**	6 weeks	6 weeks	Indirect organogenesis	Indirect organogenesis
	4 mg/L	6 weeks	4 weeks	Indirect organogenesis	Indirect organogenesis
	8 mg/L	5 weeks	4 weeks	Indirect organogenesis,	White compact callus

n.r.: not recorded during this study.

ANNEX B Table S4 Summary of the Illumina sequencing output, assembly, and annotation overview of *C.* x *powellii* "Album" transcriptome

Sequencing statistics	
Raw paired-end reads	1240830608
Clean paired-end reads	1162489247
Trinity assembly statistics	
Total Trinity gene	785475
Total Trinity transcript	1261988
Percent GC	38.48
Contig N50	1033
Median contig length	364
Average contig length	658.03
Total assembled bases	830422829
Annotation statistics	
Complete and single BUSCOs	335
Complete and duplicated BUSCOs	1128
Fragmented BUSCOs	120
Missing BUSCOs	31
Predicted ORFs	222357
ORFs annotated with UniProt SwissProt	133843
ORFs annotated with Pfam	36423

ANNEX Table S5 Summary of the biosynthetic genes identified from the C. x powellii "Album" transcriptome proposed to be involved in Amaryllidaceae alkaloids metabolism. TPM: normalized transcript per million, ORF: the size of the open reading frame in nucleotide (nt), and the corresponding top annotation.

Accession number	Name	Enzyme name	ORF type	Protein length	Gene ID	Species of top annotation (identity %)	Hit accession number	hit length	E-value	TPM (Dark + 2mg/L 2,4-D)	TPM (Dark + 4mg/L 2,4-D)	TPM (Light + 2mg/L 2,4-D)	TPM (Light + 4mg/L 2,4-D)
OQ910111	CpDAHPS1	3-deoxy-D-arabino-heptulosenate 7-phosphate synthase 1	Complete	524	Crpow_TRINITY_DN9954_c0_g1_i5	*Leucojum aestivum* (93.99%)	NP_001320125.1	1575	0	97.365	94.683	83.03	89.253
OQ910114	CpDAHPS2	3-deoxy-D-arabino-heptulosenate 7-phosphate synthase 2	Partial	517	Crpow_TRINITY_DN4592_c0_g1_i10	*L. aestivum* (89.96%)	NP_001320125.1	1554	0	16.34	28.453	160.0767	160.73
OQ910112	CpDAHPS3	3-deoxy-D-arabino-heptulosenate 7-phosphate synthase 3	Partial	343	Crpow_TRINITY_DN47353_c0_g1_i9	*L. aestivum* (92.23 %)	NP_001320125.1	1029	0	32.815	27.61667	17.09333	13.276
OQ910113	CpDHQS	3-dehydroquinate synthase	Partial	359	Crpow_TRINITY_DN10377_c0_g1_i1	*L. aestivum* (93.31 %)	NP_851279.1	1080	0	34	37.89667	53.03667	43.97
OQ910115	CpDHQSD1	Bifunctional 3-dehydroquinate dehydratase / Shikmate dehydrogenase 1	Complete	517	Crpow_TRINITY_DN1150_c0_g1_i16	*L. aestivum* (90.70%)	Q9SQT8.1	1554	0	34.6	33.74	28.3	25.243
OQ910117	CpDHQSD2	Bifunctional 3-dehydroquinate dehydratase / Shikmate dehydrogenase 2	Partial	131	Crpow_TRINITY_DN263748_c0_g2_i2	*L. aestivum* (71.76%)	Q9SQT8.1	396	1E-53	0.8	1.05	0.4566667	0.476
OQ910118	CpDHQSD3	Bifunctional 3-dehydroquinate dehydratase / Shikmate dehydrogenase 3	Partial	148	Crpow_TRINITY_DN65706_c1_g2_i1	*L. aestivum* (63.27%)	Q9SQT8.1	447	3E-19	0.37	0.09	0.093333	0.12
OQ927593	CpDHQSD4	Bifunctional 3-dehydroquinate dehydratase / Shikmate dehydrogenase 4	Partial	120	Crpow_TRINITY_DN34849_c0_g2_i2	*L. aestivum* (80.99%)	Q9SQT8.1	363	1E-58	2.28	1.513	1.386667	1.053
OQ910116	CpSK1	Shikimate Kinase 1	Complete	272	Crpow_TRINITY_DN2369_c0_g2_i2	*Elaeis guineensis* (62.71%)	XP_020274085.1	819	4E-118	5.41	4.57	8.743333	3.763
OQ910120	CpSK2	Shikimate Kinase 2	Complete	304	Crpow_TRINITY_DN7524_c0_g1_i5	*L. aestivum* (85.02%)	XP_020274085.1	915	0	15.13	15.897	18.11333	32.383
OQ910119	CpSK3	Shikimate Kinase 3	Partial	120	Crpow_TRINITY_DN10558_c0_g2_i2	*L. aestivum* (75.21%)	XP_020274085.1	360	8E-43	9.61	8.15	8.996667	9.423
OQ922005	CpEPSPS1	5-enolpyruvylshikimate 3-phosphate synthase 1	Complete	258	Crpow_TRINITY_DN5528_c1_g1_i3	*Liriope muscari* (94.42%)	AAG29739.1	777	5E-165	26.68	31.06333	79.43667	69.316
OQ910400	CpEPSPS2	5-enolpyruvylshikimate 3-phosphate synthase 2	Partial	192	Crpow_TRINITY_DN5451_c1_g1_i1	*L. aestivum* (76.92%)	AAG29739.1	492	1E-60	9.97	9.847	43.79	13.91
OQ910401	CpEPSPS3	5-enolpyruvylshikimate 3-phosphate synthase 3	Partial	112	Crpow_TRINITY_DN18590_c0_g1_i1	*L. aestivum* (97.25%)	AAG29739.1	336	2E-57	45.395	51.84	130.33	99.116
OQ916433	CpCS1	Chorismate synthase 1	Complete	459	Crpow_TRINITY_DN8367_c0_g1_i9	*L. aestivum* (92.25)	UIP35195.1	1380	0	66.195	76.04667	147.2633	100.366

OQ92759 CpCS2 8	Chorismate synthase 2	Partial	92	Crpow_TRINITY_DN293545_c0_g1_i1	*Cannabis sativa* (100%)	UIP35195.1	354	2E-77	0	0	0	0
OQ92759 CpCS3 7	Chorismate synthase 3	Partial	108	Crpow_TRINITY_DN59551_c4_g1_i1	*L. aestivum* (97.25%)	UIP35195.1	327	1E-45	0.18	0.493	1.576667	0.8833
OQ91646 CpCM1 1	Chorismate mutase 1	Complete	308	Crpow_TRINITY_DN3317_c0_g1_i11	*L. aestivum* (85.02%)	AEE77552.1	927	4E-180	14.775	17.37333	37.3933	52.36
OQ91646 CpCM2 2	Chorismate mutase 2	Complete	302	Crpow_TRINITY_DN45018_c0_g2_i1	*Asparagus officinalis* (74.06%)	AEE77552.1	885	4E-134	0.035	0.073	1.926667	0.8
OQ91646 CpCM3 3	Chorismate mutase 3	Complete	257	Crpow_TRINITY_DN13568_c1_g1_i2	*A. officinalis* (76.17%)	AEE77552.1	804	5E-121	24.155	25.593	13.8233	25.273
OQ91646 CpPAT 4	Bifunctional aspartate aminotransferase and glutamate/aspartate-prephenate aminotransferase	Complete	451	Crpow_TRINITY_DN15922_c0_g2_i2	*L. aestivum* (93.26%)	Q9SIE1.2	1356	0	17.785	20.41	38.68	40.04
OQ91646 CpADT1 5	Arogenate dehydratase/prephenate dehydratase 1	Complete	398	Crpow_TRINITY_DN11824_c0_g1_i6	*Musa acuminata* subsp. *Malaccenasis* (59.3%)	NP_974249.1	1197	3E-122	6.305	9.483	21.05667	90.13
OQ92333 CpADT2 5	Arogenate dehydratase/prephenate dehydratase 2	Complete	413	Crpow_TRINITY_DN12332_c1_g1_i1	*L. aestivum* (89.95 %)	NP_974249.1	1242	0	8.155	10.933	18.82333	21.67667
OQ92338 CpADT3 0	Arogenate dehydratase/prephenate dehydratase 3	Complete	413	Crpow_TRINITY_DN508783_c0_g1_i1	*L. aestivum* (89.95 %)	NP_974249.1	1242	0	0.28	0.223	0.2066667	0.526
OQ92333 CpADT4 6	Arogenate dehydratase/prephenate dehydratase 4	Complete	394	Crpow_TRINITY_DN7430_c0_g1_i2	*L. aestivum* (83.80%)	NP_974249.1	1185	0	11.54	11.606	7.91	8.22
OQ92337 CpADT5 9	Arogenate dehydratase/prephenate dehydratase 5	Partial	319	Crpow_TRINITY_DN77611_c0_g1_i1	*L. aestivum* (77.75 %)	NP_974249.1	1113	5E-173	0.22	0.26	0.1633333	0.18
OQ92759 CpADT6 5	Arogenate dehydratase/prephenate dehydratase 6	Complete	384	Crpow_TRINITY_DN39483_c0_g1_i8	*L. aestivum* (87.50%)	NP_974249.1	1155	0	11.37	12.027	15.29	11.416
OQ92333 CpADH1 7	Arogenate dehydrogenase 1	Complete	397	Crpow_TRINITY_DN4640_c0_g1_i10	*L. aestivum* (86.65%)	NP_198343.1	1194	0	3.29	3.577	4.403333	15.426
OQ92333 CpADH2 8	Arogenate dehydrogenase 2	Complete	265	Crpow_TRINITY_DN781_c3_g1_i9	*A. officinalis* (72.31%)	NP_198343.1	798	3E-124	4.685	3.703	2.776667	2.59
OQ92759 CpADH3 2	Arogenate dehydrogenase 3	Complete	327	Crpow_TRINITY_DN2612_c0_g1_i3	*L. aestivum* (83.59%)	NP_198343.1	984	0	8.97	9.996	6.68	6.543
OQ92333 CpPAL1 9	Phenylalanine ammonia lyase 1	Complete	712	Crpow_TRINITY_DN3203_c0_g1_i1	*L. aestivum* (92.42%)	AAC18871.1	2139	0	2.48	5.103	34.18333	40.886
OQ92334 CpPAL2 0	Phenylalanine ammonia lyase 2	Complete	499	Crpow_TRINITY_DN1223_c0_g1_i1	*L. radiata* (96.59%)	AAC18871.1	1674	0	2.23	1.82	0.7033333	1.403
OQ92334 CpPAL3 1	Phenylalanine ammonia lyase 3	Partial	212	Crpow_TRINITY_DN35605_c0_g1_i2	*L. aestivum* (89.67%)	AAC18871.1	639	2E-118	1.415	3.73	20.78667	50.976
OQ92334 CpPAL4 2	Phenylalanine ammonia lyase 4	Partial	136	Crpow_TRINITY_DN309920_c0_g1_i1	*C. sativa* (100%)	AAC18871.1	411	2E-118	0	0	0	0
OQ92334 CpPAL5 3	Phenylalanine ammonia lyase 5	Partial	139	Crpow_TRINITY_DN27471_c0_g2_i10	*Lycoris radiata* (88.96%)	AAC18871.1	489	3E-86	1.805	4.303	31.51	34.513

OQ92334 9	CpPAL6	Phenylalanine ammonia lyase 6	Partial	79	Crpow_TRINITY_DN30843_c0_g1_i1	*L. aestivum* (92.08%)	AAC18871.1	303	2E-57	0.455	1.256	3.68	28.056
OQ92335 6	CpC4H	Cinnamate-4-hydroxylase/Trans-cinnamic acid 4-monooxygenase	Complete	518	Crpow_TRINITY_DN3006_c0_g1_i22	*L. Longituba* (95.45%)	P92994.1	1518	0	50.32	91.89	254.25	407.16
OQ92335 8	CpC3H	p-coumarate 3-hydroxylase	Complete	509	Crpow_TRINITY_DN5118_c1_g2_i3	*L. aestivum* (92.24%)	Q9CA61.1	1530	0	44.545	63.473	111.28	145.15
OQ92334 6	Cp4CL1	4-coumarate:CoA ligase 1	Complete	524	Crpow_TRINITY_DN8201_c0_g2_i3	*Albuca bracteata* (79.77%)	QJD21997.1	1575	0	36.835	38.67	117.2867	87.77
OQ92335 2	Cp4CL10	4-coumarate:CoA ligase 10	Complete	442	Crpow_TRINITY_DN29724_c0_g1_i12	*N. papyraceus* (87.27%)	QJD21997.1	1626	0	7.77	7.263	13.19333	6.693
OQ92335 7	Cp4CL11	4-coumarate:CoA ligase 11	Partial	547	Crpow_TRINITY_DN29253_c0_g1_i5	*E. guineensis* (60.07%)	QJD21997.1	1644	0	1.12	1.266	0.49	0.526
OQ92335 5	Cp4CL12	4-coumarate:CoA ligase 12	Partial	559	Crpow_TRINITY_DN8984_c0_g1_i10	*L. aestivum* (62.90%)	QJD21997.1	1689	0	0.24	0.176	5.953333	0.263
OQ92338 2	Cp4CL13	4-coumarate:CoA ligase 13	Partial	268	Crpow_TRINITY_DN14588_c3_g1_i1	*N. pseudonarcissus* (83.03%)	QJD21997.1	1011	1E-158	0.045	0	0.03	0.006
OQ92338 1	Cp4CL14	4-coumarate:CoA ligase 14	Partial	101	Crpow_TRINITY_DN8463_c0_g2_i1	*N. pseudonarcissus* (88.83%)	QJD21997.1	1644	0	13.44	22.906	69.49	103.16
OQ92759 6	Cp4CL15	4-coumarate:CoA ligase 15	Partial	101	Crpow_TRINITY_DN8463_c0_g2_i1	*N. pseudonarcissus* (83.03%)	QJD21997.1	441	1E-80	0	0.046	0.1033333	0.183
OQ92334 7	Cp4CL2.1	4-coumarate:CoA ligase 2.1	Complete	548	Crpow_TRINITY_DN43473_c0_g1_i48	*A. officinalis* (81.18%)	QJD21997.1	1422	0	5.07	4.296	3.59	3.706
OQ92723 4	Cp4CL2.2	4-coumarate:CoA ligase 2.2	Complete	473	Crpow_TRINITY_DN43473_c0_g1_i41	*A. officinalis* (80.41%)	QJD21997.1	1647	0	5.07	4.296	3.59	3.706
OQ92334 4	Cp4CL3	4-coumarate:CoA ligase 3	Complete	571	Crpow_TRINITY_DN5837_c0_g1_i8	*N. pseudonarcissus* (83.63%)	QJD21997.1	1716	0	0.41	0.293	21.32333	14.796
OQ92334 5	Cp4CL4	4-coumarate:CoA ligase 4	Complete	542	Crpow_TRINITY_DN44337_c0_g1_i7	*L. aestivum* (87.38%)	QJD21997.1	1716	0	24.94	29.933	43.06	27.876
OQ92723 5	Cp4CL5.1	4-coumarate:CoA ligase 5.1	Complete	460	Crpow_TRINITY_DN9241_c0_g1_i1	*N. papyraceus* (82.06%)	QJD21997.1	1623	0	5.835	7.553	32.70333	25.93
OQ92335 0	Cp4CL5.2	4-coumarate:CoA ligase 5.2	Complete	540	Crpow_TRINITY_DN9241_c0_g1_i4	*N. papyraceus* (81.35%)	QJD21997.1	1383	0	5.835	7.553	32.70333	25.93
OQ92334 8	Cp4CL6	4-coumarate:CoA ligase 6	Complete	551	Crpow_TRINITY_DN1304_c0_g1_i18	*A. officinalis* (72.33%)	QJD21997.1	1656	0	2	1.58	1.03	1.416
OQ92335 1	Cp4CL7	4-coumarate:CoA ligase 7	Complete	536	Crpow_TRINITY_DN34817_c1_g1_i2	*L. aestivum* (89.81%)	QJD21997.1	1611	0	0.07	0.02	0.7666667	0.0466
OQ92335 3	Cp4CL8	4-coumarate:CoA ligase 8	Complete	562	Crpow_TRINITY_DN17876_c0_g2_i5	*L. aestivum* (80.93%)	QJD21997.1	1689	0	2.57	3.793	24.44	7.396
OQ92335 4	Cp4CL9	4-coumarate:CoA ligase 9	Complete	557	Crpow_TRINITY_DN4818_c1_g1_i6	*L. aestivum* (76.95%)	QJD21997.1	1674	0	1.93	1.346	11.33333	10.573

OQ92335 9	CpHCT1	Hydroxycinnamoyltransferase 1	Complete	436	Crpow_TRINITY_DN10631_c0_g1_i2	*L. aestivum* (90.83%)	OAO91238.1	1311	0	32.505	34.72	223.5367	163.746
OQ92336 0	CpHCT2	Hydroxycinnamoyltransferase 2	Complete	429	Crpow_TRINITY_DN28118_c0_g1_i2	*L. aestivum* (84.38%)	OAO91238.1	1290	0	31.6	23.113	14.33667	20.71
OQ92338 3	CpHCT3	Hydroxycinnamoyltransferase 3	Partial	215	Crpow_TRINITY_DN38312_c0_g1_i3	*L. aestivum* (91.63%)	OAO91238.1	424	6E-146	0.13	0.156	0.5533333	0.546
OQ92336 2	CpCSE1	Caffeoyl shikimate esterase 1	Complete	345	Crpow_TRINITY_DN35324_c0_g2_i20	*L. aestivum* (78.07%)	Q9C942.1	905	7E-180	0.035	0.036	0	0.023
OQ92336 4	CpCSE2	Caffeoyl shikimate esterase 2	Complete	377	Crpow_TRINITY_DN5356_c0_g1_i6	*A. officinalis* (86.13%)	Q9C942.1	1134	0	9.36	9.44	14.2333	9.463
OQ92336 5	CpCSE3	Caffeoyl shikimate esterase 3	Complete	329	Crpow_TRINITY_DN8238_c2_g2_i1	*L. aestivum* (73.07%)	Q9C942.1	990	8E-172	1.955	3.01	2.643333	1.993
OQ92336 6	CpCSE4	Caffeoyl shikimate esterase 4	Complete	347	Crpow_TRINITY_DN17256_c0_g1_i6	*L. aestivum* (89.28%)	Q9C942.1	1044	0	0.625	0.47	1.543333	0.59
OQ92336 1	CpCSE5	Caffeoyl shikimate esterase 5	Partial	326	Crpow_TRINITY_DN8687_c0_g1_i3	*L. aestivum* (87.73%)	Q9C942.1	1086	0	18.6	31.59	80.71667	95.136
OQ92759 4	CpCSE6	Caffeoyl shikimate esterase 6	Complete	345	Crpow_TRINITY_DN1629_c0_g2_i1	*L. aestivum* (88.70%)	Q9C942.1	1038	0	14.68	19.59	56.69667	36.016
OQ92336 3	CpAPX1	L-ascorbate peroxidase 1	Complete	290	Crpow_TRINITY_DN979_c0_g1_i4	*A. officinalis* (88.28%)	CAA66926.1	873	1E-171	77.705	80.473	195.05	97.336
OQ92336 7	CpAPX2	L-ascorbate peroxidase 2	Complete	251	Crpow_TRINITY_DN9047_c0_g1_i2	*Ananas comosus* (93.98%)	CAA66926.1	756	2E-149	165.8	193.667	275.0667	279.296
OQ92337 1	CpAPX3	L-ascorbate peroxidase 3	Partial	262	Crpow_TRINITY_DN524155_c0_g1_i1	*C. sativa* (100%)	CAA66926.1	789	0	0	0	0	0
OQ92336 8	CpTYDC 1	Tyrosine decarboxylase 1	Complete	518	Crpow_TRINITY_DN9870_c0_g1_i17	*N. pseudonarcissus* (87.62)	CAB56038.1	1557	0	3.655	15.043	26.523	140.84
OQ92337 0	CpTYDC 2	Tyrosine decarboxylase 2	Complete	500	Crpow_TRINITY_DN6933_c0_g1_i7	*N. pseudonarcissus* (90.80%)	CAB56038.1	1503	0	14.675	15.947	17.086	13.216
OQ92336 9	CpNBS1	Norbelladine synthase 1	Complete	155	Crpow_TRINITY_DN124400_c0_g1_i1	*L. aestivum* (71.61)	AYV96792.1	468	2E-64	0	0.006	0.27	0.013
OQ92337 2	CpNBS2	Norbelladine synthase 2	Partial	164	Crpow_TRINITY_DN163871_c0_g1_i1	*L. aestivum* (77.07%)	AYV96792.1	507	2E-61	0.11	0.166	0.05	0.476
OQ92337 4	CpN4OM T	Norbelladine 4'-O-methyl transferase	Complete	239	Crpow_TRINITY_DN7096_c1_g1_i9	*Zephyranthes bifida* subsp. *bifidal* (84.94)	A0A077EWA5.1	720	2E-141	139.03	198.95	687.54	752.626
OQ92337 3	CpNoroSyn1	Noroxomaritidine synthase 1	Complete	545	Crpow_TRINITY_DN11074_c0_g1_i12	*N.* aff. *pseudonarcissus* (71.93%)	AUG71943.1	1638	0	0.16	0.073	1.713	0.07
OQ92337 5	CpNoroSyn2	Noroxomaritidine synthase 2	Complete	417	Crpow_TRINITY_DN2907_c0_g1_i1	*N.* aff. *pseudonarcissus* (71.93%)	AUG71943.1	1140	0	0.17	0.063	6.97	0.323
OQ92337 6	CpNoroRed1	Noroxomaritidine/norcraugsodine reductase 1	Complete	276	Crpow_TRINITY_DN2246_c1_g1_i4	*L. radiata* (71.15%)	AUG71944.1	831	3E-131	15.205	18.766	34.76	19.71
OQ92337 7	CpNoroRed2	Noroxomaritidine/norcraugsodine reductase 2	Complete	259	Crpow_TRINITY_DN4979_c0_g1_i6	*N.* aff. *pseudonarci*	AUG71944.1	831	2E-142	65.435	61.246	84.10667	101.9267

						ssus (79.46%)								
OQ923378	CpNoroRed3	Noroxomaritidine/norcraugsodine reductase 3	Partial	2530	Crpow_TRINITY_DN14426_c0_g1_i3	*Leucojum aestivum* (83.47%)	AUG71944.1	756	9E-155	105.515	77.426	102.7233	125.82
KT985905.1	CpV11H	vittatine 11-hydroxylase	complete	4030	Crpow_TRINITY_DN41936_c0_g2_i15	*Galanthus* sp. MBK-2015 (72.34%)	APD78401.1	1209	4.00E-169	120.52	108.2	128.83	145.82

Note: ANNEX Table S5 was provided as a Excel file in manuscript

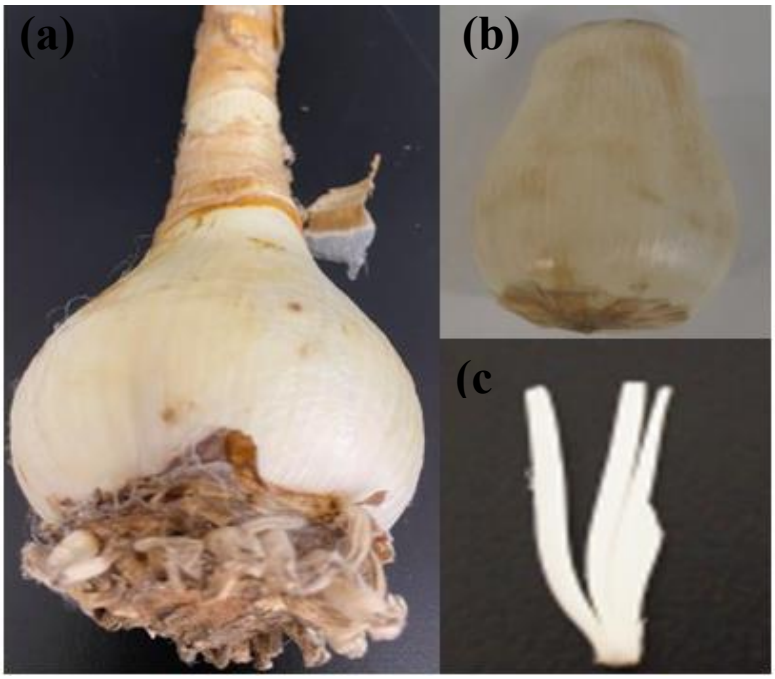

Annex Fig. S1 Explant preparation for in vitro culture of *C.* x *powellii* "Album". (**a**) Bulb of *C.* x *powellii* "Album" after cold and heat treatment. (**b**) Surface sterilized bulb. (**c**) Twin scale size explant extracted from the innermost part of the bulb.

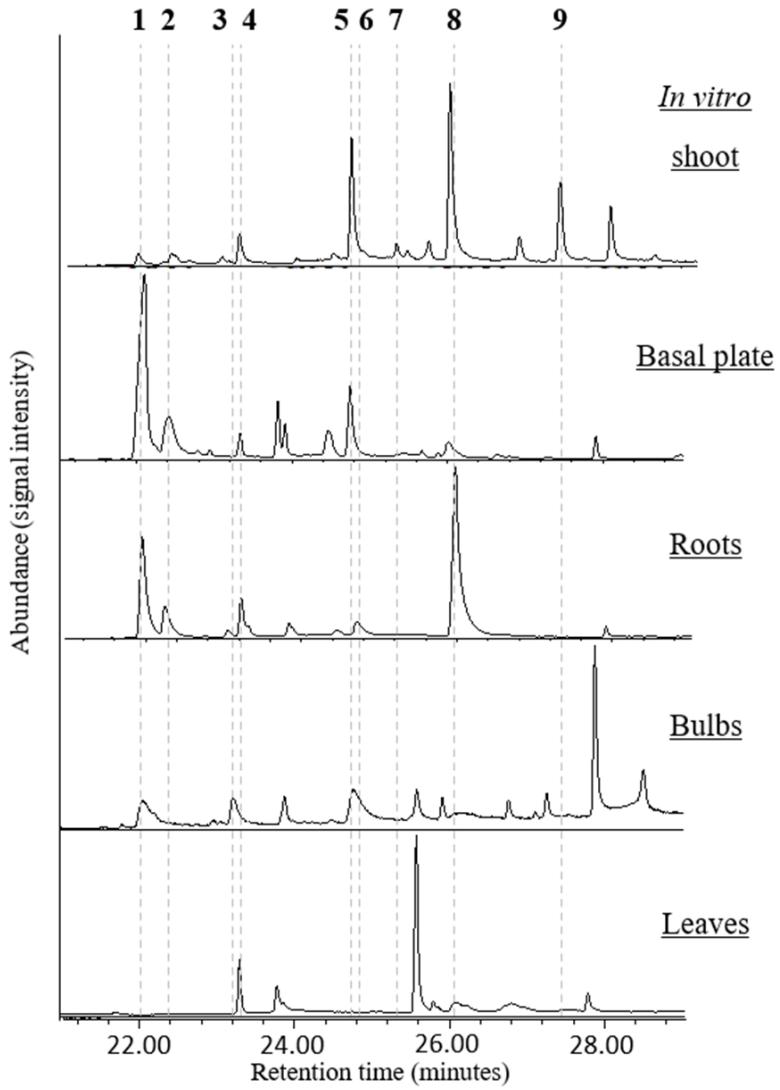

Annex B Fig. S2 Chromatographs of GC-MS analysis of C. x powellii "Album" tissues. Methanolic extracts of *in vivo* and *in vitro* tissues were analyzed. The corresponding mass for Amaryllidaceae alkaloids were identified with comparison to NIST 0.5 library. 1 : Crinan-3-ol, 1,2-didehydro(3-alpha), 2 : Crinan-3-ol, 1,2-didehydro(3-beta), 3 : Cherylline, 4 : Vittatine acetate, 5 : Powelline, 6: Epipowelline, 7: Lycorine O-acetyl, 8: Lycorine and 9: Crinamidine.

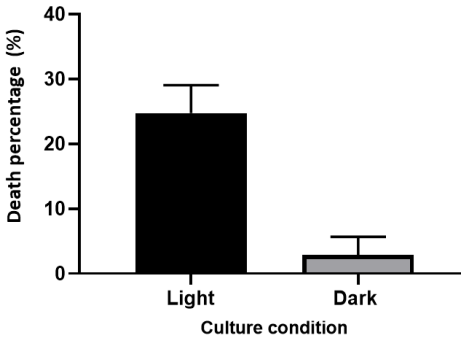

Annex B Fig. S3 Effect of light on the survival of explant. Data is present in percentage after aggregating all samples and groups by culture condition.

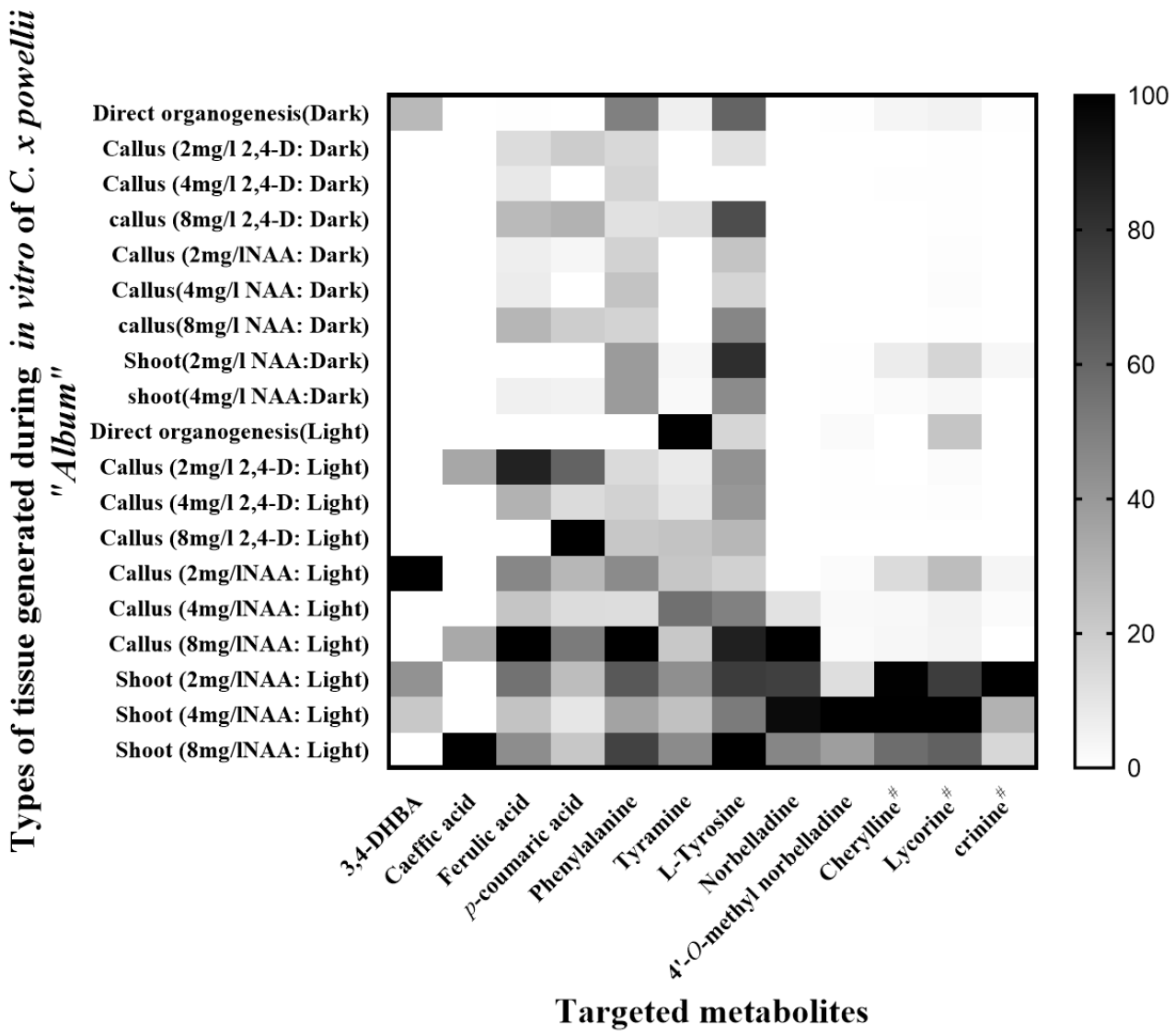

Annex B Fig. S4 LC-MS/MS analysis of targeted metabolites in tissue generated from in vitro culture of C. x powellii "Album". Heatmap shows the relative abundance of targeted metabolites in tissue culture of *C*. x *powellii*. Relative abundance corresponds to the mean value of three independent replicated values normalized to the sample with the highest level for each compound. The tissue included in the analysis in which the highest quantity of a specific compound is detected is shown as the most intense box. # Represent alkaloids which are also detected in GC-MS analysis

(a)

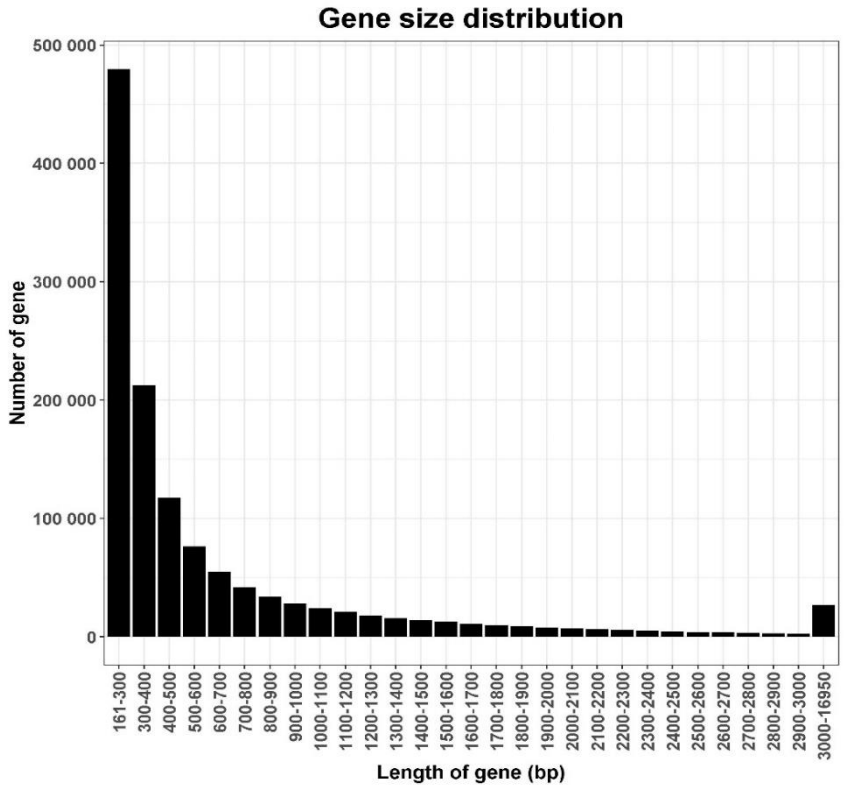
Gene size distribution
Number of gene
500 000
400 000
300 000
200 000
100 000
0
161-300
300-400
400-500
500-600
600-700
700-800
800-900
900-1000
1000-1100
1100-1200
1200-1300
1300-1400
1400-1500
1500-1600
1600-1700
1700-1800
1800-1900
1900-2000
2000-2100
2100-2200
2200-2300
2300-2400
2400-2500
2500-2600
2600-2700
2700-2800
2800-2900
2900-3000
3000-16950
Length of gene (bp)

(b)

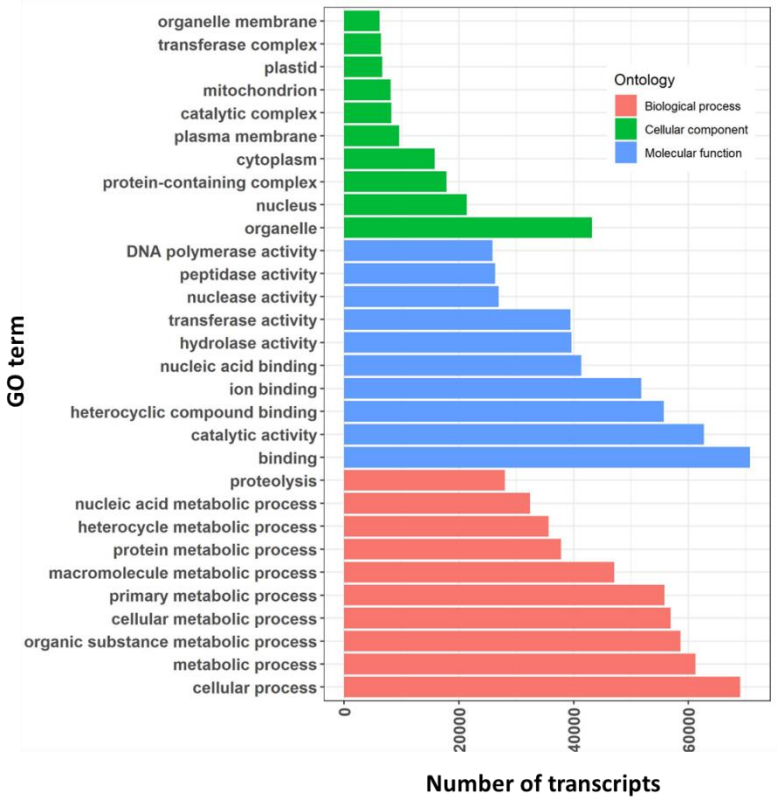
GO term
organelle membrane
transferase complex
plastid
mitochondrion
catalytic complex
plasma membrane
cytoplasm
protein-containing complex
nucleus
organelle
DNA polymerase activity
peptidase activity
nuclease activity
transferase activity
hydrolase activity
nucleic acid binding
ion binding
heterocyclic compound binding
catalytic activity
binding
proteolysis
nucleic acid metabolic process
heterocycle metabolic process
protein metabolic process
macromolecule metabolic process
primary metabolic process
cellular metabolic process
organic substance metabolic process
metabolic process
cellular process
Ontology
Biological process
Cellular component
Molecular function
0
20000
40000
60000
Number of transcripts

(c)

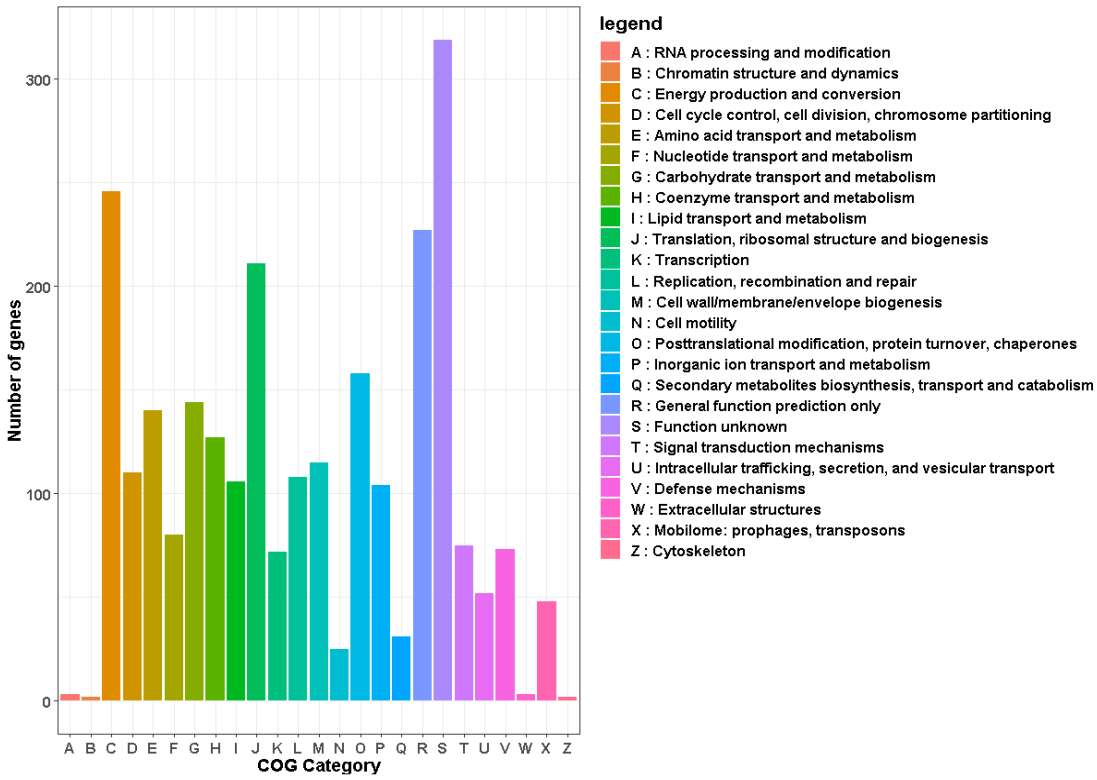

Annex B Fig. S5 Gene size distribution, GO-term analysis and COG functional classification **assemble transcriptome.** (**a**) Assembled transcriptomes were evaluated for their size distribution. The number of transcripts in each size range is presented. (**b)** Gene ontology (GO) terms of annotated *C.* x *powellii* "Album" genes separated into the three main ontologies: cellular component, molecular function and biological process. The numbers of transcripts in the ten most enriched GO terms for each of the categories are shown. (**c**) COG analysis of *C.* x *powellii* "Album" genes.

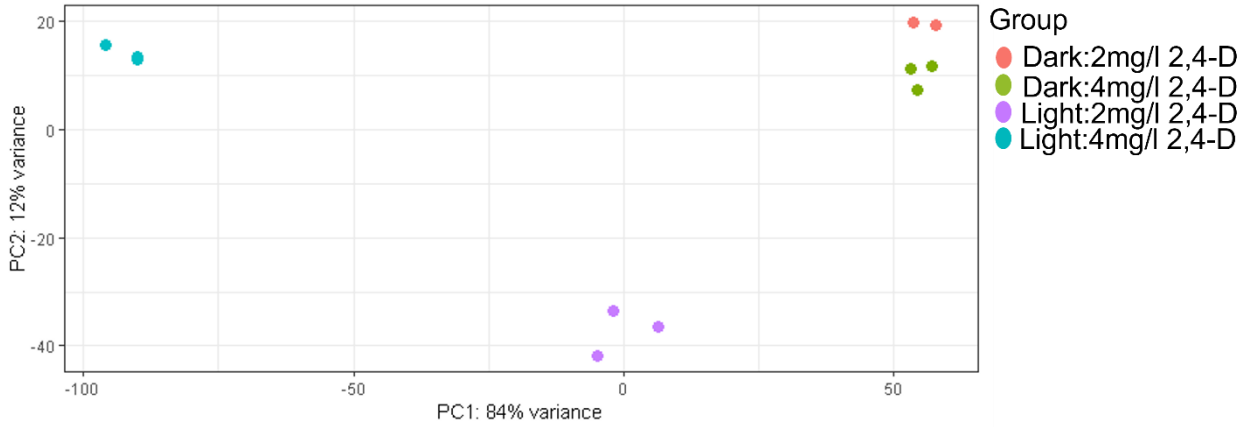

Annex B Fig. S6 Principal component analysis of RNA-seq data.

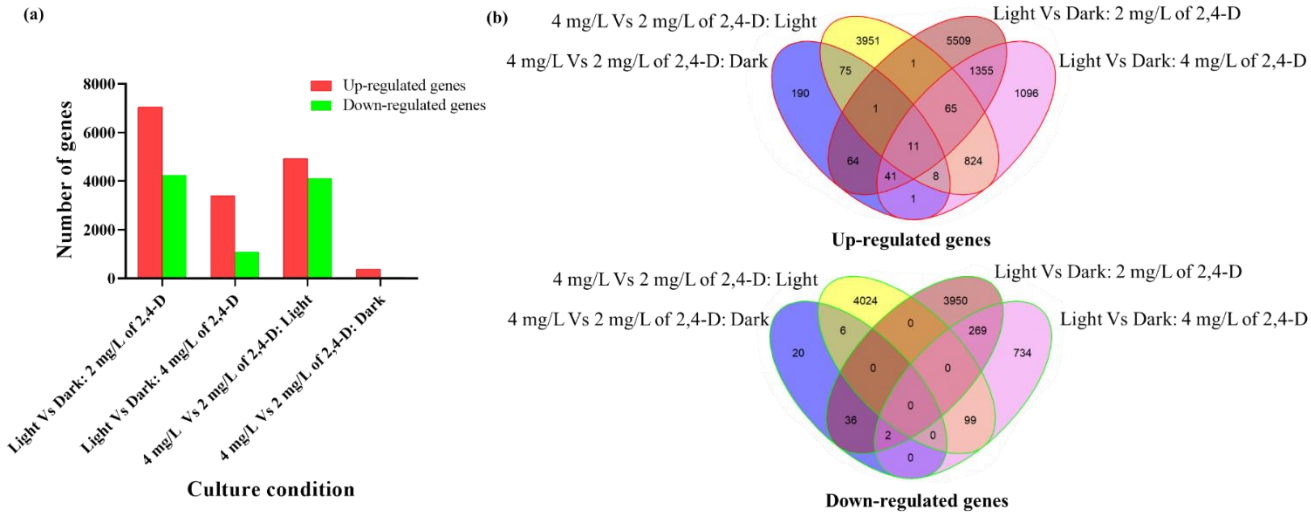

Annex B Fig. S7 Summary of differential expression analysis results. (a) Up-regulated (red) and down-regulated (green) genes were quantified. (b) Venn diagram showing the number of common and unique genes differentially expressed between the different culture conditions.

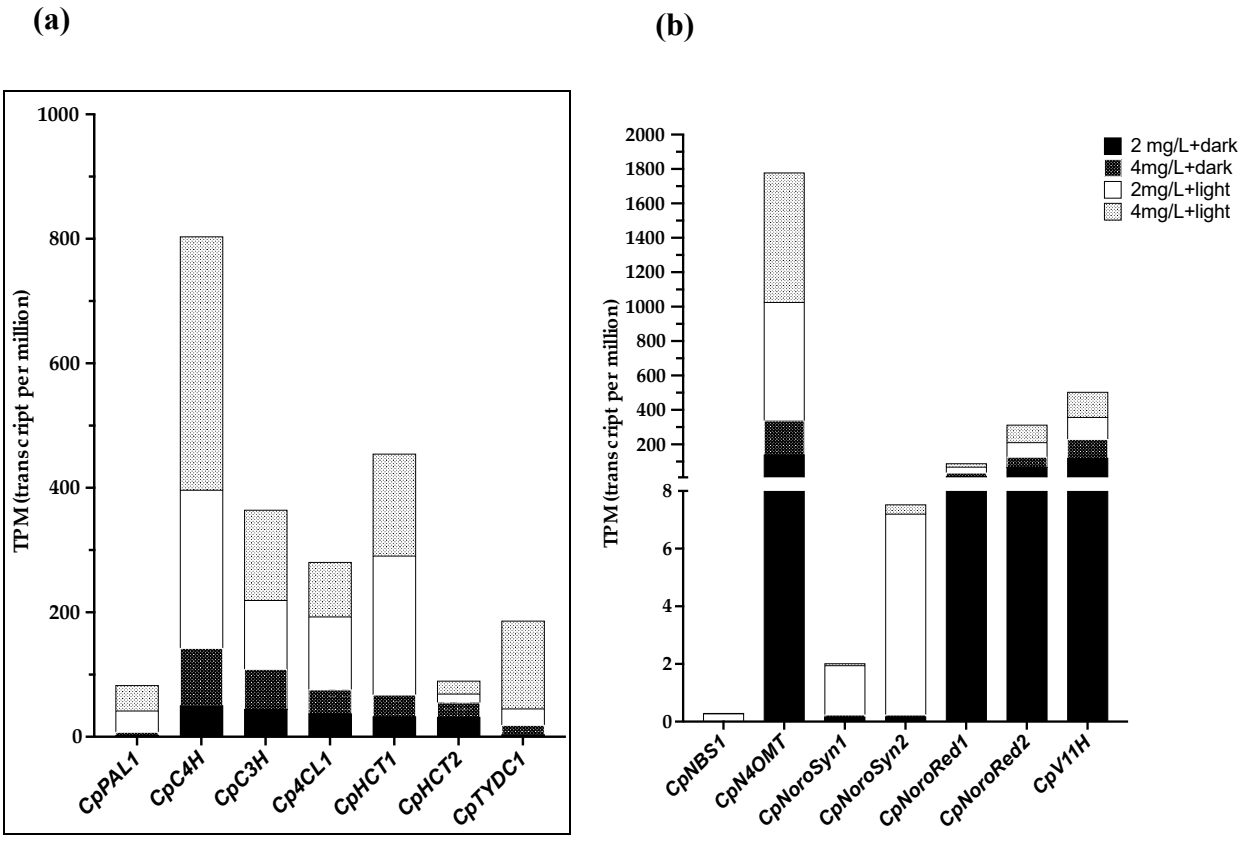

Annex B Fig. S8 Summary of differentially expressed transcripts related to the AA biosynthesis pathway with variation of light and 2,4-D concentration. (a) Precursor genes. (b) Amaryllidaceae alkaloid biosynthesis related transcripts. This figure summarizes the TPM data presented in Table S5.

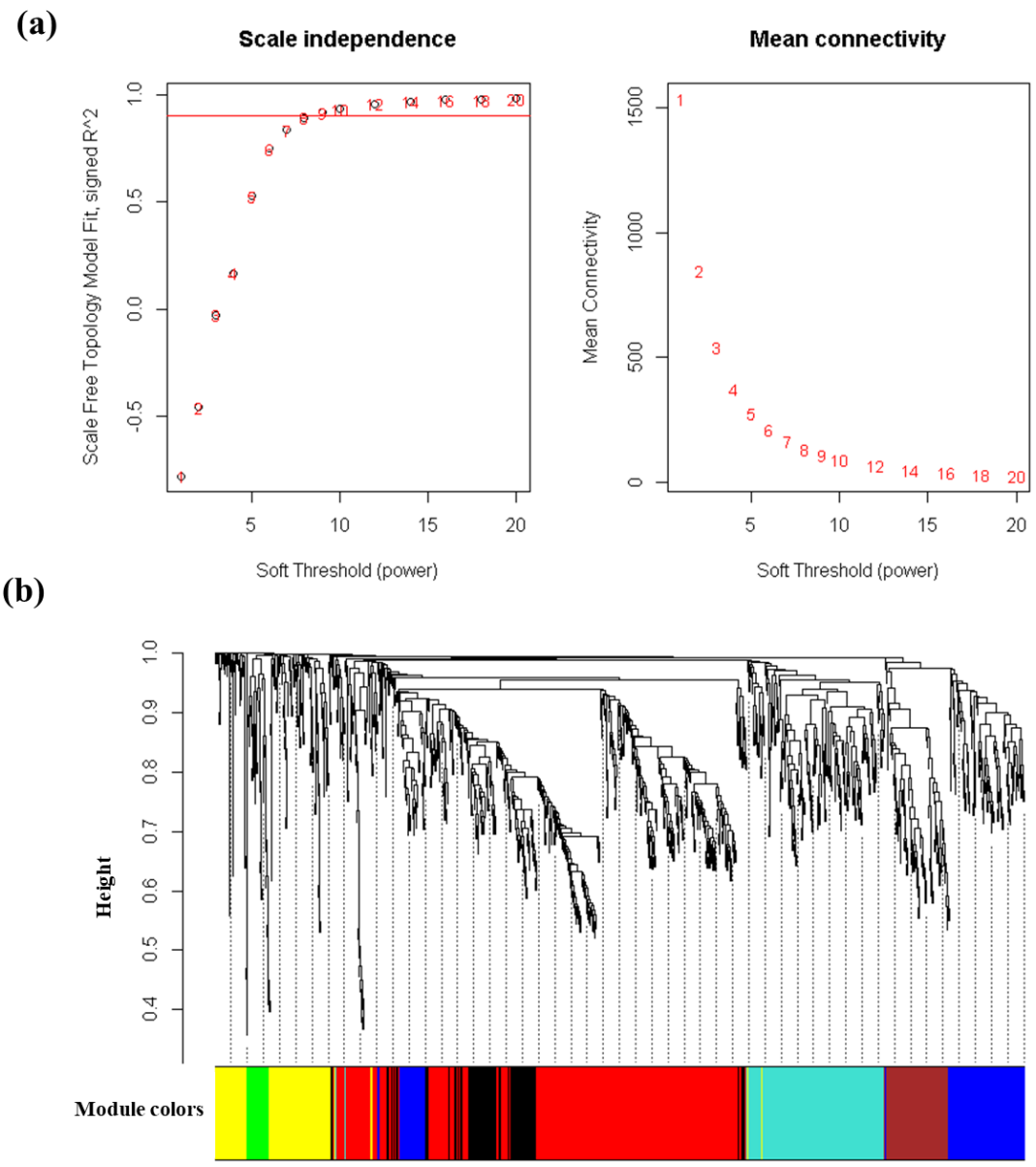

Annex B Fig. S9 WGCNA analysis of deregulated genes. (a) Determination of soft thresholding power. Left: analysis of the scale-free fit index for various soft thresholding power (β). Right: analysis of the mean connectivity for various soft thresholding power (β). (b) Hierarchical cluster tree showing seven modules of highly co-expressed genes. Each of the DEGs is represented by a leaf in the tree. Seven modules were identified, which are shown in designated colors: “blue”, “brown”, “green”, grey”, “red”, “turquoise” and “yellow

ANNEX C

Supplementary data for CHAPTER III

ANNEX C Table S1 List of primers used in this study.

Primer code	Sequence (5′-3′)	Direction	Application
NpOMT-Forward	AACGGGATCCATGGGTGCTAGCCAAGATGAT	Forward	Cloning into pMAlc2x vector
NpOMT-Reverse	ACGCAAGCTTTCAATAAAGACGTCGGCA	Reverse	
Loc-N-NpOMT-For	GGGGACAAGT TTGTACAAAAAAGCAGGCA TG GGTGCTAGC CAAGATGAT	Forward	N-terminal localization
Loc-N-NpOMT-Rev	GGGGACCACTTTGTACAAGAAAGCTGGGTC TCAATAAAGACGTCGACA	Reverse	
Loc-C-NpOMT-F	GGGGACAAGTTTGTACAAAAAAGCAGGCTT CGAAGGAGATAGAACCATGGGTGCTAGCCA AGATGAT	Forward	C-terminal localization
Loc-C-NpOMT-R	GGGGACCACTTTGTACAAGAAAGCTGGGTTT TATCAATAAAGACGTCGGCAAATAGT	Reverse	
qPCR-NpOMT-F	CCACGAGCGATTAGTGAAGC	Forward	RT-q-PCR analysis
qPCR-NpOMT-R	GGGATATCTCGACACGGG GA	Reverse	
qPCR-NBS-F	GAGGGAGGGCACTTG G	Forward	
qPCR-NBS-R	AGGAAGCATTTGCYGCATGT	Reverse	
qPCR-NR-F	AACAATGCAGGGACAGCCAT	Forward	
qPCR-NR-R	GCCGATTCGAAATTGGTGGC	Reverse	
NpHistone-F	GTCTGCCCCAACAACTGGAGG	Forward	
NpHistone-R	GCTTCCTAATCAGTAGCTCG	Reverse	

ANNNEX C Table S2 Identity and similarity (%) between characterized norbelladine O-methyltransferase and NpOMT.

		IDENTITY			
		NpOMT	**NpN4OMT**	**LrOMT**	**LaOMT**
SIMILARITY	**NpOMT**	-	96.49	97.49	92.89
	NpN4OMT	98.74	-	96.23	92.89
	LrOMT	98.74	97.49	-	93.31
	LaOMT	95.82	95.40	95.40	-

ANNEX C Table S3 Accession number of *O*-methyltransferase for phylogenetic analysis

Name of organism	Type of *O*-methyltransferase	Class of *O*-methyltransferase	Accession number
N. papyraceus	AAOMT	I	MF979869
N. sp. Aff. pseudonarcissus	AAOMT	I	AIL54541.1
Lycoris radiata	AAOMT	I	QFQ50503
Vanilla planifolia	CCoAOMT	I	AAC49913.1
Medicago sativa	CCoAOMT	I	AAC28973.1
Morus notabilis	CCoAOMT	I	EXC17316.1
Nicotiana tabacum	CCoAOMT	I	AAC49913.1
Populus tomentosa	CCoAOMT	I	ACE95173.1
Plagiochasma appendiculatum	CCoAOMT	I	KU578317.1
Danio rerio	CatOMT	I	NP-001025328.2
Egretta garzetta	CatOMT	I	KFP16811.1
Equus caballus	CatOMT	I	NP-001108007.1
Homo sapiens	CatOMT	I	NP-000745.1
Canis lupus	CatOMT	I	NP_001004074.1
Rattus norvegicus	CatOMT	I	1JR4-A
Medicago truncatula	COMT	II	DQ419914
Sorghum bicolor	COMT	II	AAL57301
Arabidopsis thaliana	COMT	II	NP-200227
Stylosanthes humilis	COMT	II	2119166A
Populus tomentosa	COMT	II	AAF63200
Medicago sativa	COMT	II	AAB46623.1
Catharanthus rosesus	BIAOMT	II	ABR20103.1
Coptis japonica	BIAOMT	II	BAB08005.1
Papaver sonmiferum	BIAOMT	II	ACN88562.1

Abbreviation: AAOMT: Amaryllidaceae Alkaloid *O*-methyltransferase, CCoAOMT: caffeoyl CoA *O*-methyltransferase, CatOMT: catecol *O*-methyltransferase, COMT: caffeic acid O-methyltransferase and BIAOMT: Benzylisoquinoline *O*-methyltransferase

ANNEX C Table S4: ***Np*OMT catalytic site residues interacting with ligands, metal ion, and SAM**.

Active Site residues	Ligand	Score	Interactions		
			Hydrophobic	H-bonds	Other
Asp6, Asp7, Tyr8, Ala9, Leu10,	Mg^{2+}	Na	Nd	nd	Metal ions Asp155 (n=2), Asp181, Asn182
Ile11, His12, Lys13, Glu46,	10 ps	Na	Nd	nd	Glu59, Lys13, Asp155, Asp181
Lys47, His48, Glu49, Trp50,	25 ns	Na	Nd	nd	Glu59 (n=2), Asp155 (n=2), Asp181(n=2)
Ser51, Ser52, Ala53, Ile78, Gly79, Val80,	SAM	Na	Tyr81	Val55, Tyr81, Tyr84, Ser85, Asp103, (n=2), Val104, Ala132, Asp155, Asp157 (n=2)	Salt bridge: Asp155
Tyr81, Ile102, Asp103, Val104, Asn105, Phe108,	10 ps	Na	Tyr81	Val55, Gly79, Tyr81, Tyr84, Ser85 (n=2) Asp103(n=2), Val104, Ala132, Asp157	Salt bridge: Asp155
Ser130, Glu131, Ala132, Leu133, Pro134,	25 ns	Na	Val55	Gly79, Tyr81, Tyr84, Ser85 (n=2), Asp103(n=2), Ala132, Tyr164	Salt bridges: Asp103
Asp155, Ala156, Asp157,	3,4-DHBA to isovanillin	-10.03	Trp185	Ser52, Lys158, Asn182, Tyr186	Mg^{2+} (n=2)
Lys158, Asn160,	3,4-DHBA to vanillin	-9.44	Trp 185 (n=2)	Asp155, Lys158, Asn182	Mg^{2+} (n=2)
Tyr164, Asp181,	Caffeic acid to isoferulic acid	-9.67	Trp185, Tyr186	Ser52, Lys158, Asn182, Tyr186	Mg^{2+} (n=2)
Asn182, Trp185,	Caffeic acid to ferulic acid	-9.62	Trp185 (n=2)	Ser52, Lys158, Asn182	Mg^{2+} (n=2)
Tyr186, Ser188, Tyr194, Leu197,	Norbelladine to 3ˈ-*O*-methylnorbelladine	-10.77	Asp157, Lys158 (n=2), Trp185, Ala204	Ser52, Asp155, Lys158, Ser159, Asn182	Mg^{2+} (n=2)

His198, Glu200,	10 ps	Na	Trp50 (n=2), Ala53	Ser52, Lys158, Asn182, Glu201	Trp185
Glu201, Ala204, Asp230,	25 ns	Na	Trp50, Trp185	Lys13, Trp50, Ala156, Lys158, Asn182	nd
	Norbelladine to 4'-*O*-methylnorbelladine	-11.34	Trp185 (n=2), Tyr186 Leu197	Ser52 (n=2), Ala53, Lys158, Asn182, Ser188, Tyr194, Glu201	π−stacking Trp185 (n=2), Tyr186; Mg^{2+} (n=1)
	10 ps	Na	Ty186 (n=2)	Ser52, Lys159, Asn 182 (n=2), Ser188, Tyr194, Glu201	Trp185 (n=2)
	25 ns	Na	Lys13, Tyr186 (n=2)	Ile11, Lys13, Asp155	nd
	4'*O*-methylnorbelladine to 3'4'*O*-dimethylnorbelladine	-10.24	Trp185 (n=2), Tyr186, Leu197	Ser52, Lys158, Asn182	π−stacking Trp185 (n=2), Tyr186, Mg^{2+}

Na: not applicable, nd: not detected. The score is in (kCal/mol).

ANNEX C Table S5: **MRM transitions and instrumental parameters used for HPLC-MS/MS analyses in ESI+ and ESI-**

Compound name	Retention time (min)	Precursor (m/z)	Product (m/z)	Fragment (V)	CE (V)	Polarity (ESI +/-)
3,4-dihydroxybenzaldehyde	15.795	137	119	114	20	Negative
			108		26	
			92		26	
3'-O-methylnorbelladine	16.875	274	**137**	105	18	Positive
			121		15	
			109		40	
4'-O-methylnorbelladine	15.630	274	**137**	105	18	Positive
			122		40	
			94		40	
11-hydroxyvittatine	4.529	288	226	105	26	Positive
			196		34	
			153		40	
3',4'-O-dimethylnorbelladine	16.668	288	**151**	100	10	Positive
			135		40	
			107		40	
Caffeic acid	18.344	181	**163**	76	5	Positive
			135		10	
			117		21	
Ferulic acid	19.588	195	**177**	81	5	Positive
			145		20	
			117		21	
Galanthamine	4.655	288	270	120	14	Positive
			225		18	
			213		22	
Haemanthamine	12.204	302	211	105	22	Positive
			196		34	
			181		30	
Homolycorine	15.892	316	300	115	30	Positive
			298		22	
			94		26	
Isoferulic acid	19.762	195	**177**	81	5	Positive
			145		20	
			117		21	
Isovanillin	18.566	153	125	86	10	Positive
			93		13	

			65		25	
Lycorine	3.963	288	270	92	20	Positive
			177		20	
			147		28	
			119		40	
Narciclasine	18.367	308	**248**	82	28	Positive
			218		36	
			202		40	
Norbelladine	7.181	260	**138**	86	5	Positive
			123		20	
			121		17	
Pancracine	6.468	288	**270**	95	18	Positive
			185		34	
			165		40	
Papaverine	18.004	340	324	165	40	Positive
			202		27	
			171		40	
p-coumaric acid	19.448	165	**147**	76	5	Positive
			119		17	
			91		20	
Tazzetine	17.216	332	**314**	90	14	Positive
			181		30	
			153		40	
Trans-cinnamic acid	21.296	147	**103**	65	9	Negative
			77		20	
Vanillin	18.740	153	125	86	10	Positive
			93		13	
			65		25	
Crinine	10.113	272	226	105	26	Positive
			196		34	
			136		26	

Notes: The quantifier ion for each compound is bold and qualifier ions are not

(a)

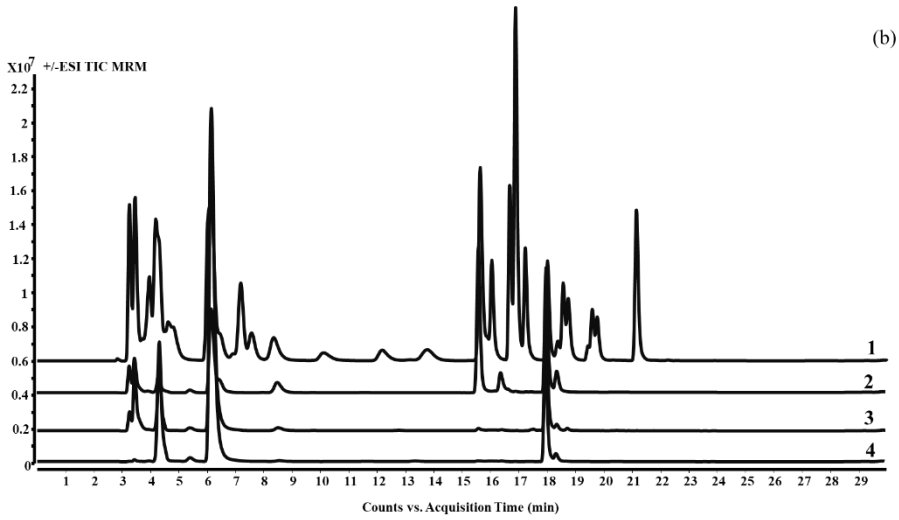

(b)

Target compound	Retention time (min)	[M+H]+(m/z)
Tyramine	3.449	138
Vanillin	18.740	153
Caffeic acid	18.344	181
Norbelladine	7.181	260
4'-*O*-methylnorbelladine	15.630	274
3',4'-*O*-dimethylnorbelladine	16.668	288
Haemanthamine	12.204	302
Narciclasine	18.367	308
Pancracine	6.468	288
Vittatine	10.113	272
11-hydroxyvittatine	4.529	288
Lycorine	3.963	288
Galanthamine*	4.655	288

ANNEX C Fig. S1. Targeted metabolites analysis on *N. papyraceus* during the vegetative stage. (a) LC-MS/MS chromatography (1) standard mixture, (2) leaves, (3) bulb, and (4) roots of *Narcissus. papyraceus*. (b) Retention time (min) and M+H +(m/z) mass of identified compounds. * Indicates the low-level detection of the compound.

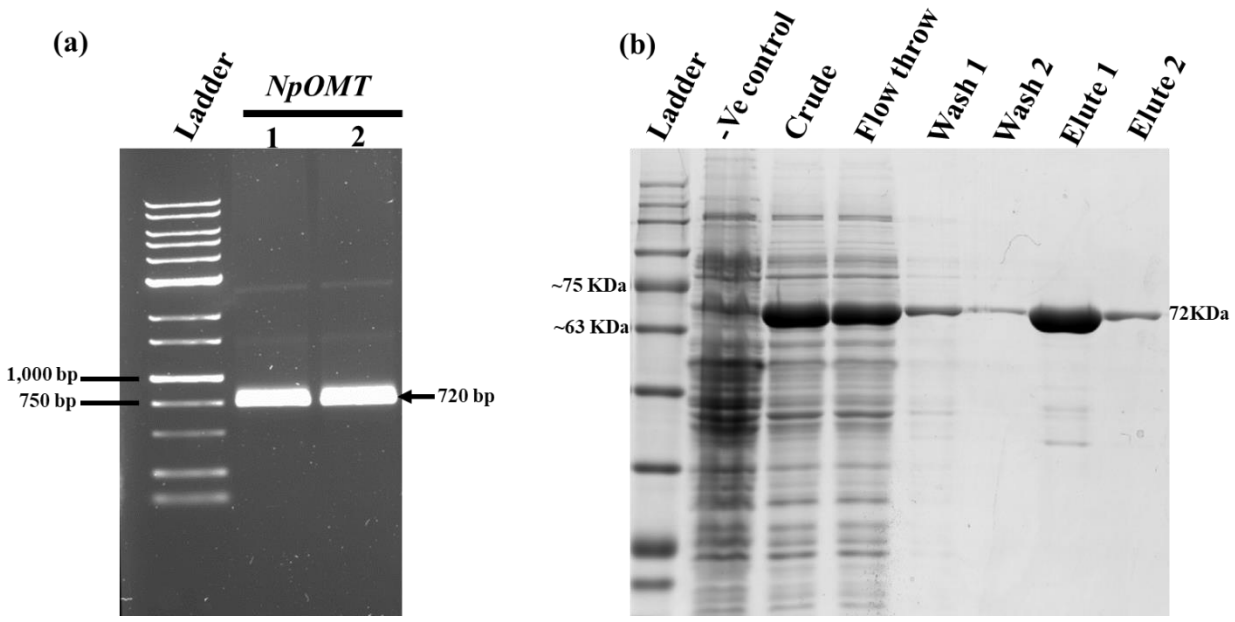

ANNNEX C Fig. S2. Heterologous expression of NpOMT in *E. coli* and purification of NpOMT. (a). PCR amplification of Np*O*MT from cDNA of *N. papyraceus*. Lane 1 and 2 show amplified NpOMT. (b) SDS-PAGE analyses of induced expression and purification of recombinant NpOMT.

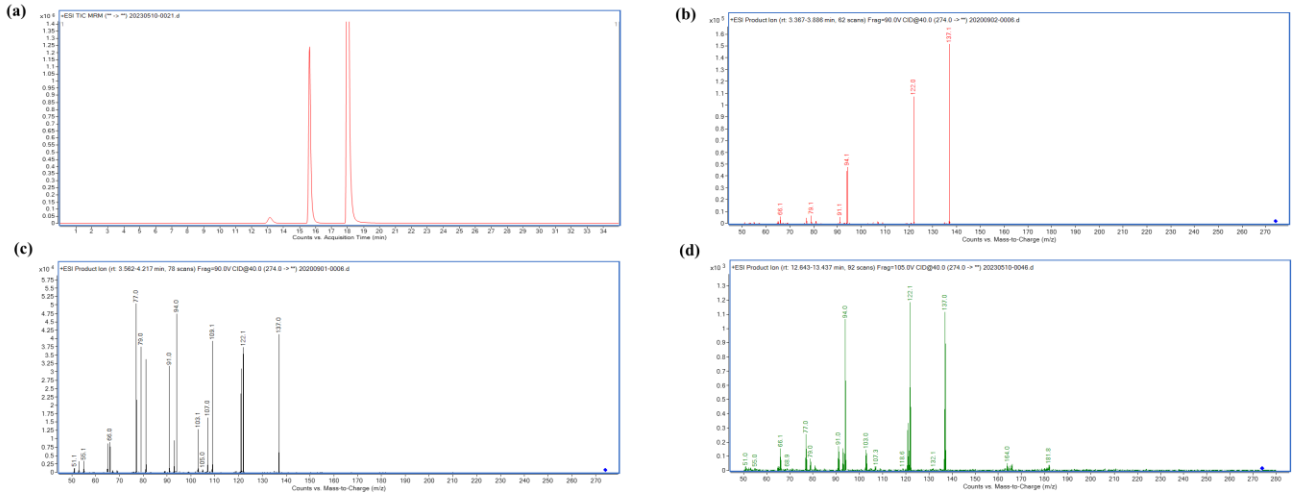

ANNEX C Fig. S3. LC-MS/MS analysis of peak iv corresponding to figure 3.4 (b). (a) +ESI TCI MRM of NpOMT enzymatic reaction with NpOMT. (b) Fragmentation of peak (unknown) obtained at 13.1 min, (c) Fragmentation of standard 4ˈ-*O*-methylnorbelladine. (d) Fragmentation of standard 3ˈ-*O*-methylnorbelladine.

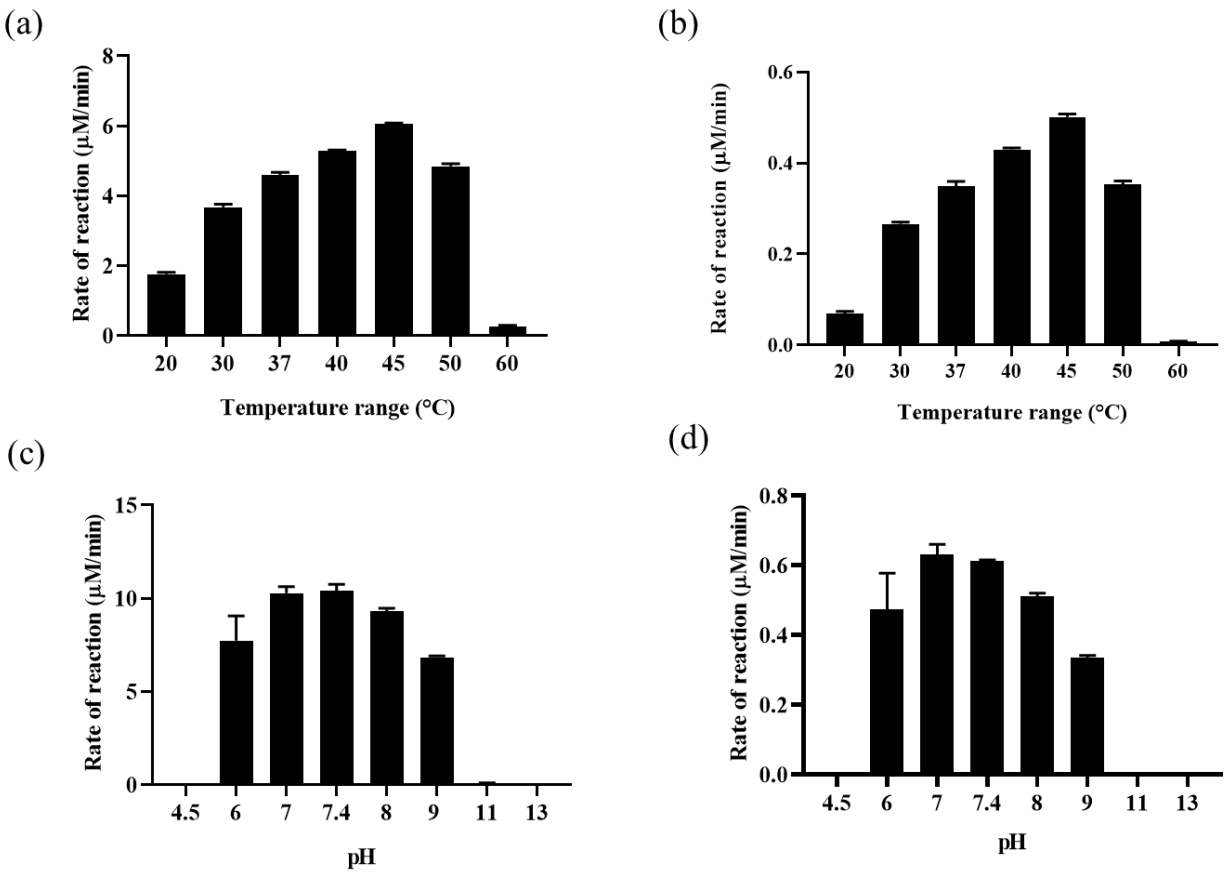

ANNEX C Fig. S4. Optimization pH and temperature for enzymatic reaction of *Np*OMT with 3,4-DHBA. (a) Effect of temperature on the formation of vanillin. (b) Effect of temperature on the formation of isovanillin. (c) Effect of pH on the formation of vanillin. (d) Effect of pH on the formation of isovanillin. All experimental values represent the means of three replicates ± standard deviation.

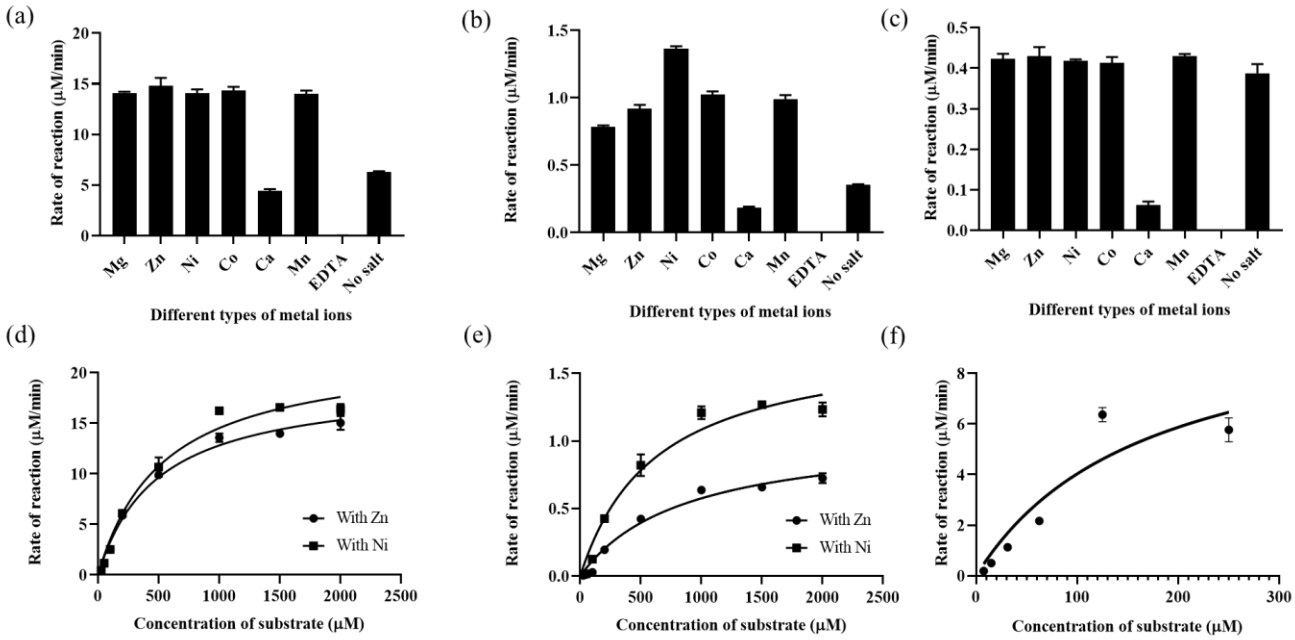

ANNEX C Fig. S5 Biochemical characterization of *Np*OMT. Effect of different divalent metal ions on formation of (a) vanillin, (b) isovanillin, and (c) 4′-*O*-methylnorbelladine. The steady-state kinetic parameters for NpOMT catalyzed reaction for the formation of (d) vanillin, (e) isovanillin, and (f) 4′-*O*-methylnorbelladine. All experimental values represent the means of three replicates ± standard deviation.

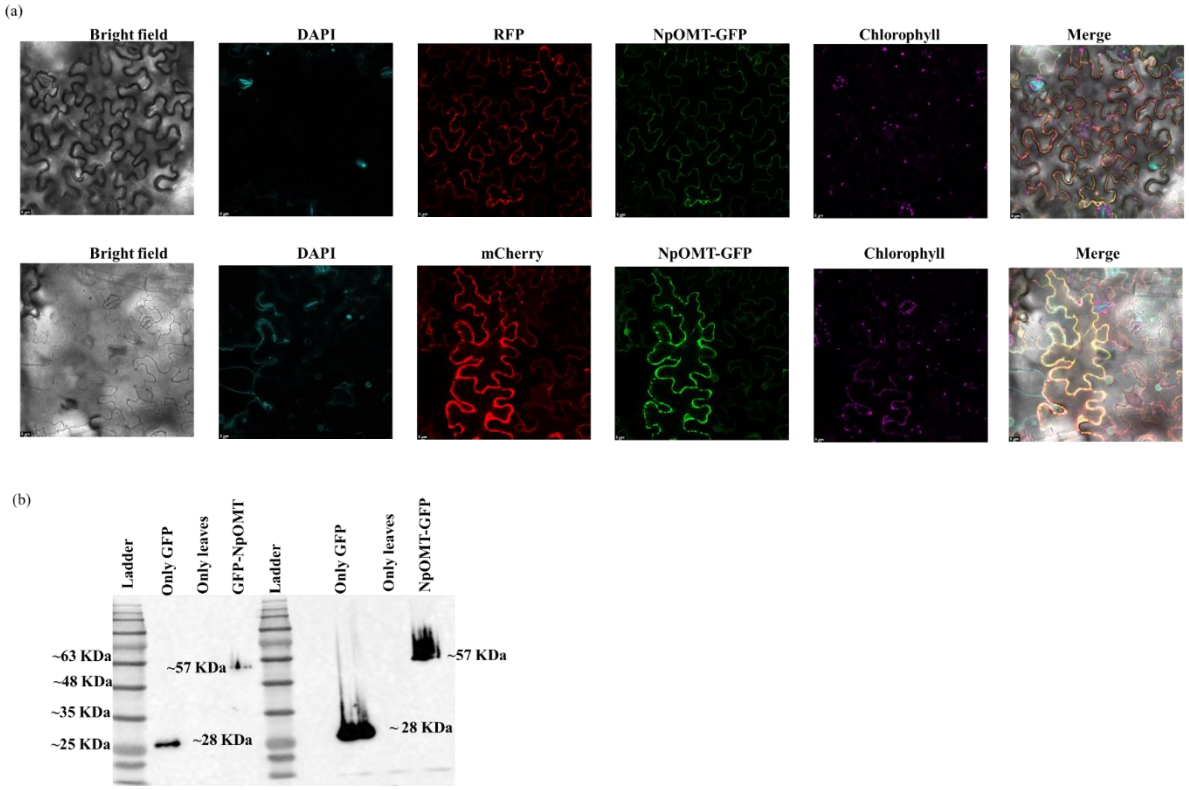

ANNEX C Fig S6 Cellular location of C-terminal GFP tagged *Np*OMT and confirmation the integrity of GFP-tag *Np*OMT. (a) C-terminal GFP fusion *Np*OMT was co-expressed with red fluorescent protein (RFP) and mCherry protein in epidermal cell of *Nicotiana benthamiana* levaes and image were taken after 48 hrs with confocal microscopy. DAPI was used as positive control for nucleus marker. Bright field, DAPI, RFP or mCherry, *Np*OMT-GFP, chlorophyll and merge image are shown. Scale bars in image represent 5 μM. (b) Western blotting of only GFP (~28 KDa), only leveaves, GFP-*Np*OMT(N-terminal GFP tagged *Np*OMT) and NpOMT-GFP (C-termial tagged *Np*OMT).Predict sized GFP tagged *Np*OMT was ~57(28 + 29) KDa.

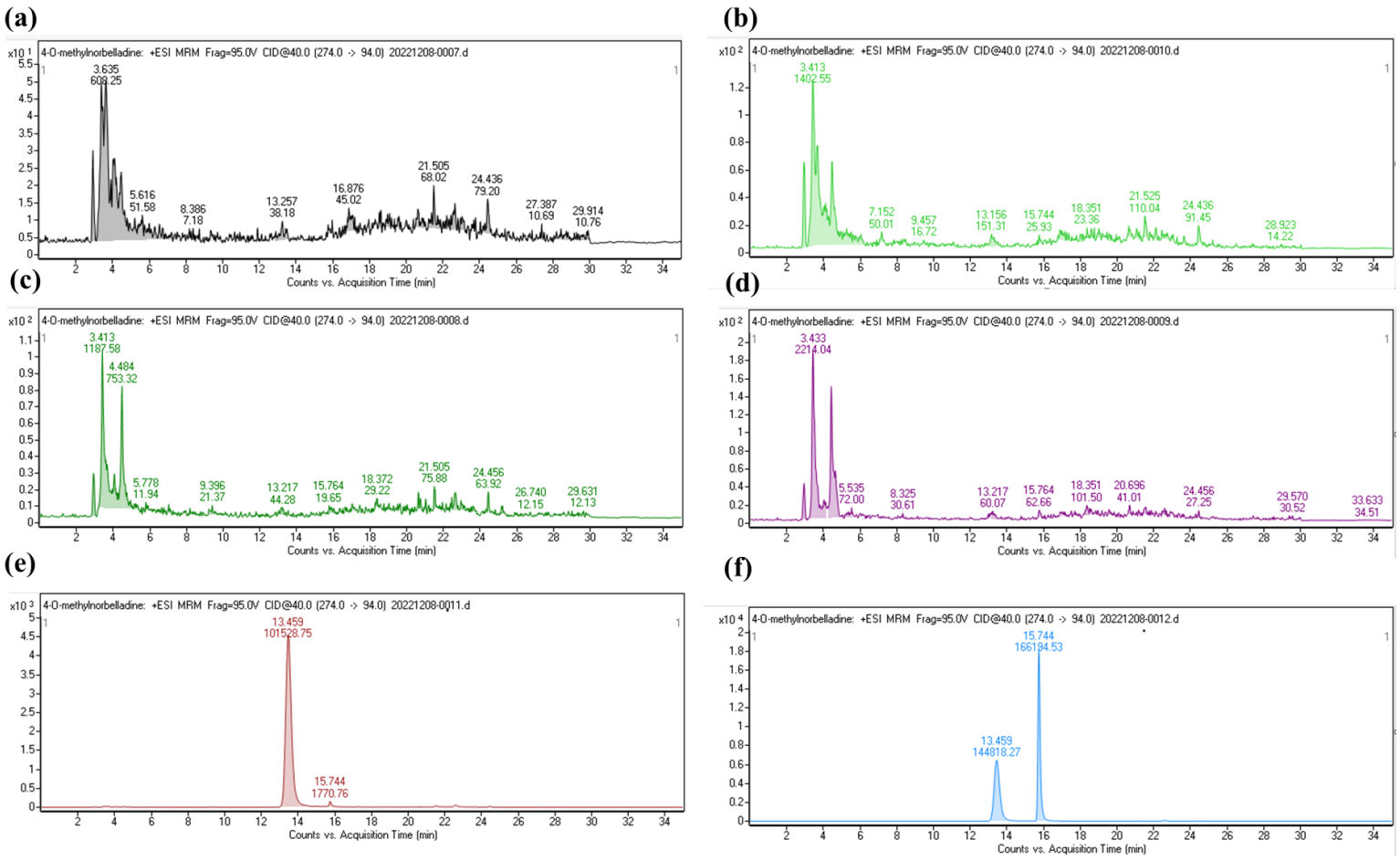

ANNEX C Fig. S7. Enzymatic assay of *Np*OMT with norbelladine in *Nicotiana benthamiana.*
The enzymatic reaction was done with N-terminal GFP tag *Np*OMT and 50 µM norbelladine was infiltrated. The formation of products was monitored was confirmed by LC-MS/MS analysis of methanolic extraction of norballadine infiltered leaves after 24 hours. (a) LC-MS/MS analysis of only leaves with transit expression of *Np*OMT, (b) LC-MS/MS analysis of transit expression of *Np*OMT infiltered with methanol, (c) LC-MS/MS analysis of GFP expressed leaves, (d) LC-MS/MS analysis of N-terminal GFP tag *Np*OMT expressed leaves, (e) LC-MS/MS analysis of norbelladibe infiltered leaves with GFP expressed and (f) LC-MS/MS analysis of norbelladine infiltered leaves with N-terminal GFP tag *Np*OMT expressed leaves.

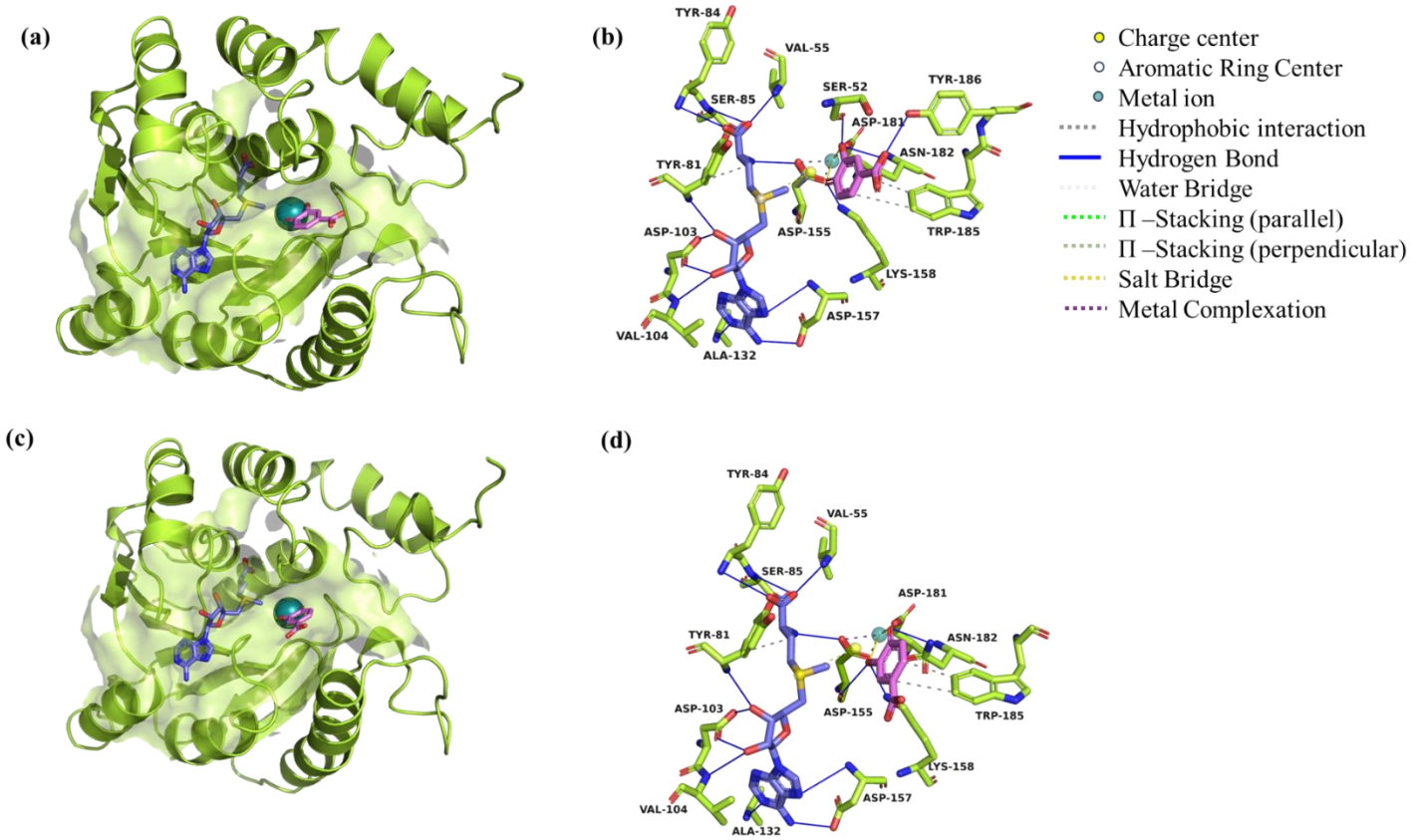

ANNEX C Fig. S8. Molecular docking study on *Np*OMT interacting with 3,4-DHBA. (a) and (b) NpOMT interacting with 3,4-DHBA for the formation of vanillin. (c) and (d) NpOMT interacting with 3,4-DHBA for the formation of isovanillin.

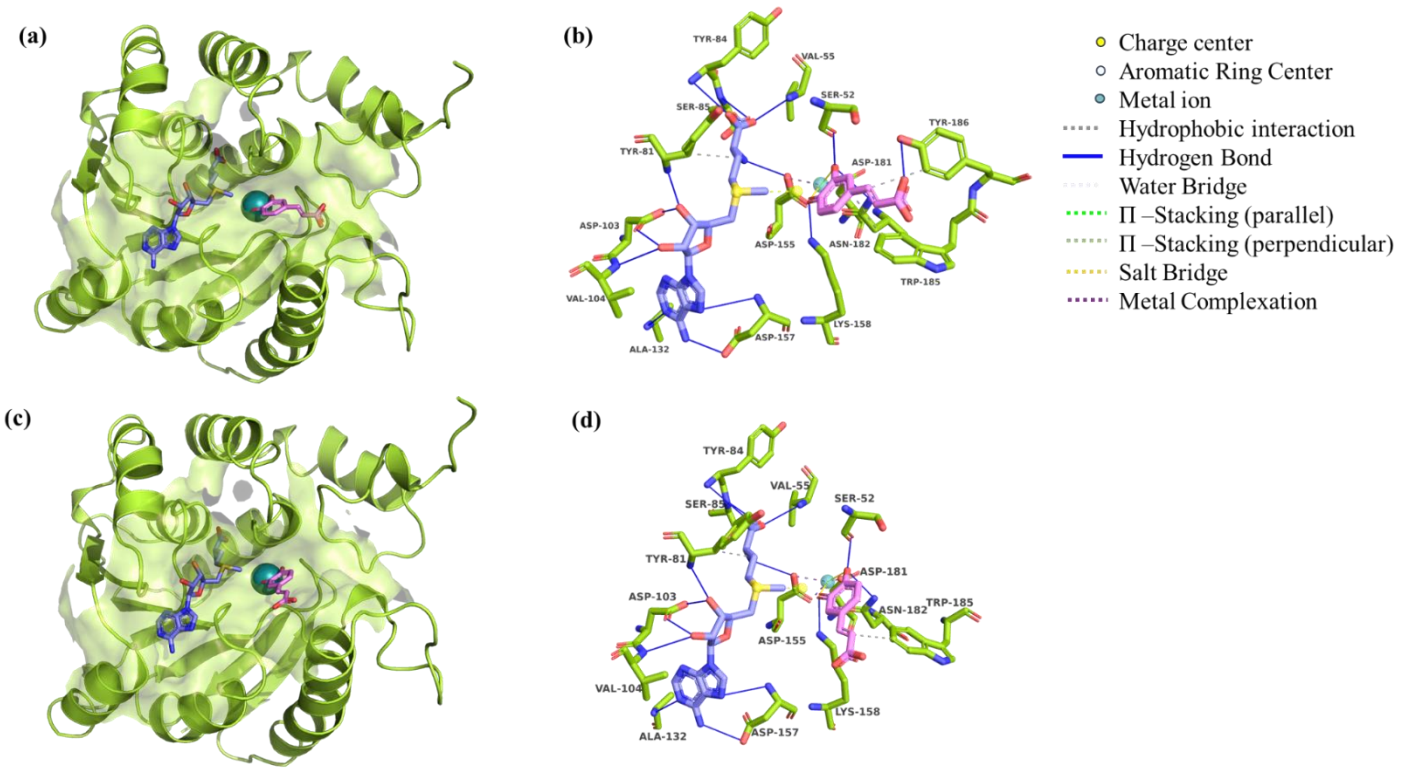

ANNEX C Fig. S9 Molecular docking study on *Np*OMT interacting with caffeic acid. (a) and (b) NpOMT interacts with caffeic acid for the formation of ferulic acid (c) and (d) NpOMT interacts with caffeic acid for the formation of isoferulic acid.